ELECTRO-CATALYTIC SUPPORTS FOR NOBLE METALS FOR EXPLOITATION AS ELECTRODES FOR FUEL CELLS

A THESIS

submitted by

T. MAIYALAGAN

for the award of the degree

of

DOCTOR OF PHILOSOPHY

DEPARTMENT OF CHEMISTRY
INDIAN INSTITUTE OF TECHNOLOGY MADRAS
CHENNAI-600 036, INDIA

APRIL 2007

Dedicated
to
My beloved Parents

THESIS CERTIFICATE

This is to certify that the thesis entitled **"ELECTRO-CATALYTIC SUPPORTS FOR NOBLE METALS FOR EXPLOITATION AS ELECTRODES FOR FUEL CELLS"** submitted by **Mr. T. Maiyalagan** to the Indian Institute of Technology, Madras for the award of the degree of Doctor of Philosophy is a bonafide record of research work carried out by him under our supervision. The contents of this thesis, in full or in parts, have not been submitted to any other Institute or University for the award of any degree or diploma.

Date:

Place:

Prof. B. Viswanathan
Research Guide
National Center for Catalysis Research
Department of Chemistry
Indian Institute of Technology, Madras
Chennai – 600 036

Prof. U. V. Varadaraju
Research Guide
Material Science Research Center
Department of Chemistry
Indian Institute of Technology, Madras
Chennai – 600 036

ACKNOWLEDGEMENTS

I would firstly like to express my deepest appreciation to my research supervisor **Prof. B. Viswanathan**, for his patience, inspiration, guidance, support, constant encouragement and advice at each and every stage of my research programme. It has been a great opportunity for me to work in his group and gain extensive research experience in the field of nanomaterials and catalysis science. I wish to express my deep attitude to the co-supervisor **Prof. U. V. Varadaraju** for his great assistance and help during my study.

I sincerely thank **Prof. M. S. Gopinathan**, **Prof. B. Viswanathan,** (late) **Prof. S. Vancheesan**, **Prof. M. N. Sudheendra Rao,** (late) **Prof. G. Sundarajan** the former Heads and **Prof. Prof. S. Sankararaman**, the present Head of the Department of Chemistry, IIT Madras for providing the necessary facilities during my research programme.

All my doctoral committee members were very supportive and gave proper direction for my research work. I take this opportunity to thank my doctoral committee members **Prof. R.P.Viswanath, Prof. T.K.Varadarajan**, **Prof. A. Subrahmanyam and Prof. V.R.K Murthy.**

During the course of my PhD-work I have benefited from discussions with and the assistance of all members of the National Centre for Catalysis Research (NCCR).

I am also thankful to **Prof. T.K.Varadarajan** for his encouragement during my research tenure.

I am extremely thankful to my seniors **Dr. V. Raghuveer** and **Dr. B. Rajesh** for their constant help and encouragement during my **Ph.D** programme.

I would like to express my sincere gratitude to **Mr. A. Narayanan, Mrs. Bhavani Kumar, Mr. Surya prakash, Mrs. Latha and Mr. Mohan** for extending their help at various stages of my research.

I also wish to express my sincere thanks to my colleagues in NCCR **Mr. Sankaran, Mr.Navaladian, Miss. Helen, Mrs. Chandravathanam, Mr.Venketeswara Rao, Mr. Satayananda Kishore, Mr. Himakumar, Mr. Indraneel, Miss Rajeswari, Mrs. Janet,** for their friendly behavior**.**

I am also thankful to my friends **Arun prasad, Amaladoss, srinivasan, Jayaseelan, Suresh, Antony, Santha Kumar, Koteeswara rao, Balaji, Anand and Velu mahalingam** for their timely help.

I am extremely grateful to **Mr. V. Baskar** for computer help during my typing the thesis.

Most of all, I express my deep appreciations to Sujatha and my parents for tireless encouragement, support, inspiration, friendship, and love.

Financial support from Council of Scientific and Industrial Research (CSIR), New Delhi is gratefully acknowledged.

T. Maiyalagan

ABSTRACT

Key words: Direct Methanol Fuel Cell (DMFC), nitrogen containing carbon nanotubes, conducting polymer nanotubes, nanocomposite, nanostructured electrodes, anode catalysts, electrocatalyst, platinum and methanol oxidation

Direct Methanol Fuel Cells (DMFCs) using polymer electrolyte membranes are promising candidates for portable power sources. It possess a number of advantages such as a liquid fuel, quick refueling, low cost of methanol and the compact cell design making it suitable for various potential applications including stationary and portable applications. DMFCs are also environmentally friendly. Although carbon dioxide is produced, there is no production of sulfur or nitrogen oxides. The development of commercial DMFCs has nevertheless been hindered by some important issues. The most important ones are cost of the platinum and the membrane (Nafion). With the eventual goal of improving the overall electrode performance of the DMFC, this study is concerned with an investigation of the issues and effect of various nanostructured supports on its performance. The aim of this research was to improve the performance of electrodes for direct methanol fuel cells (DMFCs). To reach this objective, nanostructured supports of different materials were synthesized by template synthesis.

The work presented is a compilation of different nanostructured electrodes as supports by template-synthesis for methanol oxidation. Nitrogen containing carbon nanotubes are of potential significance for a number of advanced technological applications. Currently, considerable interest exists in the possible applications of nitrogen containing carbon nanotubes for fuel cells. Metal oxides like TiO_2, WO_3 supports with a well-ordered nanostructure have also been developed. Physical properties and

nanostructure were elucidated. Developed nanostructured supports can be integrated with the nanostructured electrocatalysts. Characterizations of these nanostructured materials and the associated electrochemical properties have been studied. Conducting polymer nanotubes and nanostructured organic-inorganic hybrid nanocomposites have also been developed. The developed nanostructured electrocatalysts have been evaluated for methanol oxidation.

CONTENTS

LIST OF TABLES

LIST OF FIGURES

LIST OF SCHEMES

ABBREVIATIONS

AFM	-	Atomic Force Microscopy
CNT	-	Carbon Nanotube
CO	-	Carbon Monoxide
CV	-	Cyclic Voltammetry
DMFC	-	Direct Methanol Fuel Cell
EDX	-	Energy Dispersive X-ray Analysis
EDOT	-	Ethylenedioxythiophene
EPR	-	Electron Paramagnetic resonance Spectroscopy
FTIR	-	Fourier Transform Infrared Spectroscopy
N-CNT	-	Nitrogen containing Carbon nanotube
PEDOT	-	Poly (3, 4-Ethylenedioxythiophene)
PEMFC	-	Polymer Electrolyte Membrane Fuel Cell
PPP	-	Poly (paraphenylene)
PVP	-	Polyvinylpyrrolidone
PPY	-	Polypyrrole
PVI	-	Poly (***N***-vinylimidazole)
Pt	-	Platinum
Ru	-	Ruthenium
SEM	-	Scanning Electron Microscopy
SSCE	-	Saturated Sodium Chloride Calomel Electrode
TEM	-	Transmission Electron Microscopy
TGA	-	Thermogravimetric Analysis
UV-Vis	-	Ultra Violet – Visible Spectroscopy
V_2O_5	-	Vanadium Pentoxide
XRD	-	X-ray Diffraction

NOTATIONS

Å	-	Angstroms
θ	-	Angle
λ	-	Wavelength
h	-	hour
K	-	Degree Kelvin
°C	-	Degree Celsius
T	-	Temperature
V	-	Volume
A	-	Absorbance
eV	-	Electron Volt
mV	-	Milli Volt
E	-	potential (V)
t	-	time (s)

CHAPTER 1

INTRODUCTION

1.1 INTRODUCTION

In today's society there is an enormous demand for energy. Environmental concerns necessitate that new energy sources must be efficient and have zero (or very low) emissions. The fuel cell is an emerging technology that can meet these demands. A fuel cell is defined as an electrochemical device that can continuously convert chemical energy into electrical energy (Viswanathan and Scibioh, 2006). Much like a battery, a fuel cell produces electrical energy. However, unlike a battery, the reactants are continuously supplied and products are continuously removed. Hence, a fuel cell does not store energy (Van *et al*., 2006). Typically, hydrogen is the fuel consumed at the anode; oxygen (usually from air) is consumed at the cathode. In an acid electrolyte, the cell reactions are as follows:

Anode: $H_2 \longrightarrow 2\,H^+ + 2\,e^-$

Cathode: $O_2 + 4\,H^+ + 4\,e^- \longrightarrow 2\,H_2O$

The main advantage a fuel cell has over heat engines is that they are theoretically more efficient and produce no noxious emissions (Jewulski and Rak 2006). Also, fuel cells operate very quietly, reducing noise pollution (Dyer, 2002). Because of these advantages, fuel cells are being developed for numerous commercial and military applications, such as automobiles, portable electronic devices, mobile and stationary power generation.

Sir William Grove invented fuel cells around 1839. But it is only in the last 40 years, since the commercial fuel cell systems were applied in space technology, that their

properties are highly desirable for specific applications. Because the efficiency of electrochemical energy conversion by fuel cells is high, the interest has lead to an intensive development of components and of better cell designs. Therefore it can be expected that performance will improve significantly in the near future (Appleby, 1990).

There are, however, several hurdles that must be overcome before fuel cells can become a commercially viable technology on a large scale (Chalk *et al.,* 2000). Cost is one such factor. The required catalyst, membrane and cell hardware (e.g. bipolar plates) are expensive, resulting in a very high initial cost. Also, hydrogen storage requires a large (weight and volume) storage system. This reduces the operational range of portable fuel cell devices. There is much research for better ways to store hydrogen. In particular, storing hydrogen in carbon nanotubes and metal hydrides has received a great deal of attention recently.

1.2 THE PROMISE OF FUEL CELLS

Compared to internal combustion engines, fuel cell has an efficient conversion process. The internal combustion engine is less efficient due to the conversion of chemical energy into thermal energy and then thermal energy to mechanical energy. If cars were powered by electricity generated from fuel cell, there would be no combustion involved.

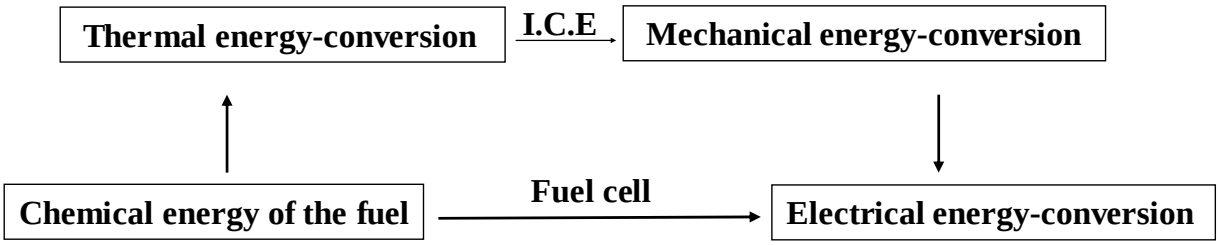

Scheme 1.1 Direct energy conversion with Fuel cells in comparison to conventional internal combustion engine (ICE).

The need for an efficient, non-polluting power source for vehicles in urban environments has resulted in increased attention to the option of fuel cell powered vehicles (Lashway, 2005). Of the various fuel cell systems, the PEM fuel cell technology seems to be the most suitable one for transportation applications. This is due to its low temperature of operation (hence, faster cold start), excellent CO_2 tolerance and a combination of high power density and high-energy conversion efficiency. Moreover, there is no free corrosive liquid in PEM fuel cells. They are able to withstand large pressure differentials. The corrosion problems of the materials are minimal. They have demonstrated longevity (Patil and Zegers, 1994).

1.2.1 Choice of Fuels

The technical characteristics, economic feasibility and infrastructure requirements of PEFC electric engines are impacted greatly by the fuel chosen, with large difference between these impacts for the fuels that are presently being considered for transportation applications: hydrogen, methanol, and gasoline or related petroleum distillate fuels.

Hydrogen Fuel has the highest energy density, but lack of fuel infrastructure, bulky storage system and safety concerns have motivated fuel cell developers to look for alternative fuel. Indeed, Toyota, Daimler-benz, Ford and other leading developers have shifted their initial emphasis from hydrogen to methanol. Methanol is the only practical carbonaceous fuel that has significant electrochemical reactivity at fuel cell electrodes in the temperature range of interest for portable applications (Wang, 2002).

Table 1.1. Chemical and Electrochemical Data on Various Fuels

FUEL	ΔG^0, kcal/mol	E_0 theor (V)	E_0 max (V)	Energy density (kWh/kg)
Hydrogen	-56.69	1.23	1.15	32.67
Methanol	-166.80	1.21	0.98	6.13
Ammonia	-80.80	1.17	0.62	5.52
Hydrazine	-143.90	1.56	1.28	5.22
Formaldehyde	-124.70	1.35	1.15	4.82
Carbon monoxide	-61.60	1.33	1.22	2.04
Formic acid	-68-20	1.48	1.14	1.72
Methane	-195.50	1.06	0.58	-
Propane	-503.20	1.08	0.65	-

It is seen from the Table 1.1 that hydrogen is the most promising fuel because of its maximum energy density and the maximum voltage that can be derived which is closer to the theoretical value. However, the use of hydrogen as fuel is always associated with the complexity in storing and handling which drive one to reflect on an alternative fuel. Electrochemists are challenged to use a fuel, which is easily transportable and easily converted into energy from the liquid state. Next to hydrogen, methanol is the favourable fuel from the aspects of cost, efficiency, availability, existence in liquid state, stability, oxidizing ability, and electrical yield per gram of fuel. Though methanol has lower energy density than hydrogen, it is attractive over other fuels which pose problems. For instance ammonia has a limitation not only in its storage and handling but also the maximum voltage that can be derived is lesser than that of either hydrogen or methanol; Hydrazine has higher theoretical cell voltage than all the other fuels, but it exhibit the problem of self decomposition leading to the

mixed potential and therefore the experimental value obtained will not be truly accounted for by the complete electrochemical combustion of the fuel. Since the other fuels such as formaldehyde, carbon monoxide and formic acid are already in their partially oxidized form, the power density derived from them will be practically lower than other fuels. The use of hydrocarbon such as methane, propane and their higher homologues required reformation to be effectively used as fuels. Carbon monoxide resulting from reforming of hydrocarbons acts as a poison for anode electrocatalysts in low temperature fuel cells, and its removal from the fuel source is a challenging task. Other potential contaminants such as sulphur containing compounds may pose further and new requirements for catalysts and their development. Methanol can be electro-oxidized at a fuel cell anode either directly or indirectly. If used indirectly, methanol is initially reformed to give hydrogen in a high temperature step. The reactor required to accomplish this, however, both lowers practical power densities and rises the inherent thermal signature of the overall power source system. As a consequence, there are strong incentives for developing fuel cells that directly oxidize methanol as a fuel in their anodic compartments (Scibioh *et al*., 2002).

It is therefore, desirable to use a fuel, which is easily transportable and easily converted into energy from the liquid state. What is needed, therefore, is the will to enter markets of fuel cell developers and manufacturers to combat the anticipated increase in energy demand.

1.2.2 Classification of Fuel Cells

Fuel cells are generally classified according to the type of electrolyte and the operating temperature (Carrette *et al.,* 2001). The most common types of fuel cells, characterized by the electrolyte are listed in Fig 1.1.

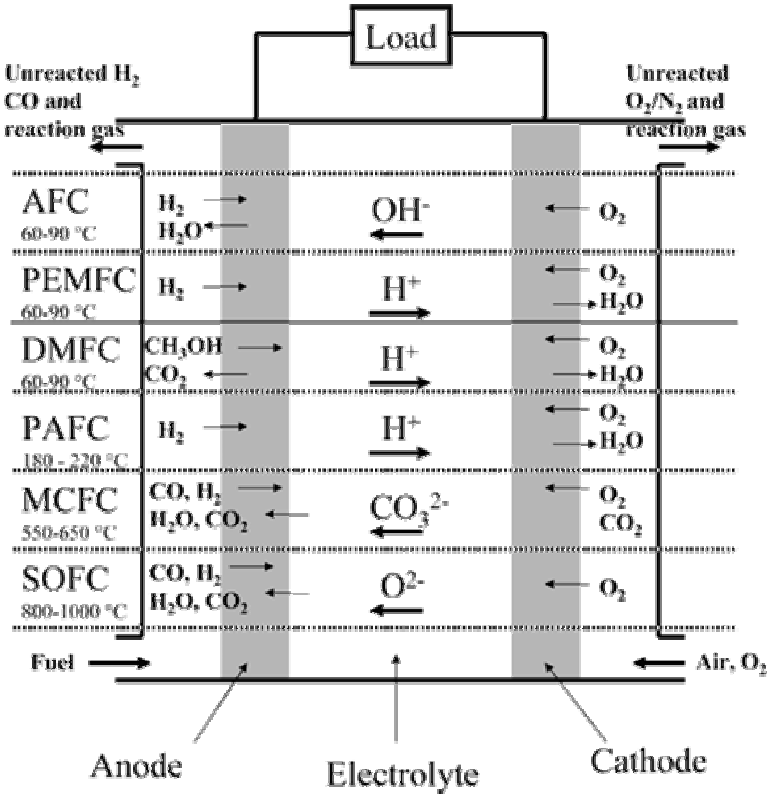

AFC : Alkaline Fuel Cells
PEMFC: Proton Exchange Membrane Fuel Cells
DMFC: Direct Methanol Fuel Cells
PAFC: Phosphoric acid Fuel Cells
MCFC: Molten Carbonate Fuel Cells
SOFC: Solid Oxide Fuel Cells

Fig. 1.1 Types of fuel cells.

1.3 DIRECT METHANOL FUEL CELLS

The direct methanol fuel cell (Fig. 1.2) is a special form of low temperature fuel cell based on PEM technology. Among many types of fuel cells, the Direct Methanol Fuel Cell (DMFC) deserves special attention due to relatively cheap, abundant, easy for handling and storage feeds (from one side methanol and from another side oxygen/air). Methanol is a favoured fuel as it is easily obtained from natural gas or renewable biomass resources. It has a high specific energy density, it is liquid at operating temperatures and most of all, the existing infrastructure for transporting

petrol may easily be transformed to support methanol. Methanol is one of the few alcohols that can be fed directly into a fuel cell and can be converted electrochemically at the anode. DMFC has potential in transport application .It works at low temperature, does not produce much heat which otherwise has to be eliminated by some cooling device, has a short start-up period, it can be easily refilled, has low polluting emission (ideally carbon dioxide and water) and as a portable power source (for example in laptops, pocket calculators, mobile phones). To be competitive at the market, the DMFC has to be able to operate at conditions close to ambient conditions and to deliver a high power density at low costs (Lamy *et al.*, 2001).

The typical design of a DMFC is shown in Fig. 1.2. It consists of an anode at which methanol is electro-oxidized to CO_2 through the reaction,

$$CH_3OH + H_2O \longrightarrow CO_2 + 6\,H^+ + 6\,e^- \quad E^0 = 0.016\ \text{V/ SHE}$$

and the cathode at which oxygen (usually as air) is reduced to form water

$$3/2\ O_2 + 6\,e^- + 6\,H^+ \longrightarrow 3\,H_2O \qquad E^0 = 1.229\ \text{V/ SHE}$$

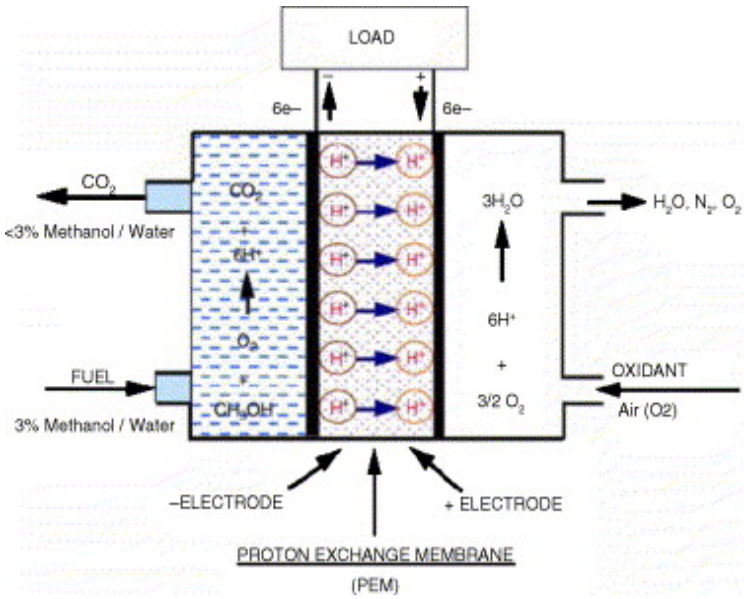

Fig. 1.2. A schematic representation of the reactions in a direct methanol fuel cell

The DMFC can be fed with a gaseous or liquid fuel feed. The liquid DMFC generally uses methanol diluted in water (typically 1 -2 M) and only a fraction of the methanol is used at the anode. It is, therefore, important to recycle the effluent and replenish it to keep the concentration in the fuel feed constant. To be able to achieve this, methanol sensors are an important part of the fuel cell system.

There are many advantages of employing methanol as the fuel (as opposed to hydrogen). Methanol is a liquid; hence its storage and transportation are less complicated. Also, methanol could be supplied through the existing gasoline infrastructure. Although hydrogen can be generated *in situ* from methanol using a reforming process, the reformer unit further complicates the fuel cell system. Also, reformed hydrogen contains significant levels of CO that poison the Pt catalyst (Arico *et al*., 2001).

The build up and operation principle of a DMFC stack equals that of an H_2-PEFC stack with the main difference that a liquid mixture of water and methanol is fed to the anode. Methanol is electrochemically oxidized at the anode resulting in the production of CO_2 and the delivery of $6H^+$ ions. This reaction proceeds with a standard reversible potential of 0.046 V. On the cathode side, oxygen reduction and the production of water take place. The theoretical overall cell potential amounts to 1.18 V, which is slightly lower than that of H_2-PEFC.

Anode: $CH_3OH + H_2O \longrightarrow CO_2 + 6\,H^+ + 6\,e^-$ $\quad E_0 = 0.046$ V

Cathode: $\frac{1}{2}\,O_2 + 2\,H^+ + 2\,e^- \longrightarrow H_2O$ $\quad E_0 = 1.23$ V

Cell Reaction: $CH_3OH + \frac{1}{2}\,O_2 \longrightarrow CO_2 + H_2O$ $\quad E_0 = 1.18$ V

Compared to the H_2-PEFC a slightly higher operating temperature of 100-120°C can be realized due to the high water content at the anode (feeding the anode with a liquid methanol/water mixture), which keeps the membrane in a well-humidified state. There is an option to use the liquid water/methanol feed stream to cool the stack, thereby making a separate cooling circle needless. However, despite the similar standard cell potential (1.18 V vs. 1.23 V) and the slightly increased temperature tremendous polarization losses ($\eta \sim 0.3$ V vs. $\eta \sim 0.05$ V for the H_2 oxidation) lead to a 0.2 to 0.4 V reduced operation voltage of a DMFC. In addition methanol shows a high diffusion rate through the state of the art polymer membranes (methanol crossover). The methanol loss on the anode side (up to 50% methanol crossover) and the decrease of the cathode potential due to the build up of a mixed potential (simultaneous oxygen reduction and methanol oxidation) are responsible for extended efficiency losses. The application of thicker membranes reduces the methanol crossover but on the other hand increases the ohmic resistance. Thin membranes with a low ohmic resistance, which still act as a methanol barrier, are subject to research.

Almost certainly, the DMFC will require platinum-based catalysts for the fuel electrode, and probably also for the air electrode (Neergat *et al*., 2002). Given the high cost of platinum, the amount of the metal must be minimized in order to match the cost of an equivalent heat engine. In addition, there is the question on the availability of platinum supplies. It has been estimated that if 50 million vehicles powered by such a device were manufactured each year, then the amount of platinum required would far exceed the current production of platinum. However, more than 95% of the platinum would be recoverable at the end of a vehicle's life (Zhao *et al*., 2007). The issue of platinum supply alone would still present some difficulties.

Nevertheless, if the catalytic problem can be solved and sufficiently small amounts of platinum can prove effective, then a substantial share of the vehicle market could be captured with all the associated benefits to the environment. Thus, DMFC as the 'philosopher's stone' for road vehicles and its successful development would greatly assist progress towards a sustainable transportation sector (Hohlein *et al*., 2000).

In spite of these advantages, why do we not see vehicles powered by DMFCs on our streets today? The answer is quite simple. The performance of the state-of-the-art cell at an acceptable cost is substantially poorer than that required for road transportation applications. Additionally, there are obvious technological advances which have been made over the last century, and particularly during the last 20 years, in the performance of its competitors, namely, internal combustion engines. Such engines in modern vehicles cost only a few tens of dollars per kilowatt, and this provides severe competition indeed (Barbir and Gomez 1996).

The major difficulties that are encountered in improving the efficiency of the DMFC can be listed as below.

- Acid electrolytes must be employed because carbonate formation is a serious problem in alkaline solution, particularly, at the current densities that are regarded as commercially desirable. The acid electrolyte causes problems of corrosion and is responsible for the slow electrode kinetics of the reduction of oxygen at the cathode.

- Similar electrocatalysts were proposed for both anode and cathode, leading to the problem of mixed potentials at both electrodes and consequently, a marked

reduction in efficiency. This is particularly difficult at the cathode, and partitioning the cell with a membrane to avoid 'chemical short circuits' will introduce a further source of inefficiency and resistance.

- The anode reaction is slow near the thermodynamic potential, with the catalysts that are currently used. A large over-potential loss is therefore encountered.
- The catalysts currently used for the anode are all based on a high platinum content.

These catalysts are easily poisoned by impurities and more seriously by the products of the anodic reaction itself.

Now a days, in fuel cell technology, especially in DMFCs, which are being considered for long as the most difficult fuel cell technology due to methanol crossover and catalytic inefficiency, steady progress has been made in various fields such as catalysis, electrolytes, electrode structure, theoretical understanding of gas diffusion and fuel cell engineering (Dohle *et al*., 2000).

1.3.1 Comparison between the H_2-PEFC and the DMFC

The schematic current-voltage curves for the half-cell reactions H_2 Oxidation, methanol oxidation and O_2 reduction is presented in Fig. 1.3. The dashed lines describe the ideal current voltage behavior if only the ohmic polarization (cell resistance) has to be taken into account and other polarization losses are entirely neglected.

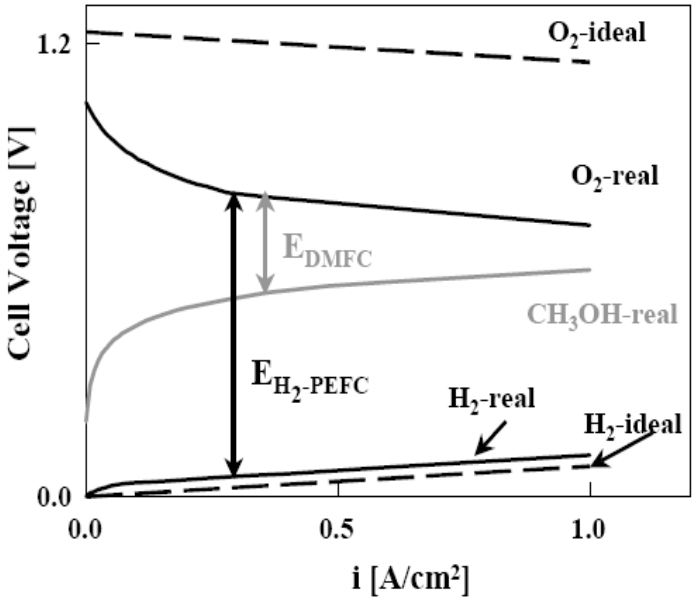

Fig. 1.3. Characteristic current-voltage curves (schematic) of a H_2-PEFC and a DMFC (Hogarth and Hards, 1996)

In the low current density region the real current-voltage behavior for the O_2 reduction and the methanol oxidation deviate noticeably from the ideal behavior. For the H_2 oxidation only a slight deviation is observed. These deviations are due to activation losses. With increasing overpotential transition to a linear current-voltage behavior is observed. In this region the current-voltage behavior is exclusively determined by ohmic losses. It is obvious that during the operation of a cell with pure hydrogen, cathodic losses are mainly responsible for the cell voltage losses whereas anodic losses are negligible (note that this is not true when using hydrogen from on-board reforming because of CO poisoning). For current densities in the range of 0.1 to 1.0 A/cm^2 cell potentials of 0.7 to 0.8 V can be realized. This results in ~ 0.4 W/cm^2 and a voltage efficiency of ~ 60% (Hogarth and Ralph, 2002)

1.3.2 Issues in DMFC

1.3.2.1 The Noble Metal Issue

In spite of many attempts in the last decade by researchers and fuel cell developers to create a non-platinum catalyst, platinum remains the catalyst of choice, since apart from its passivity in an acid electrolyte, it has demonstrated appreciable activity for the methanol electro-oxidation reaction and probably too, as a component of the air electrode catalyst. In the latter case, however, the possibilities of non-noble metal catalysts are more promising (Appleby, 1996).

Appleby (1992) has estimated that if all road vehicles in the year 2010 were powered with the better performing hydrogen–air fuel cells which use a solid polymeric acid electrolyte, then the requirement for platinum would still be about five times the total amount of the metal that has been mined to date. Of course, such vehicles would not require catalytic converters, which also contain platinum, but the amounts of platinum in such converters are one-to-two orders of magnitude less than those in fuel cells. The challenge to the developers of DMFCs is even greater, given the poorer performance of this system. However, there are quite a few advantages that are associated with fuel cell technology. First, the platinum is more than 95% recoverable at low cost and the actual cost of the platinum catalyst is only the interest on the money required to purchase the catalyst during its lifetime plus the costs of recovery of the platinum from the used catalyst (Zhao *et al*., 2007). Second, as shall be seen later, there is substantial scope for improving the performance of the methanol electrocatalyst. Third, the world vehicle population will not be replaced overnight; it will be an evolutionary process in which the appearance or non-appearance of a platinum alternative catalyst will dictate the extent to which fuel cells penetrate the

vehicle market. It is worth emphasizing the areas where improvements would be advantageous:

- The activity of the anode must be further improved by identifying a suitable catalyst for use at ambient conditions;
- The current loadings of noble metals need to be reduced. In order to reduce the usage of precious metals and thus cost, the best possible performance has to be extracted from a given amount of the catalyst. This aspect can be subdivided into catalyst preparation, pretreatment and characterization. Other issues such as catalyst support, interactions and choice of a suitable support are also involved.

It can be safely stated that neither the limited supply of platinum nor even the cost is seen to be sufficiently serious to place an embargo on the future research and development of the DMFC.

1.3.2.2 Slow electro-oxidation kinetics

Various surface intermediates are formed during methanol electro-oxidation. Methanol is mainly decomposed to CO which is then further oxidized to CO_2. Other CO like species is also formed: COH_{ads}, HCO_{ads}, $HCOO_{ads}$ (Sundmacher *et al.,* 2001). Principle by-products are formaldehyde and formic acid. Some of these intermediates are not readily oxidizable and remain strongly adsorbed on the catalyst surface. Consequently, they prevent fresh methanol molecules from adsorbing and undergoing further reaction. Thus electro-oxidation of intermediates is the rate-limiting step. The poisoning of the catalyst surface seriously slows down the oxidation reaction. Besides, a small percentage of the intermediates desorb before being oxidized to CO_2 and hence reduce fuel efficiency but undergoing in complete oxidation. Thus, a very

important challenge is to develop new electro-catalysts that inhibit the poisoning and increase the rate of the reaction. At the same time, they should have better activity toward carbon dioxide formation.

1.3.2.3 Methanol Crossover

In PEM fuel cells, one of the functions of the membrane is to stop fuel and oxygen to reach the electrode on the other side and undergo oxidation. However, in DMFC, the fuel diffuses through Nafion membrane. Due to the hydroxyl group and its hydrophilic properties, methanol interacts with the ion exchange sites and is dragged by hydronium ions in addition to diffusion as a result of concentration gradient between anode and cathode.

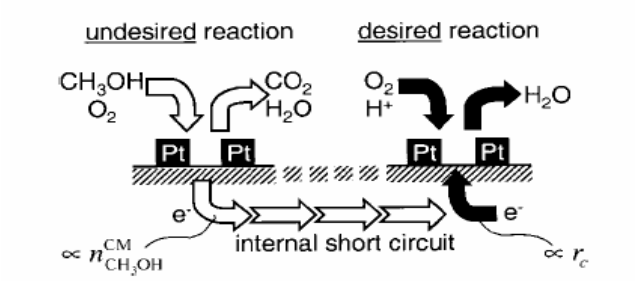

Fig. 1.4. Cathodic oxygen reduction and undesired methanol oxidation with internal short circuit created by crossover (Zhou *et al.,* 2001).

Methanol that crosses over reacts directly with oxygen at the cathode. Electrons are brought directly from the anode to the cathode along with methanol resulting in an internal short-circuiting and consequently a loss of current (Fig. 1.4). Besides, the cathode catalyst, which is pure platinum, is fouled by methanol oxidation intermediates similar to anode (Zhou *et al.,* 2001).

1.4 ELECTRO-OXIDATION OF METHANOL

The electro-oxidation of methanol is a subject of intensive research in the context of the development of the direct methanol fuel cell (Wasmus and Kuver 1999). Though the reaction proceeds faster in alkaline medium than in acidic medium, an acidic electrolyte is generally preferred for practical applications since carbonate residues are not formed in this electrolyte. The choice of the electrocatalyst material is then confined to Pt, however, which has a low activity for the methanol electro-oxidation:

$$CH_3OH + H_2O \longrightarrow CO_2 + 6\,H^+ + 6\,e^- \quad E^\circ = 0.04\ V$$

Thermodynamically this reaction is favourable (the equilibrium potential of methanol oxidation to CO_2 is close to the equilibrium potential of hydrogen reaction). In reality the overpotential of methanol oxidation is higher than that of hydrogen oxidation. The difference in kinetics of these two reactions is due to the fact that hydrogen oxidation is a simple reaction involving transfer of only two electrons, while methanol oxidation involves the transfer of six electrons and many adsorbed intermediates and side-products. Some of the reaction intermediates can irreversibly adsorb on the catalyst surface and hinder further reaction. In general, kinetics of a reaction with adsorbed intermediates and many elementary steps is greatly influenced by the catalyst (electrocatalyst). Thus, it is very important to develop an electrocatalyst which will improve the kinetics of methanol oxidation (decrease the overpotential of the reaction) and which will be resistant to poisoning.

An acidic environment is useful to reject the CO_2 produced during the electro-oxidation of methanol. Sulfuric acid solution has been the most commonly used medium.

1.5 MECHANISM OF METHANOL OXIDATION

Methanol oxidation is a complicated process; it has many steps and intermediates. The best catalyst to facilitate this oxidation process is Platinum (Hamnett, 1997). The mechanism for methanol oxidation can be viewed in terms of two basic functionalities: (a) electro-sorption of methanol onto the substrate and (b) addition of oxygen to adsorbed carbon-containing intermediates to generate CO_2, which can be alternatively facilitated by the second metal in alloy systems.

Few electrode materials are capable of adsorbing methanol; in acid medium only platinum and platinum-based catalysts show sensible activity and stability. Adsorption of methanol seems to take place through a sequence of steps. In the following general mechanism, proposed steps (1)-(4) are associated with the electrosorption process and the subsequent steps involve oxygen transfer or oxidation of surface bound intermediates. Though the mechanism of methanol oxidation almost remains same on both platinum and platinum based (Pt-M) catalysts (Watanabe and Motoo, 1975; Arico *et al.,* 1996; Wang *et al.,* 1996), the adsorption of water and further decomposition to give the oxophilic speciecs take place at a lower potential on the bimetallic surfaces (M), which leads to the easy removal of the oxidation intermediates (Steps 6b)

$$CH_3OH + Pt(s) \rightarrow Pt\text{-}CH_2OH + H^+ + e^- \quad (1.1)$$

$$Pt\text{-}CH_2OH + Pt(s) \rightarrow Pt_2\text{-}CHOH + H^+ + e^- \quad (1.2)$$

$$Pt_2\text{-}CHOH + Pt(s) \rightarrow Pt_3\text{-}COH + H^+ + e^- \quad (1.3)$$

$$Pt_3\text{-}COH \rightarrow Pt\text{-}CO + 2Pt(s) + H^+ + e^- \quad (1.4)$$

$$Pt(s) + H_2O \rightarrow Pt\text{-}OH + H^+ e^- \quad (1.5)$$

$$PtOH + Pt\text{-}CO \rightarrow 2Pt + CO_2 + H^+ e^- \quad (1.6a)$$

(or)

$$PtOH\ M\text{-}CO \rightarrow Pt\text{-}M + CO_2 + H^+ + e^- \quad (1.6b)$$

(or)

where M= Ru, Mo, Sn

$$Pt\text{-}CO + H_2O \rightarrow Pt\text{-}COOH + H^+ + e^- \quad (1.6c)$$

$$Pt\text{-}COOH \rightarrow Pt(s) + COOH^+ + e^- \quad (1.7)$$

$$Pt\text{-}CH_2OH \rightarrow Pt(s) + HCHO + H^+ + e^- \quad (1.8)$$

$$Pt_2\text{-}CHOH + Pt\text{-}OH \rightarrow HCOOH + H^+ + e^- \quad (1.9a)$$

(or)

$$Pt_2\text{-}CHOH + H_2O \rightarrow 2Pt(s) + HCOOH + 2\,H^+ + e^- \quad (1.9b)$$

$$Pt_3C\text{-}OH + Pt\text{-}OH \rightarrow 3Pt(s) + Pt\text{-}COOH + H^+ + e^- \quad (1.10)$$

$$Pt_3C\text{-}OH + H_2O \rightarrow 2Pt(s) + Pt\text{-}COOH + H^+ + e^- \quad (1.11)$$

From left to right, in Fig.1.5 shows methanol adsorption followed by methanol dehydrogenation, adsorption of blocking CO intermediate, dissociation of water and formation of OH_{ads}, reaction between CO and OH adsorbed and CO_2 evolution

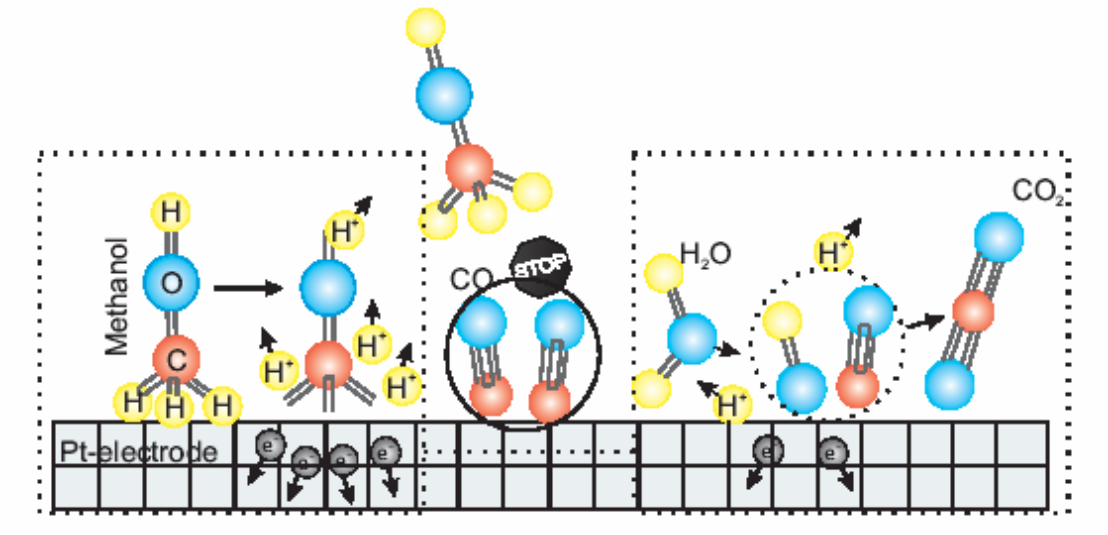

Fig. 1.5 Schematic presentation of the different reaction steps during methanol oxidation on a model catalyst surface (Vielstich 2003).

1.6 ELECTRO-CATALYSTS FOR METHANOL OXIDATION

1.6.1 Pure metal catalyst

The reported studies on bulk platinum lead to the following essential features:

a) Electrosorption of methanol is slow on bulk platinum at lower potentials, with activation energy of 35 kJ/mol.

b) Sequential proton stripping from methanol takes place, giving a series of multiply bonded intermediates that eventually convert to linearly bonded CO. Evidence for short-lived hydrogenated intermediates on platinum arises from IR, DEMS, time resolved and product studies (Wasmus and Kuver, 1999).

c) At potentials above -0.5 V/NHE, there is a steady loss of adsorbed CO from the surface of platinum and a gain of CO_2. Above 0.7 V, the surface is almost free from CO_{ads} (Sriramulu *et al.,* 1999).

d) Morphology appears to play an important role in determining the activity of platinum, with roughened platinum showing higher activity and this increased activity is associated with (i) Easier adsorption of methanol at energetically favoured sites such as steps and kinks. (ii) Formation of isolated low-coordinate platinum ad-atoms, which take place during roughening. It was also suggested that such platinum atoms may easily be oxidized as evidenced by XPS, giving rise to a Pt-O species at potentials far below than that required for planar platinum atom oxidation. (iii) A decrease in strong specific adsorption of H_2SO_4 on large planar areas of

the platinum is known to inhibit methanol adsorption (McNicol *et al.*, 1999).

e) Studies on methanol adsorption and oxidation on single-crystal surfaces of platinum show considerable sensitivity to the Miller indices of these surfaces: (i) the rate of methanol adsorption is highest on Pt (110) surface, with instantaneous potential-step measurements giving currents as high as 156 mA/cm^2 for the initial chemisorption process. (ii) the adsorption of methanol to form linearly bonded CO is most extensive on Pt (100) and surfaces with (100) terraces. (iii) Substantial multiple-bonded adsorbate is present on Pt (211) surface and this is applicable to Pt (110) in sulphuric acid electrolyte. (Parsons and Vander Noot, 1987).

f) Studies on electrochemical kinetics are associated with surface pre-treatment and control over the surface coverage of intermediates. Kinetics analyses suggest two extreme types of mechanism for methanol oxidation on platinum: one involves attack of water on CO molecules on the outside of the chemisorbed CO from the edges of the islands in a type of Reppe process, and the second involves rate-limiting migration of CO from the edges of the islands to active sites, perhaps to Pt-O, as identified by XPS. Currents are always higher on roughened platinum than on equilibrated platinum, at least for potentials below about 0.55-0.6 V/NHE. Above this potential, CO_{ads} is oxidized rapidly from the platinum surface, and FTIR studies suggests that intermediates such as Pt_3COH may be oxidized directly to CO_2 at higher potentials. This change of mechanism at higher potentials has also been detected by the presence of formyl radicals using

spin-trap EPR studies. The listing of essential feature of the studies on the bulk platinum indicates the geometry and reactivity of the active sites for methanol oxidation (Xia *et al.,* 1996).

1.6.2 On platinum particles

The oxidation of methanol on platinum particles is of technological importance than that on bulk platinum. The essential findings are:

a) Considerable controversies exist regarding the "size-effects" towards methanol oxidation (Wasmus and Kuver, 1999). Goodenough *et al.,* (1988) reported on optimal diameter of 2 nm. This size effect is a consequence of structure-demanding nature of the adsorption process. However, Watanabe (2003) do not find any evidence for size effect and commented on the earlier findings that they were flawed by failure to control the inter-particle distance.

b) Spectroelectrochemical studies such as in situ IR for Pt particles revealed a decrease in linearly bonded CO with an increase in the bridged form at higher coverages (Beden *et al.,* 1991).

c) The rate of chemisorption of methanol on Pt particles is faster than that on bulk platinum at lower potentials suggesting that methanol chemisorption is favoured on steps or at defective crystallographic sites (Christensen *et al.,* 1993).

1.6.3 Methanol Oxidation on Pt Based Alloys

1.6.3.1 Pt-Ru

The most successful binary catalyst for methanol oxidation in sulphuric acid is Pt-Ru. A proposed role for Ru in conjuction with Pt for methanol oxidation is its function in

enabling desorption of catalyst poisons from Pt surface. For optimum activity, ruthenium should be in a solid solution with Pt (Burstein *et al.,* 1997). The role of ruthenium in the mechanism of methanol oxidation is not straight forward, although the successive de-protonation of methanol through a series of adsorbed intermediates leading to intermediate (Ru) $(Pt)_2COH$, which is then oxidized to CO_2. This suggests that the optimum ratio of Pt to Ru is 2:1, assuming a uniform distribution of Ru in Pt. However, the difficulty in achieving such ideal structures probably explains the various reported optimized Pt to Ru ratios between 9:1 to 1:1.

The anodic oxidation of methanol on Pt-Ru has been studied by many groups and the results from these investigations are in good agreement. Pt-Ru catalyst form chemisorbed oxygen species at potentials (ca 0.25 V vs RHE). Thus typically there is an overpotential barrier between 0.25-3.0 V before significant oxidation currents are observed.

Recent investigations on highly dispersed Pt-Ru catalyst by stripping voltammetry of CO suggest that the surface metal alloy domains of atomic ratio Ru: Pt catalysts are key for higher DMFC anode activity (Dinh *et al.,* 2000).

The catalytic activity of Pt-Ru depends not only on maximizing the surface area and providing a surface with maximum number alloy sites of atomic ratio 1:1 but also on the presence of Ru oxides. The presence of various oxides, primarily amorphous hydrous oxides of Ru, has an inhibiting effect on surface activity, although they can play a role in terms of enhancing proton conductivity. The above conclusions were substantiated by Arico *et al.,* (2000) in which they analysed and compared the performance of commercial (E-TEK) catalyst with an in house catalyst prepared by a

colloidal method. The E-TEK catalyst contained a substantial amount of RuO_2 whilst the in house catalyst did not.

The role of hydrous ruthenium oxide as a catalyst promoter has been highlighted recently in terms of its mixed electronic and proton conductivity (Rolison *et al.,* 1999). Commercial Pt-Ru black catalysts were shown to contain a high proportion of ruthenium oxide which was essential for their high catalytic activity. The formation of anhydrous oxides of Ru has a deleterious effect on methanol oxidation. Pt-Ru catalysts are not subjected to temperatures higher than 423 K, to ensure high activity. In summary the authors conclude that a proton conducting, electrocatalytic, corrosion resistance RuO_xH_y component in Pt-Ru electrocatalysts expresses three key properties:

(a) Electronically conducting
(b) Proton conducting
(c) Is an innate good water dissociater, which is one of the mechanisms for proton movement in the material

1.6.3.2 Pt-Sn catalysts

Controversy exists as to the activity of Pt-Sn alloys for methanol oxidation. Whereas some workers report poor activity (Wang *et al.,* 1996), this is disputed by others (Wei *et al.,* 1996). This contradiction may well be due to the binary binary system not being an alloy but simply a mixture of the two metals. Additionally it is known that electrodeposited or electrosorbed Sn on Pt is a good catalysts for methanol oxidation. It has been suggested as a possible explanation as to why some apparent Pt-Sn alloys are active catalysts while others are not (Wasmus *et al.,* 1999). Furthermore, Sn may leach from the catalysts under acidic conditions and be re-adsorbed electrochemically

at Pt sites producing a Sn modified Pt surface suitable for methanol oxidation. This is undesirable for DMFCs in long-term use due to inevitable variations in performance and possible migration of ionic tin into the electrolyte membrane and possibly to the cathode surface.

Shukla *et al.,* (1999) used X-ray photoelectron spectroscopy (XPS) to study the effect of Sn and Ru additions to platinised carbons in order to elucidate differences in mechanistic behaviour. They argued that, Sn produced a modification in the electronic environment around Pt-sites (through a charge transfer in the Pt-Sn alloy), Ru-sites in Pt-Ru alloys promoted the formation of lattice bonded oxygenated species in the vicinity of methanolic residues adsorbed on Pt-sites. XPS showed the presence of stongly bonded oxygen species on Sn sites in the Pt-Sn system, which would limit the oxidation of methanol to CO_2 in relation to labile-bonded oxygen. The work confirmed the observation that Pt-Sn catalyst is excellent for methanol oxidation at low potentials (Markovic *et al.,* 1997), but that at higher potentials Pt-Ru catalysts were more effective, when labile bonded oxygen would be present on the surface.

Abdul-Rahim (2000) prepared Pt-Sn catalysts by electrodepositing Sn onto Pt substrates and found that the surface concentration of Sn was a defining factor in the activity of the catalysts produced. In addition it was shown that repeated potential cycling from the potential for oxygen evolution to that for hydrogen evolution enhanced the activity. Such cycling was found to have only a minimal effect on the catalyst stability.

In addition to binary Pt-Sn catalysts, ternary and quaternary, including Ru and W (Arico *et al.,* 1999; Arico *et al.,* 1996) catalysts have been prepared and appear promising.

1.6.4 Catalyst Promoters for methanol oxidation

The promotion of Pt by a range of metals (and oxides) to enhance methanol oxidation is well known. The species that have had a reported positive effect on methanol oxidation are summarized in Table 1.2. Of the catalyst promoters considered, significant recent activity was focused on the use of Ru, Sn and W with Pt.

Table 1.2. Effect of catalyst promoters on methanol oxidation

Promotion by	Catalyst promoter	Comment
Alloying and dissolution to produce highly reticulated surfaces	Cr, Fe, Sn	Typically less than 100 mV lower potential than Pt.
Surface adatoms	Sn, Bi	
Alloys	Ru, Sn, Mo,Os, Ir,Ti,Re	Ru has the best effect. Sn, Mo, Os and Re are substantial promoters.
Metal oxides	Ru	Hydrous Ru oxide is the most active catalyst.
Base Metal oxides	W, Ti, Nb, Zr, Ta	W oxide is a notable promoter. Small effect for other metal oxides

Though metals like Bi, Pb, Mo, Sb, In and their oxides or alloys enhance the activity of Pt for methanol oxidation, they dissolve in acid medium during the course of the reaction.

1.6.5 Metal Carbides

Base electrocatalysts have been suggested earlier for methanol electro-oxidation. Electrocatalyst made from base materials must be able to resist corrosive action of the acid electrolytes. Since base metallic materials are themselves thermodynamically

unstable in acid medium. Requirement for any base electro-catalyst is that it is passive towards corrosion. Tungsten carbide has been regarded as promising catalyst that can replace noble metals for the anodic oxidation of methanol (Kudo *et al.,* 1983; Okamoto *et al.,* 1987). The catalytic activity exhibited by the tungsten carbide is almost comparable to that of the noble metal platinum (Kudo *et al.,* 1985).It was reported that such a catalytic activity results from closer similarity in the electronic structure between WC and platinum. The electro-catalytic activity of WC and tungsten based double carbides (W, M) C (where M = V, Cr, Mn, Ni and Mo) was investigated mainly with the focus on methanol oxidation in sulphuric acid (Kawamura *et al.,* 1987). Only Mo containing carbide is found to be able to promote methanol oxidation activity. The magnitude of the over potential required to drive methanol oxidation reaction on the carbide surface is -0.3 V, which is almost comparable to that observed on platinum. However, carbide catalysts were prepared by chemical vapor deposition method (CVD) using tungsten and molybdenum carbonyls, which is rather expensive. Later, (W, Mo) carbide active powder have been made using lyophilized ammounium salt of tungstic and molybdic acid, which was turned into oxide powder by treatment at 973 K in air, followed by carburizing with CO gas. To activate the carbide further, alkaline activation treatment was given to (W, Mo) C. (W, Mo) C has been shown to exhibit some electrocatalytic activity for methanol oxidation (Burstein *et al.,* 1996; Machida and Enyo, 1990) in acidic medium. In order to develop a cheaper preparation method for the production of tungsten carbide powder catalysts, Burstein (1997) synthesized the tungsten carbide by reducing the oxide powder in the flow of methane and hydrogen at 1096 K. But it shows no significant activity for the methanol oxidation. Moreover, the material exhibits significant passivity towards corrosion, suggesting the requirement for

specific surface composition and geometry in order to achieve electrocatalytic activity for methanol oxidation. The carburized Ni/W (Burstein *et al.,* 1997), prepared by mixing equimolar proportions of nickel nitrate and sodium tungstate; after drying, the tungstate was reduced in a methane/hydrogen atmosphere at 1096 K, was studied for electrochemical oxidation of methanol in sulphuric acid medium.

This material showed very low corrosion rate in acid and exhibits significant activity for methanol oxidation upto a potential of -0.6 V vs SHE, after which the transpassivation of the state occurred and the corrosion current increased. The oxidation is enhanced in the transpassive region. Though, the methanol oxidation is taking place, but it takes place at high potentials, which is of little interest in the fuel cells. The Co was also tried in place of Ni, but significant activity was not observed for the methanol oxidation in sulphuric acid. The carburized Ni/W and Ru/W were compared for the methanol oxidation, it was found that Ni based catalysts showed a minimal potential of 0.3 V (SHE) for methanol oxidation was observed at 2.5 mA/cm^2, whereas for the Ru based catalysts, the minimal potentials of 0.7 V (SHE) for methanol oxidation was observed at 2.5 mA/cm^2. These electrodes are found to exhibit irreproducibility and scatter from one electrode to another, the potential at which methanol oxidation occurs at a rate comparable between these two catalysts, is higher for Ru based electrode: it is an inferior catalyst. Though, the carbides exhibit measurable activity for methanol oxidation, comparable to that of platinum, the synthesis of the electrode material is expensive thus limiting immediate implementation.

1.7 EFFECT OF THE ELECTROLYTE ON METHANOL OXIDATION

The performance of a catalyst vary with the nature of the electrolyte due to difference in the ionic conductivity, the degree of adsorption of acid radicals on the catalyst surface and the influence of corrosion on stability. In general, high acid concentrations tend to reduce the activity of Pt catalysts, especially above 5 M. Phosphoric acid at high concentrations (> 5 M) has been shown to facilitate better activity to methanol oxidation than sulphuric acid at the same concentration (Andrew *et al.,* 1977); however the best electrolyte at low temperatures (333 K) has been shown to be 3 M sulphuric acid. The oxidation of methanol at high temperatures (eg 473 K) in phosphoric acid (>96%) on Pt and Pt alloy catalysts (with Sn, Ru, Ti) has been shown to be reasonably fast. This research may have relevance to the use of alternative PEM systems, eg phosphoric acid doped Polybenzimidazole. Cyclic voltammetric study of methanol oxidation in phosphoric acid has been conducted to determine the preferred composition of solution of chloroplatinic acid and ruthenium chloride for the preparation of Pt-Ru catalysts (Lee *et al.,* 2000) Trifluoromethane sulphuric acid (TFMSA) has been examined as an alternative acid for methanol oxidation but no conclusive evidence exists for superior performance and controversially, poisoning of the catalysts is reported from sulphur (Hughes *et al.,* 1977; Adams *et al.,* 1980).

It has been reported that the addition of silicotungstic acid ($H_4SiW_{12}O_{38}$) in low concentration (10 mmol dm^{-3}) to sulphuric acid accelerates the reaction rate by up to 100 % for methanol oxidation on Pt-Ru catalysts (Burnstein *et al.,* 1997). This result has relevance to the work on the investigations on alternative membranes for reduced crossover of methanol.

There are reports of methanol oxidation at higher pH using carbonate and bicarbonate electrolytes and potassium or sodium hydroxide. For the former electrolytes, no advantage has been gained in terms of improved activity over sulphuric acid. In the case of caustic sodium or potassium hydroxide electrolyte, although attractive in terms of achievable current densities, the issue of carbonation of the electrolyte is a practical problem of greater significance.

There is a considerable amount of literature on the oxidation of methanol in the alkaline electrolytes (see reviews by Mc Nichol *et al.,* 1999 and Wasmus *et al.,* 1999). Methanol oxidation in alkaline electrolytes has been investigated by several research groups, using for example Pt (Triopkovic *et al.,* 1998; Drazic *et al.,* 1999), Pd (Prabhuram and Manoharan 1998), nickel hydroxide (Kowal *et al.,* 1997) and chemically modified nickel (Ciszewski and Milczarek, 1996). The oxidation of methanol in alkaline solutions is not particularly structure sensitive. The chemisorption bonding of (CHO) on Pt is weak and oxidation takes place easily without irreversibly blocking the catalyst sites. A report on methanol oxidation in alkaline solution (on unsupported Pt powder) has shown impressive polarization characteristics in comparison to those obtained in acid solution (Prabhuram and Manoharan, 1998). In alkaline solution, current densities for methanol oxidation (at fixed potentials) were atleast an order of magnitude greater than those in acidic electrolytes.

1.8 ROLE OF PREPARATION METHOD

Nanoparticles are key components in the advancement of future energy technologies. Thus strategies for preparing nanoparticles in large volume by techniques that are cost-effective are required. Catalytic activities depend critically on their size-

dependent properties. Nanoparticles are further indispensable as electrocatalysts in fuel cells and other electrochemical converters. The desire to increase the activity per unit area and decrease the necessary amount of the expensive catalytic standard, platinum, have spurred innovative approaches for the synthesis of platinum-alloy nanoparticles by wet chemistry, colloidal routes, and microemulsion methods. (Devarajan and Sampath, 2004; Raimondi *et al.,* 2005)

1.8.1 Impregnation method

Impregnation means soaking up of a dissolved metal precursor, *e.g.* $PtCl_6^{-2}$, into the pores of a support, *e.g.* Vulcan XC 72 carbon, before reduction of the metal precursor to metal nanoparticles. Impregnation occurs by capillary action. The procedure is shown schematically in the top flow line of Fig.1.6. This method is simple and has been the most common method used for electrocatalyst preparation over the years. The reduction step can be chemical or electrochemical. The common reducing agents are hydrazine, borohydride, formic acid, and hydrogen. In the case of hydrogen, temperature elevation to above 573 K under an inert atmosphere is required. Control of the size and size distribution of particles depend on many factors. The morphology of the porous substrate and the pore size distribution will play a major role in terms of penetration and wetting of the precursor and also providing the confinement for nanoparticle growth. Reaction time, kinetics and mass-transfer of reducing agent will also affect the nucleation and growth of the nanoparticles. The major drawback of the impregnation method is the lack of size control of metal particles except when the porous substrate has a narrow pore size distribution in highly ordered mesoporous carbon (Joo *et al.,* 2001). A distribution of particle sizes from nanometer to micron scale is commonly observed. Hydrogen can penetrate better into the micropores of the

porous matrix. Using the electrochemical method for the reduction step, the reaction time and hence the growth of the particle can be controlled by the amount of current passed (Zoval *et al.,* 1998). The electrochemical reduction method, however, also depends on the connectivity and uniformity of the current conduction network of the porous matrix and the nucleation and growth processes are restricted to the charged interface without three-dimensional homogeneity.

1.8.2 Colloidal method

The colloidal method, widely used for synthesizing metal nanoparticles with size control, has been reviewed (Bonnemann and Richards 2001, Roucoux *et al.,* 2002). The procedure is shown schematically in the second flow line of Fig. 1.6. In the presence of a protective agent, such as surfactant molecules, the metal precursor is chemically reduced or reacted to form metal nanoparticles. A narrow size distribution is achieved as the colloidal metal nanoparticles are stabilized either by steric hindrance or by electrostatic charges. Colloidal metals can form in the organic medium (organosols) or aqueous medium (hydrosols). In the case of adsorbed ions or charged colloids, protection from merging into larger particles is provided by the electrostatic repulsion of like charges. On the other hand, steric stabilization can be provided by coating the metal core with organic chain molecules. Examples of common protecting ligands include NR_4^+, PPh_3, PVP, and PVA.

Though the colloidal method can provide a narrow size distribution of metal nanoparticles, the major drawback is the presence of the protecting agent, which may also hinder the catalytic function of the nanoparticles. The organic protecting shell can be removed by washing with an appropriate solvent or by decomposition at elevated temperature in an inert atmosphere. Before the removal of the protecting agent,

adsorption into a protecting microporous catalyst support is necessary to prevent agglomeration into larger metal particles.

It would be preferable to use the alternative route of preparing colloidal nanometals without the use of protecting agents. This can be achieved for certain metals by appropriate combination of precursor, solvents, reducing agent and electrolyte. In the recent work of (Wang *et al.,* 2000) the use of sodium hydroxide dissolved in ethylene glycol as solvent appears to be suitable for the preparation of a number of metal nanoparticles, especially for platinum, without the use of a protecting agent. The procedure is illustrated in the third process line of Fig. 1.6. The electrocatalytic performance of supported platinum nanoparticles prepared by this method has been reported recently (Zhou *et al.,* 2003). Dissolution or precipitation of the colloidal metal nanoparticles requires careful control of process parameters, *e.g.* pH and water concentration. The colloidal metal nanoparticles may be protected by glycol, which serves as both a solvent and the protecting agent. The glycol can be removed by electro-oxidation during usage as an anode. The glycol colloidal process is attractive for large-scale synthesis of metal nanoparticles.

1.8.3 Microemulsion method

The microemulsion method is illustrated as the bottom process of Fig. 1.6. This method may offer unique flexibility in the simultaneous control of size and composition of mixed metal nanoparticles. The chemical reaction is confined within a microemulsion, which is a tiny drop of precursor containing liquid engulfed by surfactant molecules. The microemulsion is uniformly dispersed in a continuous liquid phase, which is immiscible to the precursor containing liquid phase. The size of

the microemulsion is of the order of a few nanometers to hundreds of nanometers and is determined by the balance of surface free energy mediated by the surfactant molecules and the free energy difference arising from the immiscibility of the two liquid phases. Normally, the dispersed liquid phase is oil and water forms the continuous medium. The reverse microemulsion is the water-in-oil microemulsion. A co-surfactant is sometimes added to modify the size of the microemulsion. Supercritical carbon dioxide has also been used as the continuous medium for the microemulsion method and gives additional ease in separation of the nanoparticle from the medium. Since chemical steps are conducted within the microemulsion, which serves as a micro- or nano-scale reactor, a narrow particle size distribution can be obtained accordingly. The introduction of a reducing agent, *e.g.* hydrazine, into the miroemulsion is achieved by stirring and the reaction time is in the order of minutes. The size and distribution of the nanoparticle can be further controlled and improved by a two-microemulsion method with the reducing agent also confined in a separate emulsion (Bommarius *et al.,* 1990, Wang *et al.,* 1997). The two-microemulsion technique has been applied to synthesize mixed metal nanoparticles of Pt–Co and Pt–Ru (Zhang and Chan, 2003). The final composition of the mixed metal nanoparticles can be easily controlled by the ratio of the metal precursor solutions.

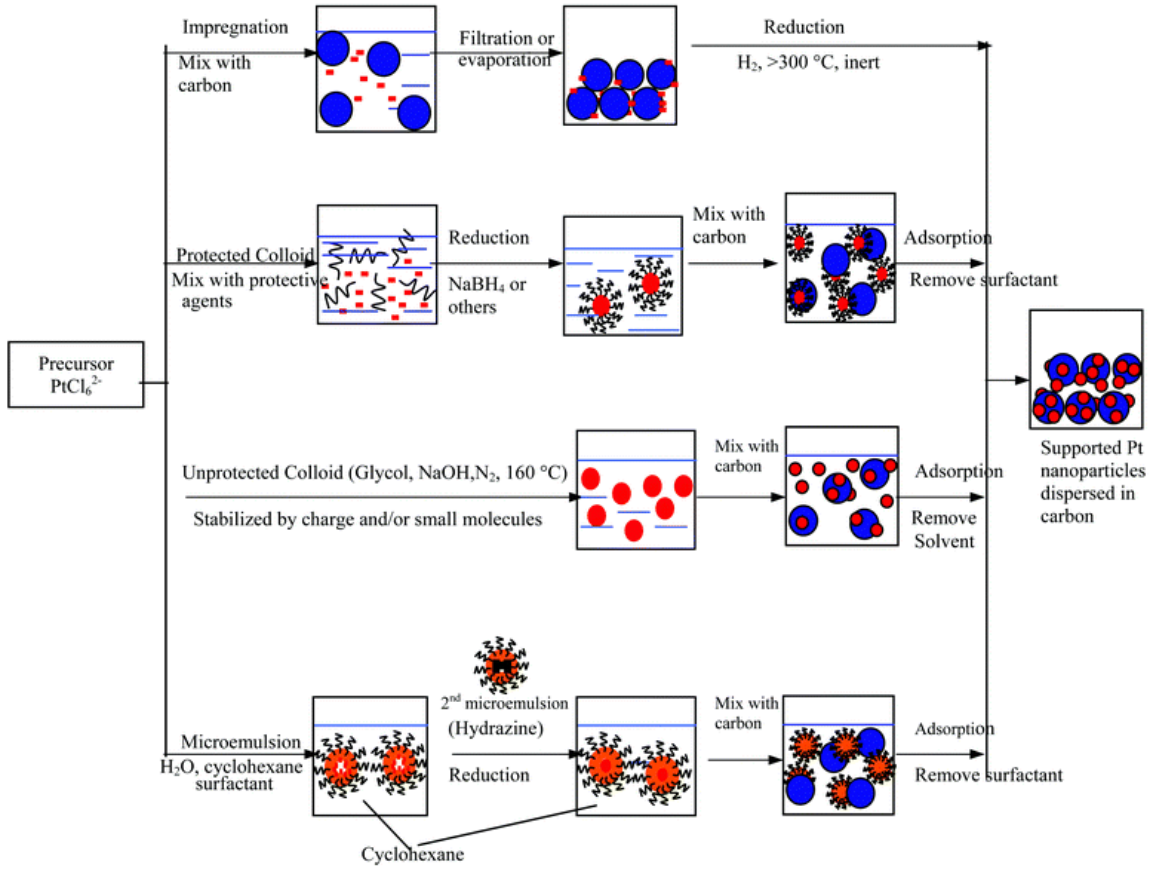

Fig. 1.6 Chemical methods to synthesize supported platinum nanoparticles with different size control methodologies. (Chan *et al.,* 2003)

Weight to oil microemulsion method offers good composition and size control. Unprotected colloidal method could be a low cost alternative.

1.9 PARTICLE SIZE EFFECT

The role of particle size on the electrochemical behaviour of supported metal particles has been extensively discussed in literature as mentioned earlier. No definite conclusions have been drawn on the influence of particle size towards the performance of carbon supported Pt for methanol oxidation. Frelink *et al.*,(1995) have carried out a systematic study on the oxidation of methanol at Pt/C catalysts with different particle sizes. Carbon black (Vulcan XC-72) with the specific surface area (BET) of 240 m^2/g was used as support. The catalysts were obtained by different

methods of preparation such as ion-exchange, impregnation, colloidal and impregnated-sintered catalysts. The particle size ranges between 1.2 and 10 nm. The specific activity was found to decrease with decrease in the particle size in the range 4.5 to 1.2 nm. The dependence of the activity on the particle size was explained in terms of its effect on adsorbed hydroxyl species or the number of the methanol adsorption sites.

1.10 ON SUPPORTED METAL PARTICLES

Dispersed micro/nano particles of noble metals supported on high surface area materials are of considerable interest to catalysis. This is in part due to their unique physical and chemical properties (Watanabe *et al.,* 1987 and Shukla *et al.,* 1994). The primary function of the support is to separate the individual particles physically in order to diminish the rate of agglomeration (Stoyanavo *et al.,* 1999). The physical properties of nanoparticles depend strongly on the perturbations that arise from large fraction of metal atoms residing at the particle surface and may show a marked difference from those characterizing the bulk solid state. Support plays a major role in determining the mechanical and thermal stability of the particles while helping them in highly dispersed state (Attwood *et al.,* 1980).

The choice of a suitable support is a factor, which affects the performance of supported catalysts. Interactions between the catalysts and the support have been identified to modify the intrinsic catalytic activity. In studies of methanol oxidation, supports so far employed for dispersing active metal particulates are carbon and conducting polymers. For instance, in case of carbon supports, nature of functional groups *i.e.,* lowers concentration of acid/base groups and carbons with sulfur and nitrogen-based functionalities have shown enhanced catalytic activity. However, till

today, to the best of our knowledge there is no report available which precisely deals with molecular level interactions that are taking place between the conducting polymer support and supported metal particles. Despite the extensive efforts of research to date, such an understanding is yet to evolve.

1.11 CATALYST SUPPORT

The support for the metal nanoparticles turns out to be as important as the nanoparticles for providing their dispersion and stability. The need for electrical conductivity has ruled out conventional catalyst supports such as molecular sieves and alumina. Electron transfer kinetics is known to largely depend on electrode materials and their surface properties. Such investigations are both fundamentally interesting and practically useful. Studies on electron transfer are particularly important for carbon based materials because those materials, such as GC, graphite, fullerene and diamond, with different electronic and structural properties, have been proved to possess distinctly different electrochemical properties from each other (Ramesh and Sampath, 2003).

Except for fundamental studies, low surface area single crystal metals and graphite are undesirable as support materials. In addition to electrical conductivity and surface area, hydrophobicity, morphology, porosity, corrosion resistance is also important factors in chosing a good catalyst support. Based on these considerations, carbon is the best catalyst support material for low temperature fuel cells. Carbon black and activated carbons have been extensively used as catalyst supports, with Vulcan XC-72 being the most representative. The most common supported catalyst is platinum supported on high surface area carbon and is used in both the cathode and anode (Dicks, 2006). In the last decade, a number of new catalyst supports with various

mesostructures and nanostructures have been reported. These include carbon nanotubes, metal oxide nanotubes and conducting polymer nanotubes with or without a high degree of order (Park and sung, 2006). However, in the following section it will be shown that the supporting material can influence the catalytic activity of fuel cell electrodes.

1.12 CARBON AS CATALYST SUPPORT

The use of carbon as catalyst support is continuously growing and there are number of reports available (Auer *et al.,* 1998) is an attempt to relate metal dispersion with the properties of the support. The main reasons are:

1. Carbon has sufficient electronic conductivity and chemical stability under fuel cell operating conditions.

2. Surface area of noble metal catalysts is greatly increased by using carbon support.

3. Primary function of the support to diminish rate of agglomeration of the metal particles in operation, and improve the stability of electrocatalyst.

4. Surface functional groups of the carbon support have a pronounced effect on the dispersion of the catalysts.

5. It is relatively easy to get uniform and highly dispersed catalyst even when catalyst loading is more than 30 wt % (to obtain better PEM fuel cell reactions, higher loading catalysts are expected).

6. The activity of electro-catalysts have been improved through the interaction between metal and support

7. Carbon supported catalysts are more stable than non-supported catalysts in relation to catalysts agglomeration under fuel cell operating conditions.

It is important to optimize carbon support and metal loading in order to obtain sufficient reaction in the catalyst layer. The structure of the carbon support in the catalyst layer can directly affect the platinum utilization, as well as degradation mechanisms that lead to decreased performance. Currently used supports, that are commercially available, include Vulcan XC-72, Black Pearls BP 2000, and Ketjen Black. All of these supports are carbon blacks with high degrees of graphitic character. These supports provide high electronic conductivity, uniform catalyst dispersion, corrosion resistance, and sufficient access of gas reactants to the catalyst (Ismagilov, 2005).

1.12.1 ROLE OF CARBON FUNCTIONALITY

The physiochemical properties of carbon are strongly influenced by the presence of chemical species on the surface. In addition, the surface structure of the carbon affects its physiochemical properties because the reactivity of carbon atoms with unsatisfied valences on edge sites is greater than that of carbon atoms in the basal planes. Consequently, the chemical properties of carbon vary with the relative fraction of edge sites and basal –plane sites on the surface. Because carbon blacks have a high surface to volume ratio, chemical species are readily adsorbed on the surface and they have a major impact on the chemical properties on the carbon black. Numerous reviews are available on this topic (Donnet, 1968, 1982). It is known that surface groups have a pronounced effect on the formation of the dispersed metal phase of supported catalyst. The surface of carbon black support is composed of graphene layers. Functional groups, which are predominantly oxygen, nitrogen or sulphur

based, are located at the edges of the graphene planes, or are present as heteroatom functionalities within the planes. The design of supported catalysts, such as Pt/C, is advanced by information concerning metal-support interactions between surface carbon functional groups and the particulate metal. Considerable amount of literature is centered on the metal-support interaction between carbon functionality and particulate Pt and the influence it on particle size and dispersion. The chemical nature of oxygen groups of carbon was the subject of many investigations. In order to study the effect of carbon surface functional groups have on fuel cell Performance, Jia *et al.,* (2001) explored the effect of increasing the hydrophilicity of the carbon support. Supported catalysts treated with nitric acid were shown to outperform untreated catalysts. This was attributed to increased proton conductivity of the catalyst layer, most likely due to the formation of surface carboxylic acid groups.

Roy *et al.,* (1997) found that carbon blacks with nitrogen, sulphur and phosphorus functionalities initiate the formation of particulate Pt with reduced dimensions relative to untreated carbon blacks. The size decrease was attributed to strong binding between the Pt particles and carbon support during the preparation of catalyst process. For untreated, N- and S-functionalized carbons the mean potential of methanol oxidation was reported to be 604, 554 and 633 mV, respectively at +50 mA/cm^2, and the corresponding Pt particle size was 2.5, 1.5 and 1.0 nm (O > N > S/P) (at all electrodes Pt content = 0.7 mg/cm^2). Electrocatalysts prepared with nitrogen-functionalized carbon showed the highest activity towards methanol oxidation. The sulphur-functionalized electrode showed the lowest activity towards methanol, suggesting the existence of a specific interaction between Pt and sulphur on the carbon support, which inhibited the rate of the reaction. Nitrogen-functionalization was accompanied by an increase in basicity of the carbon support, while sulphur

functionalization resulted in increase in acidity. XANES technique was employed to identify the specific types of carbon functionality, which interact with Pt. In the case of nitrogen-functionalized support support pyridinic and pyrolic groups were present, while in sulfur functionalized support aromatic S-H functionality and inorganic sulphate species were present. The nitrogen functionality in the carbon support determines the size of Pt by bonding with the lone pair of electrons at the nitrogen site in a sp^2 hybridized orbital in the plane of the ring. These N–sites, which predominate in untreated carbon black, were less negative than oxygen sites. The assumption was that during catalytic action, Pt might bind more strongly to pyridinic sites, thereby preventing Pt particles from sintering to the extent observed on untreated carbons. The increased electron donation from pyridinic nitrogen-functionality to Pt might be responsible for the enhancement in the kinetics of methanol oxidation sites. There was no poisoning effect from the sulphate, which is present in untreated carbon, but sulphur-functionalized carbon where poisoning was observed is attributed to the organic-type sulphur generated from P_4S_{10} residual phosphorous.

Vulcanized carbon (VC) is a standard catalyst support despite of its innate sulphate content because of its favourable electrochemical properties. Organically bound sulphur native to VC has both, advantageous and disadvantageous effects on the catalytic activity of Pt. Sulphur hetereo atoms improve the dispersion and surface area of Pt catalysts supported on carbon by serving as nucleation sites or anchors for Pt clusters. Swider and Rolison (1996) probed the interaction between nanoscale Pt and the sulphur in vulcanized carbon (XC-72). Adsorption of sulphur on the surface of Pt changes its surface energy, including both, adverse and favourable effects.

A systematic study of the effect of the chemical nature of the carbon support on the characteristics of the final catalysts is essential.

1. 13. ELECTRO-CATALYSTS SUPPORTED ON CARBON AEROGELS

Extensive research has been conducted on dispersing the catalyst on carbon supports to increase the efficiency of use and lower the loading of catalyst. Carbon particles are prone to self-agglomeration thus blocking the approach of reactants to active site and limiting the overall activity. Of the limited research centered on supported catalysts within an aerogel structure, the predominate literature is centered on incorporating Pt into a form of carbonized aerogel.

Anderson *et al*., (2002) suggests overcoming the agglomeration tendencies of carbon by immobilizing the carbon-supported catalyst in a silica aerogel network (see Fig.1.7). The Pt_{coll}/C was added to silica *prior* to the gel point so that formation of the 3-dimensional silica network would act as a binding agent. The final product was a conductive, mesoporous structure with carbon black as the electron-conducting support. Average Pt particles sizes for the technique were 3 nm and the optimal reported particle size in a H_2/O_2 fuel cell is ca. 3 nm (Kinoshita 1990). The Pt_{coll}/C-SiO_2 catalyst tested yielded lower CO stripping potentials and a higher surface Pt to total Pt ratio than Pt_{coll}/C (w/o aerogel) and Pt/C (E-TEK). More importantly, the aerogel catalysts prepared had the highest current per mass loading of Pt than other Pt/C systems, under methanol oxidation conditions (Fig. 1.8).

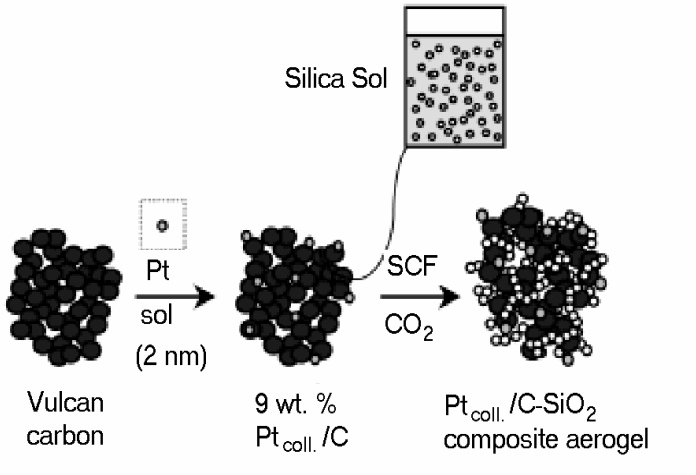

Fig. 1.7. Synthesis proposed for $Pt_{coll.}$/C-SiO_2 aerogels (Anderson *et al.*, 2002)

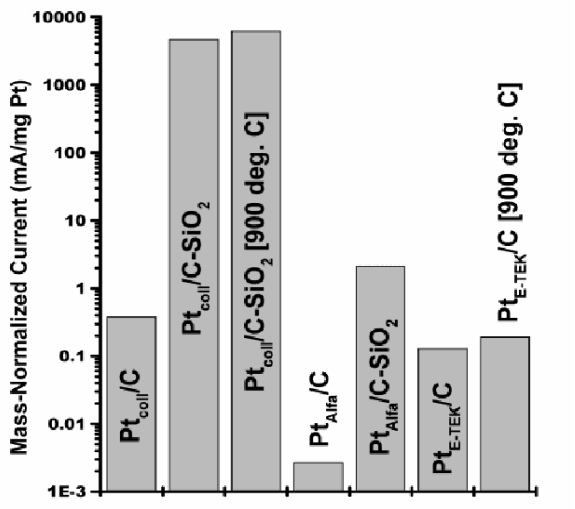

Fig.1.8. Electrocatalytic activity towards methanol oxidation. Currents measured at 300 s after chronoamperometric step to 360 mV vs. SHE and values were mass normalized (Anderson *et al.*, 2002)

1.14 NANOSTRUCTURED CARBONS AS CATALYST SUPPORT

Decreasing the amount of precious metal in the electrode catalysts is a major challenge in the development of fuel cells. Such a reduction in the amount of metal catalyst in most cases can be achieved by increasing the active area of platinum that is actually utilized on an electrode surface. One way to achieve this

is by using high surface area carbon supports, which generally enable higher utilization of the metal catalyst (Kamat, 2006).

CNT and GNF can also be used efficiently as supports for metals in fuel cell electrodes in order to replace the classically used carbon blacks. In comparison with the most widely used Vulcan XC-72R carbon support which has an electronic conductivity of 4.0 S cm^{-1} and specific surface area of 237 m^2 g^{-1}. CNT and CNF have significantly higher electronic conductivities of 104 and 103–104 S cm^{-1}, respectively (Thess *et al.,* 1996; Rodriguez; 1993) and extremely high specic surface areas of 200–900 m^2 g^{-1} (Serp *et al.,* 2003). Furthermore, Vulcan XC-72R has a large ratio of micropores, which are smaller than 2 nm, while CNT and CNF have no micropores smaller than 2 nm (Li *et al.,* 2003).

For Vulcan XC-72R support, the Pt nanoparticles may sink into the micropores, which will reduce the number of three-phase boundary reactive sites, thus reducing the Pt utilization (Thompson *et al.,* 2001; Matsumoto *et al.,* 2004). The unique surface structures and excellent mechanical and thermal properties of CNT/CNF, as well as their high electric conductivity and surface area are expected to offer great potential for catalyst supports (Rodriguez *et al.,* 1996). However, since CNT and CNF are relatively inert, it is necessary to modify the nature and concentration of surface functional groups in order to deposit Pt particles on their surface (Chen *et al.,* 2006; Kim and Mitani, 2006). Therefore their pretreatment process and Pt deposition methods could affect the Pt catalyst dispersion and catalytic activity for fuel cell reactions. Various methods have been reported on the synthesis of Pt/CNT and Pt/CNF catalysts. The synthesis methods, which are critical for Pt/CNT and Pt/CNF catalyst preparation, should play a vital role in Pt utilization.

1.14.1 Carbon nanofibers support

Carbon nanofibers are successfully used as catalyst support in direct methanol fuel cells, where they could improve oxidation activities of the catalyst in comparison to Vulcan carbon as catalyst support or unsupported catalyst. CNFs are also used as platinum catalyst support in PEFCs, effecting a high activity for methanol oxidation and oxygen reduction (Tang *et al.,* 2004; Maldonado *et al.,* 2004; Steigerwalt *et al.,* 2001). Research by Ismagilov *et al.,* (2005) suggested the use of CNF to combat the sintering that the basal graphitic planes of other carbon supports induce, and to provide a stronger interaction between the platinum and support. In CNF, the edges of the graphitic plates form the outer surface of the support. The edges could support the platinum so that it would form smaller particles and maintain a more uniform distribution of the platinum dispersion. There are three different kinds of CNF: one with graphene planes arranged perpendicular to the filament axis (known as the deck of cards type), one with the graphene planes at an angle of 45 ° to the filament axis (known as the fishbone type), and one with the planes parallel to the filament axis (known as the parallel type). These three types of fibers are illustrated in Fig 1.9.

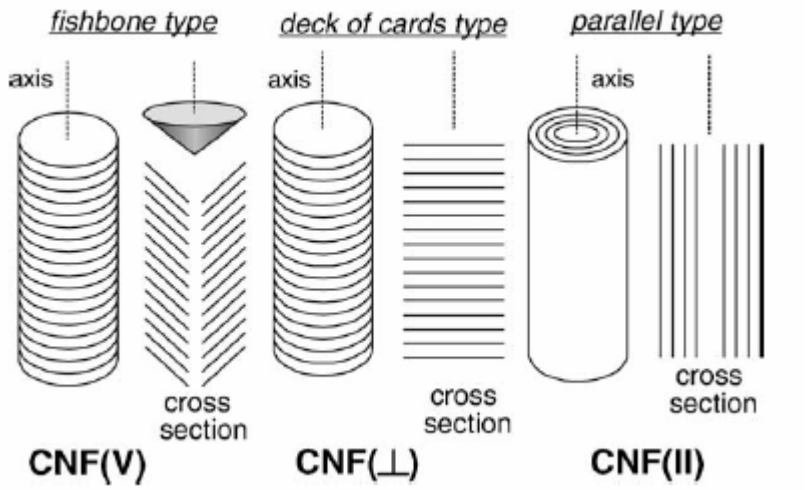

Fig. 1.9 This figure illustrates the configuration of the graphene plates with respect to the central axis of the three different types of carbon nanofibers. (De Jong and Geus 2000)

The edges of the graphene plates would theoretically produce smaller platinum particles more uniformly distributed around the support. Bessel *et al.,* (2001) have reported a 400 % higher activity for methanol oxidation of Pt supported on graphite nanofibers compared to the activity of Pt supported on Vulcan XC-72 carbon, and it is interesting that the self-poisoning also decreases by 48 %. It has been proposed that the physiochemical environment of Pt and the structure of the graphite nanofibers might play a predominant role in the higher activity and stability that were observed. But the oxidation mechanism is still to be probed

1.14.2 Carbon nanotubes

Carbon nanotubes (CNTs) are unique materials, with interesting mechanical and electronic properties. Due to their closed topology and tubular structure, they find a number of applications in nanoelectronic devices, for storage of hydrogen and other gases and as a catalyst support. Martin *et al.,* (1994) explored template-synthesis method for the preparation of micro- and nano-structured materials with cylindrical pores of uniform diameter. Kyotani *et al.,* (1997) used a combination of chemical vapour deposition (CVD) and template-synthesis methods to synthesize carbon nanotubes with highly aligned ensembles of uniform hollow tubes (20–200 nm) with open ends, which make them suitable for filling with desired materials. Che *et al*., (1998) used metal (electrocatalytic materials such as Pt, Ru and Pt/Ru) filled carbon nanotubes for the study of electro-oxidation of methanol. Both, C/Pt/Nafion and C/Pt-Ru/Nafion nanocluster membrane electrodes exhibit high electrocatalytic activity for methanol oxidation. The current density of methanol oxidation at C/Pt nanocluster membrane electrodes was ~ 20 times higher than bulk Pt electrodes.

This enhancement in current density was attributed to both the high surface area and high electrocatalytic activity of nanoclusters dispersed inside the CNTs.

A template method was also used to prepare tubular carbon structures–alumina composites which were filled with platinum (1.2 nm particles), platinum-ruthenium (1.6 nm) or platinum–tungsten (10 nm) oxide in order to be used as electrodes in methanol oxidation (Rajesh *et al.,* 2003). The authors have found that the electrochemical activity follows the order: Pt-WO_3/CNT>Pt-Ru/CNT>Pt/CNT. They have also compared the activities and stabilities with those electrodes prepared from commercial carbons such as Vulcan or E-TEK carbon (Rajesh *et al.,* 2002). In this case, the order for activity and stability is Pt-WO_3/CNT>Pt-Ru/E-TEK-Vulcan>Pt/CNT>Pt/E-TEK-Vulcan>bulk platinum. The higher electrochemical response of CNT based materials has been correlated to the higher available electroactive surface area.

1.14.3 Mesoporous carbon

Ryoo *et al.,* (1999) reported the synthesis of a new type of meoscopically ordered nanoporous (or mesoporous) carbon molecular sieve by carbonizing sucrose inside the pores of the MCM-48 mesoporous silica molecular sieve. Jun *et al.,* (2000) reported the synthesis of ordered mesoporous carbon material using the ordered mesoporous silica molecular sieve (SBA-15). This synthesis was the first example of ordered mesoporous sieve retaining the structural symmetry for silica template. Joo *et al.,* (2001) reported the Pt nanoparticles supported on ordered mesoporous arrays of carbon as electrode material for oxygen reduction in perchloric acid medium. The diameter of Pt clusters has been controlled below 3 nm and the high dispersion of these metal clusters exhibited promising electrocatalytic activity for oxygen reduction,

which could prove to be practically relevant for fuel cell technologies (Raghuveer and Manthiram, 2004; Chai *et al.,* 2004; Su *et al.,* 2005)

It is known that interaction between carbon support and catalyst modify the catalyst activity, and interactions depend on nature of surface atoms of carbon. In case of carbon support, there is lack of uniform distribution of surface atoms. Further, it is difficult to reproduce the exact surface composition. Since the overall electronegativity on the support surface governs the dispersion of catalytic particles, one has to have a control over the surface heteroatoms with respect to their amount and distribution.

An alternative is to develop a catalyst support that is permeable to gases and water, while conducting both protons and electrons efficiently. These requirements make it manadatory that the catalyst layer is thin and placed close to the hydrophobic diffusion layer. These materials could replace carbon layer and should provide enhanced performance. Conducting polymers (Lyons, 1994; Chiang and Macdiarmid, 1986) with heteroatoms offer good performance over the above addressed issues: There is uniform distribution of heteroatoms in conducting polymers as there are repeating monomer units with a regular fashion. Further, unlike carbon, controlling the deposition parameters could vary the morphology of the polymer. The catalytic particles can be incorporated either in two or three dimensional fashion according to the preparation methods adopted.

1.15 CONDUCTING POLYMER CATALYST SUPPORTS

The dispersion of the catalyst is an important factor for governing the utilization and the overall activity of methanol oxidation. One way of achieving high catalyst utilization is by dispersing the catalyst within a conducting polymer. By imbedding

the metal particles in polymeric films, the reduction of catalytic activity or efficiency due to physical or chemical loss of catalyst can be suppressed. Polymer films are frequently more effective than monolayers of adsorbed or covalently bound catalyst since they display better stability and a higher active site concentration. In the case of electrocatalysis at modified electrodes, good electronic/ionic conductivity of film or support is also necessary. Efficient electrocatalytic systems would require mutual metal support interactions leading to activation of both dispersed metal and a matrix toward electrode processes (Chandler and Pletcher, 1986; Malinauskas 1999). Modification of electrode surfaces provides an active catalytic species at the effective spatial region and combines the experimental advantages of heterogeneous catalysis with the benefits of a three dimensional distribution of active centers typically characteristic of homogeneous catalysis. In practice, a good electro-catalyst should exhibit both high reactivity towards the substrate molecules in solution and have the ability to transfer electrons rapidly in the microstructure in order to avoid transport limitations. It is essential to identify the conditions (choice of matrix, reactive components and rigid anchoring groups) for preparation of thin but three-dimensional polymeric films, which are active for the electrooxidation of methanol. A great deal of research aims at providing the right morphology of catalytic surface in order to reduce the level of loading of Pt and to reduce the poisoning of the electrode due to CO during methanol oxidation.

Various studies have examined the electrocatalytic activity of platinum microparticles dispersed on/in electronically conducting polymers such as polyaniline (Kost *et al.,* 1988; Esteban *et al.,* 1989; Hable and Wrighton, 1991), polypyrrole (Strike *et al.,* 1992; Yang *et al.,* 1997; Xue *et al.,* 1998). Swathirajan and Mikhail (1991) reported the methanol oxidation on Pt-Sn deposited on conducting poly (3- methylthiophene).

Other conducting polymers studied, include poly (N-methylpyrrole), (Kulesa *et al.,* 1999), poly (2-hydroxy-3-aminophenaizine), (Kelaidopoulou *et al.,* 1999) and copolymer of pyrrole-dithiophene (Laborde *et al.,* 1990) for electrooxidation of methanol.

The two probe or four probe methods are generally used to measure the conductivity of these polymers. But, since the ex-situ conductivity measurements some times did not reflect the true picture under the operating conditions, Schiaven *et al.,* (1989) and Wilbourn and Murray (1998) reported the measurement of conductivity by impedance spectroscopy was very attractive as it not only gives the ohmic resistance of the polymers but also the charge transfer resistance which is helpful in understanding better the electrode and electrolyte interface (Musiani, 1990; Kostecki *et al.,* 1993; Kvarnstorm and Ivusaka, 1997; Lee *et al.,* 2000; Vork and Barendrecht, 1989; Bathelet and Guglielm 1996)

Most of the conducting polymers used in the studies of electrooxidation of methanol contains S, N and/or O heterocycles in their backbone. For electrooxidation of methanol on polymer supports, the dispersed metal used was Pt with or without ad atoms.

1.15.1 N-Containing Polymers

1.15.1.1 Polyaniline

Polyaniline (PANI), is an interesting material, easy to synthesize both chemically (Malinauskas, 2001) and electrochemically (Zotti *et al.,* 1988) in aqueous medium, generally homogeneous, strongly adherent to the support and chemically stable in acid medium. Examination on PANI films using SEM studies showed that it has a rough morphology and porous texture providing high surface area. But compared with other

conducting polymers such as polypyrrole (Cai and Martin, 1991) and polythiophene (PTH) the conductivity of PANI is poor. i.e., about 1-40 S/cm at room temperature for PANI prepared by common methods. The conductivity of PANI films doped with camphor sulphonic acid (CSA) in m-cresol can reach as high as 300 S/cm. Wan,(1998) synthesized by a new 'doping-dedoping–redoping ' method, doped PANI films with high conductivity (about 200-300 S/cm) at room temperature using HCl H_2SO_4, $HClO_4$, H_3PO_4 and p-toluene sulphonic acid. PANI can be prepared by chemical oxidation (Adams *et al.,* 1997), or by electrochemical techniques. Of the electrochemical techniques, the potential cycling method (Pokhodenko and Krylov, 1991) is a good choice, since this technique provides various parameters related to the degree growth. This allows one to have maximum amount of control over the control over the quality of the PANI films. The charge transfer property of polyaniline was discussed by (Heeger, 1989; Gholamian and Contractor, 1988 and Stiwell and Park, 1988). Promising results have been reported for electro oxidation of methanol on Pt based particle dispersed in PANI film. Kost *et al.,* (1988) studied the electrooxidation of methanol on Pt particles deposited on PANI films. They exhibited higher catalytic activity by a factor of 3 than bulk platinum electrode. Moreover, a drastic decrease in poisoning effect was shown by Laborde *et al.,* (1994) using in *situ* electrochemically modulated infrared reflectance spectroscopic (EMIRS) studies, which showed no significant CO_{ads} signal. Napporn *et al.,* (1996) studied the usefulness of PANI for the electrooxidation of oxygenated molecules containing one carbon atom (methanol, HCHO, HCOOH) at highly dispersed Pt based electrodes (Pt, Pt-Ru, Pt-Sn and Pt-Ru-Sn) and showed that electrodes composed of particles of Pt and of a second (or a third) metal inserted in conducting polymer matrix exhibit weak poisioning effects compared with pure Pt particles.

1.15.1.2 Polypyrrole

Polypyrrole was found particular utility in the rapidly expanding field of chemically modified electrodes (Lyons, 1994). Depending on the preparation conditions the conductivity of the polymer can be varied. The electrocatalytic effect depend on several factors, for example, diffusion co-efficient of any depolariser not only depends on film thickness but also on surface morphology and the bulk structure of the material. This will in turn effect the measured conductivity and the doping levels seen for given conditions, but are themselves dependent on polymerization condition used. Number of factors which effect the conductivity and the electrochemical property of material (Penner *et al.,* 1998; Pickup and Osteryoung, 1984; Zhou *et al.,* 1987; Pyo *et al.,* 1994) can be explained in terms of steric interactions which effect the conjugation of the π system. i.e., by disrupting the planarity of the polymer backbone and by effecting the degree of orbital overlap, or due to structural changes involving coordination of the ion. These include nature of substituents on the pyrrole ring, the position at which the monomers are linked and the nature of dopant anion. Recently, Zhou and Heinze, (1999) observed a structural diversity of PPY during electro polymerization of pyrrole and proposed diverse mechanisms for various events occurring during film formation. Strike *et al.,* (1992) utilized PPY film coated on Au electrode to disperse Pt particles for electrooxidation of methanol. The Pt was deposited either at a constant potential or by using a pulse train. From cyclic voltametric studies, it was found that in the absence of methanol, the Pt does not have a dramatic effect upon the electrochemical properties of PPY film over the range 0.1 to 0.7 V/SCE and this observation was in agreement with previous literature for galvanostatically grown films. A considerable difference was seen between the electrodes Au/PPY/Pt (300 nm PPY, 200$\mu g/cm^2$) exhibits the current of 1.5 mA.

These modified electrodes exhibit both better electrocatalytic activity and an increased resistance to poisoning when compared to bulk platinum.

1.15.1.3 Poly-N-methylpyrrole

Poly-N-methylpyrrole (PMPY) has a conductivity of 0.001 S/cm at room temperatures, which are five orders of magnitude less than PPY. The ionization potential value of 3.9 eV reported for PMPY is identical to that of PPY, which is expected. The methyl group is linked to the nitrogen atom and the nitrogen $2p_z$ orbital has no contribution to the top of the upper valence band, which determines the ionization potential value. Kuleza *et al.,* (1999) demonstrated the usefulness of poly-N-methylpyrrole as a matrix for the fabrication of a composite film containing spatially dispersed platinum and highly reactive Ru oxo centers for electrooxidation of methanol. It is note worthy that this polymer is stable at positive potentials and, while oxidized attains a conducting state. By the introduction of polynuclear Ru/CNRu (cyanoruthenate), the overall stability of a composite film is increased and this is attributed to the strong interaction between ionic Ru/CNRu sites and positively charged cations in the rigid polymer (PMPY) matrix. These properties have allowed the preparation of fairly thick films in which active Ru oxo centers can be fully utilized for catalytic oxidations

1.15.2 S – Containing Polymer (Poly (3-methyl) thiophene (PMT))

PMT is an electronically conducting polymer, stable in acid electrolytes and has good conductivity of about 100 S/cm in the doped state but the resistivity increases by nine orders of magnitude when the polymer is not doped. Even though, many of the properties of polythiophene (PT) are similar to polypyrrole as in both cases the basic structure is essentially the same, PT has not been used so far for electro oxidation of

methanol. One of the important reasons is that the electroactive domain of PT lies between 0.5 to 1.0 V/SCE, which in not the region for methanol oxidation. Structure of PT is essentially retained even when heavily doped, and chain lengths upto 300 have been calculated for poly (3-alkyl thiophene). Electrochemically prepared chemical was amorphous, even though it was suggested that polymer was basically granular or fibrillar (chemically prepared material was crystalline). The material was apparently quite porous, with columetric data providing evidence that thiophene polymers have a large internal surface area.

Morphology depends on number of factors including nature of substrate, the growth rate and the current and potential at which polymerization proceeds. Thin films are highly homogeneous and show little evidence for solvent incorporation but as film thickness was increased the homogeneity was lost, possibly due to cumulative effect of structural defects such as chain folding, cross-linking, - coupling etc., or as a result of inhomogeneity of the electric field at the polymer surface, use of high monomer concentration tends to produce powdery film. Electrochemically prepared PMT showed high degree of order (Zhao and Pickup, 1994), again with predominantly– linking between thiophene rings, whilst unsubstituted PT has a greater degree of disorder due to possibility of –linkage. Sulphur of the thiophene ring does not play a large part in determining the electronic structure of the material (if the sulphur carried a significant portion of the charge on the chain, this symmetry would be disrupted), and that it merely stabilizes the lower energy form of the non-degenerated polymer chain of the backbone. Optical and XPS studies showed that unsubstituted and substituted polythiophenes have highly mobile spin in the polymer chains, and proposed that the conduction mechanism involves 3D variable-range hoping.

Swathirajan and Mikhail, (1992) studied the electrooxidation of methanol using Pt-Sn particles dispersed on poly 3-methyl thiophene (PMT).

1.15.3 N, S – Containing Polymer (poly (pyrrole-thiophene))

All conducting polymers have a defined domain of electroactivity and although polythiophene appears promising owing to its excellent chemical and electrochemical stability but it's it electroactivity potential range from 0.5 to 1.0 V/SCE does not fit with electrooxidation of methanol. Thus in order to extend this working range, copolymer poly (pyrrole-thiophene) has been used, as a conducting matrix and this has been electroactive between 0.0 and 1.0 V/SCE. Laborde *et al.,* (1990) investigated the electrocatalytic properties of a conducting copolymer modified by the inclusion of a small amount of (0.1 mg/ cm^2) dispersed platinum for electrooxidation of three molecules: hydrogen, formic acid and methanol. The onset potential for methanol oxidation was 0.55 V/RHE band the maximum current density of 2.0 mA/cm^2 observed at 0.9 V/RHE.

1.15.4 N, O – Containing polymer (Poly (2-hydroxy-3-aminophenazine))

Poly (2-hydroxy-3-aminophenazine) (pHAPh) is a stable, redox active, ladder polymer formed from a low oxidation potential monomer (2-hydroxy-3-aminophenazine). The electroactive potential range of pHAPh, is wider than those of polyaniline, polythiophene and polypyrrole. The electro polymerization of HAPh on Pt electrodes was studied (Keledopoulou *et al.,* 1994). Keladopoulou *et al.,* (1999) studied the electrooxidation of methanol on dispersed electrodes containing Pt, Pt-Sn and Pt/M (M=Pb, TI & Bi).

Rajesh and Viswanathan (2000) have prepared methanol oxidation catalysts using polymer films of 1.5 dihydroxynaphthalene (1, 5-DHN). The polymer films were electropolymerised onto carbon and Pt was electrodeposited from chloroplatinic acid. This structure gave better methanol oxidation characteristics than Pt alone or Pt co-deposited with the 1, 5 DHN conducting polymer.

Poly (o-phenylenediamine) can be obtained by electrochemical polymerization of monomer o-phenylenediamine or by the chemical oxidative polymerization of monomer o-phenylenediamine. One of these properties relate to an unusual dependence of the electric conductivity on the redox state of this polymer. As opposed to PANI or PPY, POPD shows the conductivity in its reduced state, whereas its oxidized state is insulating. This determines the electrochemical properties of POPD, since many electrode redox processes of solution species have been shown to take place within a relatively narrow potential window, corresponding to the reduced (conducting) form of this polymer. Within this potential window, electrocatalytic oxidation of some species proceed, making it possible to use POPD for electrocatalytic applications, like e.g. the electro oxidation of coenzyme NADH, electro oxidation of methanol (Golabi and Nozad, 2002) and oxygen reduction (Ohsaka *et al.,* 1991; Li *et al.,* 1998; Premkumar and Ramaraj, 1996)

1.15.5 Pt on Proton conducting polymers

In this context of discussion on ion conducting polymers it is worth mentioning the role of Nafion, a perfluorinated sulfonic acid polymer with excellent chemical, mechanical and thermal stability. In DMFC membrane electrode assemblies (MEA), the catalytic particles were coated with Nafion, which acts as a polymer electrolyte and the catalyst binder. Morita *et al.,* (1991) described the enhancement of catalytic

activity of Pt micro particles for the oxidation of methanol by dispersing them into Nafion film and by subsequent RF-plasma treatment. The time-course of current density at 0.3 V/SSCE for 30 min duration showed that the initial activity was larger by a factor of 1.5 on Pt-Nafion /GC (Nafion film thickness=500 nm) than Pt/GC. The oxidation current decayed with the polarization time on both electrodes, but faster on Pt/GC. Thus, the activity at Pt-Nafion/GC was larger by a factor of 2.1 than Pt/GC at 30 min. The current density at 30 min for Pt-Nafion/GC is dependant on film thickness. For thin Nafion film (<100 nm), a part of the individual Pt particles with a diameter of 100-200 nm was exposed directly to the bulk solution out of polymeric film, and hence no activity enhancement was found but when film thickness was increased from 250-500 nm the activity increased by a factor of 1.5-2.0 at 30 min. This increase was approximately same as that (2 times) of the Pt chemically plated to Nafion membrane (Pt-SPE) as reported by Aramata and Ohnishi, (1984). It is worth noting that the electrode carries only 20 μg/ cm^2 of Pt, which were two orders of magnitude less than that of Pt/SPE. The activity enhancement by Nafion film is attributed to the interaction between the particles and film, and/or an environment change of the Pt particles in the Nafion matrix. Further, RF-plasma treatment makes a Nafion film structurally more compact due to cross-linking, so that the film becomes more hydrophobic.

The importance of cyclic voltammetric and chronoamperometric techniques is reflected by the fact that, the evaluation of activity of methanol oxidation on the catalytic particles dispersed on all these conducting polymers (both electron and proton conducting polymers) was based on these techniques.

1.15.6 Catalytic particles dispersed on mixed proton-electron conducting polymer as electrode for methanol oxidation

Lefebvre *et al.,* (1999) prepared a variety of Pt and Pt-Ru supported catalysts by chemical deposition on chemically prepared poly (3, 4-ethylenedioxythiophene)/ poly (styrene-4-sulphonate) (PEDOT/PSS) and PEDOT/polyvinyl sulfate (PVS) composites. They show high electron and proton conductivities, facilitate rapid electrochemical reaction rates of thick layer of catalysts. The importance of mixed proton and electron conductivities in the direct methanol fuel cells has been reported by Rolison *et al.,* (1999). The methanol electrooxidation using these polymers are under investigation. Ghosh *et al.,* (2000) have prepared PEDOT-PSS, an electronically conductive electroactive polymer blends with an ion conducting polymer, polyethylene oxide (PEO), to increase ionic mobility in the material. As super capacitor electrodes, the blends gave higher energy densities at high power densities compared to the pure PEDOT-PSS and this enhancement in electrochemical properties was attributed to both intrinsic ionic conductivity of the PEO and the swelling of the former in liquid electrolyte solution, creating space for ionic movement. By suitably fabricating mixed electronic and ionic conducting polymers as supports for catalytic particulates, the utilization of catalytic particulates may be enhanced.

1.16 TEMPLATE SYNTHESIS OF CONDUCTING POLYMERIC NANOTUBES

Currently there is a considerable interest in nanostructured poly heterocyclics, since they exhibit novel properties largely as a consequence of their infinite small size. A possible approach for building such nanoscale objects involves the use of nanoporous host material as the templates. Penner and Martin (1986) described a new

template (Poly carbonate nucleopore and alumina anapore membranes) method for preparing polypyrrole nanotubes. Later organic micro and nanotubes of polyaniline polypyrrole and poly (3-methyl) thiophene (Cai and Martin, 1989; Martin *et al.,* 1996; Dyke and Martin, 1990) have been prepared. Even polyacetylene fibrils (Liang *et al.,* 1990), metal microtubules (Brumlik and Martin, 1991) and molecular filtration membrane (Jirage *et al.,* 1997) have been prepared inside the pores of these membranes. Champagne *et al.,* (2000) and Delvaus *et al.,* (2000) synthesized electrochemically polyaniline and polypyrrole nanotubes using the pores of nanoporous polycarbonate (PC), particle track etched membrane (PTM) as templates. It has been shown that the conducting polymer synthesized by the template method has enhanced the conductivity and charge transport properties compared to the conventionally synthesized conducting polymers.

1.17 CATALYSTS BASED ON THE METAL OXIDE SUPPORTS

The influence of dispersing metal oxides (Al_2O_3, Cu_2O, ZnO_2, TiO_2, Fe_2O_3, SiO_2, RuO_2) with a commercial Pt-Ru catalyst for methanol oxidation in phosphoric acid. At 423 K, catalyst made by mixing with Fe_2O_3 were identified as giving the best performance in terms of reduction polarization compared to Pt-Ru alone, the electrodes used had loading of 0.15mg cm^{-2}.

Biswas *et al.,* (1991) studied the electrocatalytic activity of a graphite based Pt electrode modified with In + Pb mixed oxide towards methanol oxidation in 0.5 M H_2SO_4. A more negative zero-current potential around 70 mV/RHE was realized on a Pt/In + Pb mixed oxide/GC with Au compared with 95 mV/RHE for Pt/In + Pb mixed oxide/GC without Au. These were close to the theoretical oxidation potential ~ 30mV in acidic solutions.

Perovskite oxides have been studied as potential materials because they offer surface basicity character, which affect the oxidative dehydrogenation steps in methanol oxidation, and are stable particularly in alkaline medium (Biswas *et al.,* 1992)

In recent years, it is found that certain metal oxides**,** such as RuO_2 (Gu *et al.,* 2006; Chen *et al.,* 2005), WO_3 (Zhang *et al.,* 2006; Park *et al.,* 2006), ZrO_2 (Bai *et al.,* 2005), MgO (Xu *et al.,* 2005) and CeO_2 (Wang *et al.,* 2007; Shen *et al.,* 2006), can enhance the catalytic activity for ethanol or methanol electrooxidation through synergetic interaction with Pt. The dehydrogenation capability of the WO_3 has been effectively used for methanol electrooxidation. It was well known that oxides like WO_3, MoO_3 and V_2O_5 can form their respective bronzes by dehydrogenation. Among these oxides, WO_3 has been used along with Pt and Pt-Ru for electrooxidation of methanol (Wasmus and Kuver, 1999; Babu *et al.,* 1998).

Nanoporous TiO_2 was also found to be an effective support for the oxidation of methanol (Hayden *et al.,* 2001). It has been shown that carbon with basic surface oxides are the most effective type of support. Electrochemical oxidation of methanol, ethanol, glycerol and ethylene glycol (EG) on novel Pt–CeO_2/C catalysts in alkaline media have been studied and shows an improved performance in terms of the electrode activity and the poisoning resistance (Xu *et al.,* 2004). Rare earth oxides LnO_x (Ln = Sc, Y, La, Ce, Pr and Nd) as modifications to prepare the catalysts for methanol electrooxidation in acid electrolyte. (Tang and Lu 2006)

VO_x-NTs were used to act as catalyst supporting material (Zhang *et al.,* 2006). Well-dispersed Pd nanoparticles supported on VO_x-NTs were successfully prepared through a simple reductive process. Compared with other supporting materials, VO_x-NTs can be easily synthesized as a pure product in gram quantities by low temperature

hydrothermal synthesis and have reactive defects on their surface. The prepared Pd/VO_x-NTs composites showed an excellent electrocatalytic activity and long-term stability for methanol oxidation in alkaline medium.

1.18 COMPOSITE MATERIAL AS SUPPORTS

Au/TiO_2 is added to a PtRu/C electrode to improve the performance of a direct methanol fuel cell (DMFC). In CO-stripping and methanol oxidation voltammetry, PtRu/C-Au/TiO_2 composites exhibits better activity for CO and methanol oxidation than PtRu/C. The performance of the DMFC is also improved by addition of Au/TiO_2 to the PtRu/C electrode. The improved performance of the PtRu/C-Au/TiO_2 composite catalyst is explained in terms of preferential oxidation of CO or CO-like poisoning species that are generated during the oxidation of methanol on PtRu/C (Kim *et al.,* 2006).

Zhang *et al*., (1999) prepared Pt/MoOx/C composite electrode by co-deposition method and carried out electro-oxidation of methanol in acidic medium. XPS data revealed the presence of Mo in 6, 4& 3 oxidation states. The composite electrode exhibited better performance than platinisd carbon electrode. A surface redox mechanism which involves (i) Mo (VI)/(IV) couple in substoichiometric lower valence MoOx ($2<x<3$) and (ii) the proton spill over effect from hydrogen molybdenum bronzes were two proposed explanations for the enhanced catalytic activity of this system.

Pt–RuO_2/C composite using boron-doped diamond (BDD) electrode as the substrate for electrochemical experiments shows superior performance than the glassy carbon electrode, probably related to the very low capacitive currents of that material. Ideally, a catalyst support material that is both electronically and ionically conductive is

desired (Suffredini *et al*., 2006). Conducting polymer composite consists of one polymer that is electronically conductive (*e.g.*polyprrole, poly(3, 4-ethylenedioxythiophene)), and one that is a proton conductor (*e.g.* polystyrenesulfonate). This material was tested as a replacement for carbon and reasonable performance was achieved. However, low Pt utilization and polymer stability are still issues.

Methanol oxidation reaction operates in acid medium and hence requires both the catalyst and support to be stable. The building of efficient nanocomposite electrode is very important. This principle has been followed by several researchers, describing the preparation of nanocomposites in which nanoparticles of Pt, Pd, Cu, etc. are combined with PPy, PAni, PTh etc to form efficient electrocatalytic electrodes. The dispersion of Pt particles in PAni matrix and their ability for enhancing methanol oxidation has been extensively discussed (Hable *et al.,* 1996). Similarly, the formation of a series of such mono and bimetallic electrodes using Pd, Cu, Pd/Cu and Cu/Pd catalyst in conjunction with PAni has been reported to show efficient oxidation of formic acid and methanol.

Pt nanoparticles (4 nm) supported at polyaniline–V_2O_5 composite show better activity and stability in methanol electro-oxidation than a bulk Pt electrode (Rajesh *et al.,* 2005). Pt–Ru alloy nanoparticles dispersed in poly (*N*-vinylcarbazole) or poly(9-(4-vinyl phenyl carbazole) show a good performance in a direct methanol fuel cell, although somewhat lesser activity than for carbon-supported electrode (Choi *et al.,* 2003)

Novel nanocomposite Pt/RuO_2.xH_2O/carbon nanotube catalysts for direct methanol fuel cells. This combination of RuO_2.xH_2O, which donates and accepts protons and

electrons, with Carbon nanotubes (CNTs) which compensate the loss of electron cond. caused by the RuO_2 coating, improves electrode microstructure and lowers electrode resistance. The result is that this nanocomposite catalyst performs well for direct electrooxidation of MeOH in fuel cells (Cao *et al.*, 2006).

1.19 OBJECTIVE AND SCOPE OF THE PRESENT STUDY

Development of electrodes with maximum utilization of Pt on different types of supports for methanol oxidation is an area of research interest in this study. The main objective of the present study is to synthesize and study the electrochemical properties of different support materials as electrodes for methanol oxidation for Direct Methanol Fuel Cells.

The main objectives of this study include:

1. Synthesize electrocatalysts with high electrocatalytic activity for methanol oxidation

2. Develop unconventional supports for platinum catalysts for methanol oxidation and compare the methanol oxidation activity of nanostrucured supported catalysts with that of the commercially available Vulcan XC-72 based catalysts.

3. Synthesize nitrogen containing carbon nanotube supported Pt electrodes for methanol oxidation.

4. Synthesize TiO_2 nanotubes by template method has been developed and the nanotubes are employed as support for Pt.

5. Synthesize Pt/WO_3 nanorods as anode electro-catalyst for methanol oxidation in DMFC application.

6. Electrochemical Synthesis of Pt deposited conducting polymer nanotube electrodes for methanol oxidation.

7. Synthesis and electrochemical activity of Pt supported on PEDOT-V_2O_5 polymer nanocomposite electrodes for methanol oxidation.

8. Physio-chemical characterization of the synthesized electrode materials.

9. Evaluation of performance of elctrooxidation of methanol in acid medium on the above synthesized electrode materials.

CHAPTER 2

EXPERIMENTAL METHODS

2.1. CHEMICALS AND MATERIALS USED

The Whatman Anapore Membrane (Alumina) with pore diameter, thickness and percentage porosity of 200 nm, 60 μm and 65% respectively was purchased from Alltech Associates Incorporation, U.S.A.

Glassy Carbon (GC) disc (0.07 cm^2) and polishing kit was purchased from Bio Analytical System. U.S.A. Carbon block was purchased from Industrial Carbon Manufacturers, India.

Phosphotungstic acid, Polyvinylpyrolidone (Sisco Research Laboratory, India) and 3,4-ethylene dioxythiophene (Fluka) were used after distillation and stored in nitrogen atmosphere. *N*-vinylimidazole (Fluka) was purified by distillation under reduced pressure prior to use. α,α′-azoisobutyronitrile (Fluka) (AIBN) was purified by recrystallization from methanol. Benzene was used without further purification. 30% HBF_4 were purchased from Fluka and used as received. 5 wt% Nafion were purchased from Aldrich. All the noble metal chlorides were purchased from M/s Hindustan Platinum Ltd., India.

All other chemicals and solvents used in the investigation were of analytical (AR) grade and were obtained from (Sisco Research Laboratory, India) or E.Merck, India. These chemicals were used as such without further purification.

2.2 PURIFICATION OF GASES

2.2.1 Purification of Argon

High pure argon from M/s. Karnataka Oxygen Ltd., was bubbled though a series of gas washing bottles. The first two of the wash bottles contained 50 g of amalgamated zinc and 200 ml of 0.1 M ammonium metavanadate in hydrochloric acid. The next two traps had distilled water and concentrated sulphuric acid respectively to remove vanadium and moisture from the gas stream. Finally, the gas was passed through a silica gel column to absorb traces of moisture and thus dry argon gas free of oxygen was obtained.

2.2.2 Purification of Hydrogen

Hydrogen gas obtained from M/s. Indian Oxygen Ltd. was purified through a heated trap containing reduced copper powder kept at 623 K followed by traps containing potassium hydroxide pellets, fused calcium chloride and silica gel. Hydrogen of high purity thus obtained was used for the reduction of the catalysts.

2.3 PHYSIOCHEMICAL CHARACTERISATION

2.3.1 X-ray diffraction studies

The XRD patterns were obtained for the powdered samples recorded with a Philips (Philips generator, Holland model PW1140) automated powder diffractometer at room temperature. The diffraction patterns were recorded using a Ni filtered Cu K_α radiation at a scanning rate of 3 deg/min and a chart speed of 3 mm/deg.

2.3.2 Infrared spectroscopic studies

Infrared studies in the range 4000-400 cm^{-1} for samples were recorded on Shimadzu photometer. The samples were mixed well with KBr in 1: 100 ratios and then pelletized.

2.3.3 UV-Vis spectroscopic measurements

UV-Vis spectra were recorded with CARY-5E UV-Vis- NIR spectrophotometer. For samples, the spectra were recorded in nujol mode at room temperature. The sample was diluted with nujol oil and ground well in a mortar. The resulting paste was then soaked on a Whatmann-41 filter paper and was introduced in to the spectrometer. Prior to that, background correction was done with nujol-soaked filter paper.

2.3.4. Thermogravimetric Analysis (TGA)

Thermogravimetric analysis (TGA) was conducted using TGA7 (Perkin-Elmer, Norwalk, CT) where the sample was maintained at 120 ºC for 2 hours and then heated to 850 ºC with a heating rate of 10 ºC/min in high purity nitrogen atmosphere.

2.3.5. Estimation of Metal(s) loading

The bulk metal on the catalyst/electrode were analysed by Inductively Coupled Plasma Atomic Emission Spectrometer (ICPAES, Model 3410, ARL) after calibration with standard solution containing known metal content. The metal was extracted from the catalyst/electrode by boiling in aqua regia.

2.3.6. Elemental Analysis

The C, H and N analysis was done using the Heraeus CHN analyzer.

2.4 ELECTRON MICROSCOPY STUDY

2.5. SCANNING ELECTRON MICROSCOPY (SEM) STUDY

The surface morphology and composition of the deposited material were studied using a Hitachi S-3600N Scanning Electron Microscope (SEM), equipped with an Energy Dispersive Spectroscopy (EDS) detector. The sample in powdered form or a portion of the electrode was attached on the carbon tape (Adhesive tape, normally used in SEM measurements for conduction purpose) and mounted on the SEM sample holder and imaged.

2.6. TRANSMISSION ELECTRON MICROSCOPY (TEM) STUDY

Transmission Electron Microscope (TEM) analysis of the deposited carbon material was performed on a JEOL JEM 2010 electron microscope operated at 200 KeV with a point-to-point resolution of 2.3 Å. TEM samples were prepared by dispersion of the carbon material in alcohol and drops of dispersed material were placed on copper TEM grids and dried for TEM analysis.

2.7. ATOMIC FORCE MICROSCOPY

Contact mode AFM measurements were performed with a Digital Instruments Dimension 3000, using micro-fabricated cantilevers with force constants of approximately 40 N/m. The ratio of amplitudes which are used in feedback control was adjusted to 0.6 of the free air amplitude for all the reported images. All samples were dehydrated at 80 ^{o} C for 24 hr under vacuum conditions. The samples were then imaged immediately in a relative humidity of about 35%.

2.8. ELECTROCHEMICAL MEASUREMENTS

All electrochemical studies were carried out using the BAS 100 electrochemical analyzer. A conventional three-electrode cell consisting of the GC (0.07 cm^2) working electrode, Pt plate (5 cm^2) as counter electrode and Ag/AgCl reference electrode was used for the cyclic voltammetry (CV) studies. The CV experiments were performed using 1 M H_2SO_4 solution both in the absence and presence of 1 M CH_3OH at a scan rate of 50 mV/s. All the solutions were prepared using ultra pure water (Millipore). The electrolytes were degassed with nitrogen gas before the electrochemical measurements.

CHAPTER 3

SYNTHESIS AND ELECTRO-CATALYTIC ACTIVITY OF METHANOL OXIDATION ON NITROGEN CONTAINING CARBON NANOTUBES SUPPORTED Pt ELECTRODES

3.1 INTRODUCTION

Carbon materials possess suitable properties for designing of electrodes in electrochemical devices. Therefore, carbon is an ideal material for supporting nano-sized metallic particles in the electrodes for fuel cell applications. Carbon has the essential properties of electronic conductivity, corrosion resistance, surface properties and low cost as required for the commercialization of fuel cells. The conventional support namely carbon black is used for the dispersion of Pt particles (Uchida *et al*., 1995). New novel carbon support materials such as graphite nanofibers (GNF) (Bessel *et al*., 2001**,** Steigerwalt *et al*., 2001), carbon nanotubes (CNT) (Li *et al*., 2003**,** Kim *et al*., 2004, Wang *et al*., 2004), carbon nanohorns (Yoshitake *et al*., 2002) and carbon nanocoils (Hyeon *et al.,* 2004), provide alternate candidates of carbon support for fuel cell applications. Bessel *et al*., (2001) and Steigerwalt *et al*., (2001) used GNFs as supports for Pt and Pt–Ru alloy electro-catalysts. They observed better activity for methanol oxidation. The high electronic conductivity of GNF and the specific crystallographic orientation of the metal particles resulting from well-ordered GNF support are believed to be the factors for the observed enhanced electro-catalytic activity. In heterogeneous catalysis, one of the important tasks is the determination of the number of active sites in the catalyst. For a given catalyst, the number of active sites present is responsible for the observed catalytic activity. Considerable amount of research has been devoted towards understanding the number of active sites as well as

the role played by the carrier of the supported catalysts. The most efficient utilization of any supported catalyst depends on the percentage of exposed or the dispersion of the active component on the surface of the carrier material. Among the various factors that influence the dispersion of active component, the nature of the support and the extent of the active component loading are of considerable importance.

Carbon nanotubes, because of their interesting properties such as nanometer size, electronic properties and high surface area, have been receiving increased attention in recent years for their application in fuel cells as supports for catalyst (Wang *et al*., 2004). Modification of the CNTs alters the catalytic activity of the supported catalyst. Doping the carbon with heteroatom could be particularly an interesting way for tuning the surface and electronic properties. Incorporation of nitrogen in the CNT results in the enhancement of conductivity, due to the contribution of additional electron by the nitrogen atom (Stephan *et al*., 1994; Glerup *et al*., 2003). Doping with high concentrations of nitrogen leads to an increase in the conductivity due to the raise in Fermi level towards the conduction band (Czerw *et al*., 2001; Terrones *et al*., 2002). The profitable effect of nitrogen functionalities on the performance of porous carbon used as an electrode material in the electric double layer capacitors has been reported (Jurewicz *et al*., 2003; Zeng *et al*., 2002). The presence of nitrogen atom in the carbon support also generates specific surface properties including enhanced polarity, basicity and heterogeneity in terms of hydrophilic sites. This modification is of great interest when considering the application to catalysis and electrochemistry.

Carbon with nitrogen, sulphur and phosphorus functionalities promotes the formation of Pt particulates relative to unfunctionalised carbon. Electrocatalysts prepared with nitrogen-functionalised carbon showed the highest activity towards methanol

oxidation (Roy *et al*., 1996). While sulphur-functionalised electrode showed the lowest activity towards methanol oxidation, suggesting the existence of specific interaction between Pt and sulphur on the carbon support which inhibited the rate of the reaction (Swider and Rolison; 1996, 2000). Nitrogen functionalisation was accompanied by an increase in basicity of the carbon support, while sulphur functionalisation resulted in an increase of acidity. Nitrogen sites on carbon surfaces were generated using pyrolyzed porphyrins and heterocycles on carbon supports for fuel cell applications (Tarasevich and Bogdanovskaya, 1987; Tarasevich *et al*., 2004). The presence of nitrogen functional groups in the carbon framework has also a substantial effect on the catalytic activity in direct methanol fuel cells (Shukla *et al*., 1994, Roy *et al*., 1997).

N-doped CNF electrodes exhibit enhanced catalytic activity for oxygen reduction over non-doped CNF. However, higher dispersion and the electrocatalytic activity of methanol oxidation of Pt particles on nitrogen containing carbon nanotube support has been reported (Maldonado *et al*., 2005, Sun *et al*., 2005). For the application of carbon nanotubes in catalysis, it is important to know to what extent surface morphology, structure and chemistry are effective and how many effective sites are present on the surface. The nitrogen atoms present in the support generate catalytically active sites; such a site of nitrogen on carbon nanotubes appears to be advantageous in providing active sites for methanol oxidation. In the present investigation the role of nitrogen surface functionality on the carbon nanotube supported Pt electrodes for the electrocatalytic activity for methanol oxidation was evaluated both for CNT and N-CNT and the observed activities are compared with that of the conventional electrodes.

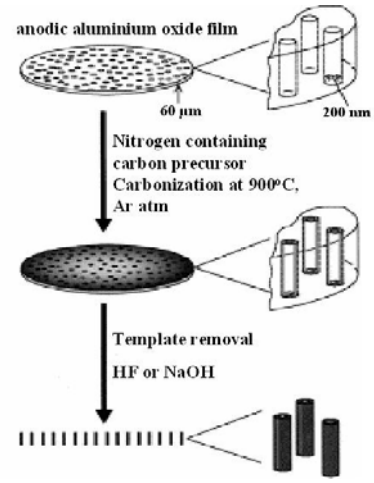

Scheme. 3.1 Scheme for Template assisted chemical synthesis of highly ordered nitrogen containing carbon nanotubes

In this work, Pt catalyst supported on nitrogen containing carbon nanotubes electrode was studied. By using nitrogen containing carbon nanotubes as support, CNT acts as three-dimensional electrode which may remain open and favor material diffusion during the electro-catalytic reaction. Nevertheless, there are no reports on the catalyst used nitrogen containing carbon nanotubes as support of catalyst in fuel cells.

3.2 EXPERIMENTAL

3.2.1 Synthesis of CNTs from poly (paraphenylene)

Carbon nanotubes have been synthesized by carbonizing the polyparaphenylene polymer inside the alumina template. Polyparaphenylene was prepared on the alumina membrane template according to the method of Kovacic and Oziomek (1964). In this method, alumina membrane template was immersed in a benzene monomer solution. The monomer undergoes cationic polymerization with $AlCl_3$ and $CuCl_2$. The polymerization temperature was kept at 45 ^{0}C. The stirring speed was maintained around 400-500 rpm for 2 h. Nitrogen was purged throughout the experiment. During this process, the polymer was formed from the monomers and is deposited within the pores of the alumina template. After polymerization, the alumina template was washed using water and ethyl alcohol to remove $CuCl_2$ and aqueous acid. This synthesis method based on template yielded the tubules of the desired polymer within the pores of the alumina membrane by controlling the polymerization time and temperature. After polymerization on the membrane, the membrane was washed with deionised water and then dried. Subsequently, the membrane was carbonized in an electric furnace at 1173 K under argon atmosphere. The resulting carbon-alumina composite was immersed in 48 % HF at room temperature for 24 h to remove the alumina template. This is then washed with hot water to remove the residual HF.

3.2.2 Synthesis of N-CNTs from poly (vinylpyrolidone)

Polyvinylpyrrolidone (PVP, 5 g) was dissolved in dichloromethane (20 ml) and impregnated directly into the pores of the alumina template by wetting method. After complete solvent evaporation, the membrane was placed in a quartz tube (30 cm length, 3.0 cm diameter) kept in a tubular furnace and carbonized at 1173 K under Ar

gas flow. After 3 h of carbonization, the quartz tube was naturally cooled to room temperature. This was followed by the same procedure as described above to remove the alumina template. The nanotubes were then washed with distilled water to remove the residual HF and was dried at 393 K.

3.2.3 Synthesis of N-CNTs from poly (pyrrole)

Pyrolysis of nitrogen containing polymers is a relatively easy method for the preparation of carbon nanotube materials containing nitrogen substitution in the carbon framework. Nitrogen containing carbon nanotubes were synthesized as follows: the pyrrole monomer has been polymerized on the surface and the pore walls of the alumina template by suspending alumina template membrane in an aqueous pyrrole (0.1 M) solution containing 0.2 M ferric chloride hexahydrate, then to this 0.2 M *p*-toluene sulphonic acid was added slowly and the polymerization was carried out for 3 h. This leads to the black coating of polypyrrole on the template membrane. The surface layers are removed by polishing with fine alumina powder and this is ultrasonicated for 5 min to remove the residual alumina, which was used for polishing. Then the membrane was placed inside a quartz tube (30 cm length, 3.0 cm diameter) kept in a tubular furnace and carbonized at 1173 K under Ar gas flow. After 3 h of carbonization, the quartz tube was cooled to room temperature. This was followed by the same procedure as described above to remove the alumina template.

3.2.4 Synthesis of N-CNTs from poly (N-vinylimidazole)

Poly (***N***-vinylimidazole) was synthesized on the alumina template by polymerization of ***N***-vinylimidazole in benzene with AIBN as initiator. Thus, *N*-vinylimidazole (50 ml) and AIBN (0.5 g) were dissolved in 250 ml benzene and polymerized at

333 K under nitrogen atmosphere for 48 h. This was followed by the same procedure as described above to remove the alumina template.

3.3. LOADING OF Pt CATALYST ON THE CARBON NANOTUBES AND NITROGEN CONTAINING CARBON NANOTUBES

Platinum nanoclusters were loaded inside both the CNT and the N-CNT as follows; the C/alumina composite obtained (before the dissolution of template membrane) was immersed in 73 mM H_2PtCl_6 (aq) for 12 h. After immersion, the membrane was dried in air and the ions were reduced to the corresponding metal by 3 h of exposure to flowing H_2 gas at 823 K. The underlying alumina was then dissolved by immersing the composite in 48 % HF for 24 h. The membrane was then removed from the HF solution and treated in the same way as for the unloaded CNT to remove the residual HF. This procedure resulted in the formation of Pt nanocluster loaded CNT and N-CNT. The complete removal of fluorine and aluminum is confirmed by EDX analysis.

3.3.1. Preparation of Working Electrode

Glassy carbon (BAS Electrode, 0.07 cm^2) was polished to a mirror finish with 0.05 μm alumina suspension before each experiment and served as an underlying substrate of the working electrode. In order to prepare the composite electrode, the nanotubes were dispersed ultrasonically in water at a concentration of 1mg mL^{-1} and 20 μL of the aliquot was transferred on to a polished glassy carbon substrate. After the evaporation of water, the resulting thin catalyst film was then covered with 5 wt% Nafion solution. And the electrode was dried at 353 K and is used as the working electrode.

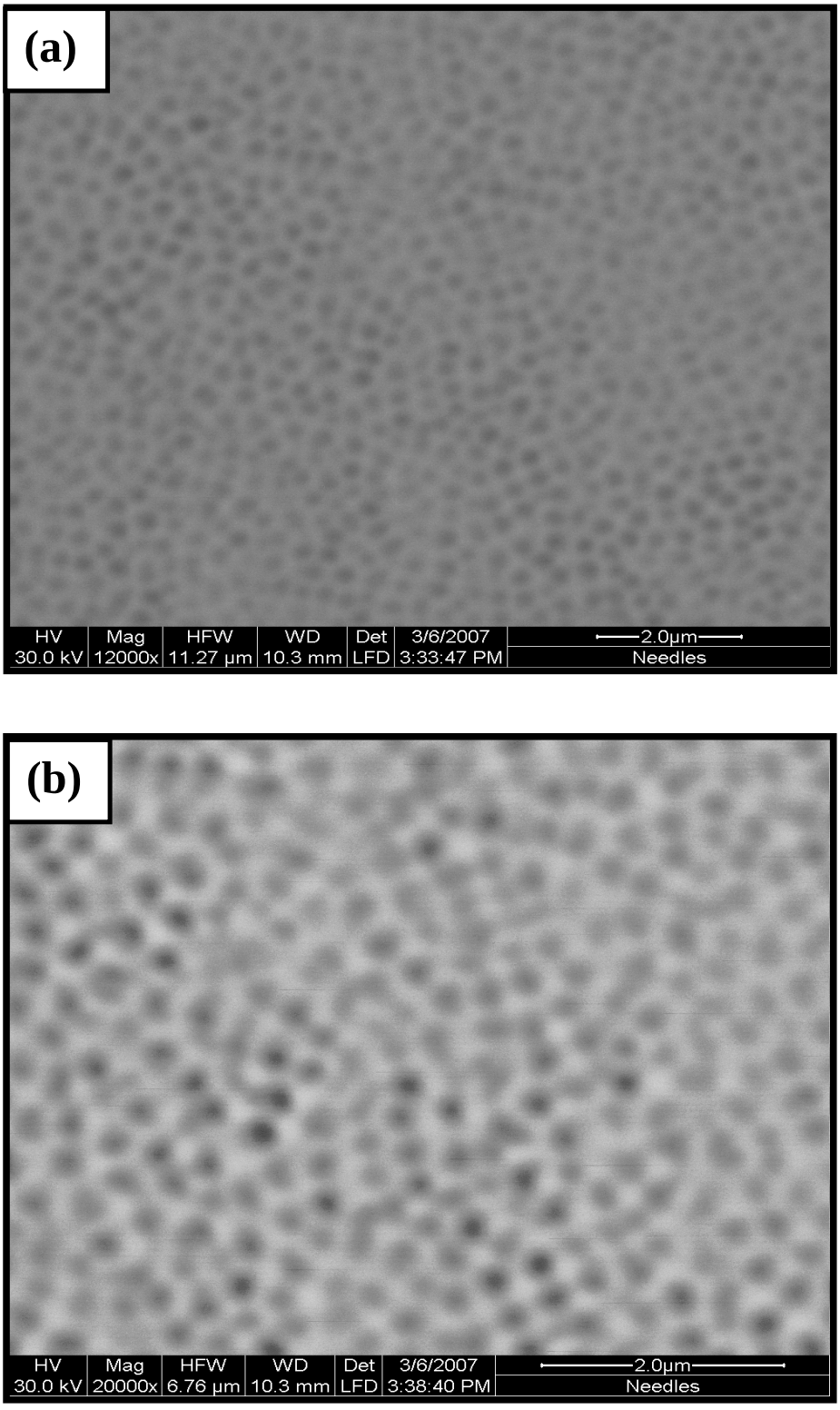

Fig. 3.1. SEM Image of AAO template; (a) low-magnification and (b) high-magnification

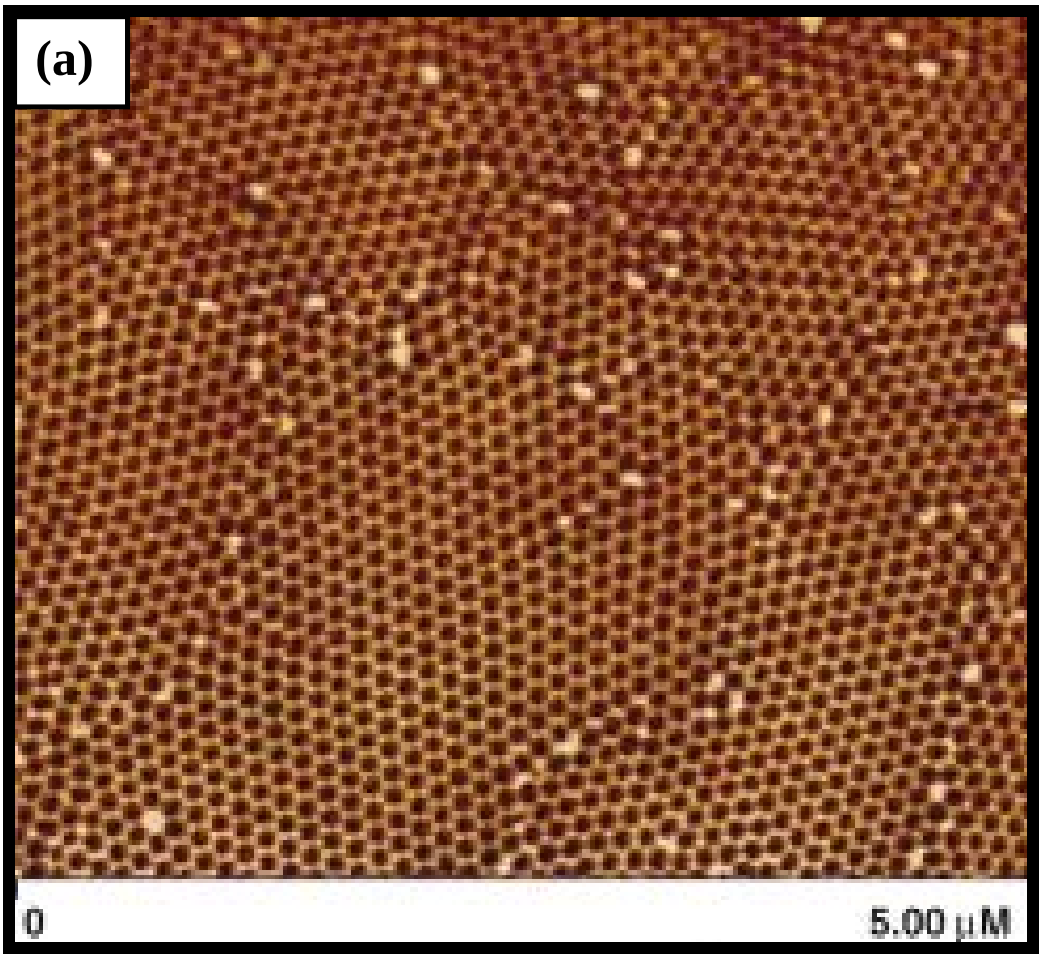

Fig. 3.2 AFM Image of AAO template

3.4 ELECTRON MICROSCOPY STUDY

3.4.1 Scanning Electron Microscopy study

The surface cross sectional view of alumina membaranes (pore diameter 200 nm) is shown in Fig 3.1 a-b. Fig 3.1.b shows the uniform pore present in the membrane. The pores and channels of the membrane have been effectively utilized for the polymerization and subsequent carbonization for the formation of the carbon nanotubes. AFM image show the surface morphology of AAO membranes to consist of periodically arranged pores.

The scanning electron micrographs (SEM) of the carbon material are shown in Fig.3.2(a). The Vulcan XC-72 carbon support well known as carbon black is shown in Fig. 3.2 (a). The agglomerated globular morphology and rough surface of the carbon particles can be observed.

The top view of the vertically aligned CNTs from poly paraphenylene is shown in Fig.3.4 (a). Fig. 3.5. (a)-(c) SEM images of N-CNTs from poly (vinyl pyrolidone) shows the hollow open structure and well alignment verified by SEM. Fig. 1 (c) shows the Pt deposited carbon nanotubes.SEM images of well aligned N-CNTs prepared from poly(pyrrole) , poly(N-vinylimidazole) are shown in 3.7a and 3.8 (a-b).

3.4.2 Atomic Force Microscopy study

The AFM images of the synthesized N-CNTs from poly (vinyl pyrolidone) deposited on a silicon substrate are shown in Fig.3.5 (d). The AFM tip was carefully scanned across the tube surface in a direction perpendicular to the tube axis. From the AFM images, a part of the long nanotube appears to be cylindrical in shape and is found to be terminated by a symmetric hemispherical cap. Because of the finite size of the AFM tip, convolution between the blunt AFM tip and the tube body will give rise to an apparently greater lateral dimension than the actual diameter of the tube (Tsang *et al*., 1996).

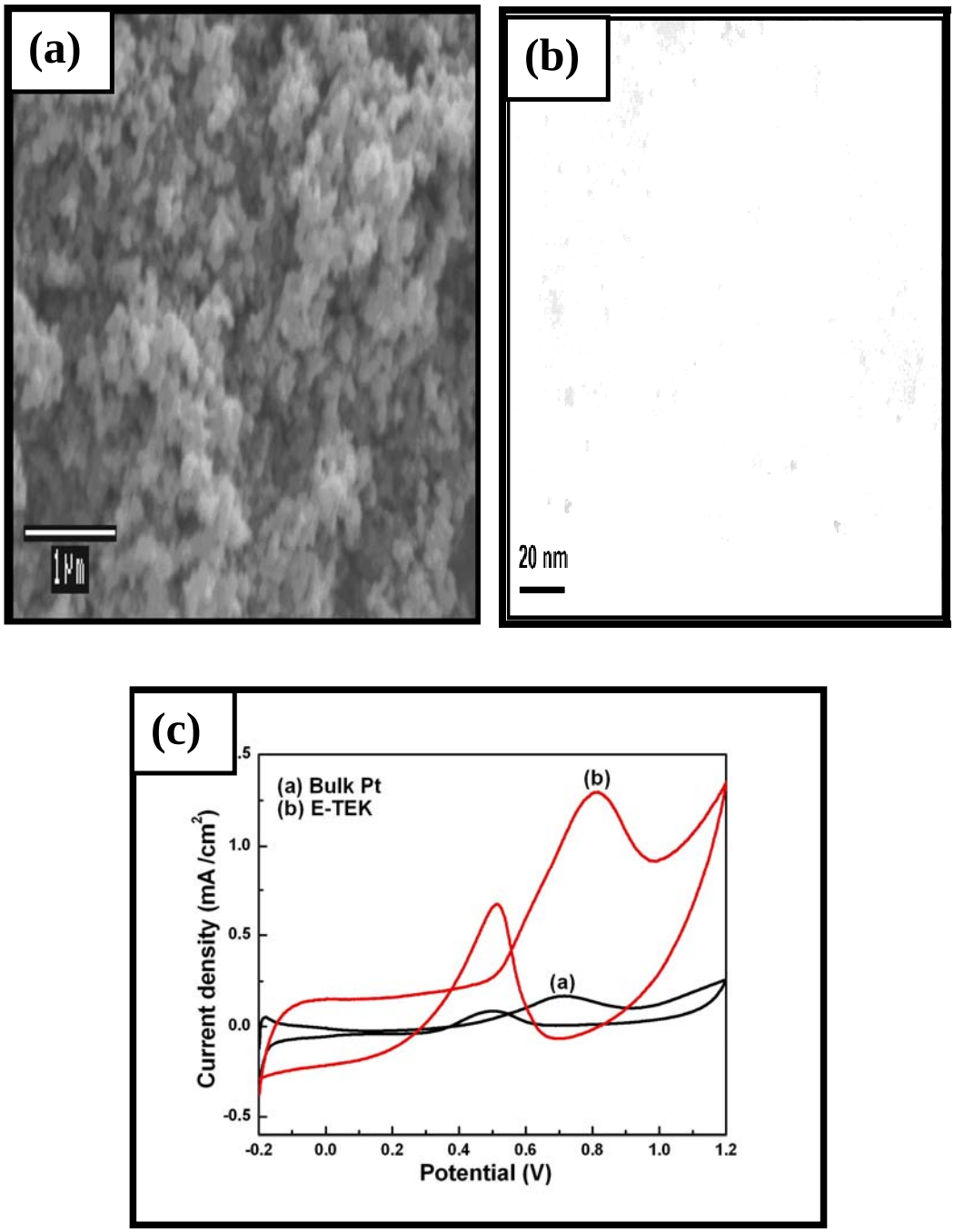

Fig. 3.3. (a) SEM Image of Vulcan carbon support (b) TEM image of Pt supported Vulcan carbon support and (c) cyclic voltammetry of the Pt supported Vulcan carbon catalyst in 1 M H_2SO_4/1 M CH_3OH run at 50 mV/s

.

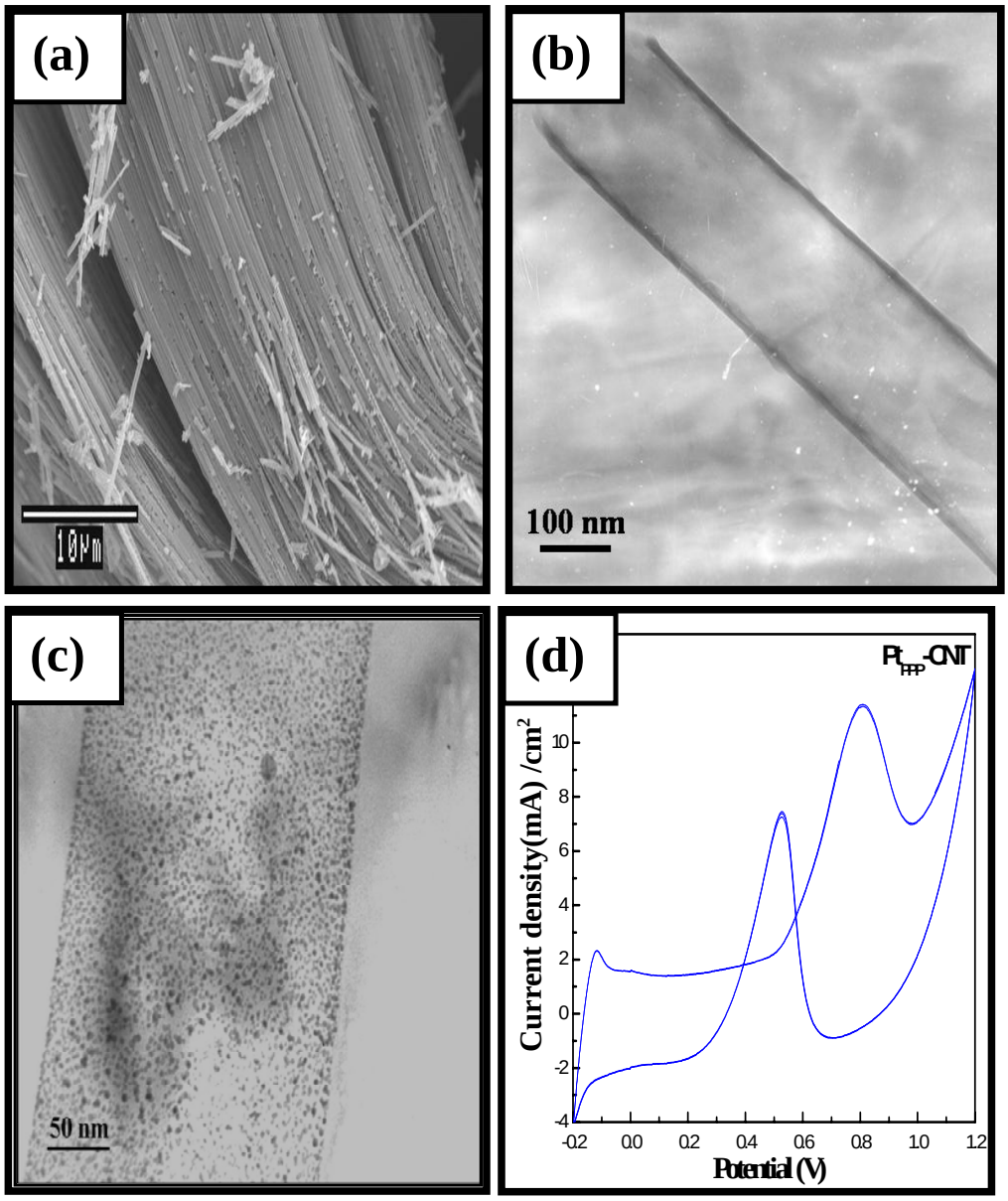

Fig. 3.4. (a) SEM Image of carbon nanotube support from poly paraphenylene (b) TEM image of carbon nanotube support (c) TEM image of Pt supported carbon nanotube support and (d) Cyclic voltammograms of GC/CNT_{PPP}-Pt-Nafion in 1 M H_2SO_4/1 M CH_3OH run at 50 mV/s

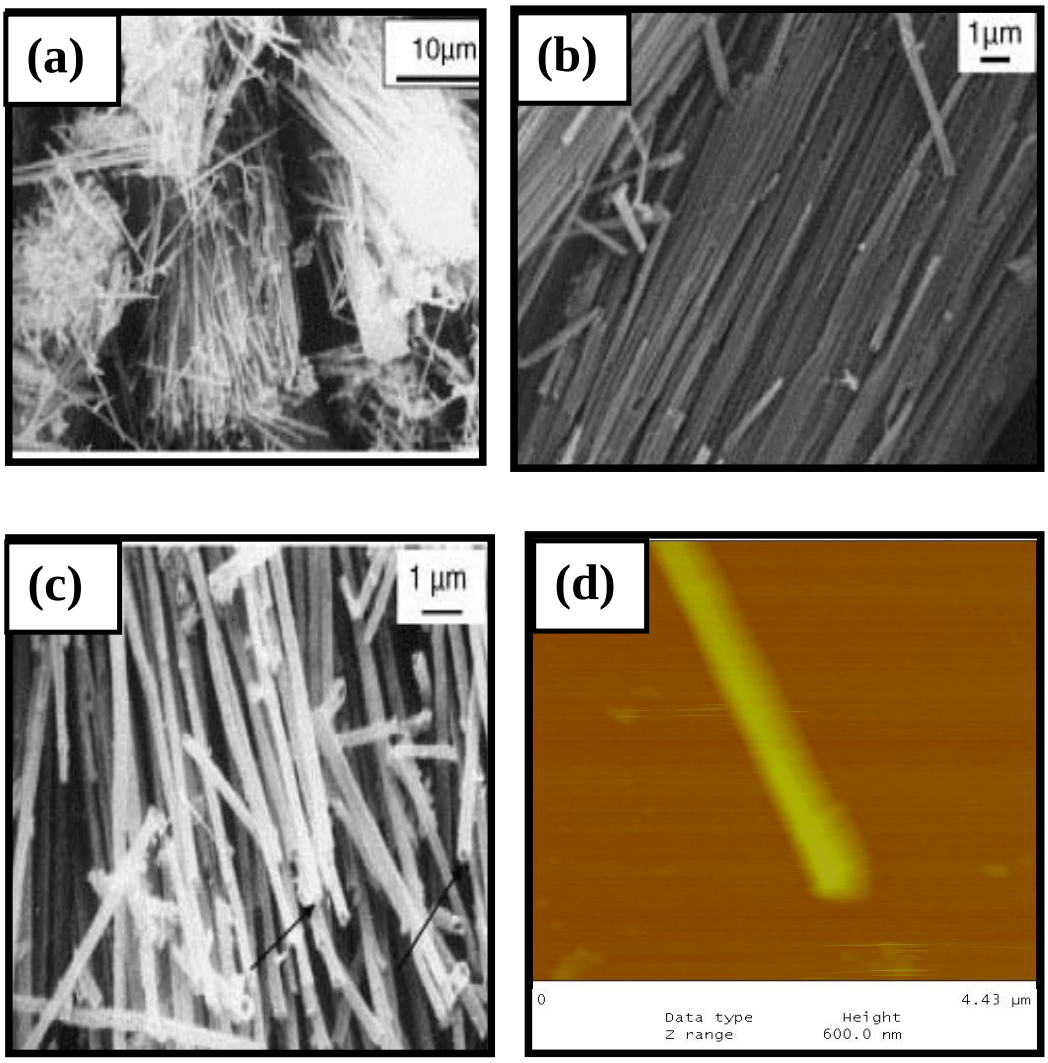

Fig. 3.5. (a)-(c) SEM images of N-CNTs from poly (vinyl pyrolidone) (d) AFM image of the N-CNT on silicon substrate

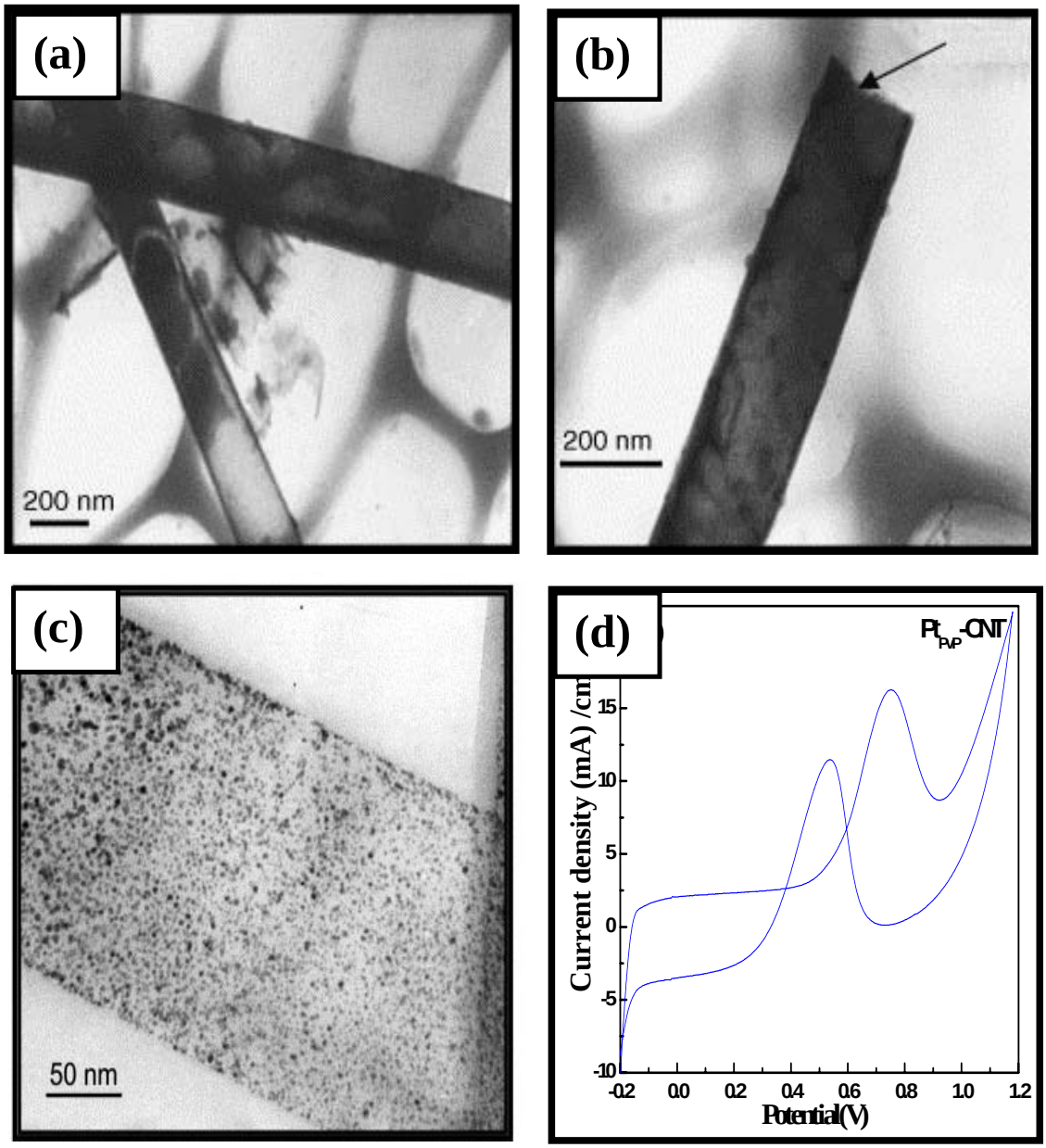

Fig. 3.6. (a)-(b) TEM images of N-CNTs from poly (vinyl pyrolidone) (c) TEM images of Pt deposited N-CNTs (d) Cyclic voltammogram of GC/CNT_{PVP}-Pt-Nafion in 1 M H_2SO_4/1 M CH_3OH run at 50 mV/s

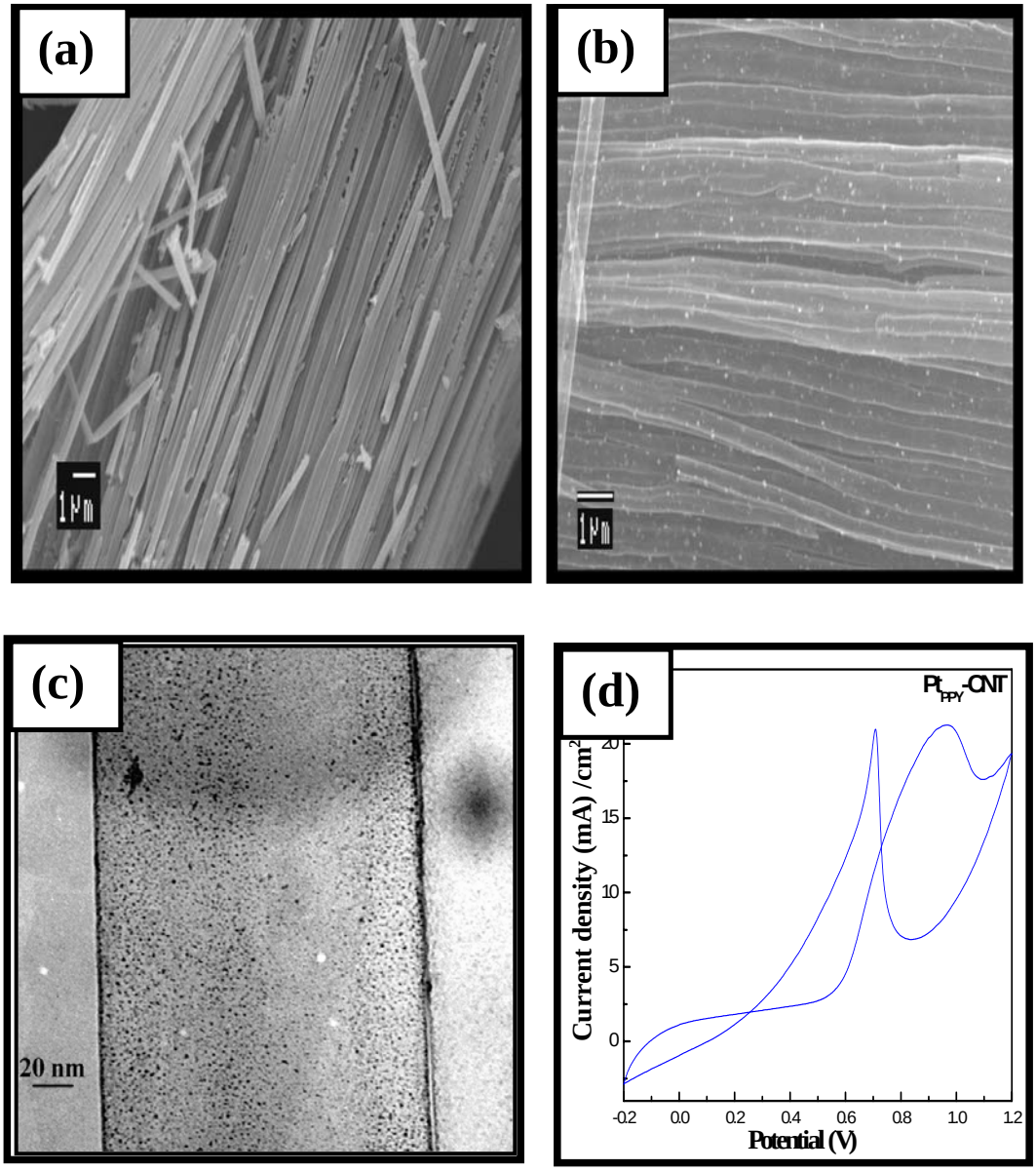

Fig. 3.7. Scanning electron micrographs of N-CNTs support from poly (pyrrole) (b) SEM images of Pt deposited N-CNTs (c) TEM images of Pt deposited N-CNTs (d) Cyclic voltammograms of GC/CNT_{PPY}-Pt-Nafion in 1 M H_2SO_4/1 M CH_3OH run at 50 mV/s

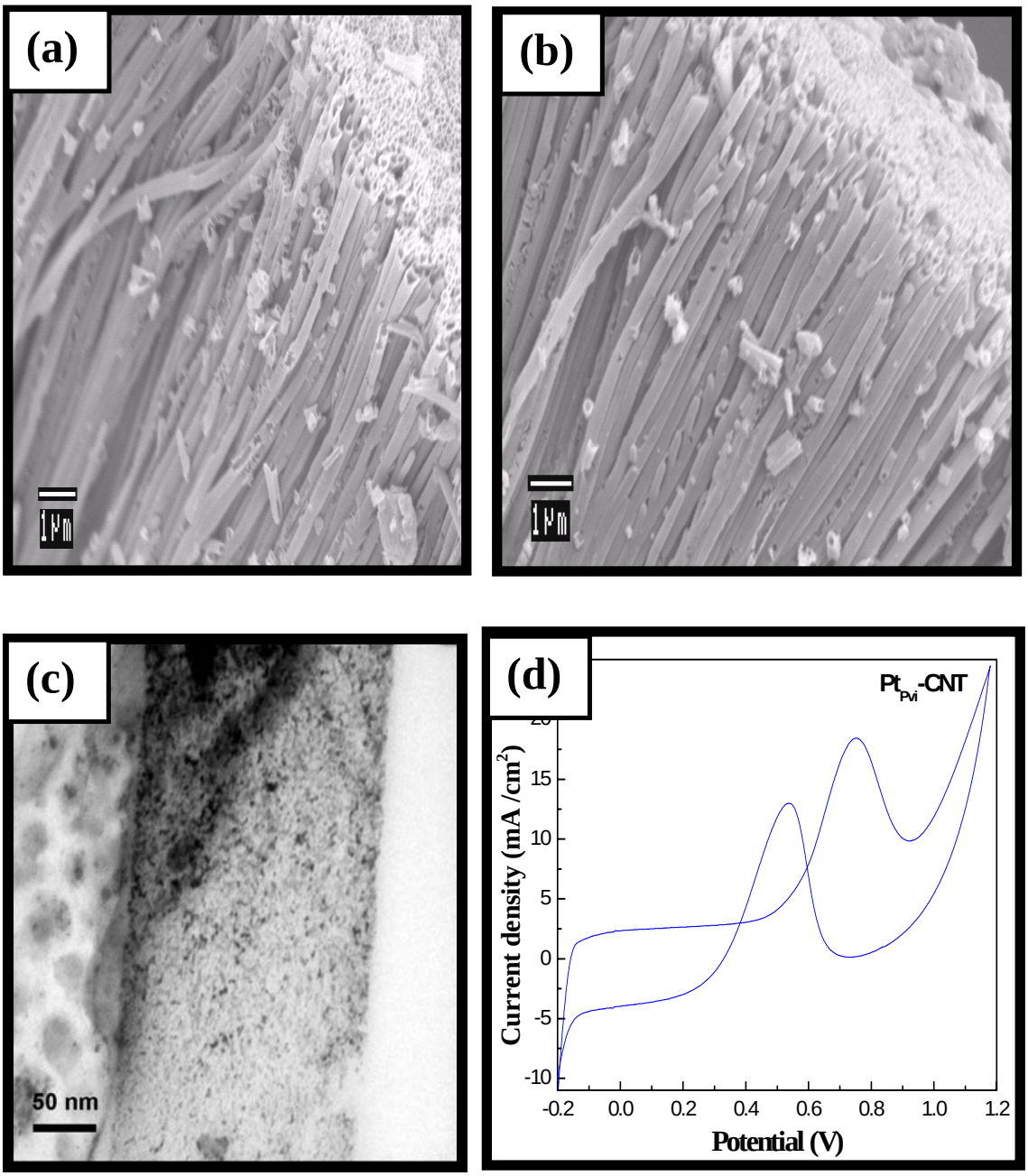

Fig. 3.8. (a-b) Scanning electron micrographs of N-CNTs support from poly (vinyl imidazole) (c) TEM images of Pt deposited N-CNTs and (d) Cyclic voltammograms of GC/CNT_{PVI}-Pt-Nafion in 1 M H_2SO_4/1 M CH_3OH run at 50 mV/s

3.4.3 Transmission Electron Microscopy study

The TEM images of Vulcan carbon support are as shown in Fig. 3.3b. The TEM image of the carbon nanotubes from poly paraphenylene is shown in Fig. 3.4 (b).

The open end of the tube was observed by TEM, which showed that the nanotubes were hollow and the outer diameter of the nanotube closely matches with the pore diameter of the template used i.e., with a diameter of 200 nm and a length of approx. 40–50 μm. Since no catalyst has been used for synthesis of nitrogen containing carbon nanotubes, it is worth pointing out that the nanotubes produced by template synthesis under normal experimental conditions are almost free from impurities.

The platinum catalyst has been supported on the nanotubes via impregnation. The TEM image of Pt nanoparticles deposited on CNT_{PPP} obtained from poly paraphenylene is shown in Fig. 3.4 (c) and the Pt particle size is 3.6 nm. TEM images of N-CNT_{PVP} obtained from poly (vinyl pyrolidone) are shown in Fig. 3.6 (a-b). It is evident from the images that there is no amorphous material present in the nanotube. Fig. 3.6(c) shows the TEM image of Pt nanoparticles filled N-CNT_{PVP} obtained from poly (vinyl pyrolidone). TEM pictures reveal that the Pt particles have been homogeneously dispersed on the N-CNT_{PVP} and particle sizes were found to be around 3 nm. Fig. 3.7(c) shows the TEM image of Pt nanoparticles filled N-CNT_{PPY} obtained from poly (pyrrole) and the Pt particle size is 2.6 nm. It can be seen from the images that there is no aggregation of Pt nanoparticles on the surface of the N-CNT, indicating that the surface functionalisation of the support also affects the dispersion of the Pt particles. The N-CNT anchors Pt particles effectively, leading to the high dispersion of Pt particles on their surface. The TEM pictures clearly revealed that the Pt particles have been homogeneously well dispersed on the nanotubes. Since the incorporation of nitrogen in CNT promotes the dispersion of nanoparticles on the surface. Further increase in the nitrogen content on the carbon nanotube surface, the Pt particle tends to agglomerate as shown in Fig. 3.8(c) and their particle size tends to increase and average particle size was found to be around 3 nm. The particle size of Pt

for the CNT supported electrode shows particle size of around 3.2 nm while the N-CNT supported electrode with nitrogen content 10.5 % shows particle size of around 2.3 nm.

3.5 ELECTRO-CATALYTIC ACTIVITY OF THE CATALYST

Platinum is the best electro-catalyst for methanol oxidation reaction in direct methanol fuel cells (DMFC). The dispersion of platinum nanoparticles on the support greatly affects the activity of the catalyst. Hence, the modification of the support surface to create surface functional groups compatible to Pt becomes the only choice. The electro-catalytic activity of methanol oxidation of the Pt/N-CNT electrodes with variation in nitrogen content has been evaluated, which is then compared with that of the Pt/CNT electrode and the conventional carbon supported platinum (E-TEK, Pt/C 20 wt %) electrode. The cyclic voltammograms of bulk Pt and commercial E-TEK catalysts in 1 M H_2SO_4 / 1 M CH_3OH run at a scan rate of 50 mV/s are shown in Fig. 3.2 (d). The cyclic voltammograms of methanol oxidation activities of Pt supported on the CNT and N-CNT electrodes with variation in nitrogen content was evaluated.

It is evident that the oxidation current observed with the Pt supported N-CNT_{PPY} electrode with 10.5 % nitrogen content is showing more than sixteen fold increase in the current compared to 20 wt % Pt/C (E-TEK) electrode. The Pt/N-CNT_{PPY} electrode with 10.5 % nitrogen content is showing higher electrocatalytic activity for methanol oxidation than the other N-CNT, CNT electrode and commercial 20-wt % Pt/C (E-TEK) electrode. Pure bulk Pt electrode is showing an activity of 0.167 mA/cm^2. The Pt/N-CNTs showed a higher activity of 11.3 mA/cm^2 compared to that of Pt/CNT, which shows an activity of 7.9 mA/cm^2. Whereas the conventional 20-wt % Pt/C (E-TEK) electrode shows a lesser activity of 1.3 mA/cm^2 compared to the carbon

nanotube supported electrode. These differences, which are related to both the functional groups of the support and the particle size, lead to structures that will ultimately serve to influence the catalytic activity. The higher electrocatalytic activity of the N-CNT electrode is due to higher dispersion and a good interaction between the support and the Pt particles.

The Vulcan carbon support has randomly distributed pores of varying sizes which may make fuel and product diffusion difficult whereas the tubular three-dimensional morphology of the nitrogen containing carbon nanotube makes the fuel diffusion easier. The Vulcan carbon contains high levels of sulfur (ca. 5000 ppm or greater), which could potentially poison the fuel-cell electrocatalysts (Swider and Rolison; 1996). The Pt particles can be anchored to the surface of the carbon nanotubes by nitrogen functional groups. The Pt particles coordinating with the nitrogen on the surface determines the strength of the metal-support interaction. The observed effect of metal–support interaction between N-CNT and platinum may have a control in the growth of a particular crystalline plane of Pt. Consequently, the metal-support interaction greatly influences the methanol oxidation activity. According to the model of van Dam and van Bekkum the ionization behaviour of the carbon surface based on independent acid and basic groups, leads to the conclusion that the acidic oxygen surface groups should be considered as weak anchoring sites (Swider and Rolison; 2000). On this basis, the carbon surface basic sites of nitrogen act as anchoring sites for the hexachloroplatinic anion and are responsible for the strong adsorption of platinum on the carbon nanotube surface. The nature of the carbon surface basic sites is still a subject of discussion. The carbon surface basic sites are frequently associated with pyrone like structure. In N-CNT, the surface active sites are essentially of Lewis type and are associated with the π-electron rich regions within the basal planes.

The nitrogen functionality on the carbon surface develops basic sites with moderate strength and shows strong interaction with H_2PtCl_6 during impregnation, which would favour the Pt dispersion on the carbon surface. The high Pt dispersion on the nitrogen containing carbon nanotubes support is attributed to the surface properties of the carbon nanotubes, resulting in strong Pt/N-CNT interaction.

Table 3.1. Electrocatalytic activity of nitrogen containing carbon nanotube supported Pt electrodes for methanol oxidation

Electrode	Nitrogen content (%)	Activity Ip (mA/cm^2)
Pt	-	0.076
GC/ 20% Pt/C (ETEK)Naf	-	1.3
GC/CNT_{PPP}-Pt -Naf	0.0	12.4
GC/CNT_{PVP} -Pt -Naf	6.63	16.2
GC/CNT_{PPY} -Pt -Naf	10.5	21.4
GC/CNT_{PVI}-Pt -Naf	16.7	18.6

The N-CNT electrodes show higher catalytic activity compared to CNT electrodes, which shows the catalytic effect of nitrogen functionalisation on the carbon nanotubes. Finally, the dispersed platinum electrodes obtained by stabilization of colloidal metallic particles on N-CNT support with nitrogen content 10.5 % display a high activity for the oxidation of methanol. Therefore it is likely that the influence of the composition of the support and in particular the nitrogen functionalisation of the carbon nanotube support directly influences the catalytic properties of the Pt particles. In addition, particle aggregation is not observed indicating that the surface morphology of the support also affects the dispersion of the Pt particles. The nitrogen containing carbon nanotubes lead to higher dispersion of Pt particles on its surface,

which is attributed to the surface properties of the nitrogen containing carbon nanotube and this result in a strong Pt/N-CNT interaction. On the contrary, lack of active sites on CNT results in fewer but larger Pt particles on the surface of CNT.

In order to see the effect of the nitrogen content in the carbon nanotube, the catalytic activity was evaluated by increasing the percentage of nitrogen in the carbon nanotube from zero to 16.7 %. The variation of nitrogen content has been done by fixing the polymer source. It is evident from Table 3.1. The catalytic activity for methanol oxidation increases as nitrogen content increases. There is a decrease in the activity when nitrogen content is increased above 10.5 %. The nitrogen containing carbon nanotubes prepared from polypyrrole precursor shows high catalytic activity and stability towards methanol oxidation.

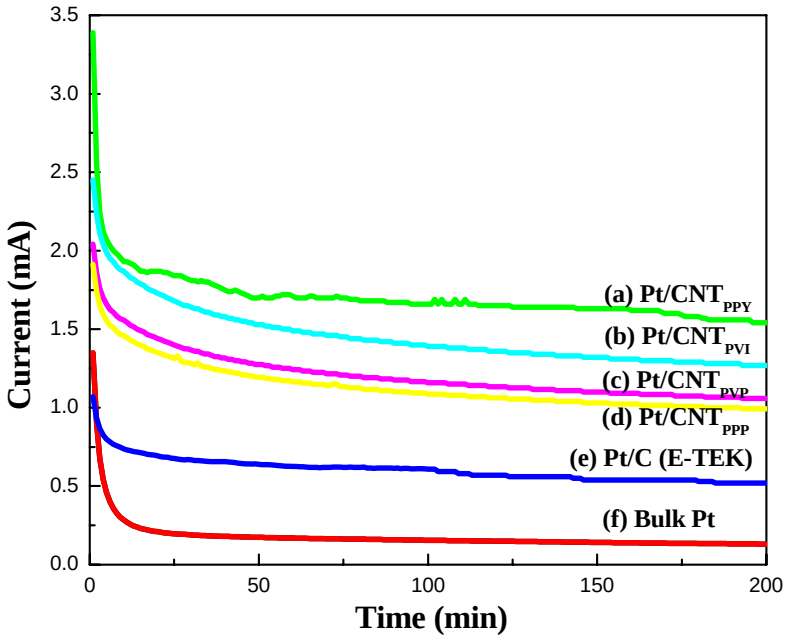

Fig 3.9. Chronoamperogram curves for (a) Pt/N-CNT_{PPY}, (b) Pt/N-$CNT_{PVI,}$ (c) Pt/N-CNT_{PVP} (d) Pt/CNT_{PPP}, (e) carbon supported platinum, (f) 20-wt % Pt/C (E-TEK) and (g) Pt measured in 1 M H_2SO_4 + 1 M CH_3OH. The potential was stepped from the rest potential to 0.6 V vs. Ag/AgCl

3.6 CHRONOAMPEROMETRY OF THE CATALYST

Chronoamperometry was used to characterize the stability of the electrodes. Long-term stability is very important for practical applications. The current density-time plots of various electrodes in 1 M H_2SO_4 and 1 M CH_3OH at 0.6 V are shown in Fig. 3.10. The performance of Pt electrodes was found to be poor compared to that of the E-TEK, Pt/CNT and Pt/N-CNT electrodes. The N-CNT supported electrodes are found to be the most stable for direct methanol oxidation. The increasing order of stability of various electrodes is: Pt < Pt/Vulcan (E-TEK) < Pt /CNT_{ppp} < Pt /N-CNT_{pvp} <Pt/N-CNT_{Pvi} <Pt/N-CNT_{Ppy}. It must be noted that the current density (specific activity) and stability is the highest for the Pt/N-CNT_{ppy} electrodes. It is also found that the metal particle distribution on the N-CNT support and metal-support interactions are important parameters contributing to the activity of the catalyst. Thus, the higher activity of the Pt/N-CNT_{PPY} electrode with 10.5 % nitrogen content may be attributed to the small particle size, higher dispersion of platinum and the nature of CNTs supports (metal-support interaction).

3.7 CONCLUSIONS

In summary, the dispersion and electro-catalytic activity of platinum nanoparticle on nitrogen containing carbon nanotubes with variation in nitrogen content have been investigated. The amount of nitrogen in the CNT plays an important role as observed by the increase in activity and stability of methanol oxidation with Nitrogen content, probably due to the hydrophilic nature of the CNT. It is found that the Pt particles supported on N-CNT with 10.5 % nitrogen content show excellent electrocatalytic activity for methanol oxidation than the CNT and the commercial carbon supported platinum (E-TEK) electrodes. Higher activity of Pt nanoparticles supported N-CNT

has been discussed based on the metal-support interaction. The use of N-CNT as supports for Pt electrodes shows higher electro-catalytic activity, involving high platinum dispersion, strong metal-support interaction and high stability, which are important practical considerations in fuel cell technology.

CHAPTER 4

SYNTHESIS AND ELECTRO-OXIDATION OF METHANOL ON TiO_2 NANOTUBE SUPPORTED PLATINUM ELECTRODES

4.1 INTRODUCTION

Titanium dioxide (TiO_2) has been widely investigated as a key material for applications in photovoltaic cells, batteries, chemical sensing (Varghese *et al.,* 2003), optical emissions, photonic crystals, catalysis, photocatalysis (Livraghi *et al.,* 2005) and environmental pollutant decomposition (Obare *et al.,* 2005). Anatase TiO_2 electrodes are used in solar cells, lithium batteries and electrochromic devices (Hagfeldt and Gratzel 1995; Kavan *et al.,* 2000; Gratzel 2001). Nanocrystalline form of anatase TiO_2 is a promising electrode material for Li-ion batteries owing to its good Li-storage capacity, cycling-stability and safety against overcharging (Huang *et al.,* 1995, Subramanian *et al.,* 2006). Non-toxicity, environmental compatibility and low price are the other practical advantages of TiO_2. As a catalyst and/or catalyst support, it is employed in the processes of photo degradation of chlorine hydrocarbons. Recently, efforts have been directed to obtain nanostructured TiO_2-based materials with a large specific surface area. The energy band structure becomes discrete for titanium dioxide of nanometer scale, and its photophysical, photochemical, and surface properties are quite different from those of the bulk. This is due to the quantum size effect. TiO_2-based nanotubes have attracted wide attention owing to their potential for application in highly efficient photocatalysis (Adachi *et al.,* 2000), lithium ion batteries (Zhou *et al.,* 2003), photovoltaic cells (Zhu *et al.,* 2007; Adachi *et al.,* 2002; Uchida *et al.,* 2002) and environmental applications (Quan *et al.,* 2005).

Titanium dioxide is an attractive system for electrocatalysis, since if used as the support for metallic catalysts or electrocatalysts; it may enhance their catalytic activity on the basis of strong metal support interaction (SMSI) (Wang *et al.,* 2005, Lee *et al.,* 2004). TiO_2 is an effective photocatalyst for the oxidation of methanol (Mandelbaum *et al.,* 1999). Pt/TiO_2 is stable in acidic or alkaline medium and possesses higher active surface area than Pt. Pt/TiO_2 shows high activity for oxygen reduction (Baez *et al.,* 1995; Xiong *et al.,* 2004, Shim *et al.,* 2001). There are several articles which deal with the methanol oxidation reaction on TiO_2 supported Platinum catalysts (Hayden *et al.,* 2001; Ioroi *et al.,* 2005). Titanium mesh supported electrodes showed high activity for the methanol oxidation. Therefore it appears to be a promising alternative to carbon-supported catalysts (Yu *et al.,* 2004). More important in the present case, Pd/TiO_2 nanotube has been recently shown to act as a good catalyst for the oxidation of methanol (Wang *et al.,* 2005).

Many approaches, such as a template-assisted method (Sander *et al.,* 2004), electrochemical anodic oxidation of pure titanium sheet (Gong *et al.,* 2001; Macak *et al., 2005),* and methods involving chemical treatment of fine titania particles (Kasuga, *et al.,* 1998; Du *et al.,* 2001), have been reported to fabricate TiO_2 nanotubes. There are advantages and limitations in each of the above-mentioned methods. However, technical problems may arise from the difficulties in achieving uniform inner diameter of titanium oxide nanotubes. In addition, oriented nanostructures of the TiO_2 nanotubes are often more desirable for applications in photovoltaic cells, sensing, catalysis and photocatalysis. Template-synthesis method has been used to prepare nanotubes or fibrils of electronically conducting polymers (Martin *et al.,* 1993), metals (Martin 1996), semiconductors (Lakshmi *et al.,* 1997) and carbon nanotubes (Maiyalagan and Viswanathan 2005). This method entails synthesis of a

desired material within the pores of an alumina membrane, which has cylindrical pores with monodisperse diameters. The tubule of the desired material is obtained within each pore. This template approach is proved to be a versatile method for synthesizing nanomaterials because the aspect ratio of the nanostructures prepared *via* this method can be controlled.

The present work focuses on the efforts undertaken to develop unconventional supports based on platinum catalysts for methanol oxidation. The catalyst supported on metal oxide nanotubes yields a better dispersion and shows better catalytic activity. TiO_2 nanotubes of the anatase form have been synthesized by sol gel method using anodic aluminium oxide (AAO) as the template. TiO_2 nanotubes were used to disperse the platinum particles effectively without sintering and to increase the catalytic activity for methanol oxidation. The tubular morphology and the oxide nature of the support have influence on the dispersion as well as the catalytic activity of the electrode. Titanium dioxide is also known to have strong metal support interaction with Pt particles. The present chapter deals with the preparation of highly dispersed platinum supported on TiO_2 nanotubes. The catalytic activities for the methanol oxidation of the electrodes have been evaluated and a comparison with the catalytic activity of conventional electrodes is made.

4.2 EXPERIMENTAL

4.2.1 Synthesis of TiO_2 nanotubes

Titanium isopropoxide (5 mL) was added to 25 mL of 2-propanol (mole ratio $[Ti^{4+}]$/[2-propanol] = 1:20). The solution was stirred for 3 h at room temperature (298 K). The alumina template membrane was dipped in the solution for 2 min. After removal from the solution, vacuum was applied to the bottom of the membrane

until the entire volume of the solution was pulled through the membrane. The membrane was then air-dried for 60 min at 303 K, and then placed in a furnace (in air) with a temperature ramp of 2 ^{o}C min^{-1} to 873 K for 2 h. The temperature was then decreased at a ramp rate of 2 ^{o}C min $^{-1}$ to room temperature (303 K) (Lee *et al.,* 2004).

4.2.2 Synthesis of Pt/TiO_2 nanotubes

The TiO_2/alumina composite obtained (before the dissolution of template membrane) was immersed in 73 mM H_2PtCl_6 (aq) for 12 h. After immersion, the membrane was dried in air and the ions were reduced to the corresponding metal(s) by exposure to flowing H_2 gas at 823 K for 3 h. The resulting composite was immersed into 3 M aqueous NaOH for several minutes to dissolve the alumina template membrane. This procedure resulted in the formation of Pt nanoclusters loaded TiO_2 nanotubes.

4.3 CHARACTERIZATION METHODS

The scanning electron micrographs were obtained using JEOL JSM-840 model, working at 15 keV after the removal of alumina template. For transmission electron microscopic studies, the nanotubes dispersed in ethanol were placed on the copper grid and the images were obtained using Phillips 420 model, operating at 120 keV. The UV-Vis absorption spectra were obtained on a Cary 5E spectrophotometer. Micro-Raman scattering experiments were performed on a Bruker FRA106 FT-Raman at room temperature in a quasi-backscattering geometry with parallel polarization incident light. The excitation source used was an Argon ion laser operating at 514.5 nm with an output power of 20 mW. The X-ray diffraction patterns were obtained on a Philips PW 1820 diffractometer with Cu K_α (1.54178 Å) radiation.

4.4 UV-VIS ABSORPTION SPECTROSCOPY

Fig. 4.1 shows the UV-Vis absorption spectra of the anatase TiO_2 nanotube compared with that of the Degussa TiO_2. The spectral lines for both TiO_2 nanotubes and bulk TiO_2 exhibit only one characteristic absorption band which is assigned to the intrinsic transition from the valence band (VB) to the conduction band (CB). An absorbance below 370 nm was observed for the TiO_2 nanotube, which is ascribed to bulk anatase TiO_2. Here the blue shift of absorption maximum with higher band energy of TiO_2 nanotubes compared with that of the bulk TiO_2 can be attributed to the quantum-size effect (Takagahara and Takeda 1992).

4.5 RAMAN SPECTRA

The Raman spectra of fabricated anatase TiO_2 nanotubes and Degussa TiO_2 are shown in Fig. 4.2.The result of XRD analysis is supported by the Raman spectra of TiO_2 nanotubes as shown in Fig. 4(b). The vibration mode symmetries of the anatase are indicated. Raman peaks at 156.9, 206, 408.48, 529.54, 649.54 and 801 cm^{-1} were assigned to E_g, E_g, B_{1g}, A_{1g}, E_g and B_{1g}, respectively. The positions and intensity of the six Raman active modes correspond well with the anatase phase of TiO_2 (Lei *et al.,* 2001; Bersani and Lottici 1998). A weak overtone scattering (B_{1g}) at 801 cm^{-1} was observed in this study. Overtone can be found in both bulk Degussa TiO_2 and nanotube, but the intensity of overtone is very less in bulk Degussa TiO_2. This is due to the large intensity ratio of fundamental peak to overtone one makes it difficult to be observed. While for nanotube, the decreasing ratio makes it easy to be observed. No significant broadening and shift of Raman spectra were found when one compared the obtained anatase-TiO_2 nanotube with that of the bulk DegussaTiO_2.

4.6 ELECTRON MICROSCOPY STUDY

4.6.1 Scanning Electron Microscopy (SEM)

The scanning electron microscopic (SEM) images of the TiO_2 nanotubes obtained after dissolving the 200 nm alumina template membrane is shown in Fig. 4.3. It can be seen from the Fig. that an ordered array of nanotubes with uniform diameter and length is formed.

4.6.2 Transmission Electron Microscopy (TEM)

The open end and the hollow nature of the TiO_2 nanotubes is also confirmed by transmission electron microscopy (TEM) image as shown in Fig. 4.4a. The outer diameter of the nanotubes is ca. 200 nm, retaining the size and near cylindrical shape of the pores of the aluminium oxide template membrane. The TEM image of a Pt/TiO_2 nanotube electrode is shown in Fig. 4.4b, which shows that the Pt particles are highly dispersed on the TiO_2 nanotube support. The Pt particle size was found to be around 3-4 nm while their crystal structure is confirmed by the XRD method. The optimal Pt particle size for reactions in the H_2/O_2 fuel cell is around 3 nm (Kinoshita *et al.,* 1990). The importance of the Pt particle size on the activity for methanol oxidation is due to the structure sensitive nature of the reaction and the fact that particles with different sizes will have different dominant crystal planes and hence different intercrystallite distances which might influence methanol adsorption. The commercial Pt/C has a high specific surface area but contributed mostly by micropores less than 1 nm and are therefore more difficult to be fully accessible. It has been reported that the mean value of particle size for 20% Pt/Vulcan (E-TEK) catalyst was around 2.6 nm (Antolini *et al.,* 2001). The TiO_2 nanotube matrix of anatase form can provide hydroxide ions to remove CO poisoning. Methanol oxidation studies on the prepared electrode have been carried out using cyclic voltammetry.

4.7 X-RAY DIFFRACTION STUDY

The XRD patterns of the Pt/TiO_2 nanotubes as well as P-25 are shown in Fig. 4.5. Rutile and anatase were seen by XRD in P25 titania, but rutile was not seen in the TiO_2 nanotubes. The diffractograms of the synthesized TiO_2 nanotubes mainly belong to the crystalline structure of anatase TiO_2. XRD pattern of the TiO_2 nanotubes evidenced the presence of anatase as the main phase. After Pt deposition, the colour of the TiO_2 nanotubes changed to dark gray and during reduction of Pt, oxide reduction takes place and new diffraction peaks are formed. The presence of Pt could be observed at diffraction angle of 39.8° indexed to (1 1 1) plane of metallic Pt. However the peak intensity is relatively weak, presumably due to the combination of its low content and small particle size.

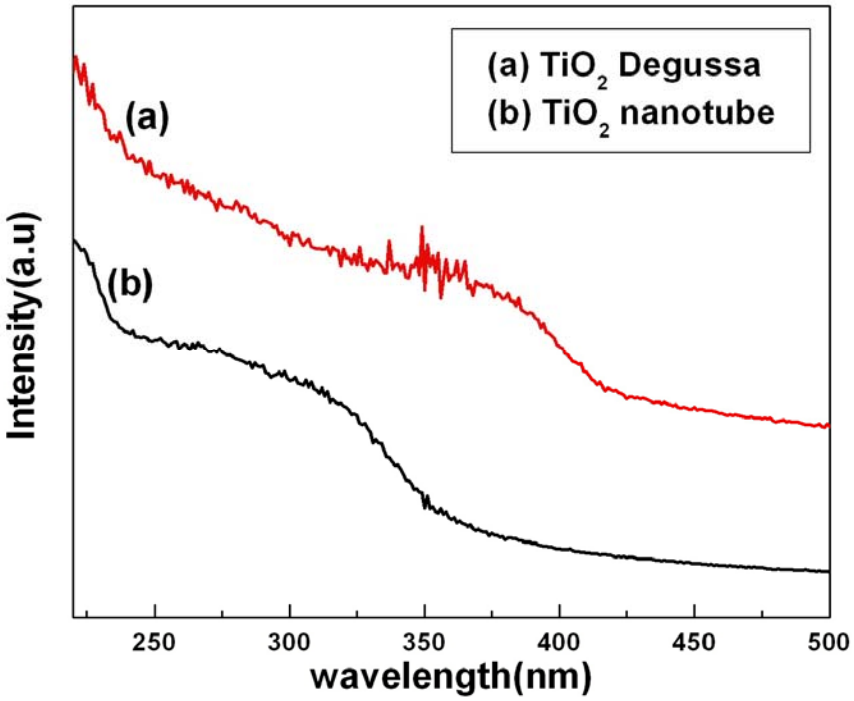

Fig. 4.1. UV–Vis absorption spectra of (a) Degussa TiO_2 and (b) anatase TiO_2 nanotube

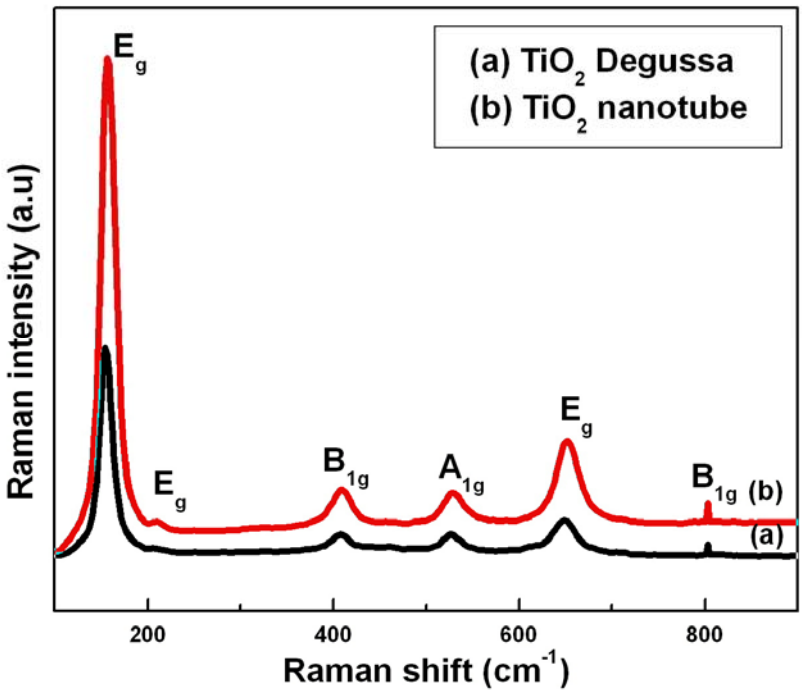

Fig. 4.2. Raman spectra of (a) Degussa TiO_2 and (b) fabricated anatase-TiO_2 nanotube (The vibration mode symmetries of the anatase are indicated)

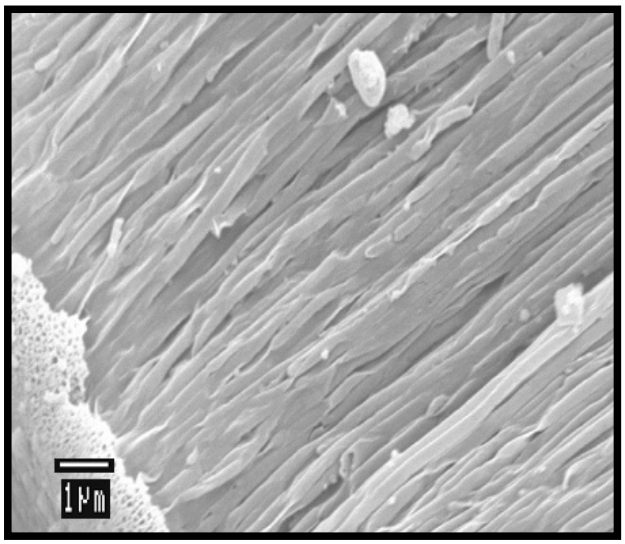

Fig. 4.3. SEM image of TiO_2 nanotubes obtained by sol gel method calcined at 650° C for 2 h

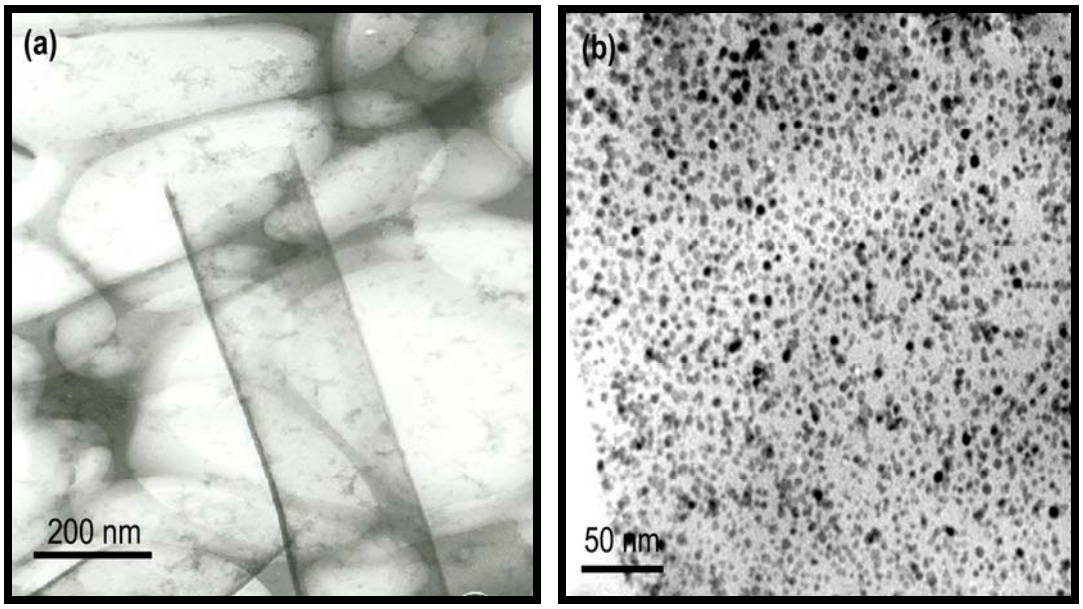

Fig. 4.4. TEM images of (a) TiO_2 nanotubes obtained by sol gel method calcined at 650 ^{0}C for 2 h (b) Pt filled TiO_2 nanotubes

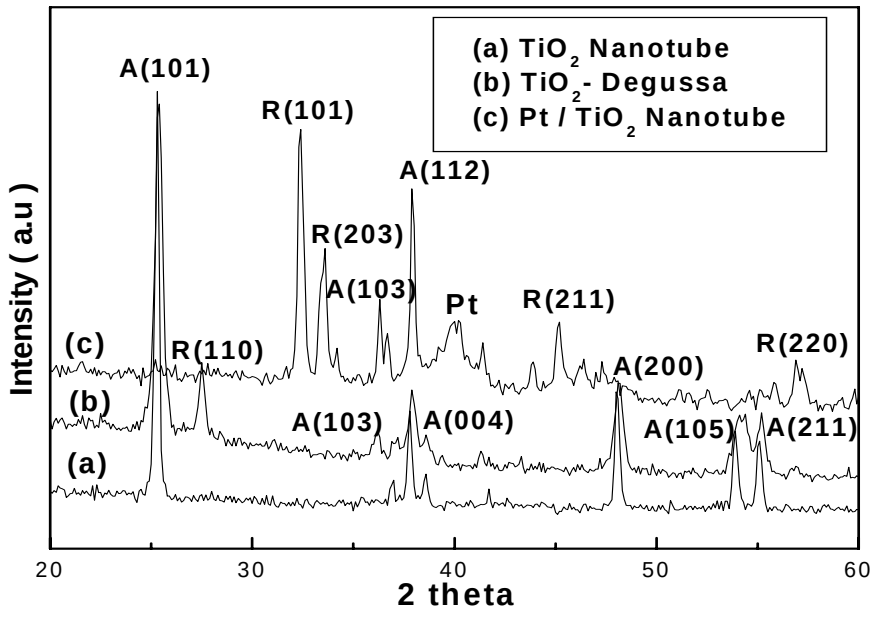

Fig.4. 5. X-ray diffraction patterns of (a) Degussa TiO_2 as a reference (b) TiO_2 nanotube and (c) Pt / TiO_2 nanotube

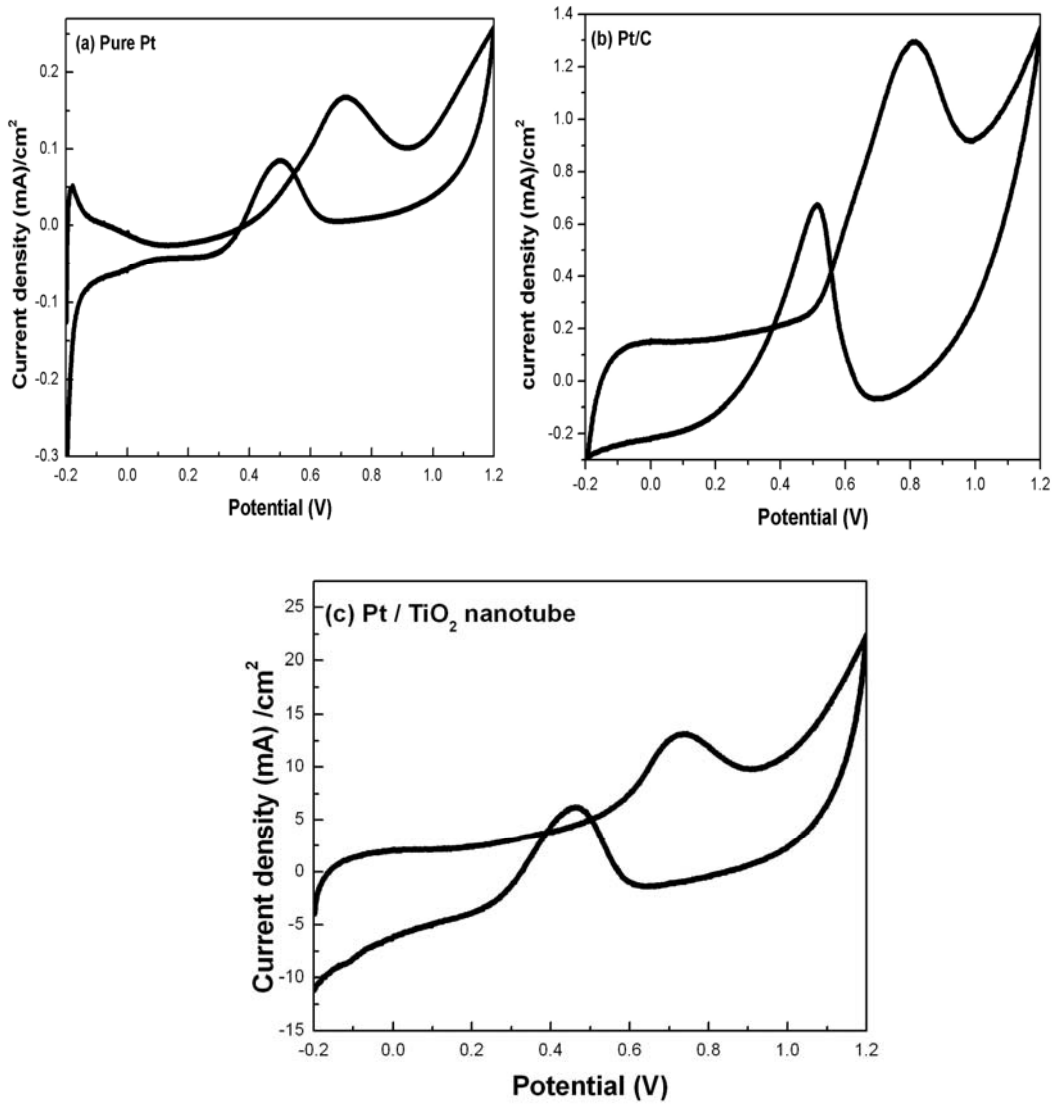

Fig. 4. 6. Cyclic voltammograms of (a) pure Pt, (b) Pt/C and (c) Pt/TiO_2 nanotube in 0.5 M H_2SO_4/1 M CH_3OH run at 50 mV/s (area of the electrode = 0.07 cm^2)

4.8 ELECTROCHEMICAL MEASUREMENTS

The catalyst was electrochemically characterized by cyclic voltammetry (CV) using an electrochemical analyzer (Bioanalytical Sciences, BAS 100). A common three-electrode electrochemical cell was used for the measurements. The counter and reference electrodes were a platinum plate (5 cm^2) and a saturated Ag/AgCl electrode respectively. The CV experiments were performed using 1 M H_2SO_4 solution in the

presence of 1 M CH_3OH at a scan rate of 50 mV/s. All the solutions were prepared by using ultra pure water (Millipore, 18 MΩ). The electrolytes were degassed with nitrogen before the electrochemical measurements.

4.8.1 Preparation of Working Electrode

Glassy Carbon (GC) (Bas Electrode, 0.07 cm^2) was polished to a mirror finish with 0.05 μm alumina suspensions before each experiment and served as an underlying substrate of the working electrode. In order to prepare the composite electrode, the nanotubes were dispersed ultrasonically in water at a concentration of 1mg ml^{-1} and 20 µl aliquot was transferred on to a polished glassy carbon substrate. After the evaporation of water, the resulting thin catalyst film was covered with 5 wt% Nafion solution. Then the electrode was dried at 353 K and used as the working electrode.

4.9 EVALUATION OF METHANOL OXIDATION ON Pt/TiO_2 NANOTUBE ELECTRODES

In order to evaluate the electrocatalytic activity of the Pt/TiO_2 nanotube electrodes for the oxidation of methanol, cyclic voltammetric studies were carried out in 0.5 M H_2SO_4 and 1 M CH_3OH. During the anodic scan, the current increases due to dehydrogenation of methanol followed by the oxidation of absorbed methanol residues and reach a maximum in the potential range between 0.8 and 1.0 V versus Ag/AgCl. In the cathodic scan, the re-oxidation of the residues is observed. On the whole, the behaviour of the Pt/TiO_2 nanotube electrodes was found to be similar to that of Pt. This suggests that the electrooxidation reaction takes place on the Pt nanoparticles, dispersed on the TiO_2 nanotube, involves basically the same reaction mechanism.

Table 4.1: Electrocatalytic activity of Pt/TiO_2 nanotube catalysts for methanol oxidation

Electrocatalyst	Specific activity ($mA\ cm^{-2}$)	Mass activity ($mA\ mg^{-1}$ Pt)
Bulk Pt	0.167	-
Pt/C	1.3	3.25
Pt/TiO_2 nanotube	13.2	33

The results of the voltammetric curves for the oxidation of methanol obtained with the Pt/TiO_2 nanotube, Pt and Pt/C (E-TEK) electrodes are shown in Fig. 4.6. The Pt/TiO_2 nanotube shows a higher current density of 13.2 mA/cm^2 compared to Pt/C (E-TEK) electrodes (1.23 mA/cm^2). The specific activity and the mass activity for the different electrodes are given in Table 4.1. The results show high electrocatalytic activity for methanol oxidation for Pt/TiO_2 nanotube electrode. It is evident that the mass activity observed with the Pt supported TiO_2 nanotubes shows around ten-fold increase in current than Pt/C (E-TEK) electrode. The Pt/TiO_2 nanotube catalyst had a better electrocatalytic activity for methanol oxidation when compared with that of bulk Pt and Pt/C (E-TEK) catalysts. This higher catalytic activity can be mainly attributed to remarkably platinum active reaction sites on the nanotube oxide matrix and the role of the TiO_2 nanotube facilitates as a path for methanol (CH_3OH) as a fuel and Protons (H^+) produced during an electrochemical reaction.

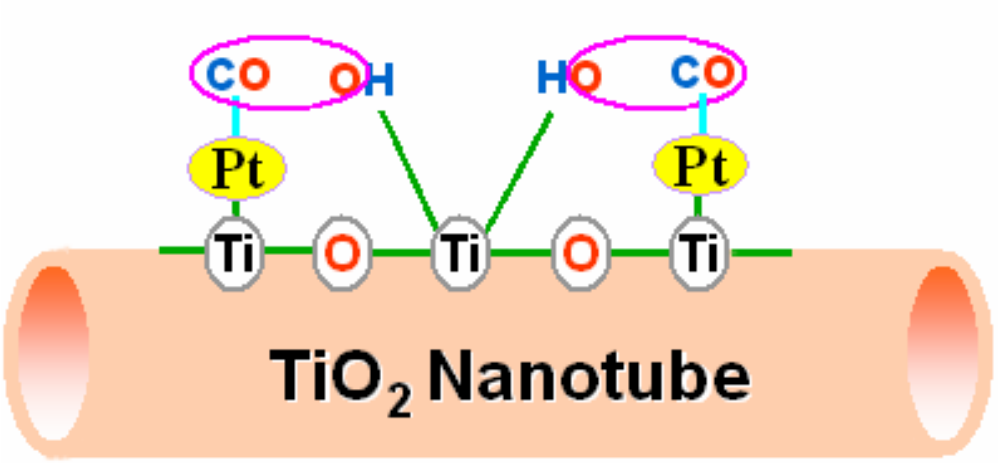

Fig. 4. 7. A possible mechanism for the removal of CO poisoning intermediates during methanol oxidation over TiO_2 nanotube supported Pt catalysts

Pt deposited onto metal oxides nanotubes, such as TiO_2, as methanol oxidation DMFC catalysts, exploiting the strong metal support interaction (SMSI). These catalysts showed good resistance to CO poisoning and had enhanced activity. The anatase form of TiO_2 nanotube, rather than rutile, was identified as contributing most performance enhancement. It is possible that TiO_2 nanotube functions in the same way as Ru does in Pt-Ru/C catalysts because hydroxide ion species could easily form on the surface of the TiO_2 nanotubes. The formation of hydroxide ion species on the surface of the TiO_2 nanotubes transforms CO like poisoning species on Pt to CO_2, leaving the active sites on Pt for further electrochemical reaction has been shown in Fig. 4.7 (Huaxin *et al.,* 1999; Takeuchi, *et al.,* 2005). The participation of the TiO_2 nanotube support. The high dispersion of Pt particles on TiO_2 nanotube electrode, OH groups generated near the Pt-oxide interface promote CO removal, and strong metal support interaction (SMSI) could be a reason for enhanced electrocatalytic activity for methanol oxidation (Tauster *et al.,* 1978; Neophytides, *et al.,* 2005).

4.10 CONCLUSIONS

The Pt was deposited on TiO_2 nanotubes in order to study the effect of the properties of the support for methanol oxidation reaction. The Pt/TiO_2 nanotube catalyst exhibits high electrocatalytic activity for methanol oxidation compared to the commercial E-TEK catalysts. Overall, the relative activities are of the order Pt/TiO_2 nanotubes > E-TEK > pure Pt. The observed improved catalytic activity of Pt/TiO_2 nanotube catalysts can be due to oxidation of CO to CO_2 by the surface hydroxyl groups of TiO_2 nanotube support which otherwise poison the active Pt sites. The electronic interaction between TiO_2 support and the Pt particles could also be another factor contributing to the observed higher activity. Further study on the detailed mechanism and stability of the TiO_2 nanotube supported catalysts are now under progress.

CHAPTER 5

SYNTHESIS AND ELECTRO-CATALYTIC ACTIVITY OF Pt SUPPORTED ON WO_3 NANORODS – ALTERNATE ANODES FOR METHANOL OXIDATION IN DIRECT METHANOL FUEL CELL

5.1 INTRODUCTION

Platinum supported on metal oxides has received attention in recent years, mainly because of its potential utility in anodes in direct methanol fuel cells (Ren *et al.,* 2004; Macak *et al.,* 2005; Hepel *et al.,* 2006; Wang *et al.,* 2005; Maiyalagan *et al.,* 2006; Gu and Wong 2006; Xu and Shen 2004; Huang *et al.,* 2006). Most often the catalyst is dispersed on a conventional carbon support and the support material influences the catalytic activity through metal support interaction. In order to achieve better dispersion of the metal, as well as to derive maximum activity from the dispersed metal sites, one has to adopt some innovative strategies. A strategy is to preferentially promote the oxidation of the intermediate species (partial oxidation products of methanol like CO and other partially dehydrogenated species) on other sites so that the noble metal sites are still available and free for the electrochemical oxidation of the fuel (Gutierrez *et al.,* 2003; Wang *et al.,* 2001). However, it is essential that the additional components employed for the reaction of the inhibiting intermediates, should not only be contributive to the overall desired electrochemical reaction but also should not render any additional impedance to the activity of the electro-catalyst as well as should not lead to the loss of electrochemical energy converted. This means that the role of the support (mainly oxides for the preferential oxidation of partial combustion products) should be cumulative and not additive. The role of tungsten

oxide nanorods is examined for use as supports for noble metals for possible application as fuel cell anodes.

Tungsten oxide is a well-known multifunctional material, especially for fuel cell applications (Hobbs and Tseung, 1969). Tungsten oxide nanorods have been utilized as support for the following reasons. Platinum catalysts supported on tungsten oxide have been extensively studied as active catalysts for the electro-oxidation of methanol (Shen and Tseung, 1994). Tungsten oxide can form hydrogen bronze (H_xWO_3) that effectively facilitates the dehydrogenation of methanol, though these catalysts exhibit high performance, tungsten oxide undergoes dissolution in acid medium and thus reduces the electrocatalytic activity. The stability of tungsten oxide in acid medium can be improved by suitably adjusting the conditions of its preparation

Application of the tungsten oxide matrix should increase the electrochemically active surface area and facilitate charge (electron, proton) distribution (Yang *et al.*, 2004). Although to the lower extent than in the case of ruthenium species, the $–OH_{ads}$ groups existing on tungsten oxide surface may induce oxidation of the poisoning CO intermediate (Shen and Tseung, 1994). The present study aims at fabrication of multi-component electrocatalytic system with optimized reactivity towards electrooxidation of methanol. On the whole, the system is multifunctional in terms of promoting oxidation of methanol.

In this chapter the preparation of Pt nanoparticles supported on the surface of WO_3 nanorods and the electro-catalytic activity for the methanol oxidation of these composite electrodes are compared with the activity of conventional electrodes. The results indicated that the as-obtained Pt/WO_3 nanorod catalysts have an excellent electro-catalytic activity for methanol oxidation than the commercial Pt/C catalyst.

5.2 EXPERIMENTAL

5.2.1 Synthesis of WO_3 nanorods

10 g of Phosphotungtstic acid ($H_3PW_{12}O_{40}$) was stirred in a 30 ml of methanol solution. The resulting colloidal suspension was infiltrated into the membrane under vacuum by wetting method. The same procedure was repeated 1 to 8 times. The upper surface of the membrane was then polished gently by sand paper (2500 grit) and dried at 368 K for 1 h. The formation of WO_3 nanorods inside alumina template (WO_3 /AAO) was further achieved by programmed temperature thermal decomposition from 95 to 500 ^{0} min^{-1} and finally calcinated at 873 K for 3 h in air. The removal of the AAO template was performed by dissolving alumina template in 10 % (v/v) HF. The WO_3 nanorod product was washed with a copious amount of deionized water, to remove the residual HF and dried at 393 K.

5.2.2 Preparation of Pt/WO_3 nanorods composites

Platinum nanoclusters were loaded on the WO_3 nanorods by conventional impregnation methods (Watanabe *et al.,* 1987). Platinum was loaded on the nanorods as follows: 5 ml of 73mM aqueous hexachloroplatinic acid (H_2PtCl_6) was mixed with 100 mg of WO_3 nanorods by stirring at room temperature. The mixture was then evaporated to dryness and the resulting material was then reduced in hydrogen atmosphere at 623 K for 3h to give Pt/WO_3 nanorods.

5.3 CHARACTERIZATION METHODS

The scanning electron micrographs were obtained using JEOL JSM-840 model, working at 15 keV after the removal of alumina template. For transmission electron microscopic studies, the nanotubes dispersed in ethanol were placed on the copper

grid and the images were obtained using Phillips 420 model, operating at 120 keV. Micro-Raman scattering experiments were performed on a Bruker FRA106 FT-Raman at room temperature in a quasi-backscattering geometry with parallel polarization incident light. The excitation source used was an Argon ion laser operating at 514.5 nm with an output power of 20 mW. The X-ray diffraction patterns were obtained on a Philips PW 1820 diffractometer with Cu K_α (1.54178 Å) radiation.

5.4 FT-IR SPECTRA

The FT-IR spectra of WO_3 nanorods recorded in the region 400–3500 cm^{-1} were shown in Fig 5.1. The broad band from 1000 cm^{-1} to 500 cm^{-1} corresponds to the W–O vibrational mode. It has been widely reported that HPW with Keggin structures gives several strong, typical IR bands at ca. 1079 cm^{-1} (stretching frequency of P–O of the central PO_4 tetrahedron), 983 cm^{-1} (terminal bands for W═O in the exterior WO_6 octahedron), 889 cm^{-1} and 805 cm^{-1} (bands for the W–O_b–W and W–O_c–W bridge, respectively)

5.5 RAMAN SPECTRA

The Raman spectra of WO_3 nanorods exhibiting bands at ~ 717 and 808 cm^{-1} are shown in Fig 5.2. These bands agree closely to the wave numbers of the strongest modes of monoclinic-WO_3. The bands at 703 and 813 cm^{-1} correspond to the stretching modes of the WO_3 (Santato *et al.,* 2001; Daniel *et al.,* 1987).

5.6 X-RAY DIFFRACTION STUDY

The XRD pattern for the as-synthesized tungsten oxide nanorods and platinum loaded tungsten oxide nanorods are given in Fig 5.3.a and 5.3.b respectively. The diffraction peaks and the peak intensities of the tungsten oxide nanorods are in good agreement

with the diffraction peaks of crystalline monoclinic phase of WO_3. XRD patterns of Pt/WO_3-Nanorods are shown in Fig. 5.3.b. The presence of Pt (111), Pt (200) peaks are found in Fig 5.3.b. Furthermore, the major diffraction peaks of Pt nanoparticles can be observed.

5.7 ELECTRON MICROSCOPIC STUDIES

The morphology of tungsten oxide nanorods was studied with SEM, AFM, transmission electron microscopy (TEM) images on a Philips CM12/STEM instrument. The scanning electron microscopy (SEM) image presented in Fig 5.4.a shows rod like morphology of the product. Further AFM image confirms the rod like morphology in Fig 5.4.b represents low magnification. The morphology of the nanorods can be confirmed with TEM micrographs shown in Fig 5.5 (a, b). The dimensions of the nanorods are matches with the outer diameter of the template used. The diameter of the nanorods was found to be around 200 nm. The presence of Pt on WO_3 nanorods can be seen from Fig 5.6.a and it is clear from the micrograph that the Pt is well dispersed all over the surface of the nanorods. The size of the Pt nanoparticles is in the range of 3-4 nm, which is evidenced from Fig 5.6. a. The optimal Pt particle size for reactions in the H_2/O_2 fuel cell is 3 nm (Kinoshita, 1990). The EDX pattern shows the presence of Pt particles present on the WO_3 nanorods. The complete removal of fluorine and aluminum has also been confirmed.

5.8 ELECTROCHEMICAL MEASUREMENTS

The catalyst was electrochemically characterized by cyclic voltammetry (CV) using an electrochemical analyzer (Bioanalytical Sciences, BAS 100). A common three-electrode electrochemical cell was used for the measurements. The counter and reference electrodes were a platinum plate (5 cm^2) and a saturated Ag/AgCl electrode

respectively. The CV experiments were performed using 1 M H_2SO_4 solution in the presence of 1 M CH_3OH at a scan rate of 50 mV/s. All the solutions were prepared by using ultra pure water (Millipore, 18 MΩ). The electrolytes were degassed with nitrogen before the electrochemical measurements.

5.8.1 Preparation of working electrode

Glassy carbon (GC) (BAS Electrode, 0.07 cm^2) was polished to a mirror finish with 0.05 μm alumina suspensions before each experiment and served as an underlying substrate of the working electrode. In order to prepare the composite electrode, the nanorods were dispersed ultrasonically in water at a concentration of 1mg ml^{-1} and 20 µl aliquot was transferred on to a polished glassy carbon substrate. After the evaporation of water, the resulting thin catalyst film was covered with 5-wt% Nafion solution. Then the electrode was dried at 353 K and used as the working electrode.

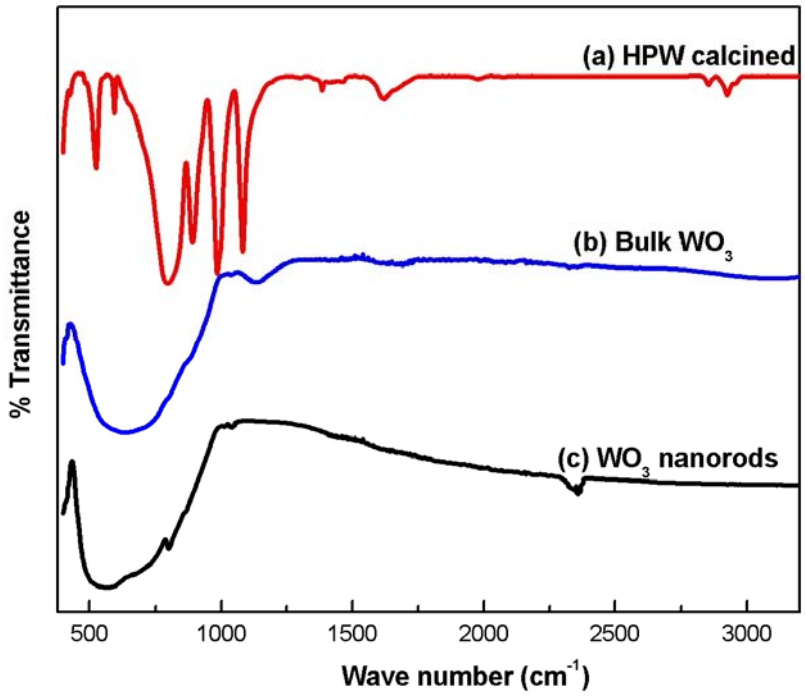

Fig. 5.1. FTIR Spectrum of the (a) calcined HPW (b) Bulk WO_3 (c) Tungsten oxide nanorods

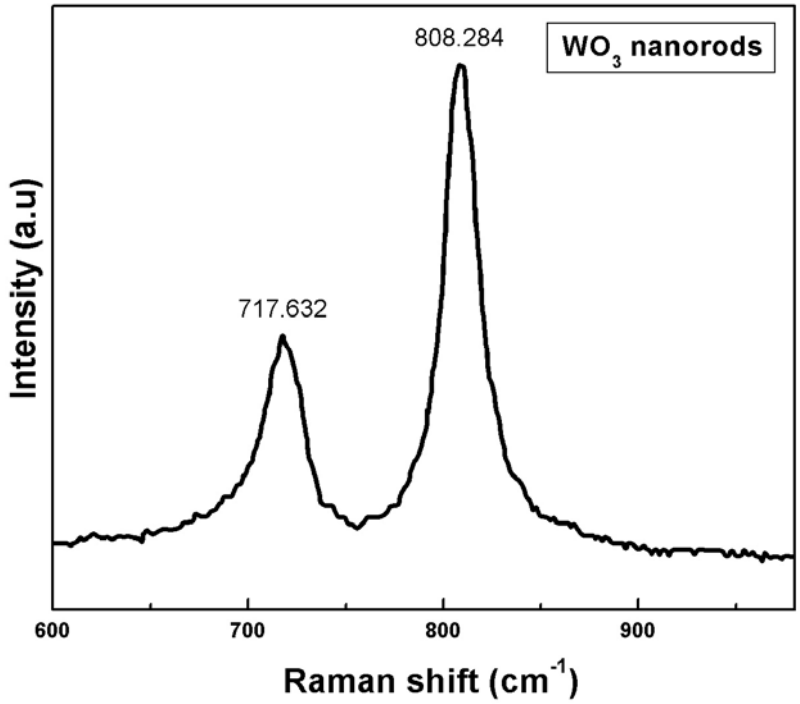

Fig. 5.2. Raman spectrum of the Tungsten oxide nanorods

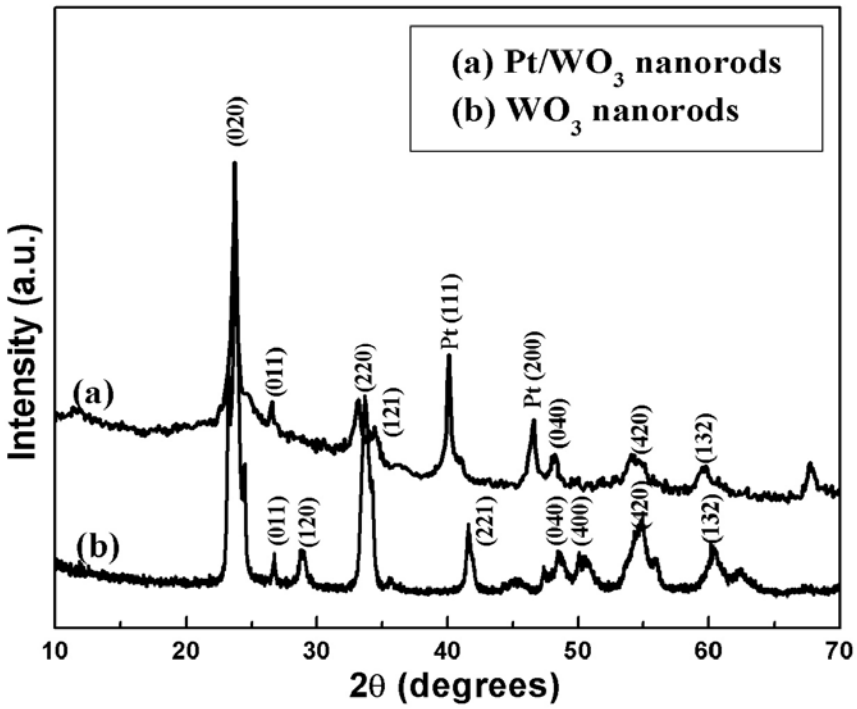

Fig. 5.3. XRD patterns of (a) Pt/WO_3 nanorods and (b) WO_3 nanorods

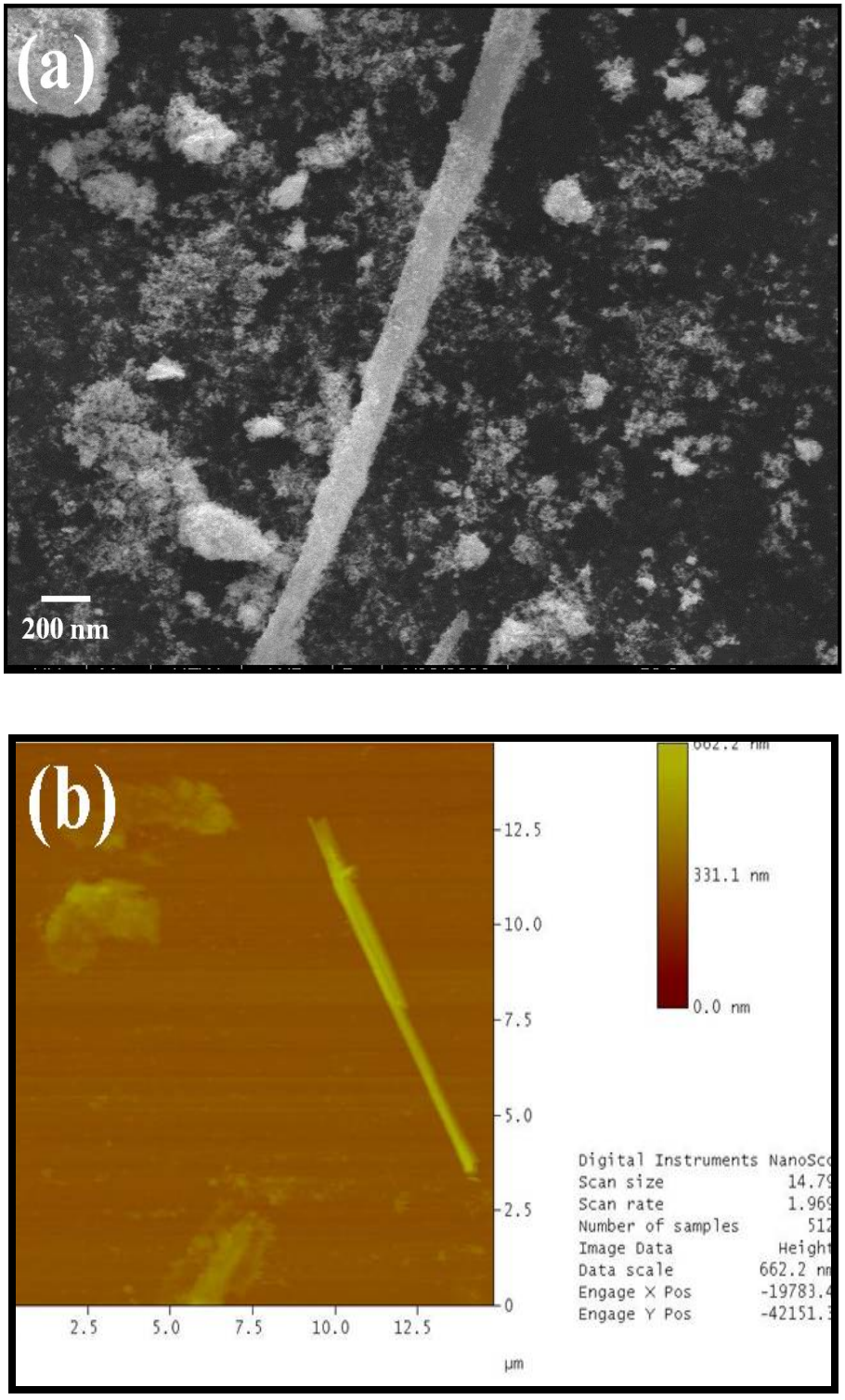

Fig. 5.4. (a) SEM Micrograph of the WO_3 nanorod (b) AFM micrograph of the nanorods

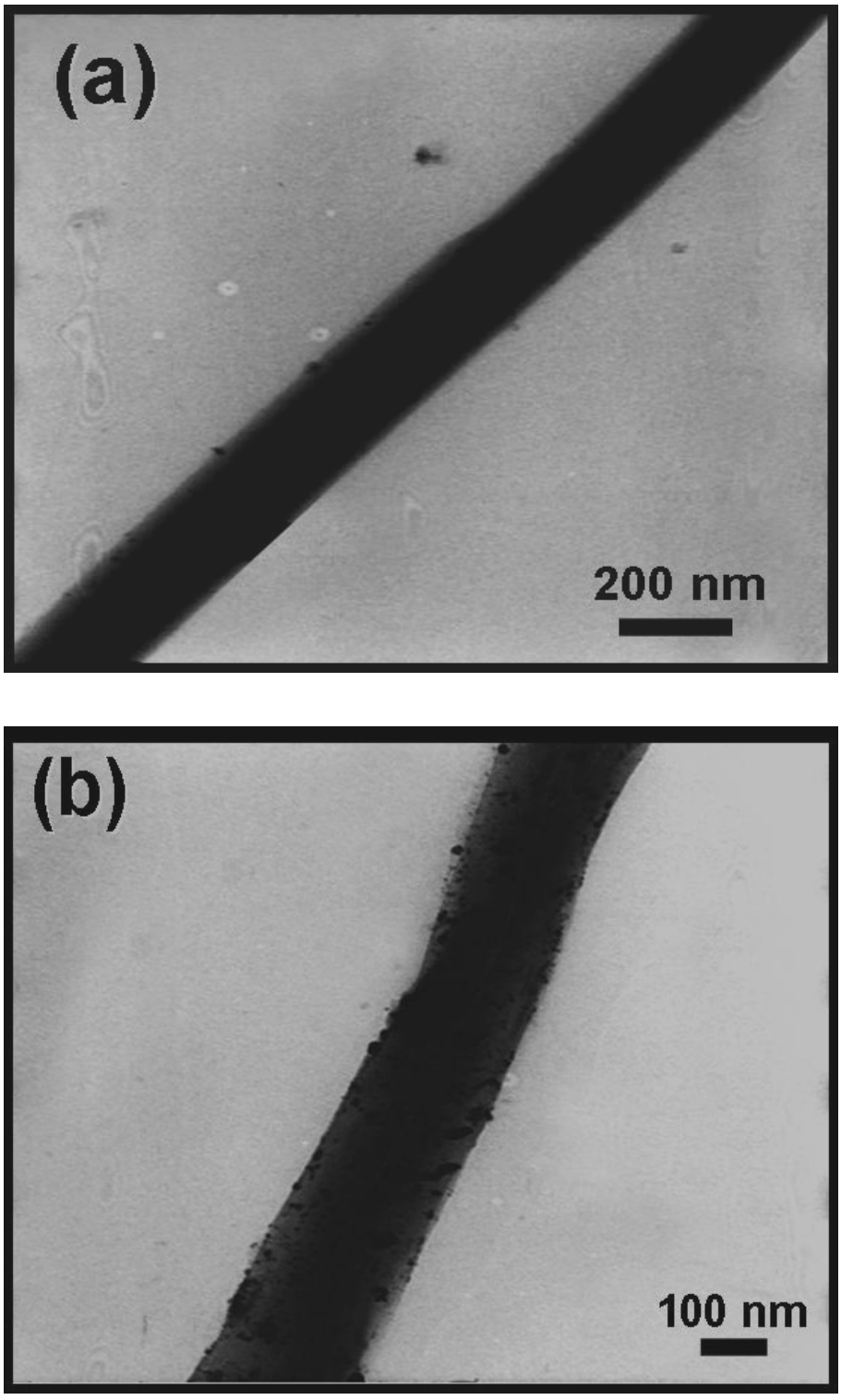

Fig. 5.5. TEM Micrographs of the nanorods (a) WO_3 nanorods (b) Pt/WO_3 nanorods

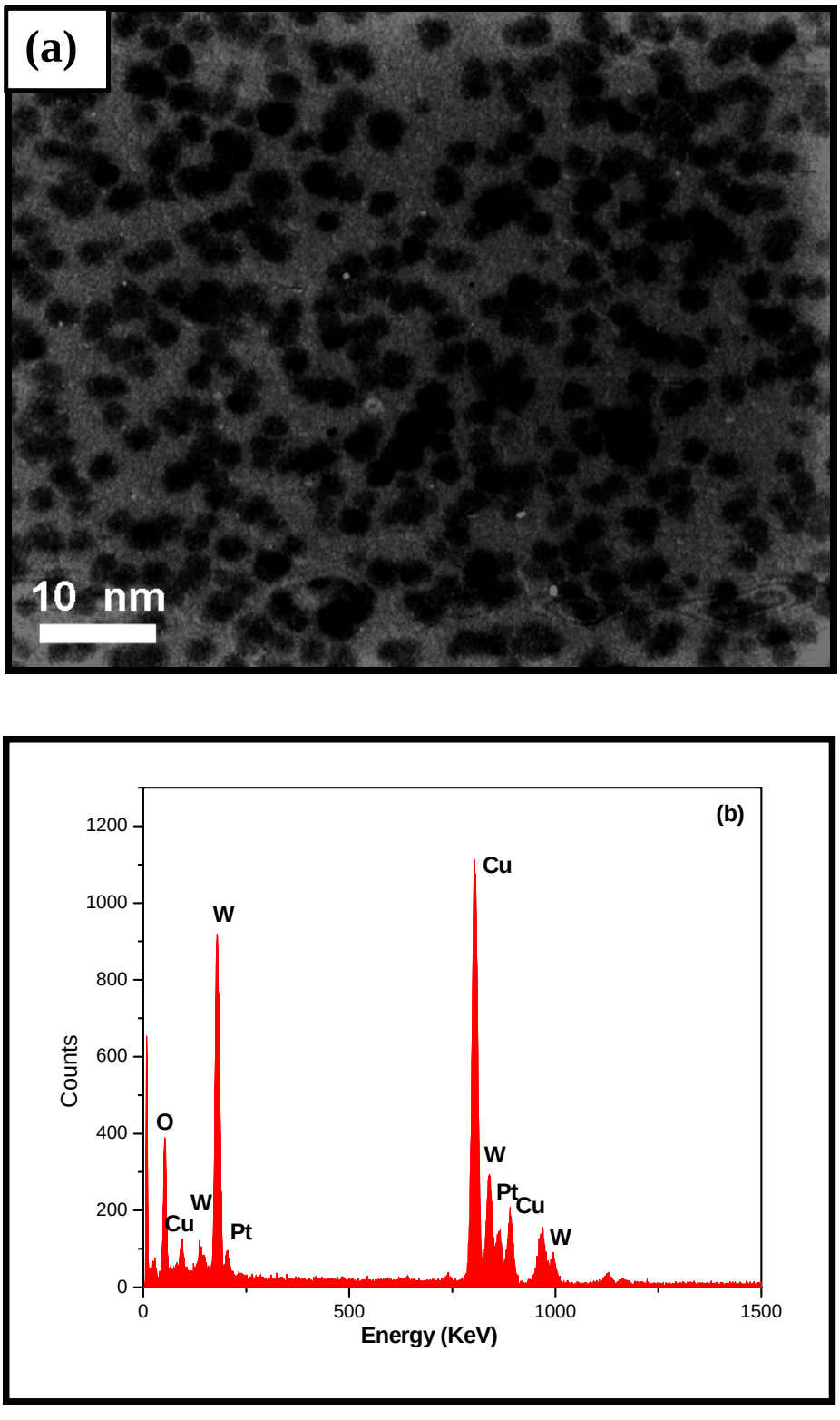

Fig. 5.6. (a) TEM Micrographs of the Pt/WO_3 nanorods (b) EDX pattern of Pt/WO_3 nanorod electrode

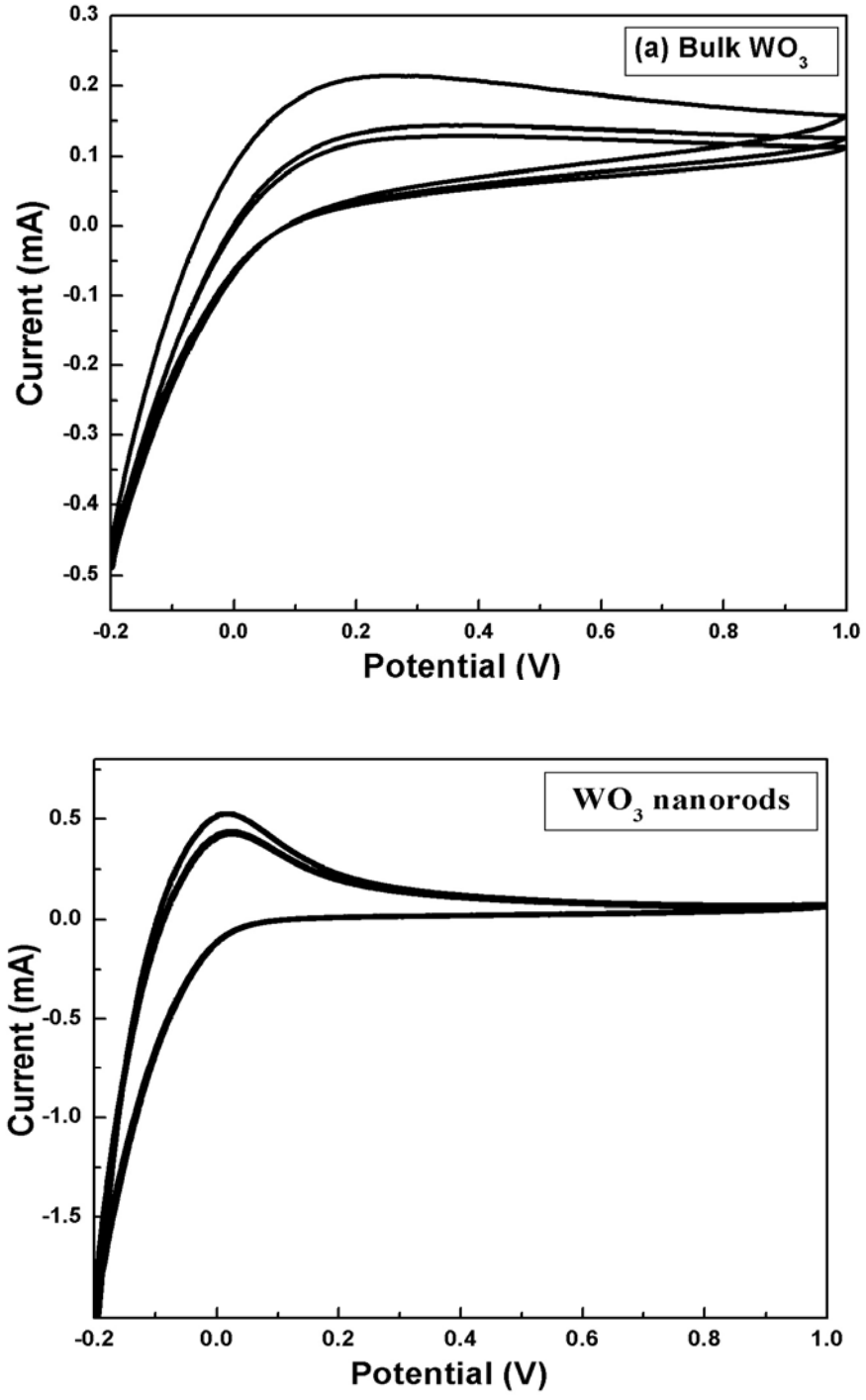

Fig. 5.7. Cyclic voltammogram for (a) bulk WO_3 (b) WO_3 nanorods in 1 M H_2SO_4 at scan rate of 50 mV s^{-1} at 298 K

5.9 ELECTROCHEMICAL BEHAVIOR OF WO_3 NANORODS

The electrochemical behavior of WO_3 nanorods was studied in 1 M H_2SO_4 was shown in Fig 5.7 b. The cyclic voltammogram (see supporting information) shows an anodic peak current at –0.07 V and it is due to the formation of tungsten bronzes by hydrogen intercalation in the tungsten trioxide. The electrochemical response due to W is seen at -0.1 V in the forward scan, which matches with the peak reported in literature (Figlarz 1989). Further, the stability of tungsten trioxides in sulphuric acid medium was evaluated by carrying out the cyclic voltammetry by repeating voltammetric cycles in 1 M H_2SO_4. There is initial decrease in current and after few cycles the peak current remained the same even after 50 cycles and this showed the stability of WO_3 nanorods in sulfuric acid medium.

5.10 EVALUATION OF METHANOL OXIDATION ON Pt / WO_3 NANOROD ELECTRODES

The electrochemical activity of platinum loaded WO_3 nanorods for methanol oxidation was studied using cyclic voltammetry in the presence of 1M H_2SO_4 and 1M CH_3OH. Fig 5.8a shows the electrochemical oxidation of methanol by Pt loaded on WO_3. (Voltammogram obtained after the peak attained a constant peak current). For comparison, methanol oxidation was also carried out with commercial 20% Pt/C (Jhonson Mathey). Fig 5.8c shows the cyclic voltammetry of WO_3 nanorods in 1M H_2SO_4 and 1M CH_3OH. Like Ru, WO_3 has no activity for methanol oxidation in acid solution. The unsupported WO_3 nanorods showed no activity towards methanol oxidation. As is shown in Fig 5.8a, two oxidation peaks are observed, which belong to the oxidation of methanol and the corresponding intermediates (Wang *et al.,* 2001).

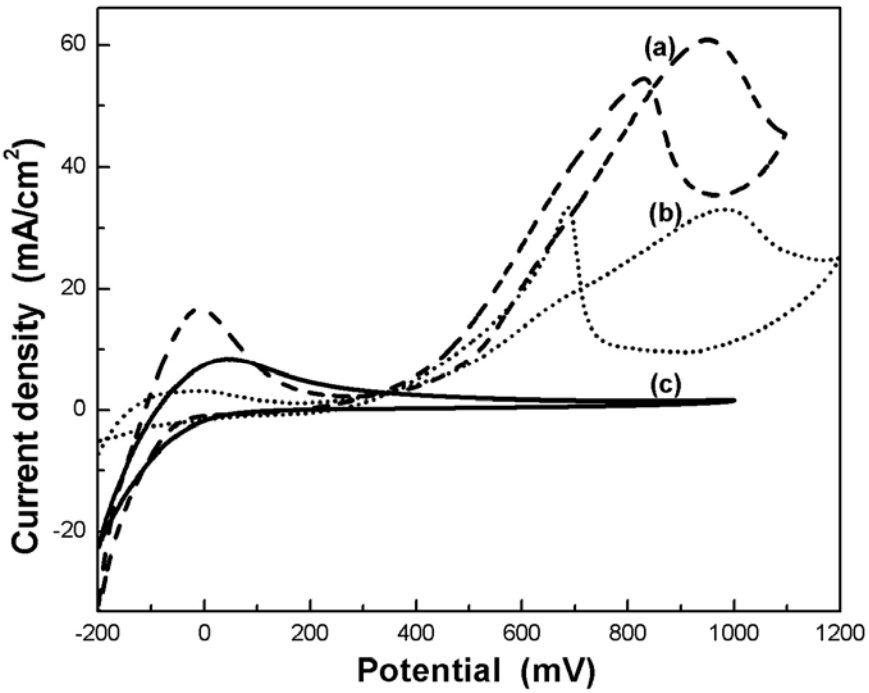

Fig. 5.8. Cyclic voltammograms of (a) Pt/WO_3 nanorods (b) Pt/C (Johnson mathey) (c) WO_3 nanorods in 1 M H_2SO_4/1 M CH_3OH run at 50 mV/s

Table 5.1. Electro-catalytic activity of Pt/WO_3 nanorods and Pt/C for methanol oxidation

Electrocatalyst	Pt loading μg/cm^2	Specific activity mA/cm^2
Pt/C	20	29.5
Pt/WO_3 nanorods	20	62.0

The methanol oxidation peak potential is lower for Pt/WO_3 than for Pt/C indicating the better performance of Pt particles supported on WO_3 nanorods. For a lower platinum loading, the WO_3 nanorods show enhanced activity than the commercial catalyst. The specific activity (mA cm^{-2}) of the platinum supported on WO_3 nanorods are almost two times higher than that of the commercial 20% platinum on carbon support (Table 5.1). The higher activity of Pt/WO_3 can be attributed to the stabilization of Pt nanoparticles and dispersion on the WO_3 nanorods. It can be

supposed from the cyclic voltammogram that the Pt/WO_3 nanorods electrode is relatively endurable for intermediate production.

According to Yoshiike and Kondo (1983, 1984) H_2O molecules are physisorbed but also chemisorbed on WO_3. The oxophilic nature of WO_3 would help in adsorbing the intermediates and thereby keeps the surface of platinum clean. It is not possible in the case of Pt supported on carbon. The advantages of using Pt/WO_3 electrode are (1) keeping the Pt site clean for chemisorption of methanol by the formation and oxidation of hydrogen tungsten bronzes during dehydrogenation of methanol on the surface of Pt/WO_3 electrode.

$$WO_3 + xPt\text{-}H \longrightarrow HxWO_3 + xPt$$

$$HxWO_3 \longrightarrow xH^+ + xe^- + WO_3$$

and (2) oxidizing the poisons such as CO, since water adsorbed on WO_3 surface can interact with CO adsorbed on Pt at the neighbouring site. Such bronzes show better catalytic activity than Pt-Ru based electrocatalyts (Park *et al.,* 2003; Hobbs and Tseung, 1969; Shen and Tseung, 1994).

The stability of electrode for methanol oxidation was evaluated by chronoamperometry Fig 5.9. compares the chronopotentiometric results of methanol oxidation in 1 M H_2SO_4 and 1 M CH_3OH at 0.6 V.Pt/WO_3 nanorods electrode not only showed higher initial activity but also is more stable than Pt/C electrode (Fig. 5.8). The probable reason could be the lower polarisation potential. At this potential, the leaching of W would not have had a pronounced effect on the stability of the electrode for methanol oxidation (Rajesh *et al.,* 2002). Also the oxophilic

nature of WO_3 is beneficial to producing hydroxyl groups on the catalyst surface, which promotes the oxidation of adsorbed CO (Shen *et al.,* 1995; Chen *et al.,* 1995).

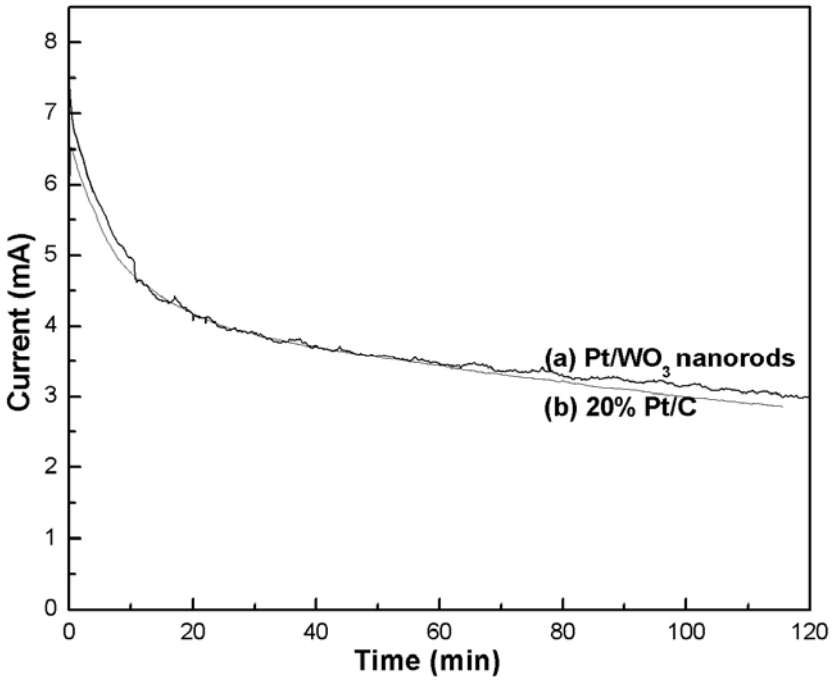

Fig. 5.9. Current density versus time curves at (a) Pt/ WO_3 nanorods (b) Pt/C Johnson Mathey) measured in 1 M H_2SO_4 + 1 M CH_3OH. The potential was stepped from the rest potential to 0.6 V vs. Ag/AgCl

5.11 CONCLUSIONS

In conclusion, a simple template synthesis has been described for preparing WO_3 nanorods by a direct calcination of Phosphotungtstic acid in the channels of the alumina template. The size of nanorods is around 200 nm matches with the diameter of the template used. The methanol oxidation activity of platinum supported on WO_3 nanorods has been studied and compared with that of the commercial catalyst. Pt/WO_3 nanorods exhibited higher methanol oxidation activity than the commercial Pt/C catalyst by a factor of two. Platinum supported on such nanorods is found to be stable

for several cycles in an electrochemical environment. Enhancement in the electro-catalytic activity is due to spill over effect in methanol oxidation and the role of tungsten oxide nanorods are examined for use as supports for noble metals for possible application as fuel cell anodes.

CHAPTER 6

ELECTROCHEMICAL SYNTHESIS, CHARACTERISATION AND ELECTRO-OXIDATION OF METHANOL ON Pt INCORPORATED TEMPLATE SYNTHESISED CONDUCTING POLY (o-PHENYLENEDIAMINE) NANOTUBES

6.1 INTRODUCTION

In recent years, catalytic particles dispersed on the conducting polymers mainly on polypyrrole and polyaniline has received considerable attention as the electrode material for methanol oxidation. Among many conducting and electroactive polymers, poly (o-phenylenediamine) (PoPD) is of great interest because of its potential use in various fields of technology. Two interesting properties of PoPD, different from those, characteristic for usual conducting polymers like Polyaniline (PANI) or Polypyrrole (PPY) make it promising for applications in electrochemical and bioelectrochemical sensors. One of these properties relate to an unusual dependence of the electric conductivity on the redox state of this polymer. As opposed to PANI or PPY, PoPD shows the conductivity in its reduced state, whereas its oxidized state is insulating. This determines the electrochemical properties of PoPD, since many electrode redox processes have been shown to take place within a relatively narrow potential window, corresponding to the reduced (conducting) form of this polymer. Within this potential window, electro-catalytic oxidation of some species proceed, making it possible to use PoPD for electro-catalytic applications, like e.g. the electro oxidation of coenzyme NADH, electro oxidation of methanol (Golabi and Nozad 2002, Golabi *et al*., 2003, and oxygen reduction (Ohsaka *et al.,* 1991, Li *et al.,* 1998, Premkumar and Ramaraj 1996)

The detailed synthetic procedures of the poly (o-phenylenediamine) nanotube and Pt incorporated template synthesized poly (o-phenylenediamine) nanotube on nafion and graphite are shown schematically in Scheme 6.1. The conventional synthesis of poly (o-phenylenediamine) and Pt deposited poly (o-phenylenediamine) nanotube was followed in the same way without the alumina membrane as the template.

The tubular morphology played a crucial role in the dispersion of the catalytic particles of the conducting poly (o-phenylenediamine). In the present investigation, Pt incorporated template synthesized conducting poly (o-phenylenediamine) nanotube has been used as the electrode for methanol oxidation. The composite material based on Pt incorporated template synthesized poly (o-phenylenediamine) has been compared with that of the Pt deposited on conventionally synthesized poly(o-phenylenediamine) for electro oxidation of methanol. These materials are characterized and studied using SEM, AFM, TEM and cyclic voltammetry.

6.2. ELECTROCHEMICAL SYNTHESIS OF POLYMER NANOTUBES

The present work was carried out in aqueous solutions. Purified water obtained by passing distilled water through a milli Q (Millipore) water purification system was used as solvent. o-Phenylenediamine (o-PD) was purchased from Aldrich.

All experiments were carried out in a conventional one-compartment cell with a Pt counter electrode and a saturated calomel reference electrode, at room temperature. First the graphite electrode is coated with nafion solution. The nafion is not only acts as binder but provides both ionic and electronic contact and favours proton transport and the membrane are hot pressed with the graphite. Second the graphite electrode was used as current collector and contact with the template membrane. The membrane together with the current collector was fixed between two teflon rings.

The area of the membrane contacted to the electrode was ca. 1 cm^2. The solution was de-aerated by bubbling dry nitrogen gas for 5 min before electrochemical polymerization. The electropolymerization of o-phenylenediamine was carried out with a BAS 100B Electrochemical Workstation (Bioanalytical Systems Inc., West Lafayette, IN). The poly (o-phenylenediamine) nanotubes were grown potentiodymanically -0.2 V to 1.2 V containing 5 mM o-phenylenediamine. The length of the nanotube was controlled by the total charges passed in the cell.

6.2.1 Deposition of Pt particles on Graphite/Naf/PoPD $_{Temp}$

Deposition of platinum particles into the PoPD nanotube by electroreduction of chloroplatinic acid (0.01 M) in 0.5 M sulfuric acid. Each electro reduction step involved ten potential cycles in the range from 0.8 to −0.3 V (scan rate =50 mV s^{-1}). Under these conditions, the amount of loaded platinum particles was determined as 0.1 mg cm^{-2} from the charge passed during the loading step.

6.2.2 Removal of template

The alumina membrane from Graphite/Naf/PoPD $_{Temp}$ and Graphite/Naf/PoPD $_{Temp}$ − Pt was removed by immersing the composite in 0.1 M NaOH for 15 min. The composite after the dissolution of the template was repeatedly washed with deionized water to remove the residual NaOH. It was subsequently immersed in 1% HBF_4 for 10 min and then washed with deionized water again. The composite after the dissolution of the template was designated as Graphite/Naf/$PoPD_{Temp}$ and Graphite/Naf/PoPD $_{Temp}$ –Pt. A similar experimental condition was adopted to prepare the template-free Pt incorporated poly (o-phenylenediamine) on graphite. The electrode was designated as Graphite /Naf/PoPD-Pt. The details of the synthetic procedure for the preparation of template synthesized poly (o -phenylenediamine) and

Pt incorporated template synthesized poly (o -phenylenediamine) are illustrated in Scheme 6.1.

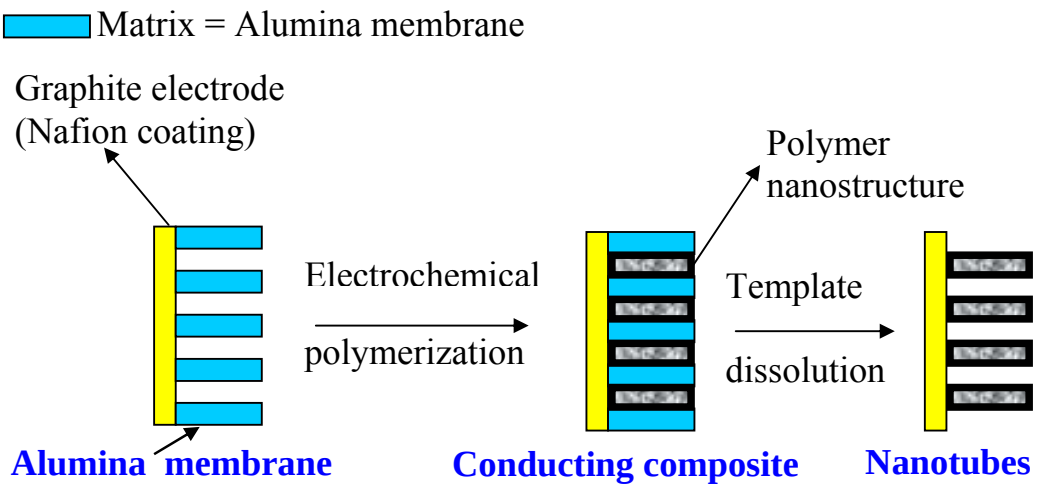

Scheme.6.1. Scheme for template assisted electrochemical synthesis of conducting polymer nanotube

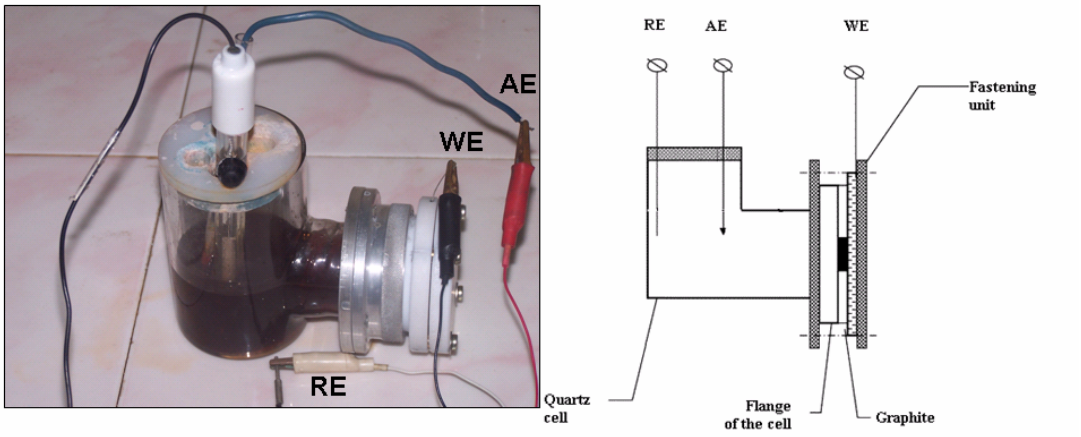

Fig. 6.1. Schematic view of an electrochemical cell for the formation of nanostructured materials RE, reference electrode; AE, auxiliary electrode; WE, working electrode (template membrane with a deposited Nation contact layer)

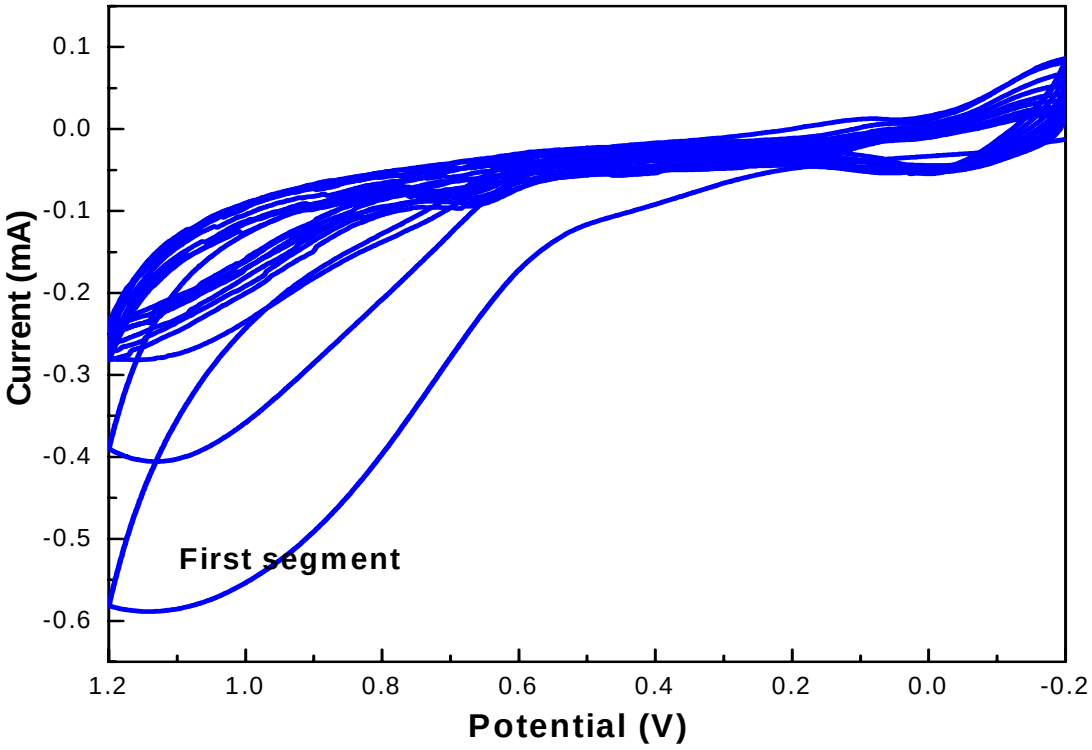

Fig. 6.2. Cyclic voltammograms obtained during the electropolymerization of o-phenylenediamine in 0.5 M oPD + 0.5 M H_2SO_4 solution (v = 50mVs^{-1})

The electrochemical properties of the nanotube electrode were compared with those of the conventionally synthesized poly (o-phenylenediamine) on graphite, using cyclic voltammetry. The Pt incorporated poly (o-phenylenediamine) nanotube electrode exhibited excellent catalytic activity and stability compared to the 20 wt % Pt supported on the Vulcan XC 72R carbon and Pt supported on the conventional poly (o-phenylenediamine) electrode. The nanotube electrode showed excellent electro-catalytic activity and stability for electro-oxidation of methanol.

6.3 CV MEASUREMENTS

The electropolymerisation of oPD monomer on the alumina template was carried out by cyclic voltammetry was shown in Fig 6.2. A broad anodic peak appeared in the

potential ranged from +0.2 V to 1.2 V, which indicated that, an oxidative process of oPD. In all the cases no reduction peak is found in the reverse scans, thus suggesting that oxidized oPD is involved in further chemical processes leading to non-reducible species in the potential range adopted.

6.4 ELECTRON MICROSCOPY STUDY

The SEM image of the conventionally synthesized conducting poly (o-phenylenediamine) is shown in Fig 6.3a. The image shows ladder morphology revealed a dense coverage of poly (o-phenylenediamine) on graphite, which are not uniform in nature. Fig. 6.3b shows the SEM image of the Pt deposited conventionally synthesized poly (o-phenylenediamine) on graphite. Though, the Pt crystallites are clearly seen from the image, the cluster size and the geometry of the Pt particles are not uniform and the cluster size was found to be high with agglomerates as seen over the scanned region. It is further evident from the image that the large Pt crystallites are randomly distributed on poly (o-phenylenediamine) and the ladder morphology of the poly (o-phenylenediamine) is also seen in the SEM image.

It is evident from Fig. 6.4a that the uniform, cylindrical, monodisperse nanotubes of PoPD after the removal of the template are projecting perpendicularly to the graphite. The open ends of the uniform nanotube are clearly seen in this image. Fig. 6.5b shows the picture of the conducting polymeric tubules taken at a tilted angle, in a different region. It is evident from the image that the density of the nanotubes is quite high, in all the regions. These tubes are uniformly distributed in a regular array on the graphite with an outer diameter (200 nm) that almost matches the pore diameter of the template.

Fig. 6.5b shows the high-resolution transmission electron micrograph (HR-TEM) of Pt incorporated template synthesized poly (o-phenylenediamine) polymer nanotube. Though the nanotubes are clearly seen, the Pt particles are not visible due to the thickness of the wall of the tubules.

In order to demonstrate the presence of Pt on the template synthesized poly(o-phenylenediamine), electron diffraction image was taken and presented in Fig 6.6b. The diffraction pattern of the Pt is seen as spots, which demonstrates that the sizes of Pt particles formed on the conventionally synthesised poly (o-phenylenediamine) polymer are large.

The electron diffraction image of the Pt deposited template synthesized poly(o-phenylenediamine) polymer nanotube is shown in Fig.6.7b, as it can be seen from the image, the diffraction pattern of the fine Pt particles is seen as number of clear concentric rings without any spot seen on the ring. This clearly revealed the presence of the fine Pt particles in/on the nanotubes. The rings correspond to the diffraction from the (111), (200), (220) and (311) planes of crystalline Pt particles.

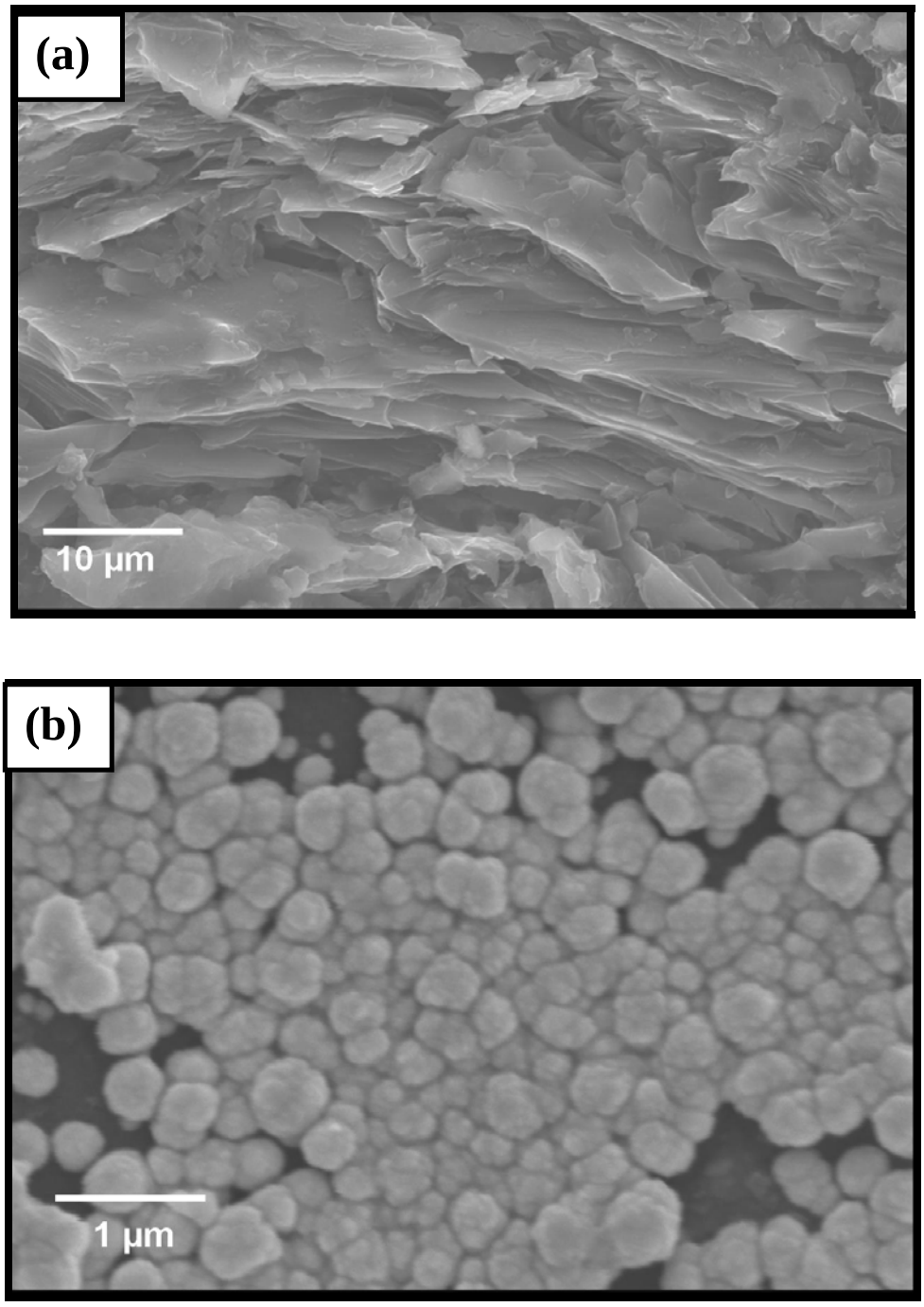

Fig. 6.3. (a) SEM images of conventionally synthesized PoPD polymer and (b) SEM Images of Pt deposited on conventionally synthesized PoPD polymer

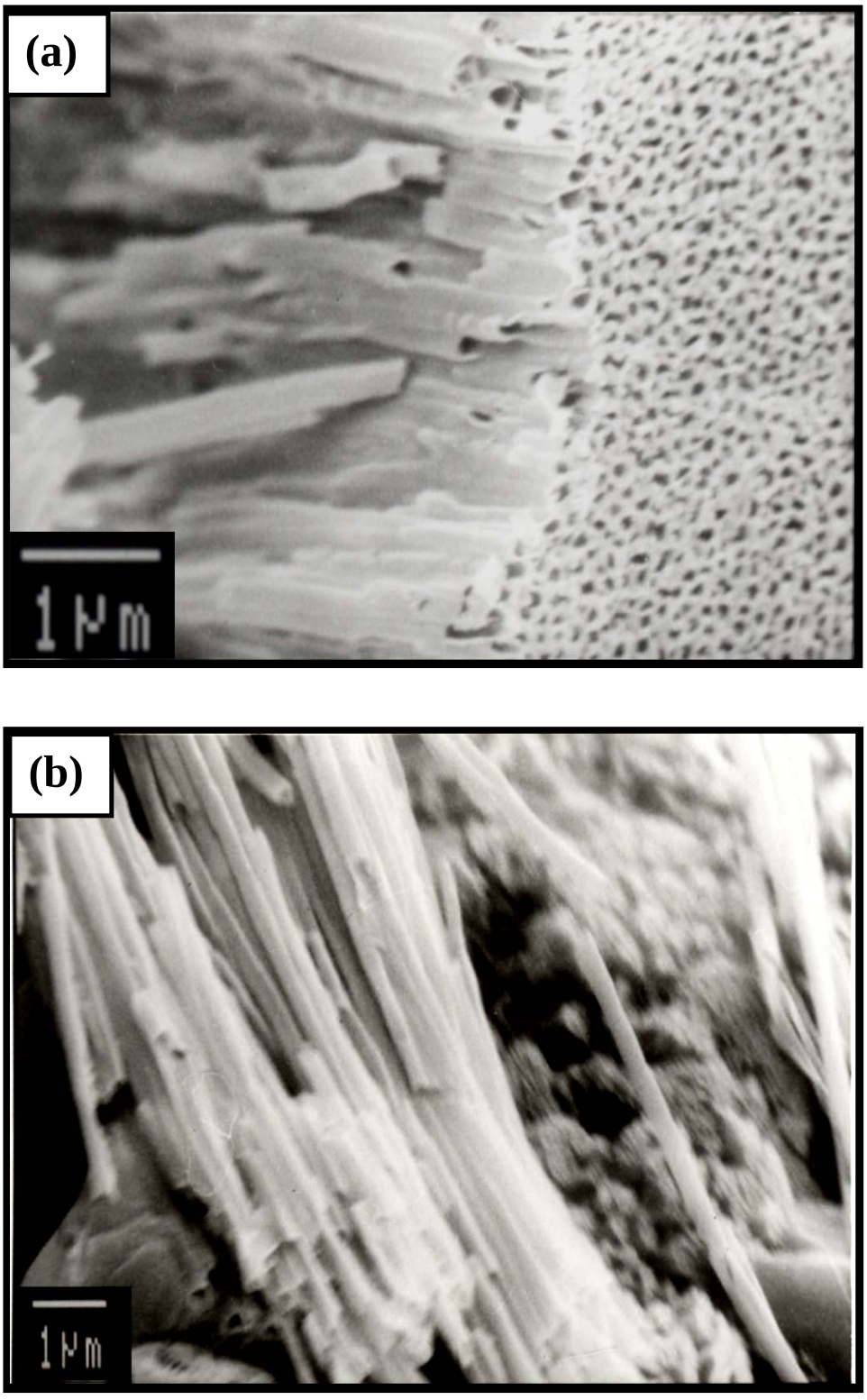

Fig. 6.4. (a-b) SEM images of template synthesized PoPD polymer nanotubes

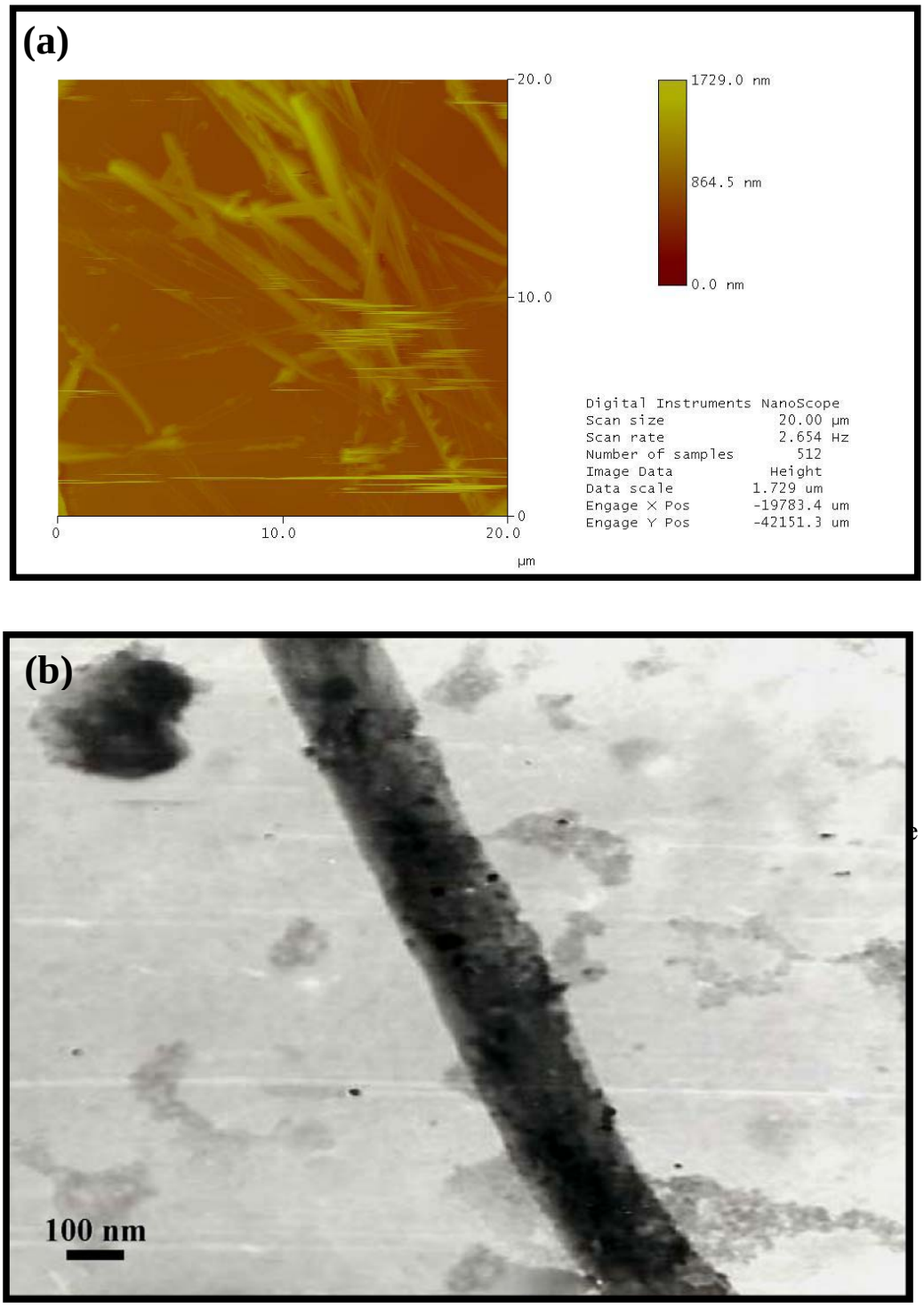

Fig. 6.5. (a) AFM images of template synthesized PoPD polymer nanotubes on the silicon substrate and (b) TEM Images of Pt deposited on template synthesized PoPD polymer nanotubes

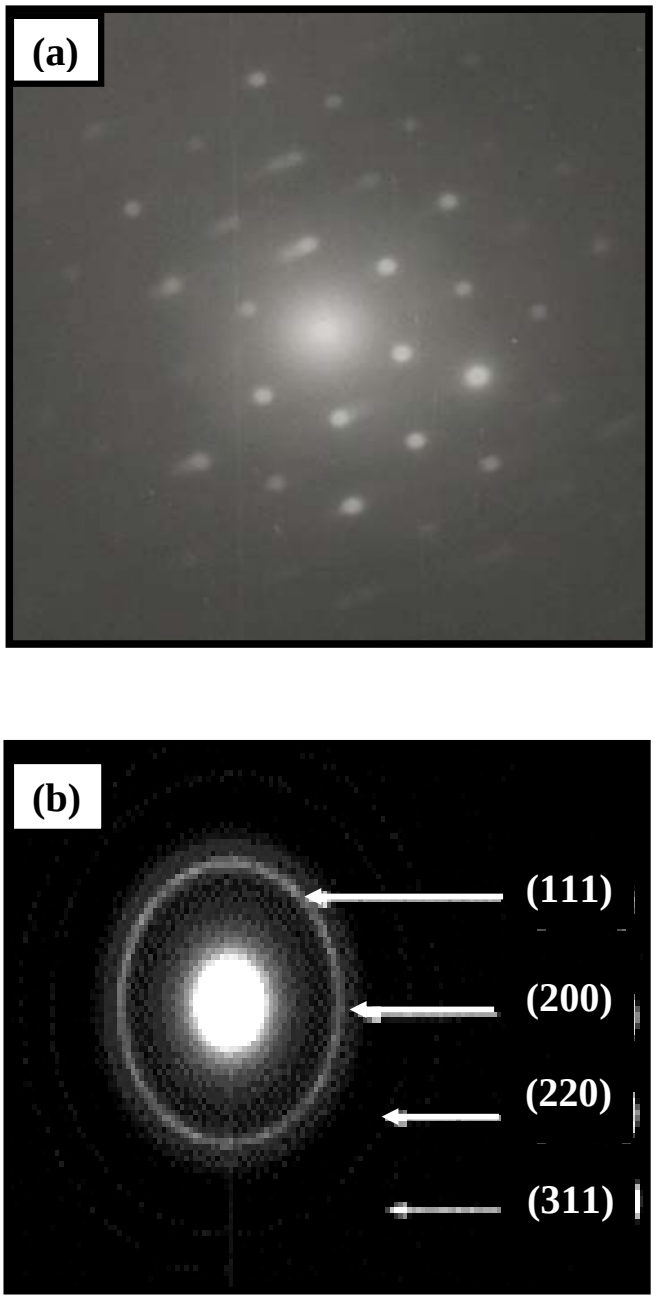

Fig. 6.6. (a) Electron diffraction pattern of Pt nanoparticles on conventionally synthesized PoPD polymer and (b) Electron diffraction pattern of Pt nanoparticles template synthesized PoPD polymer nanotubes

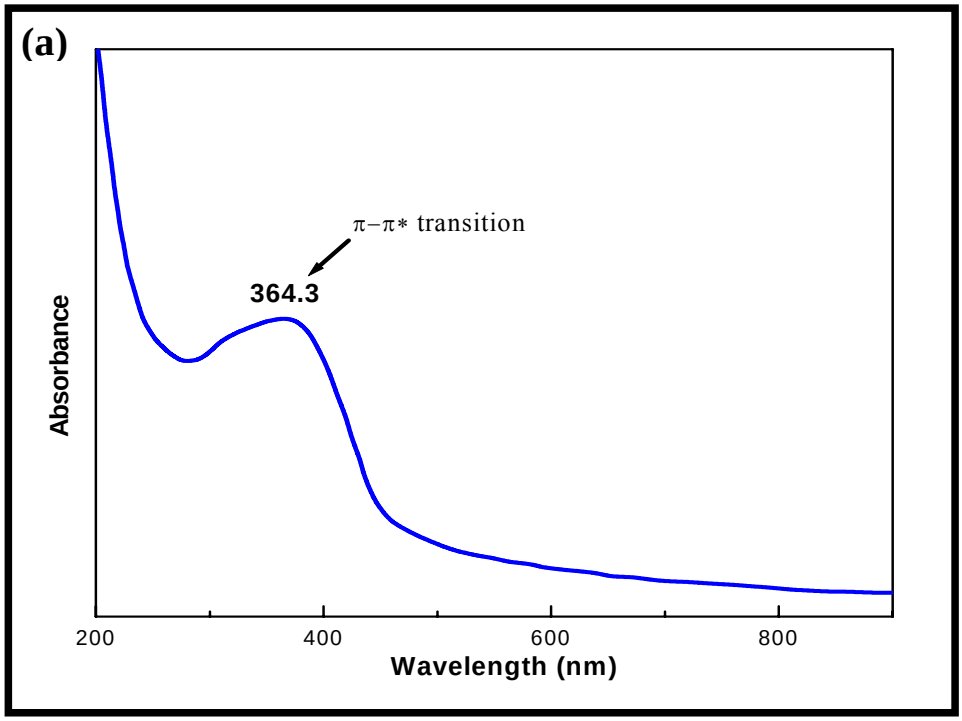

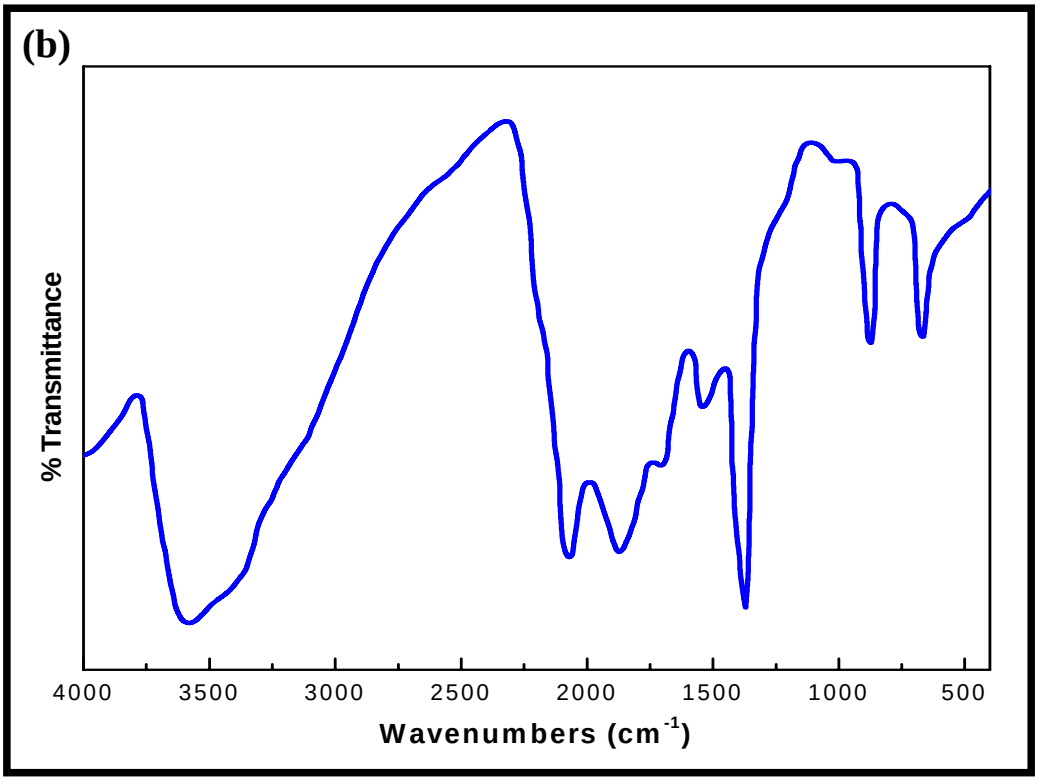

Fig. 6. 7 (a) UV–Vis absorption spectra of PoPD polymer nanotubes and (b) FTIR Spectra of PoPD polymer nanotubes in KBr pellet at room temperature

6.5 UV-VIS ABSORPTION SPECTROSCOPY

The UV–Vis absorption spectra of the PoPD nanotubes are shown in Fig. 6.7 a. A single, large absorption band around 364.3 nm is seen for PoPD. The band is due to inter-band charge transfer associated with excitation of benzenoid to quinoid moieties (optical absorption of the metallic polar on band of the conducting form).

6.6 FT-IR SPECTRA

The FT-IR spectroscopy was used to identify the structure of the PoPD. Fig. 6.7 b shows the FT-IR spectra of PoPD nanotubes. The absorption band appears around 3400 cm^{-1} corresponding to the N-H stretching vibration. The absorption bands in the 650–900 cm^{-1} regions are in the characteristic region of the substitution pattern on the aromatic ring. The band at 812 cm^{-1} assigned to the vibration of the 1,4-disubstitude ring (Guay and Dao 1989). The large band at 1450 cm^{-1} is attributed to the C=N stretching vibration. This suggests that a considerable portion of C=N bond were existed in the PoPD nanotubes. It can be noted that the presence of this band in the PoPD backbone means that the polymer chain has an extensive π conjugation between polymer chain and all nitrogen atoms. This is consistent with the results of UV–Vis spectroscopy and electrochemical experiment.

6.7 EVALUATION OF METHANOL OXIDATION ACTIVITY OF GR/NAF/PoPD$_{TEMP}$ –Pt NANOTUBE AND GR/NAF/PoPD$_{CONV}$-Pt ELECTRODES

The cyclic voltammogram of Pt-Poly (*o* -phenylenediamine) in the presence of in 1 M H_2SO_4 after the removal of the template is shown in Fig. 6.9a. A broad peak at −0.2 V in the forward scan was observed, which is due to the ionization of hydrogen on Pt. The CV for the Pt-Poly (*o* -phenylenediamine) in 1 M H_2SO_4/1 M CH_3OH after the

dissolution of the template is shown in Fig. 6.9b. The methanol oxidation was clearly evident from the CV with a maximum current density of 84 mA/cm^2. Another interesting feature of the CV is that as the applied potential increases, the methanol oxidation current density also increases without peaking at any particular potential value (in the potential range studied). In the present investigation, the potential was scanned between −0.2 and +1.0 V versus Ag/AgCl. Though, there is no peak current observed in the cyclic voltammogram for Pt incorporated template-synthesized poly (*o*-phenylenediamine) nanotube electrode, the anodic peak current observed was taken and the values are normalized per unit area (mA/cm^2). The difference between the forward and the reverse current was also found to be very low, which might suggest the better tolerance of the electrode towards the strongly adsorbed intermediates. It was also reported (Santosh *et al.,* 2006) that poisoning effect was lower on the Pt dispersed on the poly (o-phenylenediamine) than the bulk Pt electrodes.

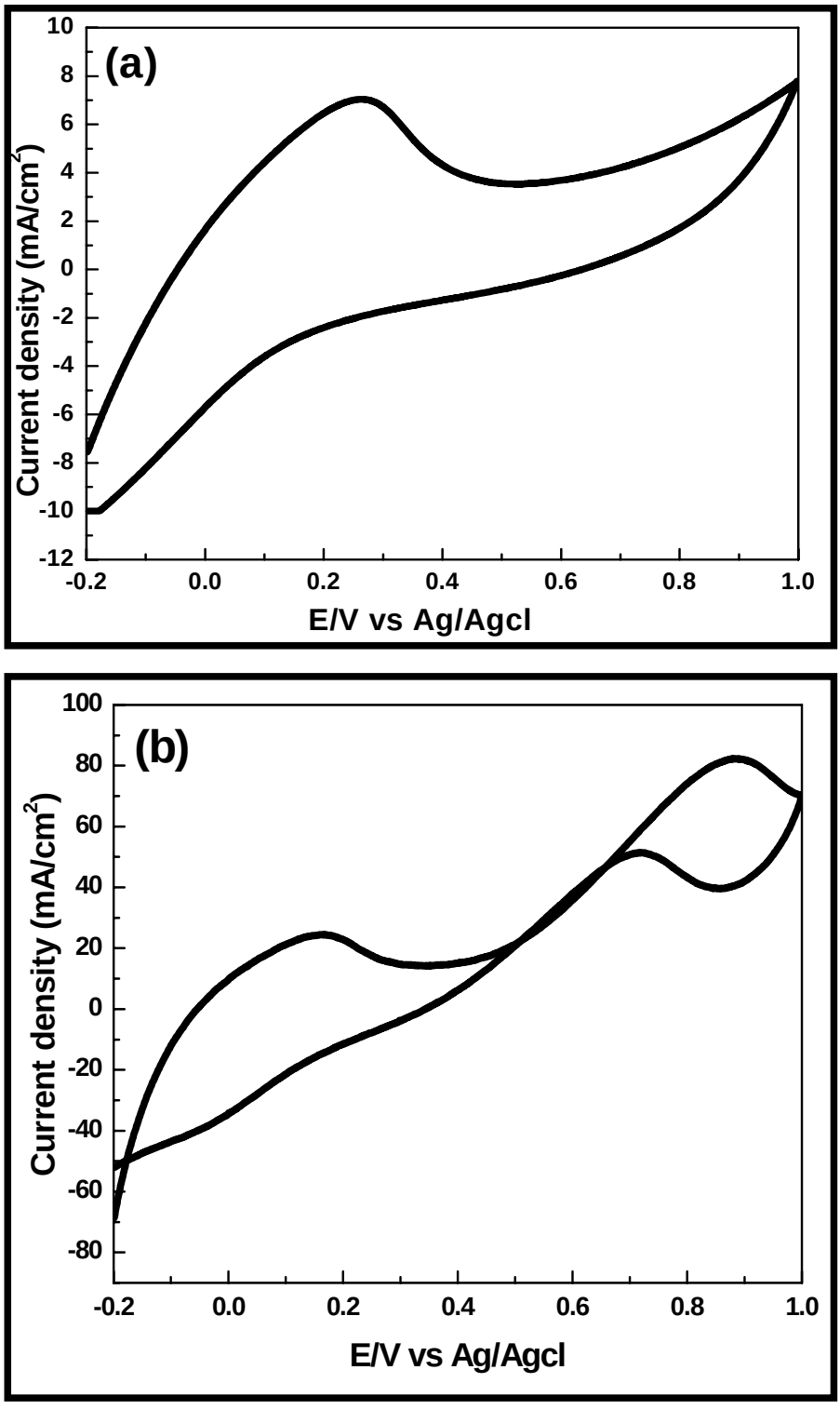

Fig. 6.8. Cyclic voltammograms of Pt incorporated template-based poly (*o*-phenylenediamine) (GR/Naf/Al_2O_3/$PoPD_{Temp}$-Pt) electrode (after the removal of template) (a) 1 M H_2SO_4 and (b) 1 M H_2SO_4/1 M CH_3OH. Scan rate 50 mV/s

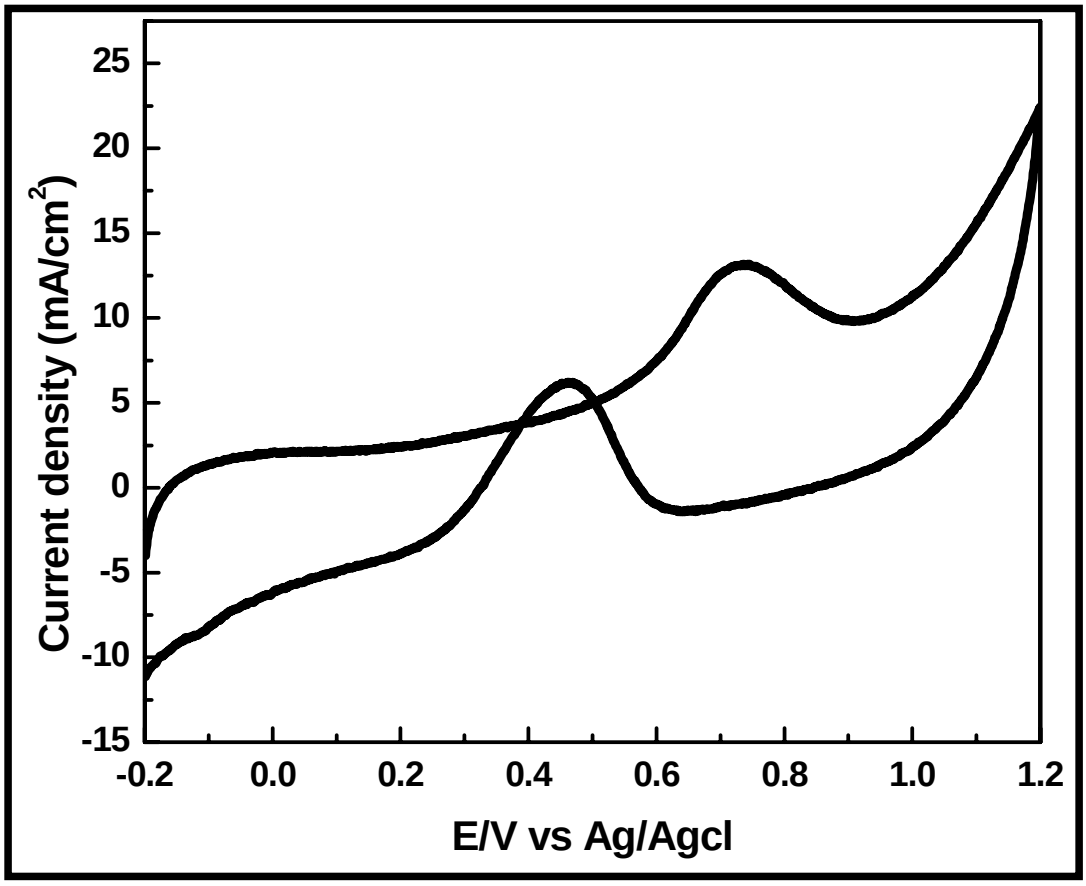

Fig. 6.9. Cyclic voltammograms of Pt incorporated conventional synthesized poly (o-phenylenediamine) (GR/Naf/Al_2O_3/$PoPD_{conv}$-Pt) electrode (after the removal of template) in 1 M H_2SO_4/1 M CH_3OH. Scan rate 50 mV/s

Fig. 6.9 shows the cyclic voltammogram of GR/Naf/$PoPD_{conv}$/Pt in 1 M H_2SO_4 and 1 M CH_3OH. It is clear from the voltammogram that the onset of methanol oxidation starts around + 0.2 V in the forward scan and peaks at 0.7 V with a peak current density of 13.3 mA/cm^2, the reverse scan shows the oxidation peak at 0.45 V with a peak current density of 6 mA/cm^2. Based on the charge deposited for the polymerisation, the thickness of the polymer was found to be 0.6 μm and the loading of Pt was found to be 600 μg/cm^2.

Since the Pt deposited on the conventionally synthesized poly (o -phenylenediamine), behaved like a bulk Pt, the curve in Fig. 6.9 was reminiscent of the Pt electrode

(Yamamoto *et al*., 1979). But, though the catalyst is, Pt deposited on the poly(o - phenylenediamine) in both the cases, the curve in Fig. 6.8b for the templated electrode for methanol oxidation was different compared to the conventional electrode. The peak potential for methanol oxidation was not observed even up to +0.8 V versus Ag/AgCl electrode for the templated system. This is the main reason for the differences in the cyclic voltammogram between the two systems. This also probably reflects that the Pt loaded on the templated system was more resistant for oxide formation than the Pt loaded on the conventional poly (o-phenylenediamine) electrode. It is well known that Pt forms platinum oxide in aqueous solutions. It is normally observed (Austin *et al*., 1984, Trasatti and Petrii 1991) that a Pt surface at +0.8 V versus Ag/AgCl should be largely oxidized and in the present study with the Pt loaded on the conventionally synthesized poly (o-phenylenediamine), the same behavior was observed and that was one of the reason for the decrease in activity of methanol oxidation (Fig. 6.9) beyond 0.7 V versus Ag/AgCl. In the case of templated system, it appears that the Pt particles in the templated nanotubes was comparatively more resistant for the Pt oxide formation and this might be one of the reason for the continuous increase in activity (Fig. 6.8b) even beyond 0.7 V versus Ag/AgCl electrode.

The activity of methanol oxidation evaluated for Pt incorporated template synthesised poly (o-phenylenediamine) and Pt deposited on conventionally synthesised poly(o-phenylenediamine) from the cyclic voltammograms are tabulated in Table 6.1.

Table 6.1 Comparison of activity of methanol oxidation between GR/Naf/ $PoPD_{Temp}$-Pt and GR/Naf/$PoPD_{Conv}$/Pt electrodes

S.No	Electrode	Onset Potential (V)	Activity*			
			Forward sweep		Reverse sweep	
			I (mA cm^{-2})	E (mA cm^{-2})	I (mA cm^{-2})	E (mA cm^{-2})
1	GR/Naf/$PoPD_{Temp}$– Pt	+0.37	84	0.82	--	---
2	GR/Naf/$PoPD_{Conv}$– Pt	+0.2	13.3	0.70	6.	0.45

* Activity evaluated from cyclic voltammogram run in 1 M H_2SO_4/1 M CH_3OH

6.8 EFFECT OF Pt LOADING ON POLY (o-PHENYLENEDIAMINE) NANOTUBES ON THE PERFORMANCE OF METHANOL OXIDATION

Fig.6.10 shows the plot of variation of performance of methanol oxidation current with Pt loading on conventionally synthesised poly (o-phenylenediamine) polymer and template synthesised poly (o-phenylenediamine) polymer nanotubes. It is evident from the plot, as the loading increases there is an increase in the activity (84 mA/cm^2) of methanol oxidation up to a loading of 600 μg/cm^2. This clearly revealed that the nanotube morphology of the poly (o-phenylenediamine) polymer helps in the fine dispersion of the Pt particles inside the poly (o-phenylenediamine) matrix. As platinum-loading increases the catalytic activity increases for the template synthesized poly (o-phenylenediamine) polymer nanotubes. This is due to the nanotubular morphology of the polymer can load platinum to a higher extent and at maximum loading there is no further increase in the catalytic activity. But as the loading increases, there is not much increase in the catalytic activity for the conventionally synthesised poly (o-phenylenediamine) polymer electrode, probably due to the agglomeration of the catalytic particles, which restrict the usage of Pt particles for methanol oxidation. The charge used for the polymerisation was 600 mC/cm^2.

6.9 EFFECT OF METHANOL CONCENTRATION

Fig. 6.11 shows the effect of methanol concentration on the anodic current of methanol oxidation for conventional and template synthesized polymer nanotube electrodes. It is clearly observed that the anodic current increases with increasing methanol concentration and levels off at concentrations higher than 0.5 M at both conventional and nanotube electrodes. We assume this effect may due to the saturation of active sites on the surface of the electrode. In accordance with this result, the optimum concentration of methanol to obtain a higher current density may be considered as about 0.5-1M. As seen in Fig. 6.11 the largest current for a given concentration of methanol was observed on the GR/Naf/PoPD $_{Temp}$– Pt electrode in same experimental conditions.

6.10 EFFECT OF TEMPERATURE

The effect of temperature on the electro-oxidation of methanol was studied. It is found that the anodic current at two different electrodes affected by temperature was shown in Fig.6.12. Current density generally increases with the rise in temperature indicating an increase in reaction kinetics. A linear increase in the peak currents with increasing temperature was observed for the conventional electrodes up to 65 °C, indicating an enhancement of the methanol oxidation rate with temperature and then the peak currents decrease. The next decrease can be attributed to the progressive evaporation of solution with increasing temperature. Considering that no azeotrope is formed in methanol water mixture, it is expected that a progressive decrease in peak current should appear during the temperature elevation, due to a loss in methanol concentration**.** However, a linear increase of the peak current is observed in practice at temperatures below 65 °C (the boiling point of methanol is 64.5 °C), which can be

assigned to the acceleration of the electrode reaction kinetics proportionally to temperature increase. There is not much increase in current density as temperature increases for template synthesized nanotube electrode. This may be due to the tubular morphology favours easier transport of methanol to the catalytic sites

6.11 CHRONOAMPEROMETRIC RESPONSE OF GR/Naf/PoPD$_{Temp}$-Pt, GC/ 20 wt.%Pt/C (E-TEK) AND GR/Naf/PoPD$_{Conv}$-Pt

Chronoamperometric experiments were carried out to observe the stability and possible poisoning of the catalysts under short-time continuous operation. Fig.6.13 shows the evaluation of activity of GR/Naf/PoPD$_{Temp}$-Pt and GR/Naf/PoPD$_{Conv}$-Pt with respect to time at constant potential of +0.6 V. It is clear from Fig. 6.13 when the electrodes are compared under identical experimental conditions; the GR/Naf/PoPD$_{Temp}$-Pt shows a better activity and stability to the GR/Naf/PoPD$_{Conv}$-Pt, GC/E-Tek and 20% Pt/Vulcan XC72 carbon–Nafion electrodes. GC/E-Tek 20% Pt/Vulcan XC72 carbon–Nafion shows higher activity and stability compared to conventional GR/Naf/PoPD$_{Conv}$-Pt electrodes. The higher activity of the polymer nanotube based electrodes demonstrates the better utilization of the catalyst. The increased utilization is mainly due to the tubular morphology of the polymer, which allows the particle to be highly dispersed, which result in lower particle size. The lower activity of GR/Naf/PoPD$_{Conv}$-Pt and GC/E-Tek 20% Pt/Vulcan XC72 carbon–Nafion electrode might be due to the poor utilization of the platinum catalyst.

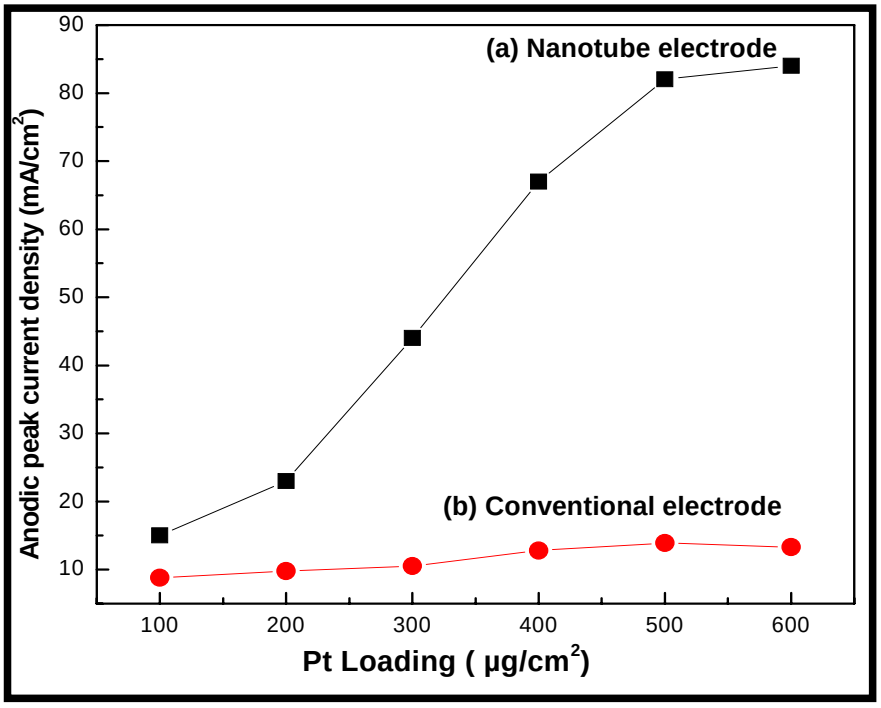

Fig. 6.10. Variation of anodic peak current density as a function of platinum loading on (a) nanotube and (b) conventional electrodes (Current densities were evaluated from CV run in 0.5 M H_2SO_4 / 1M CH_3OH at 50 mV/s)

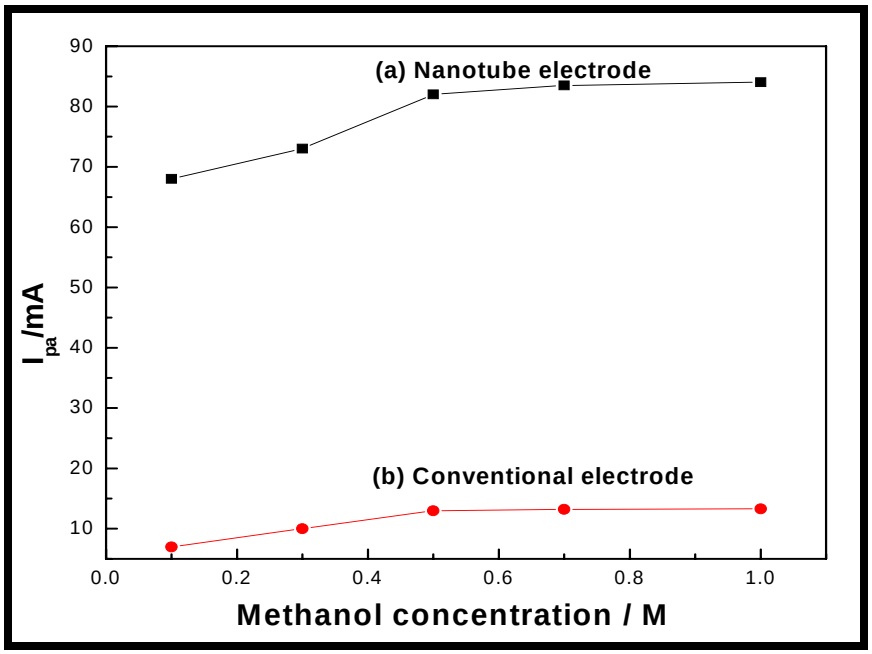

Fig. 6.11. Plot of anodic peak current of methanol oxidation as a function of methanol concentration in 0.5 M H_2SO_4 solution for (a) nanotube and (b) conventional electrodes

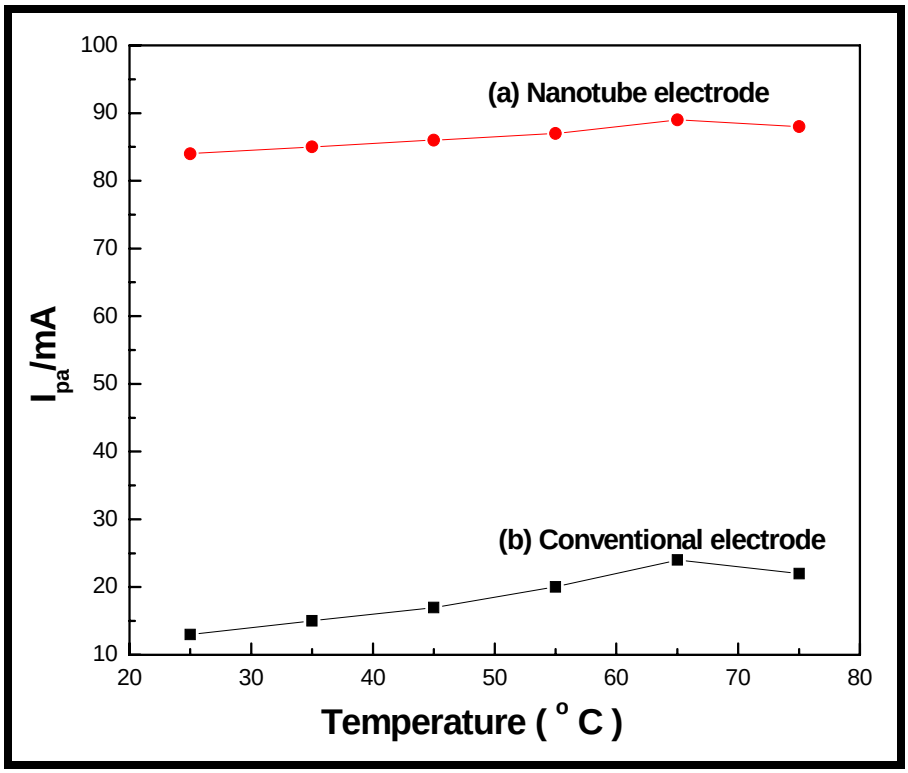

Fig. 6.12. Plot of anodic peak current oxidation as a function of temperature for: (a) GR/Naf/$PoPD_{Temp}$– Pt and (b) GR/Naf/$PoPD_{Conv}$– Pt in 0.5 M H_2SO_4/1.0 M CH_3OH

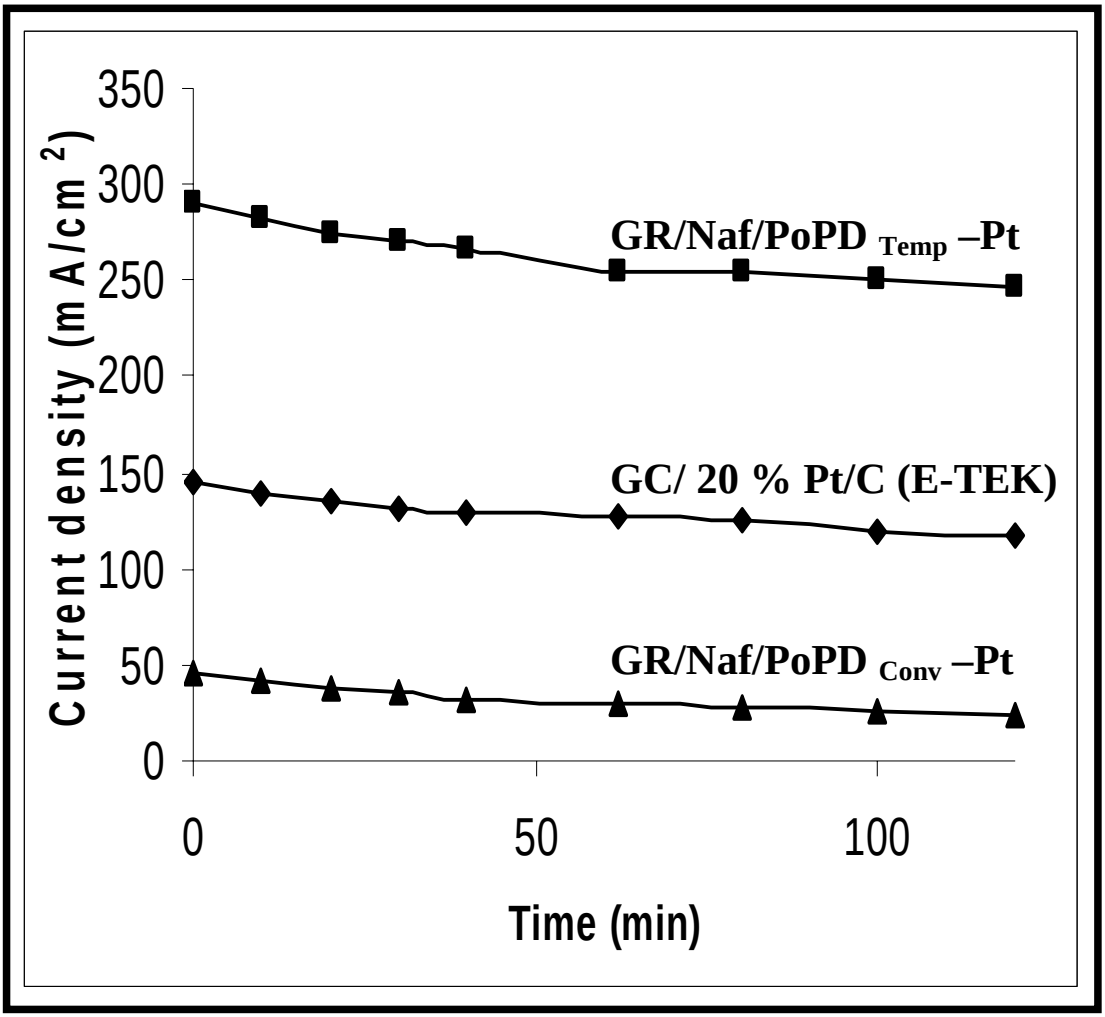

Fig. 6.13. Variation of current density with time in 1 M H_2SO_4/1 M CH_3OH at +0.6 V vs. Ag/AgCl

6.12 CONCLUSIONS

The electrochemical synthesis and characterization of conducting poly (o-phenylenediamine) nanotube and Pt incorporated nanotube by template method have been achieved. On the other hand, the SEM experiments show the dense, non-uniform and mat morphology of conventionally synthesized poly (o-phenylenediamine). The fine dispersion of Pt particles inside the nanotube was revealed from the electron diffraction image. The methanol oxidation activity of Pt incorporated template

synthesized poly (o-phenylenediamine) with a loading of 600μg/cm^2 was found to be nearly 13 times more active than Pt deposited on conventionally synthesized poly (o-phenylenediamine) with the same metal loading. It was revealed from the plot of current density vs the loading, that the Pt incorporated on template-synthesized poly (o-phenylenediamine) can accommodate more amount of Pt than conventionally synthesized poly (o-phenylenediamine). Excellent catalytic activity is observed for the electro-oxidation of methanol at the metal–polymer nanotube composite electrode. The highly dispersed platinum particles play a key role in the electrochemical behavior and catalytic activity, and the conducting polymer acts as an electron transfer matrix and a protective layer with a long time stability of electrode. The better utilization (by means of high activity at low Pt loading) and stability of the template-synthesized Pt incorporated poly (o-phenylenediamine) electrode have been demonstrated by comparing with Pt incorporated template-free conventionally synthesized poly (o -phenylenediamine) electrode. One of the major impediments to the commercialization of DMFC is the higher requirement of Pt catalyst. Increasing its utilization could considerably lower the Pt loading. The Pt incorporated template-synthesized polymeric nanotube on the graphite, not only increases the electronic–ionic contact, but also provides an easier electronic pathway between the electrode and the electrolyte, which increases the reactant accessibility to the catalytic sites.

The electro-catalytic activity of the nanotube based electrode was compared with those of the conventionally synthesized poly (o-phenylenediamine) on graphite, using cyclic voltammetry. The Pt incorporated poly (o-phenylenediamine) nanotube electrode exhibited excellent catalytic activity and stability compared to the 20-wt % Pt supported on the Vulcan XC 72R carbon and Pt supported on the conventional

poly(o-phenylenediamine) electrode. The nanotube electrode showed excellent electro-catalytic activity and stability for electro- oxidation of methanol.

CHAPTER 7

SYNTHESIS, CHARACTERIZATION AND ELECTRO-CATALYTIC ACTIVITY OF Pt SUPPORTED ON POLY (3, 4-ETHYLENEDIOXYTHIOPHENE)/ V_2O_5 NANOCOMPOSITES FOR METHANOL OXIDATION IN DIRECT METHANOL FUEL CELLS

7.1 INTRODUCTION

Considerable attention has been paid in recent years in improving the performance of existing electrode materials for methanol oxidation reaction. The research over the last few decades identified the best catalyst, so for is the bimetallic catalyst based on Pt-Ru supported on carbon for methanol oxidation. The transformation in fuel cell research for developing electrode materials shows the importance of the catalyst supports. In that process we focus our attention on composite materials based on conducting polymer based bronzes to enhance the utilization of the noble metal and also to increase the stability of the electrode for methanol oxidation. There has been a great deal of interest on preparation of conducting polymer-based nanocomposite electrodes for methanol oxidation in direct methanol fuel cells (Rajesh *et al.,* 2005). Electronic conducting polymers such as polypyrrole, polyaniline, polythiophene and poly (3, 4-ethylenedioxythiophene) can serve as porous support to disperse the platinum particles and the resulted composites have revealed some special features. (Kuo *et al.,* 2006). Among the conducting polymers, poly(3, 4-ethylenedioxythiophene) (PEDOT) is the most promising polymer due to high conductivity, wide electrochemical potential window and environment stability.

Electrically conducting oxide Xerogels are being explored as new materials in electrochemistry and for their innate ability to amplify the nature of the surfaces of technologically relevant conducting oxides in batteries, ultracapacitors and fuel cells. Vanadium oxide has received the most attention of the conducting oxides. V_2O_5 xerogels have been known for over 50 years, but it was the research by Livage and colleagues using sol gel chemical synthesis that renewed interest in these materials in the 1980s (Livage; 1996). The resulting xerogels were shown to possess a variety of electrical, optical and electrochemical properties.

Vanadium pentoxide (V_2O_5) is a popular material because of its intrinsic electrochemical redox activity to induceable change in the oxidation degree of vanadium (V) species (Folkesson and Larsson, 1989). Platinum and other noble metals have been found to catalyze the complete oxidation of sucrose and other sugars by vanadium (IV) in acid environments. As the redox potential of vanadium (IV)/vanadium (III) differs substantially from that of dioxygen/water, it might be possible to use this reaction to construct a redox type of fuel cell (Larsson and Folkesson 1993, 2005). Porphyrin doped vanadium pentoxide xerogel has been used as an electrode material (Anaissi *et al.,* 2003). Vanadium (V) oxide Xerogels is capable of intercalating metal ions or organic molecules, forming nanostructurized composite materials with a wide spectrum of possible applications, especially electrochemical ones.

The use of carbon and possibly other electronic conductors in the catalyst layer has been proposed for increasing the utilization of the catalyst by increasing electrical connectivity between catalyst particles. However, the relatively low density of carbon results in thick catalyst layers that impede the mass transport of methanol to the

catalytic sites. Furthermore, the polymer-electrolyte membrane material is acidic and most metals are not chemically stable in contact with it. Carbon material that conducts electrons (but not protons) does not contribute to the transport of protons produced in the electro-oxidation reaction.

Commonly used carbon supports (Conductex 975 and Vulcan XC-72) are good conductors of electrons. The catalyst by itself, however, cannot conduct protons. Presence of ionomer in the catalyst layer is necessary to conduct the protons. Therefore proton conduction may depend dramatically on the formulation of the catalyst layer. Recent advances in catalyst design have begun to address this limitation. As with electron conduction, thinner catalyst layers help reduce resistive losses due to proton conduction. Further, the surface chemistry of the catalyst support can be tailored appropriately; the catalyst also may lose stability due to sintering of platinum particles, dissolution of platinum, and corrosion of the carbon support.

Corrosion of the carbon support also may lead to performance loss. When carbon corrodes, the relative percentage of conductive material in the catalyst layer decreases. The resistance of the remaining dielectric material then dominates the cell resistance. Further, as the carbon support oxidizes, the thickness of the catalyst layer decreases, decreasing electrical contact with the current collector and increasing the cell resistance. Carbon corrosion also decreases the number of sites available to anchor platinum, resulting in metal sintering. The extent of carbon corrosion in the cell depends on the operating conditions and the specific chemistry of the support used. Higher operating voltage increases the degradation rate. The surface area of the carbon support also influences the rate of carbon corrosion. The higher the surface area of the carbon, the faster is the rate at which it corrodes. A catalyst maker may

attempt to lower the available support surface area by selecting an alternative carbon. The carbon support may also be modified by graphitization. When traditional carbon blacks are heated to high temperatures (*e.g.,* ~2,000 °C), lattice rearrangements occur, increasing the graphitic nature of the material and decreasing the number of active surface sites. Graphitization produces a material, which is highly resistant to oxidation and carbon corrosion. However, with fewer active sites, metal deposition on such supports is more difficult.

An alternative is to develop a catalyst support that is permeable to gases and water, while conducting both protons and electrons efficiently. Such a material could replace both carbon and Nafion in the catalyst layer and should provide enhanced performance. Elsewhere we have described the use of polypyrrole/poly(styrene-4-sulfonate) (PPY/PSS) in such a role. However, because of the poor stability of the polypyrrole we were unable to deposit appropriately small Pt particles without appreciable losses of electronic conductivity. As a consequence, the performances of the PPY/PSS supported catalysts for oxygen reduction in gas diffusion electrodes were only modest (Lefebvre *et al.,* 1999). As a π conjugated polymer, PEDOT can have high conductivity up to $20\Omega^{-1}$ cm^{-1} when prepared from chemical synthesis (Corradi and Armes 1997) and electrochemical synthesis (Niu *et al.,* 2001).

The synthesis and electrochemical studies, of a more stable conducting poly(3, 4-ethylenedioxythiophene)/ (PEDOT-V_2O_5) nanocomposites have been reported. This material was shown to have an appropriately high surface area for use as a catalyst support and to exhibit high electron and proton conductivities. Furthermore V_2O_5 is a strong oxidant, V_2O_5 acts as a good oxidation catalyst. The potentials of methanol oxidation and vanadium redox couples are shown in Fig 7.1.

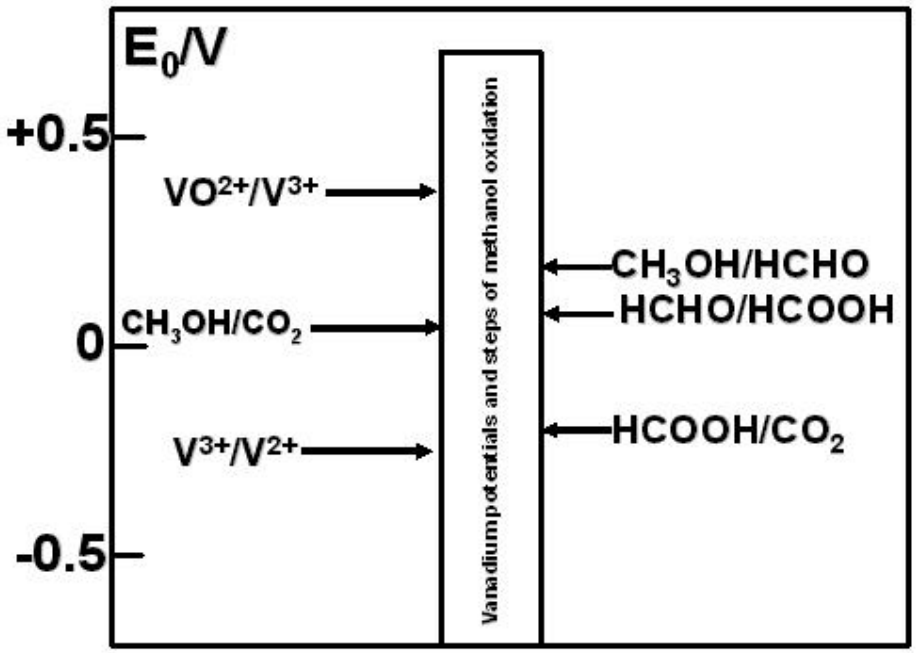

Fig. 7.1. Comparison of the potentials at which methanol is usually oxidized electrochemically and the normal redox couples (Folkesson *et al.,* 1989)

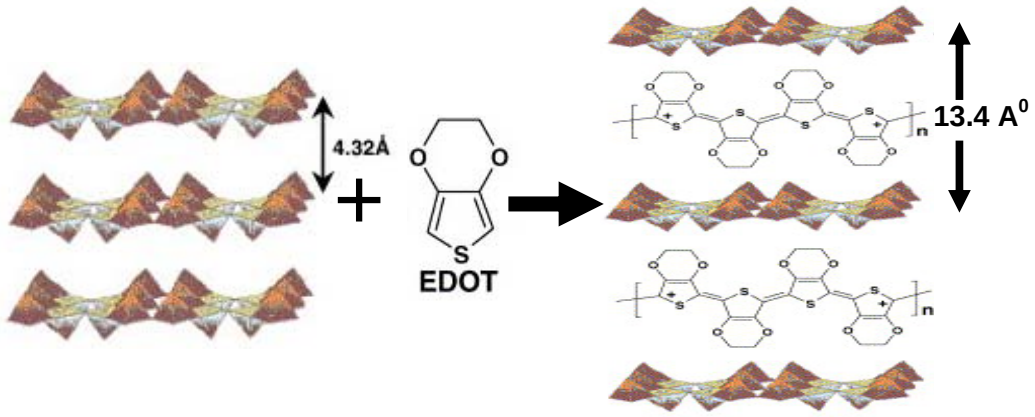

Scheme 7.1. Schematic diagram of formation of PEDOT-V_2O_5 nanocomposite

The normal potentials of the probable intermediates in the methanol oxidation are also included. Vanadium oxide redox couple has been extensively used in batteries (Sum and Skyllas-Kazacos, 1985; Sum *et al.,* 1985).

The synthesis of PEDOT-V_2O_5 nanocomposite is illustrated in scheme 7.1. Assynthesised nanocomposite with nanometer-scale Pt particles can produce excellent fuel cell catalysts. Platinum can be dispersed in such a support that leads to a decrease in the amount of expensive noble metal used. Also, such composites have improved catalytic activity for the oxidation of methanol via a better utilization of the platinum crystallites and in decreasing the poisoning effect. The typical scheme to be adopted for the preparation of Pt supported composite material is shown in scheme 7.2.

In the present investigation the composite material prepared by the former method has been used as the support for Pt and used as the electrode for methanol oxidation in acid medium. The material has been characterized and studied by X-ray diffraction (XRD), Thermogravimetric analysis (TGA), Elemental analysis, Scanning electron microscopy (SEM), Transmission electron microscopy (TEM) and cyclic voltammetry (CV). The cyclic voltammetric technique apart from being used to characterize the composite material for accessing the electrochemical stability in acid medium, the technique has also been used to evaluate the methanol oxidation in acid medium. The chronoamperometric response was monitored to evaluate the stability of the Pt supported nanocomposite material for methanol oxidation.

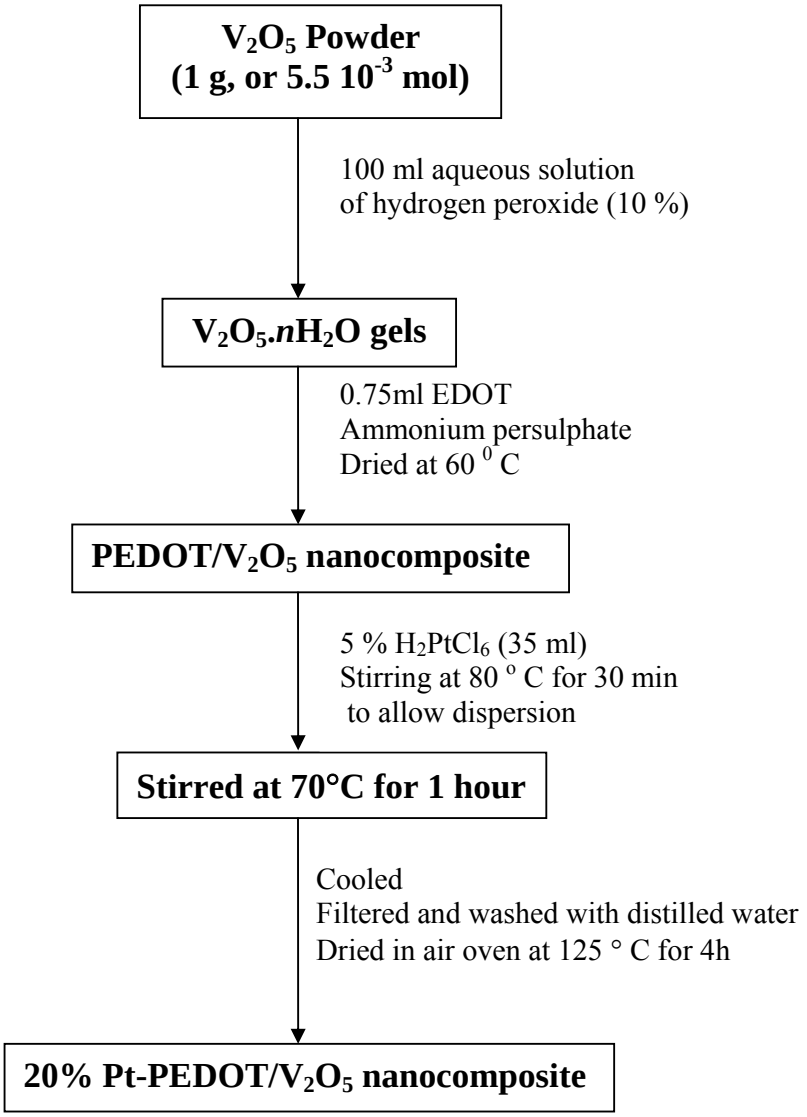

Scheme 7.2. Preparation of 20% Pt/PEDOT-V_2O_5 nanocomposite catalyst by formaldehyde reduction method

7.2 EXPERIMENTAL

7.2.1 Preparation of Poly (3, 4-Ethylenedioxythiophene)-V_2O_5 nanocomposites

Vanadium oxide (V_2O_5) powder (1 g, or 5.5 ×10^{-3} mol) is mixed with 100 ml aqueous solution of hydrogen peroxide (10%). As H_2O_2 decomposes, oxygen gas evolves and voluminous bright yellow foam forms spontaneously. Vanadium oxide reacts with

hydrogen peroxide to give $V_2O_5.nH_2O$ gels (Chandrappa *et al.,* 2002) that have a layered structure. These gels can intercalate a wide variety of inorganic and organic species, such as EDOT. In the foaming process described, gelation and intercalation both occur when the EDOT and hydrogen peroxide solutions are added to vanadium oxide powder. The monomer has been polymerised using ammonium persulfate as initiator. The intercalation of EDOT between V_2O_5 layers creates a pasty solid, while the hydrogen peroxide decomposes spontaneously in the presence of vanadium oxide. Large pores are formed by oxygen gas released through the viscous gel in the presence of EDOT: as they escape, the oxygen bubbles cause the formation of voluminous foam.

7.2.2 Preparation of Pt/ PEDOT- V_2O_5 nanocomposites and Pt/C catalyst

The nanocomposite powder (ca. 100 mg) was ground gently with a mortar and pestle then suspended in about 20 mL H_2O. H_2PtCl_6 solution was used (Aldrich) for deposition of Pt was then added in an amount slightly greater than the desired loading. The suspension was stirred at around 80^0C for 30 min to allow dispersion and equilibration, then ca. 25 molar excess of aqueous formaldehyde (BDH, 37%) was added followed by heating at reflux for 1 h. The catalyzed polymer nanocomposites were collected by filtration, washed thoroughly with water, and then dried under vacuum (25-50^0C).

The same procedure as the above was repeated for the preparation of Pt/C catalyst. The same procedure and conditions were used to make a comparison between the Pt/C and Pt/PEDOT-V_2O_5 system.

7.3 ELEMENTAL ANALYSIS

The Vanadium content was determined by ICP-OES analysis of the sample solution that was prepared by placing the composite powder in concentrated sulfuric acid to dissolve V_2O_5 in the composite, followed by dilution with water and filtration to remove the dispersed polymer solid samples. Other elements presents in the polymer were analyzed by CHNS-O analysis. The combined elemental analysis of the nanocomposites gives the following information: $(C_6H_4O_2S)_{0.40}$ V_2O_5 0.5 H_2O : C, 11.5; H, 2.25; S, 5.13; V, 40.76.

7.4 X-RAY DIFFRACTION STUDY

Fig. 7.2 shows a comparison of the powder XRD patterns for the PEDOT/ V_2O_5 nanocomposites and V_2O_5 to demonstrate the subtle structural changes upon intercalation. The X-ray diffraction pattern (Fig. 7.2 a) of the PEDOT–V_2O_5 nanocomposite was comparable with the one reported (Murugan *et al.,* 2004). Only (0 0 1) reflections are observed in the X-ray diffraction pattern, which is a typical pattern for quasi-crystalline layered materials. The strongest peak observed at low angle corresponding to the (001) plane of the layered V_2O_5 structure is directly related to the interlayer spacing. The main features of the V_2O_5 diffraction pattern in the nanocomposites are modified by the appearance of a sharp diffuse scattering feature and an increase in the intensity of the (001) peak. Nanocomposites shows a clear change in the position of the peak takes place, which indicates the (001) peak at 2θ 6.8°, which corresponds to an interlayer spacing of 13.4 A^0, respectively, compare to the interlayer spacing of V_2O_5 of 4.32 A^0. After intercalation Incorporation of PEDOT in V_2O_5 confirms increasing the interlayer spacing to 13.4 A^0.

The powder XRD patterns for Pt/C and Pt/ PEDOT-V_2O_5 nanocomposites catalysts are also shown in Fig. 7.3. The diffraction peak at 24-27° observed is attributed to the hexagonal graphite structure (002) of Vulcan carbon. Both Pt/Vulcan carbon and Pt/ PEDOT-V_2O_5 electrocatalysts displayed the characteristic patterns of Pt FCC diffraction. The peaks can be indexed at 2θ = 39.8° (1 1 1), 46.6° (2 0 0) and 67.9° (2 2 0) reflections of a Pt face-centered cubic (FCC) crystal structure.

7.5 FT-IR SPECTROSCOPIC STUDIES

The FT-IR spectra of the synthesized PEDOT-V_2O_5 nanocomposites are shown in Fig.7.4, together with those of pristine V_2O_5 and V_2O_5 xerogel. which presents the characteristic bands corresponding to PEDOT (bands in the range 1049–1600 cm^{-1}) as well as bands at lower frequencies assigned to V_2O_5 (523 and 759 cm^{-1} for V–O–V stretching modes and 1003 cm^{-1} for V=O stretching). The changes in position and shape of the vibrational peaks of the vanadium oxide framework are also significant. The V=O peak shifts from 990 to 1003 cm^{-1} while the V–O–V vibrational peaks shift from 852 and 530 cm^{-1} to 758 and 523 cm^{-1}, respectively. These changes are attributed to the greater number of V^{4+} centers present in the nanocomposite. The mechanism of this remarkable all-solid-state intra-lamellar polymerization is presumed to be coupled to the ability of vanadium centers to activate oxygen. Therefore, vanadium oxide plays a direct role in this redox event, which is consistent with its ability to catalyze several oxidation reactions of organic molecules (Centi *et al.,* 1990). The qualitative differences between spectra of b relative to nanocomposites C relate to bands at 1218 and 1105 cm^{-1} owing to the presence of excess PEDOT in these two samples.

7.6 THERMOGRAVIMETRIC ANALYSIS

The thermal stability of these materials in air was examined by TGA experiments. Fig. 7.5. gives the Thermogravimetric curves of pristine V_2O_5, V_2O_5 xerogel and PEDOT-V_2O_5 nanocomposites. Fig. 7.5b reveals that the TGA curve of V_2O_5 xerogel contains two main weight losses. The first weight loss (8 %), up to 120 °C, corresponds to the removal of the weakly bonded water. The second weight loss (16.2 %), up to ~215 °C corresponds to the loss of more strongly bound water between the layers. This is followed by a continuous weight loss up to ~420 °C, which can be attributed to the combustion of the organic polymer component, in the nanocomposite, which can be used to confirm PEDOT content in these nanocomposites. A subsequent mass gain (2.6%) up to 650 °C can be attributed to the formation of orthorhombic V_2O_5. These results suggest that the insertion and polymerization of the 3,4-ethylene dioxythiophene (EDOT) monomer is accompanied by sacrificial reduction of the V_2O_5 layers.

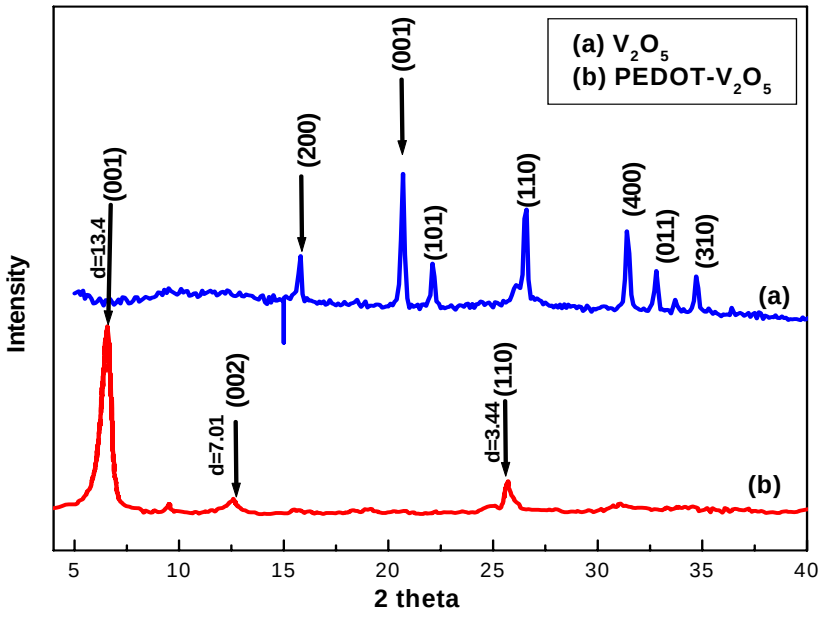

Fig. 7.2. X-ray diffraction powder pattern of (a) V_2O_5 powder and (b) PEDOT-V_2O_5 $(C_6H_4O_2\ S)_{0.4}\ V_2O_5.0.5H_2O)$ nanocomposite

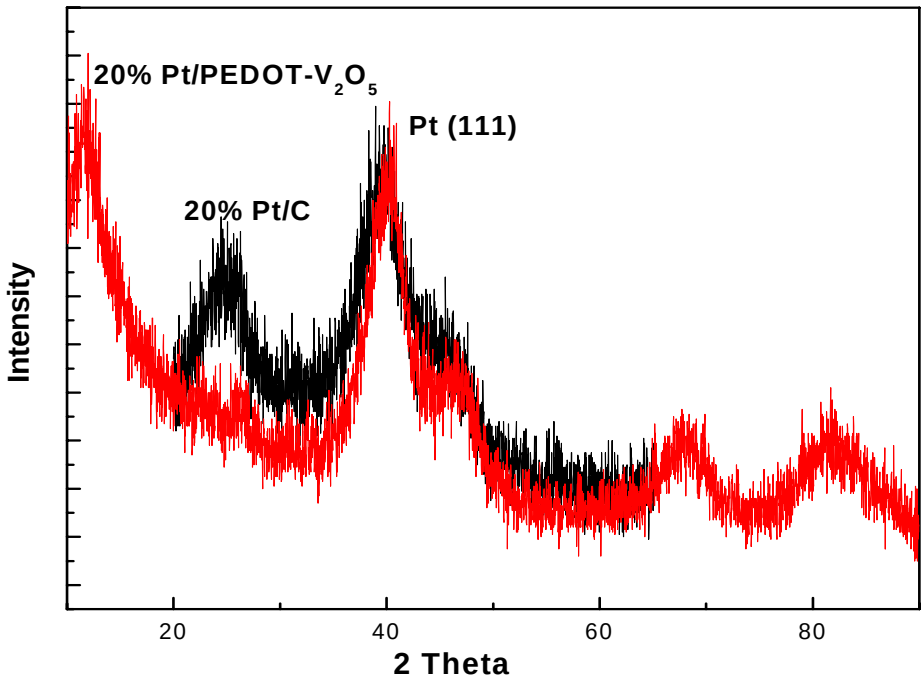

Fig. 7.3. X-ray diffraction powder pattern of (a) 20 % Pt/C and (b) 20 % Pt/PEDOT- V_2O_5 nanocomposite

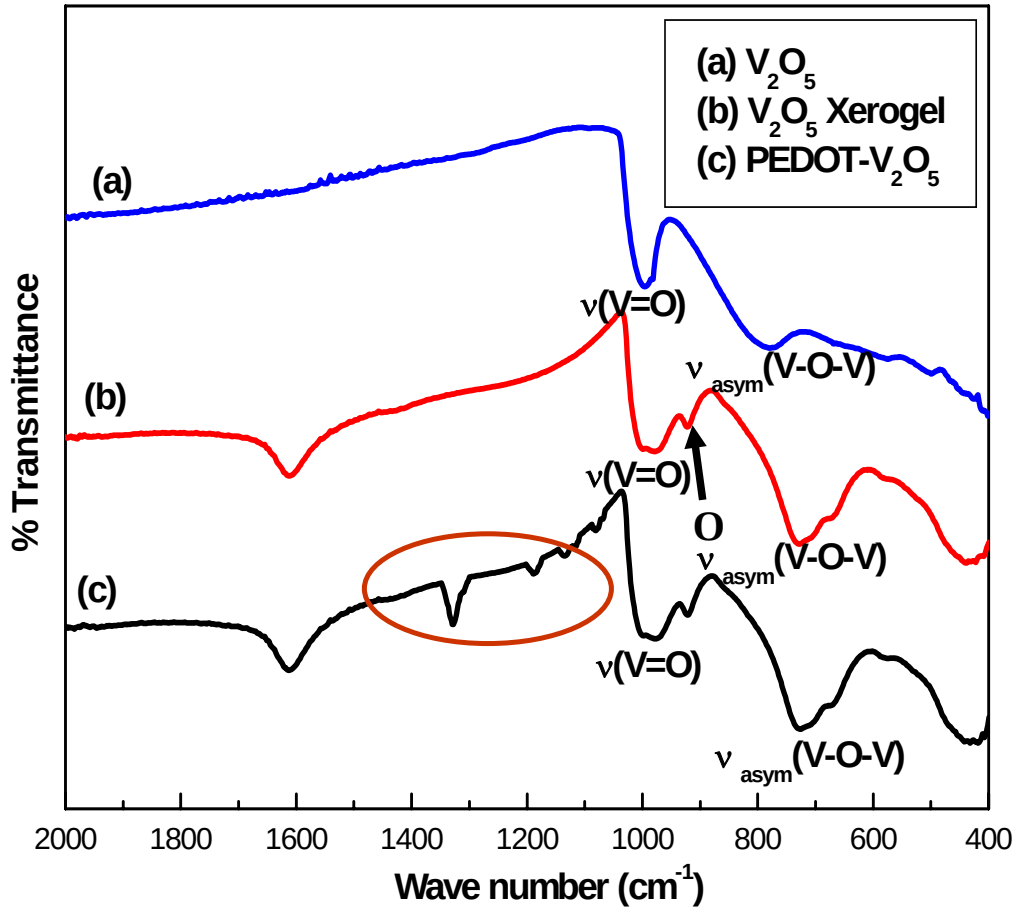

Fig. 7.4. FT-IR spectra of (a) V_2O_5 (b) V_2O_5 xerogel and (c) PEDOT/V_2O_5 nanocomposites

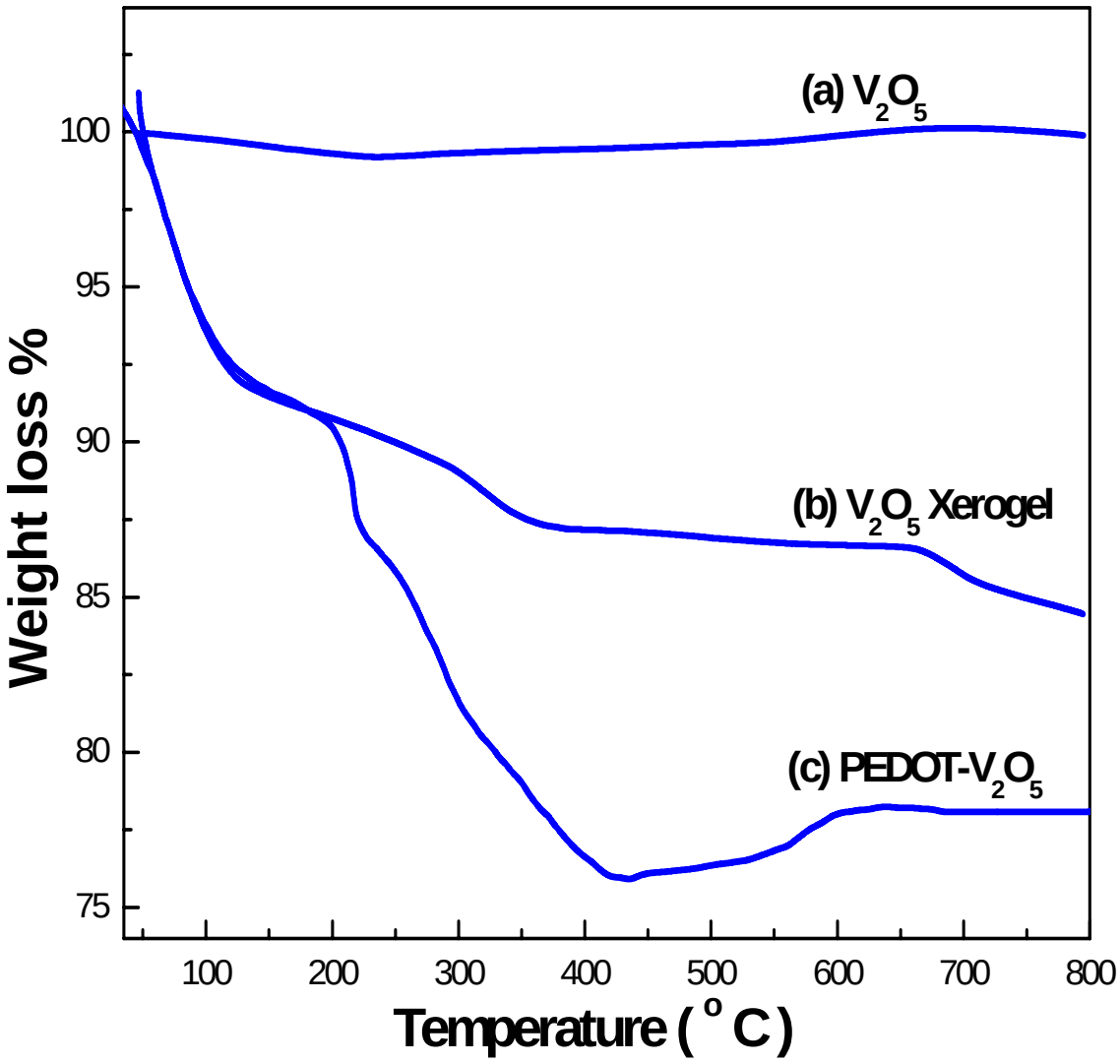

Fig. 7.5. TGA curves of (a) V_2O_5 (b) V_2O_5 xerogel and (c) PEDOT-V_2O_5 nanocomposite

7.7 ELECTRON MICROSCOPY STUDY

7.7.1 Scanning Electron Microscopy (SEM)

In order to determine the morphologies and elemental distribution of the supports before and after impregnation, SEM and EDX were performed, respectively. The scanning electron microscopic (SEM) images of both V_2O_5 and PEDOT /V_2O_5 nanocomposites are illustrated in Fig. 7.6 (a-d) respectively, where the later forms a continuous and relatively homogeneous matrix with a distinct lamellar morphology. Although, the incorporation of PEDOT into the V_2O_5 leads to morphological changes in agreement with the results of XRD patterns, these can be seen only at high resolution. More significantly, the SEM images also suggest that there is no bulk deposition of polymer on the surface of the microcrystallites.

The SEM image of the nanocomposite support after impregnation with Pt is shown in Fig 7.7a. After Pt deposition on the nanocomposite porous morphology has been developed which is suitable for catalyst support. The nanocomposite catalyst support not only provides ionic and electronic conductivity but also favours mass transport.

The EDX mapping image in a scanning electron microscope (SEM) of the nanocomposite support can provide information on the distribution of Pt. The typical EDX mapping image for the nanocomposite support after impregnation with Pt are shown in. Fig 7.7c. Fig 7.7a and 7.7c show the same area of the sample. The EDX mapping of Pt shows homogeneous distribution of platinum inside the layer of the nanocomposite, which indicates better catalyst dispersion. The EDX spectrum substantiated that the catalyst support consisted of Pt and V.

7.7.2 Transmission Electron Microscopy (TEM)

A more accurate observation of particle morphology and structure can be realized using transmission electron microscopy (TEM) as illustrated in Fig. 7.8. The TEM image of Pt/C catalyst was shown in Fig 7.8a and the average Pt particle size was 3.1 nm. The TEM image of Pt/PEDOT-V_2O_5 nanocomposite support was shown in Fig 7.8b. The Pt particles are well dispersed on the nanocomposite support. The average Pt particle size around 2.3 nm. Transmission electron micrograph of Pt nanoparticles on PEDOT-V_2O_5 nanocomposite support showing Pt nanoparticles dispersed throughout the nanocomposite support.

7.8 Electrochemical characteristics of the PEDOT-V_2O_5 nanocomposite

The electrochemical behavior of PEDOT-V_2O_5 nanocomposites was studied in 0.5 M H_2SO_4. Fig 7.9 shows the cyclic voltammogram (CV) associated with the Vanadium centers of nanocomposite: it is constituted by a first one-electron reversible wave followed by a composite wave, largely irreversible chemically. Worth of notice, the redox processes of the V-centers are located in a potential value (roughly -0.2 V to + 0.6 V)

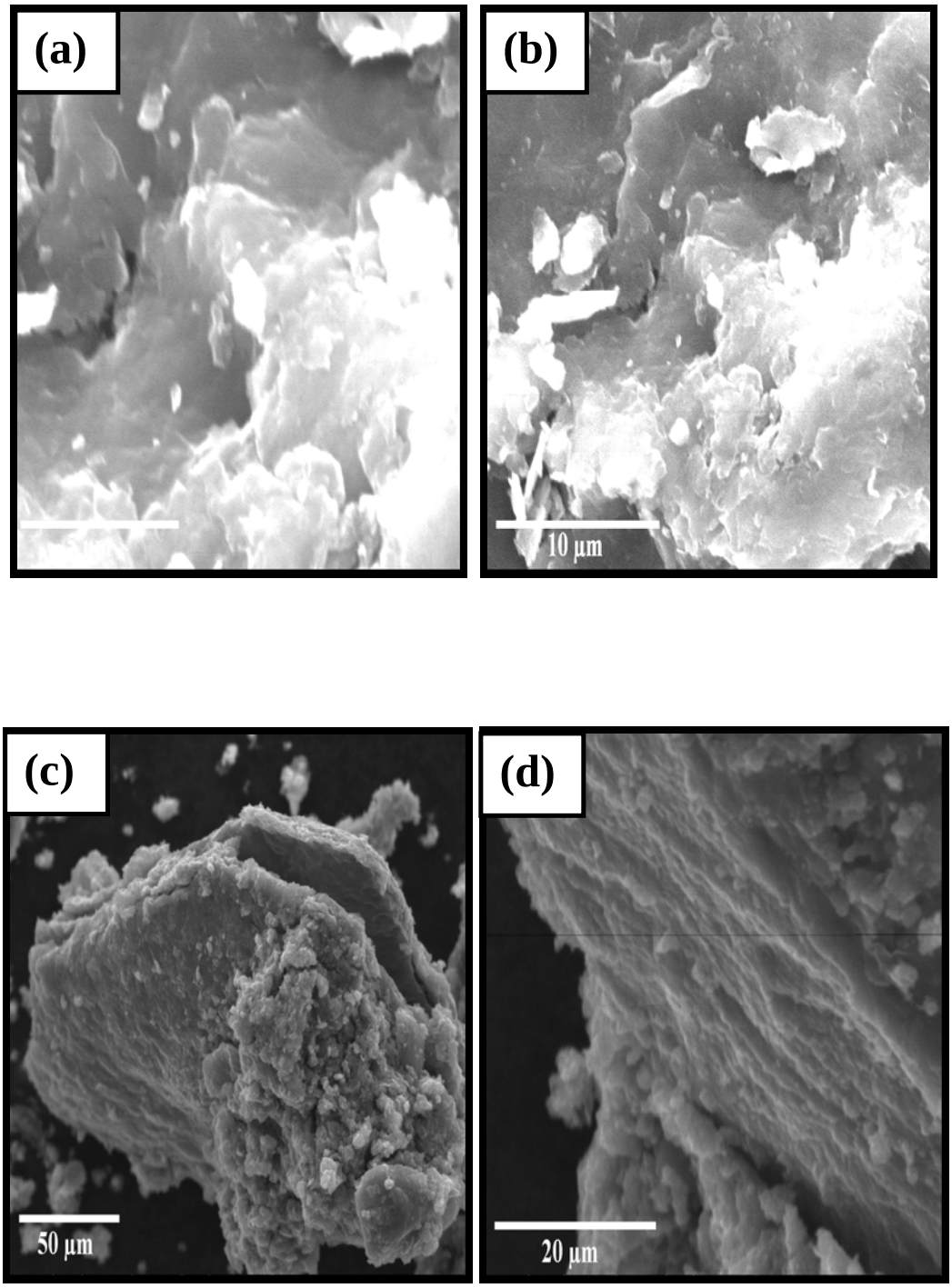

Fig. 7.6. SEM images of (a-b) V_2O_5 (c-d) layered hybrid PEDOT-V_2O_5 nanocomposite synthesized chemically with the aid of H_2O_2

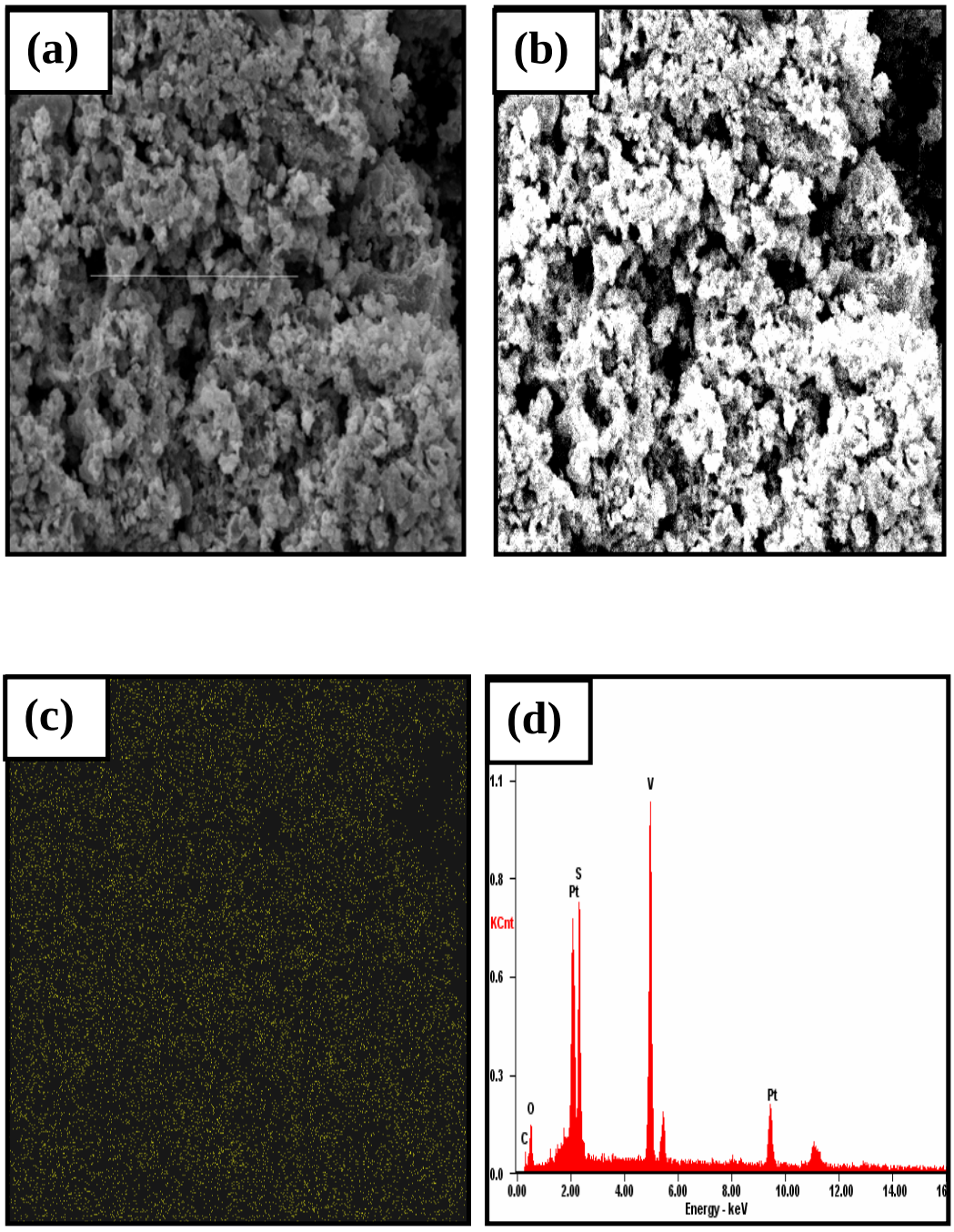

Fig. 7.7. (a-b) SEM image, (c) EDX-element distribution and (d) EDX mapping of Pt on PEDOT-V_2O_5 nanocomposite support

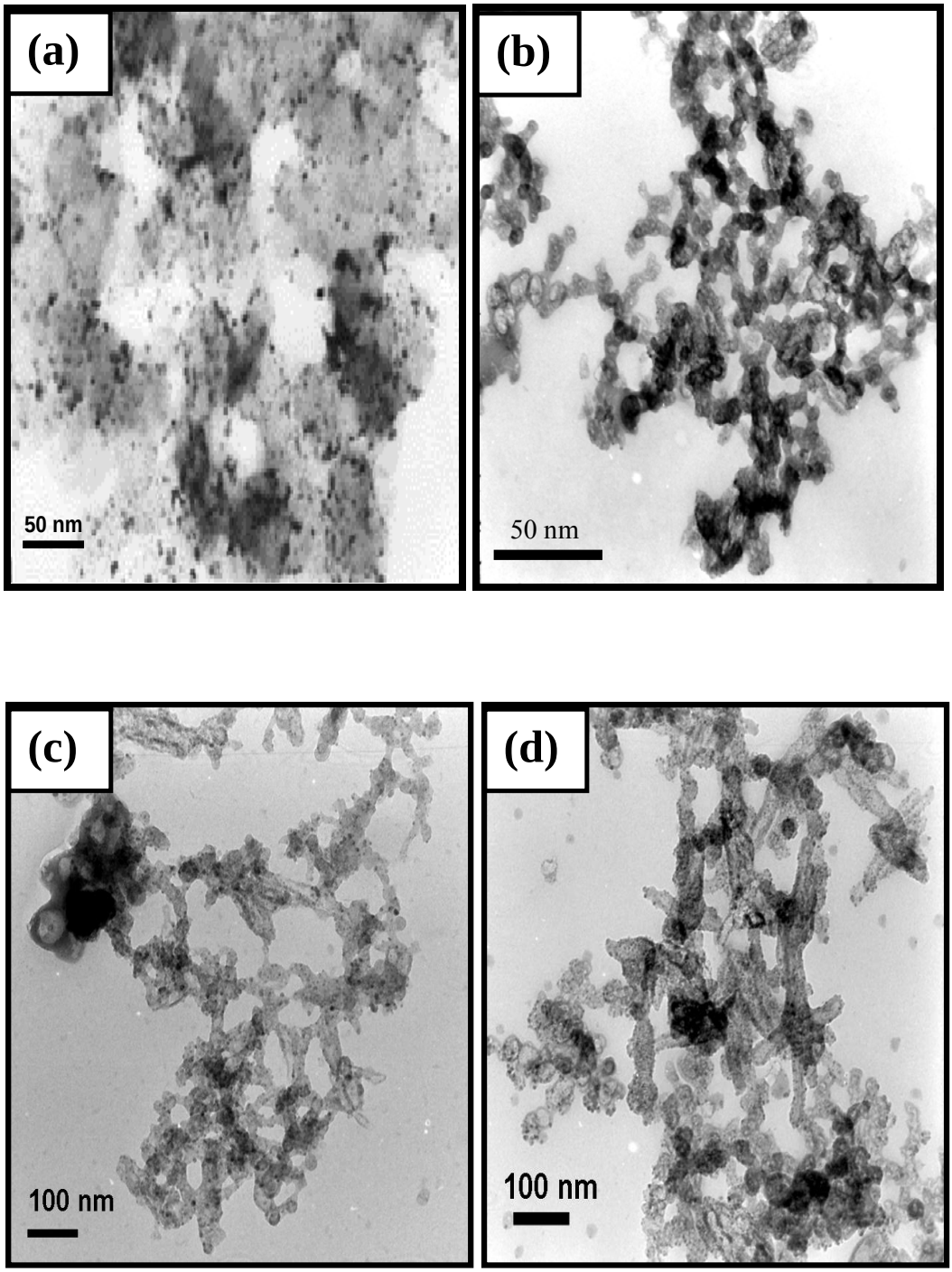

Fig 7.8. TEM image of (a) 20% Pt/C (b) PEDOT-V_2O_5 nanocomposite and (c-d) Pt / PEDOT-V_2O_5 catalyst

7.11 EVALUATION OF METHANOL OXIDATION ON Pt LOADED PEDOT-V_2O_5 NANOCOMPOSITE

Fig. 7.10a shows the Cyclic Voltammogram of Pt loaded PEDOT-V_2O_5 nanocomposite (GC/PEDOT-V_2O_5-Naf/Pt) in 1 M H_2SO_4 scanned between – 0.2 and + 1.2 V and run at 50 mV/s.

It is evident from the voltammogram that the onset of methanol oxidation starts at 300 mV and the current increases linearly with the applied potential and does not exhibit any peak in the forward scan and reaches a maximum current density of 56.4 mA/cm^2 for a Pt loading of 20 μg/cm^2. In the reverse scan there is a slight decrease in the current and there is a superposition of the voltammogram between +0.8 and +1.0 V probably suggests the tolerance of nanocomposite electrode toward the strongly adsorbed intermediates. In the present investigation, the increased methanol oxidation activity probably suggests that the vanadium pentoxide present in the matrix might have helped in the bifunctional mechanism. This is due to V_2O_5 functions as Ru does in Pt-Ru/C catalysts because oxygen-containing species could easily form on the surface of V_2O_5.

The Pt loaded conducting poly (3, 4-ethylenedioxythiophene) intercalated vanadium pentoxide nanocomposite exhibited excellent activity and stability for methanol oxidation compared to the Pt loaded on the commercial Vulcan XC 72R carbon support. The conducting poly (3, 4-ethylenedioxythiophene) not only acted as an excellent electronic support for Pt particles but also aided for an increased stability of the layered transition metal oxide, under the electrochemical operating conditions.

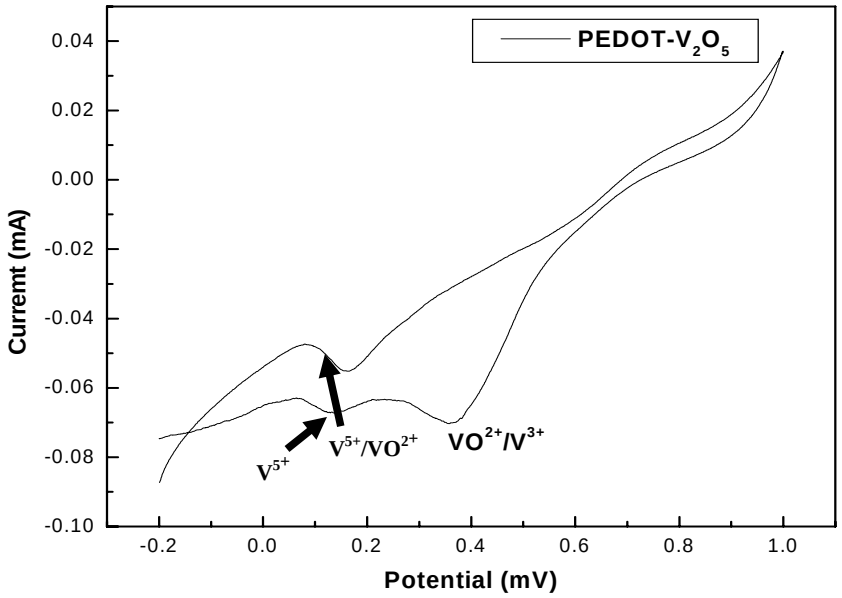

Fig 7.9. CV of PEDOT-V_2O_5 nanocomposite electrode in 0.5 M H_2SO_4 at 50 mV/s

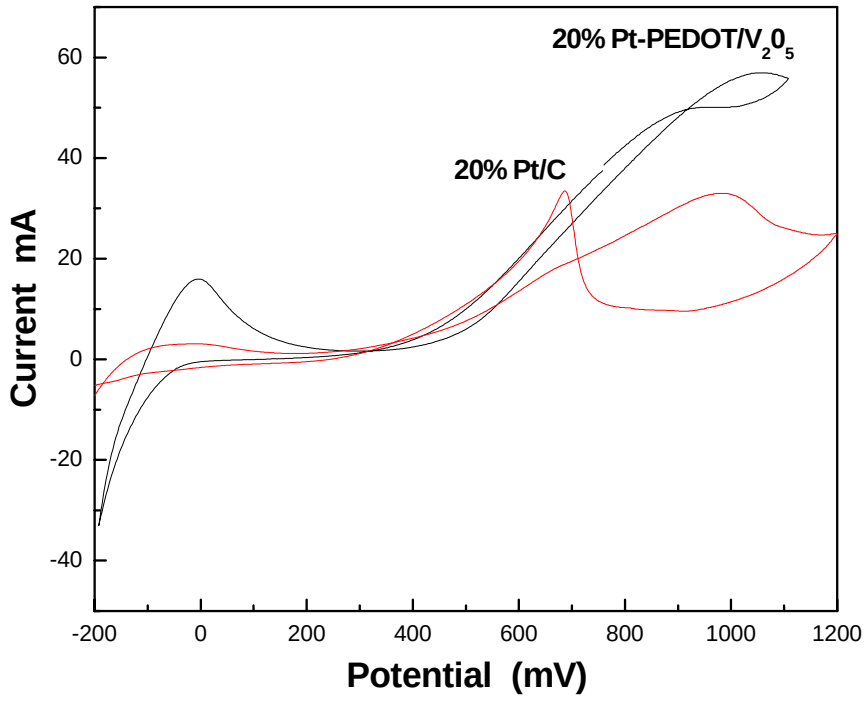

Fig 7.10. CV of (a) Pt loaded PEDOT-V_2O_5 nanocomposite and (b) Pt/C electrode in 1 M H_2SO_4/1 M CH_3OH at 50 mV/s

Although the activity observed in the present investigation is fairly high for the same loading of Pt, the activity can be further increased. The probable reason for this is the conductivity of the nanocomposite system. The conductivity of the nanocomposite system might be higher than the crystalline V_2O_5 and the conductivity of polymer nanocomposite is less than the pure conducing polymer. This is due to the conducting polymer intercalation of the layered V_2O_5 reduces the polymer conductivity, which might effect the charge transfer at the electrode/electrolyte interface. However, supporting the synthesized material on the high surface area carbon material may improve the dispersion further and the catalytic activity.

Table7.1. Methanol oxidation activity of Pt/ PEDOT-V_2O_5 catalyst prepared by formaldehyde reduction method

Catalyst	Pt loading μg/cm^2	Methanol oxidation activity mA/cm^2
Pt/$(C_6H_4O_2S)_{0.4}V_2O_5.0.5H_2O$	10	28.4
Pt/Vulcan	10	15

During cell operation, electrons and protons generated are migrating through the electrode layer. The electrode layer must exhibit good electronic and protonic conductivities to minimize resistive losses in the cell. Commonly used carbon supports (Conductex® 975 and Vulcan® XC-72) are good conductors of electrons. The catalyst by itself, however, cannot conduct protons. Introduction of ionomer such as Nafion has been used in the electrodes to improve the protonic conductivity. Nafion solution used to enhance the three-phase boundary; the electrodes are adhered to the polymer membrane by hot pressing, not in a fused state, but in a simple physically close contact state. Thus, the polymer membrane is simply brought into simple contact with the electrodes in plane, which has a limit in improving the

utilization of the platinum catalyst. Additionally, a Nafion solution itself is expensive, increasing the cost of the electrodes.

The present conducting polymer nanocomposite provides both protonic conductivity and ionic conductivity and it removes the barrier of three-phase boundary. The high porosity of nanocomposite are desirable and favourable in fuel cell electrodes because they allow for dispersion of a maximum amount of catalyst particles per unit volume of conductive support while providing sufficient structure in the support to enable access of electrolyte to catalyst particles without blocking transport of fuel, oxidant, and water to and from catalyst particles. Electrode materials designed with these considerations in mind are expected to exhibit maximum activity for fuel cell reactions and could form the basis of a new generation of power sources with much higher performance than existing devices.

7.12 CHRONOAMPEROMETRIC RESPONSE OF THE Pt LOADED PEDOT-V_2O_5 NANOCOMPOSITE

Fig. 7.11 shows the chronoamperometric response of Pt/ PEDOT- V_2O_5 and Pt/Vulcan XC 72R carbon electrodes at a constant potential of +0.6 V versus Ag/AgCl in 1 M H_2SO_4 and 1 M CH_3OH. The methanol oxidation activity and the stability for Pt/PEDOT- V_2O_5 nanocomposite based electrode were found to be higher than that of Pt/Vulcan XC 72R carbon electrode. The porous PEDOT-V_2O_5 nanocomposite leads to the high dispersion of Pt particles on its surface and also the porous morphology of the nanocomposite is favorable for the transport of methanol in the catalyst layer.

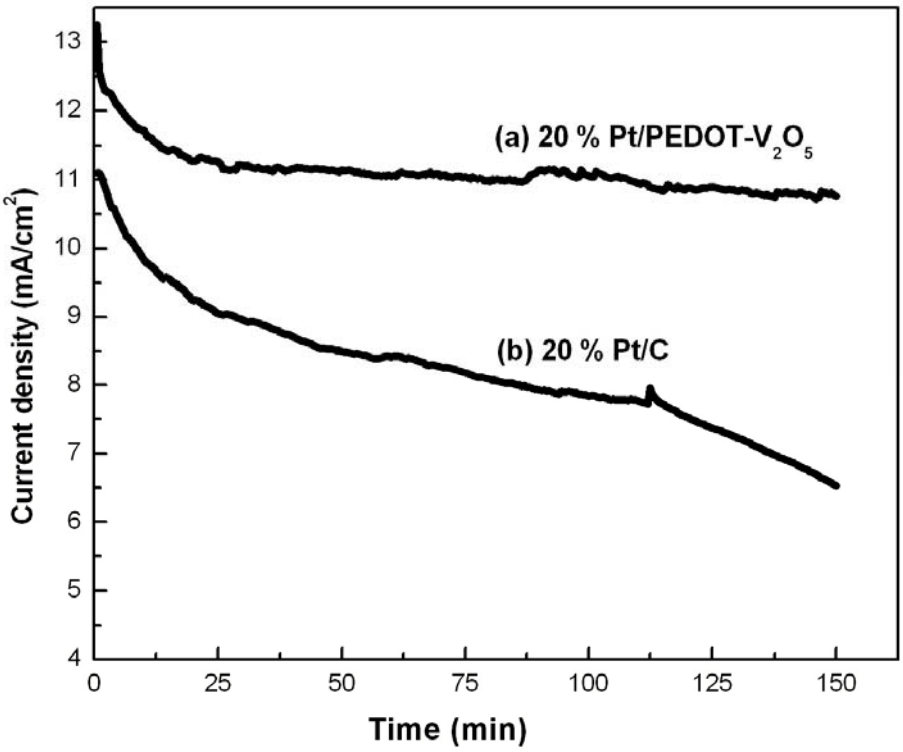

Fig. 7.11 Chronoamperometric response of (a) Pt/ PEDOT- V_2O_5 nanocomposite electrodes and (b) Pt/Vulcan XC 72R polarized at +0.6 V in 1 M H_2SO_4/1 M CH_3OH. (Pt = 10 μg cm^{-2})

7.13 CONCLUSIONS

The Pt loaded on PEDOT-V_2O_5 nanocomposite has been evaluated as the electrode for methanol oxidation in acid medium. The electrode exhibited a fairly high catalytic activity of 28 mA/cm^2 at a Pt loading of 10 μg cm^{-2}. Electron microscopic studies show the Pt supported PEDOT-V_2O_5 nanocomposite shows a porous morphology, which favours methanol diffusion. TEM investigations showed good dispersion of Pt nanoparticles on PEDOT-V_2O_5 nanocomposite with an average particle size 2.3 nm. The results also suggest that the polymer nanocomposite acts as a better catalyst support than the carbon support material by enhancing methanol oxidation. The Pt/ PEDOT-V_2O_5 catalyst synthesized and studied in this work display a series of

interesting properties (a) the presence of vanadium atom(s) is beneficial in several catalytic and electro-catalytic processes (b) Vanadium center to act as a an oxidizing center toward methanol. The high electro-catalytic activity of the Pt/ PEDOT-V_2O_5 catalyst can be attributed to the high dispersion of the Pt nanoparticles, their special surface structures on PEDOT-V_2O_5, oxidation capability and the improved capability of mass transport of methanol in the electrode. The results also suggest that, the polymer nanocomposite acts as a better catalyst support than the carbon support material by enhancing methanol oxidation. Future studies will focus on the development of carbon with PEDOT-V_2O_5 nanocomposite supported Pt catalyst and the testing of the composite anode in a DMFC.

CHAPTER 8

CONCLUSIONS

Fuel cells are considered as one of the options for energy conversion by the common man in the future. However, in spite of several decades of concerted attempts, this device has not yet evolved as an economically viable, socially acceptable, easily manipulative tool for energy conversion. It is known that there are a variety of barriers in every aspect of this energy conversion device. As far as the hardware of a fuel cell is concerned, it essentially consists of three components, namely the two electrodes and the electrolyte. Pt or Pt based noble metals are employed as electro-catalyst in both the electrodes. It is therefore natural, that there are attempts to reduce the amount of noble metal loading in the electrodes. This can be achieved by suitably dispersing the noble metals on suitable electronically conducting supports keeping in view the net energy density derivable from such a device with low metal loadings.

In order to achieve better dispersion of the metal, as well as to derive maximum activity from the dispersed metal sites, one has to adopt some innovative strategies. This thesis therefore attempts to concentrate on these two aspects of fuel cells.

- Making smaller fuel cells for portable electronic devices will require submicron-sized carbon electrode supports that minimize the use of noble metals but retain suitable catalytic activity. Carbon nano-textures have gained importance in recent times for various reasons. In order to exploit them as supports for noble metals, with a view to get better dispersion and also keeping the particle sizes of the dispersed material at the lowest sizes (~ 2 nm) possible without agglomeration, one has to generate chemically binding sites

on the conventional carbon nanotubes. Nitrogen containing carbon nanotubes are one such option and this presentation attempts to examine the possibility of utilizing nitrogen containing carbon nanotubes as supports for noble metal electro-catalysts. The electrochemical oxidation of methanol is used as the probe reaction for possible application as anodes for Direct Methanol Fuel Cells (DMFC).

- A second strategy is to preferentially promote the oxidation of the intermediate species (partial oxidation products of methanol like CO and other partially dehydrogenated species) on other sites so that the noble metal sites are still available and free for the electrochemical oxidation of the fuel. However, it is essential that the additional components employed for the reaction of the inhibiting intermediates, should not only be contributive to the overall desired electrochemical reaction but also should not render any additional impedance to the activity of the active electro-catalyst as well as should not lead to the loss of electrochemical energy converted. This means that the role of the support (mainly oxides for the preferential oxidation of partial combustion products) should be cumulative and not additive. The role of nanotubes of titania or tungsten oxide is examined for use as supports for noble metals for possible application as fuel cell anodes.

- Metal oxides provide oxygenated species for CO oxidation. Metal oxides form oxy-hydroxide species at relatively low potentials and helps in oxidizing CO intermediates and also corresponding metal redox couples favour methanol oxidation.

- Yet another possibility is the use of conducting polymers as supports. In this study this aspect has also been examined by making use of Poly(o-phenylendiamine) nanotube as support for noble metals for the oxidation of methanol.

- Another approach to avoid poisoning is to employ electronically conducting hybrid nanocomposite as electrode materials. Thus attempts were made to examine PEDOT/V_2O_5 nanocomposite as electrodes for methanol oxidation in Direct Methanol Fuel Cells.

- Many studies have shown that the catalytic activity of the most studied Pt catalyst depend on the amount and the nature of electrocatalytic support.

- The new studied catalysts form different kind of electrocatalytic supports and the PEDOT-V_2O_5 nanocomposite support showed good catalytic activity. The key is to find reproducibility in the measurements which depend on the method of preparation and the amount of Pt loading.

Future research in this area should involve further characterization of these electrodes in fuel cell mode. The activity cannot be exactly extrapolated in the fuel cell mode (Nafion as electrolyte) but since some of these electrodes were fabricated to be suitable for use in the fuel cell mode. The supported PEDOT-V_2O_5 nanocomposite could play a role in the activity and stability for methanol oxidation if they can be further supported on the high surface area carbon.

REFERENCES

1. **Abdel Rahim, M.A., M.W. Khalil and H.B. Hassan** (2000) Platinum - tin alloy electrodes for direct methanol fuel cells. *J. Appl. Electrochem.,* **30(10)**, 1151-1155.

2. **Adachi, M., Y. Murata and S. Yoshikawa** (2000) Formation of titania nanotubes with high photo- catalytic activity. *Chem. Lett*., **8** 942-943.

3. **Adachi,M., Y.Murata and S. Yoshikawa** (2003) Formation of titania nanotubes and applications for dye-sensitized solar cells. *J. Electrochem. Soc.,* **150,** G488-G493.

4. **Adams, A.A. and R.T. Folley** (1980) The stability of trifluoromethane sulfonic acid as an electrolyte in fuel cells. Reply to comments. *J. Electrochem. Soc.,* **127(12)**, 2647-47.

5. **Adams, P.N., L. Abell, A. Middleton and A.P. Monkman** (1997) Low temperature synthesis of high molecular weight polyaniline using dichromate oxidant. *Synth. Met.,* **84,** 61-62.

6. **Anderson, M.L., R.M. Stroud and D.R. Rolison** (2002) Enhancing the Activity of Fuel-cell Reactions by Designing Three-dimensional Nanostructured Architectures: Catalyst-modified Carbon-Silica Composite Aerogels. *Nano Lett.,* **2(3)**, 235-240.

7. **Andrew, M.R., B.D. McNicol, R.T. Short and J.S. Drury** (1977) Electrolytes for methanol-air fuel cells. I. The performance of methanol electro-oxidation catalysts in sulfuric acid and phosphoric acid electrolytes. *J. Appl. Electrochem.,* **7(2)**, 153-60.

8. **Antolini, E., L. Giorgi, F. Cardellini and E.Passalacqua** (2001) Physical and morphological characteristics and electrochemical behavior in PEM fuel cells of PtRu/C catalysts. *J. Solid State Electrochem.,* **5(2)**, 131-140.

9. **Appleby, A.J** (1992) Fuel cell technology and innovation. *J. Power Sources,* **37**, 223–239.

10. **Appleby, A.J.** (1990) From Sir William Grove to today: Fuel cells and the future. *J. Power Sources,* **29(1-2)**, 3-11.

11. **Appleby, A.J.** (1996) Issues in fuel cell commercialization. *J. Power Sources,* **58**, 153-176.

12. **Aramata, A. and R. Ohnishi** (1984) Methanol Electrooxidation on platinum Directly Bonded to a Solid Polymer Electrolyte Membrane. *J. Electroanal. Chem.,* **162,** 153-162.

13. **Arico, A.S., A.K. Shukla, K.M. El-Khatib, P. Creti and V. Antonucci** (1999) Effect of carbon-supported and unsupported Pt-Ru anodes on the performance of solid-polymer-electrolyte direct methanol fuel cells. *J. Appl. Electrochem.,* **29(6)**, 671-676.

14. **Arico, A.S., P. Creti, E. Modica, G. Monforte, V. Baglio and V. Antonucci** (2000) Investigation of direct methanol fuel cells based on unsupported Pt-Ru anode catalysts with different chemical properties. *Electrochim. Acta,* **45(25-26)**, 4319-4328.

15. **Arico, A.S., P. Creti, N. Giordano, V. Antonucci, P.L. Antonucci and A. Chuvilin** (1996) Chemical and morphological characterization of a direct methanol fuel cell based on a quaternary Pt-Ru-Sn-W/C anode. *J. Appl. Electrochem.,* **26(9)**, 959-967.

16. **Arico, A.S., S. Srinivasan and V. Antonucci** (2001) DMFCs: from fundamental aspects to technology development. *Fuel Cells,* **1**, 133-161.

17. **Attwood, P.A., D. McNicol, S. Brian, T. Richard and J.A. Van Amsteel** (1980) Platinum on carbon fiber paper catalysts for methanol electrooxidation. Part 1. Influence of activation conditions on catalytic activity. *J. Chem. Soc. Faraday Trans*., **76(11)**, 2310-21.

18. **Auer, E., A. Freund, J. Pietsch and T. Tacke** (1998) Carbons as supports for industrial precious metal catalysts. *Appl. Catal. A: Gen.,* **173(2)**, 259-271.

19. **Austin, D. S., J. A. Polta, T. Z. Polta, A. P. -C. Tang, T. D. Cabelka and D. C. Johnson** (1984) Electrocatalysis at platinum electrodes for anodic Electoanalysis. *J. Electroanal. Chem.,* **25**, 227-248.

20. **Babu, R.S., A.S. S. Murthy and B. Viswanathan** (1998) Electrocatalytic oxidation of methanol on platinum based catalysts. *Studies Surf.Sci.Catal.,* **113**, 787-792.

21. **Baez, V. B. and D.Pletcher** (1995) Preparation and characterization of carbon/titanium dioxide surfaces - the reduction of oxygen. *J. Electroanal. Chem.,* **382(1-2)**, 59-64.

22. **Bai, Y., J. Wu, J. Xi, J. Wang, W. Zhu, L. Chen and X. Qiu** (2005) Electrochemical oxidation of ethanol on Pt- ZrO_2 /C catalyst. *Electrochem. Commun.,* **7(11)**, 1087-1090.

23. **Barbir, F. and T. Gomez** (1996) Efficiency and economics of proton exchange membrane (PEM) fuel cells. *Int. J. Hydrogen Energy,* **21(10)**, 891-901.

24. **Barthet, C. and M. Gugliolm** (1996) Aspects of the conducting properties of the Nafion doped polyaniline. *Electrochim. Acta,* **41,** 2791-2798.

25. **Beden, B., F. Hahn, J.M. Leger, C. Lamy, C.L. Perdriel , N.R. De Tacconi, R.O. Lezna and A.J. Arvia** (1991) Electromodulated infrared spectroscopy of

methanol electrooxidation on electrodispersed platinum electrodes. Enhancement of reactive intermediates. *J. Electroanal. Chem.,* **307**, 129-38.

26. **Bersani, D. and P. P. Lottici** (1998) Phonon confinement effects in the Raman scattering by TiO_2 nanocrystals. *Appl. Phys. Lett.,* **72,** 73-75

27. **Bessel, C.A., K. Laubernds, N.M. Rodriguez and R.T. Baker** (2001) Graphite nanofibers as an electrode for fuel cell applications. *J. Phys. Chem. B,* **105 (6)**, 1115–1118.

28. **Bessel, C.A., K. Laubernds, N.M. Rodriguez and R.T. Baker** (2001) Graphite nanofibers as an electrode for fuel cell applications. *J. Phys. Chem. B,* **105,** 1115–1118**.**

29. **Biswas, P.C. and M. Enyo** (1992) Electrooxidation of methanol on graphite-supported perovskite-modified platinum electrodes in alkaline solution. *J. Electroanal. Chem.,* **322(1-2)**, 203-20.

30. **Biswas, P.C., T. Ohmori and M. Enyo** (1991) Electrocatalytic activity of a graphite-based platinum electrode modified with metal oxides towards methanol oxidation. *J. Electroanal. Chem.,* **305(2)**, 205-16.

31. **Bommarius, A.S., J.F. Holzwarth, D.L.C. Wang and T.A. Hatton** (1990) Coalescence and solubilizate exchange in a cationic four-component reversed micellar system. *J. Phys. Chem. B,* **94(18)**, 7232-9.

32. **Bonnemann, H. and R.M. Richards** (2001) Nanoscopic metal particles - synthetic methods and potential applications. *Eur. J. Inorg. Chem.,* **(10)**, 2455-2480.

33. **Brumlik, A.J. and C.R. Martin** (1991) Template Synthesis of Microtubules. *J. Am. Chem. Soc.,* **113,** 3174-3175.

34. **Burnstein, G.T., C.J. Barnett, A. R. Kucernak and K.R. Williams** (1997) Aspects of the anodic oxidation of methanol. *Catal. Today,* **38(4)**, 425-437.

35. **Burstein, G.T., C.J. Barnett, A.R.J. Kucernak and K.R. Williams** (1996) Anodic oxidation of methanol using a new base electrocatalyst. *J. Electrochem. Soc.,* **143(7)**, L139-L140.

36. **Cai, Z. and C.R. Martin** (1989) Electronically Conductive Polymer Fibres with Mesoscopic Diameters Show Enhanced Electronic Conductivities. *J. Am. Chem. Soc.,* **111,** 4238-4139.

37. **Cao, L., F. Scheiba, C. Roth, F. Schweiger, C. Cremers and U. Stimming** (2006) Novel nanocomposite $Pt/RuO_2.xH_2O$/carbon nanotube catalysts for direct methanol fuel cells. *Angew. Chem., Int. Ed. Engl.,* **45(32)**, 5315-5319.

38. **Carrette, L., K. A. Friedrich and U. Stimming** (2001) Fuel cells - Fundamentals and applications. *Fuel Cells,* **1(1)**, 5-39.

39. **Centi, G., D. Pinelli and F. Trifiro** (1990) Effects of the active phase – support interaction in vanadium oxide on TiO_2 catalysts for o – xylene oxidation. *J. Mol. Cat.,* **59(2)**, 221-31.

40. **Chai, G.S., S.B. Yoon J.H. Kim and J.S. Yu** (2004) Spherical carbon capsules with hollow macroporous core and mesoporous shell structures as a highly efficient catalyst support in the direct methanol fuel cell. *Chem. Commun.,* **(23)**, 2766-7.

41. **Chalk, S.G., J.F. Miller and F.W. Wagner** (2000) Challenges for fuel cells in transport applications. *J. Power Sources,* **86(1-2)**, 40-51.

42. **Champagne, S.D., E. Ferain, C. Jerome, R. Gerome and R. Legras** (2000) electrochemically synthesized polypyrrole nanotubules: Effects of different experimental conditions. *Eur. Polym. J.,* **34,** 767-774.

43. **Chan, K.Y., J. Ding, J. Ren, S. Cheng, and K.Y. Tsang** (2003) Supported mixed metal nanoparticles as electrocatalysts in low temperature fuel cells. *J. Mater. Chem.,* **14**, 505-516.

44. **Chandler, G. K. and D. Pletcher** (1986) The electrodeposition of metals onto polypyrrole films from aqueous solution. *J. Appl. Electrochem.,* **16(1)**, 62-8.

45. **Chandrappa, G. T., N. Steunou and J. Livage** (2002) Macroporous crystalline vanadium oxide foam. *Nature,* **416**, 702-702.

46. **Che, G., B.B. Lakshmi, C.R. Martin and E.R. Fisher** (1999) Metal-Nanocluster-Filled Carbon Nanotube: Catalytic Properties and Possible Applications in Electrochemical Energy Storage and Production. *Langmuir,* **15(3)**, 750-758.

47. **Che, G., B.B. Lakshmi, E.R. Fisher and C.R. Martin** (1998) Carbon nanotubule membranes for electrochemical energy storage and production. *Nature,* **393**, 346-349.

48. **Chen, J., M. Wang, B. Liu, Z. Fan, K. Cui and Y. Kuang** (2006) Platinum Catalysts Prepared with Functional Carbon Nanotube Defects and Its Improved Catalytic Performance for Methanol Oxidation. *J. Phys. Chem. B.,* **110(24)**, 11775-11779.

49. **Chen, K. Y., P. K. Shen and A. C. C. Tseung** (1995) Anodic oxidation of formic acid on electrodeposited Pt/WO_3 electrode at room temperature. *J. Electrochem. Soc.,* **142(4)**, L54-L56.

50. **Chen, Z., X. Qiu, B. Lu, S. Zhang, W. Zhu and L. Chen** (2005) Synthesis of hydrous ruthenium oxide supported platinum catalysts for direct methanol fuel cells. *Electrochem. Commun.,* **7(6)**, 593-596.

51. **Chiang, J.C., and A.G. MacDiarmid** (1986) Polyaniline : protonic acid doping of the emeraldine form to the metallic regime. *Synth. Met.,* **13(1-3)**, 193-205.

52. **Choi, J.H., K.W. Park, H.K. Lee, Y.M. Kim, J.S. Lee and Y.E. Sung** (2003) Nano-composite of PtRu alloy electrocatalyst and electronically conducting polymer for use as the anode in a direct methanol fuel cell. *Electrochim. Acta,* **48(19)**, 2781-2789.

53. **Christensen, P.A., A. Hamnett and G.L. Troughton** (1993) The role of morphology in the methanol electro-oxidation reaction. *J. Electroanal. Chem.,* **362**, 207-18.

54. **Ciszewski, A. and G. Milczarek** (1996) Electrocatalytic oxidation of alcohols on glassy carbon electrodes electrochemically modified by conductive polymeric nickel (II) tetrakis(3-methoxy-4-hydroxyphenyl)porphyrin film. *J. Electroanal. Chem.,* **413(1-2)**, 137-142.

55. **Corradi, R. and S.P. Armes** (1997) Chemical synthesis of poly (3,4-ethylenedioxythiophene). *Synth. Met.,* **84(1-3)**, 453-454.

56. **Czerw, R., M. Terrones, J-C. Charlier, X. Blase, B. Foley and R. Kamalakaran** (2001) Identification of Electron Donor States in N-Doped Carbon Nanotubes. *Nano Lett.,* **1(9)**, 457-60.

57. **Daniel, M. F., B. Desbat, J.C. Lassegues, B. Gerand and M. Figlarz** (1987) Infrared and Raman study of WO_3 tungsten trioxides and $WO_3.xH_2O$ tungsten trioxide hydrates. *J. Solid State Chem.,* **67(2)**, 235-47.

58. **De Jong, K.P. and J.W. Geus** (2000) Carbon nanofibers: catalytic synthesis and applications. *Catal. Rev. Sci. Eng.,* **42(4)**, 481-510.

59. **Delvaus, M., J. Duchet, P.Y. Stavaux, R. Legras and S.D. Champagne** (2000) Chemical and Electrochemical Synthesis of Polyaniline Micro-and-Nanotubules. *Synth. Met.,* **113,** 275-280.

60. **Devarajan, S. and S. Sampath** (2004) Electrochemistry with nanoparticles. *Chemistry of Nanomaterials,* **2**, 646-687.

61. **Dicks, A. L.** (2006) The role of carbon in fuel cells. *J. Power Sources,* **156(2)**, 128-141.

62. **Dinh, H.N., X. Ren, F.H. Garzon, P. Zelenay and S. Gottesfeld** (2000) Electrocatalysis in direct methanol fuel cells: in-situ probing of PtRu anode catalyst surfaces. *J. Electroanal. Chem.,* **491(1-2)**, 222-233.

63. **Dohle, H., J. Divisek and R. Jung** (2000) Process engineering of the direct methanol fuel cell. *J. Power Sources,* **86(1-2)**, 469-477.

64. **Donnet, J.B.** (1968) Chemical reactivity of carbons. *Carbon,* **6(2)**, 161-76.

65. **Donnet, J.B.** (1982) Structure and reactivity of carbons: from carbon black to carbon composites. *Carbon,* **20(4)**, 267-82.

66. **Drazic, D.M., A.V. Tripkovic, K.D. Popovic and J.D. Lovic** (1999) Kinetic and mechanistic study of hydroxyl ion electrosorption at the Pt (111) surface in alkaline media. *J. Electroanal. Chem.,* **466(2),** 155-164.

67. **Du, G. H., Q. Chen, R. C. Che, Z. Y. Yuan and L. M. Peng** (2001) Preparation and structure analysis of titanium oxide nanotubes. *Appl. Phys. Lett.,* **79,** 3702-3705.

68. **Dyer, C.K.** (2002) Fuel cells for portable applications. *J. Power Sources,* **106**, 31-34.

69. **Dyke, L.S.V. and C.R. Martin** (1990) Electrochemical Investigation of Electronically Conductive Polymers. 4. Contolling the Super Molecular Structure Allows Large Transport Rates To Be Enhanced. *Langmuir,* **6,** 118-1123.

70. **Esteban, O.P., J.M. Leger, C. Lamy and E. Genies** (1989) Electrocatalytic oxidation of methanol on platinum dispersed in polyaniline conducting polymers. *J. Appl. Electrochem.,* **19(3)**, 462-4.

71. **Figlarz, M.** (1989) New oxides in the WO_3-MoO_3 system. *Prog. Solid-State Chem.,* **19**,1-46.

72. **Folkesson, B. and R. Larsson** (1989) On the kinetics of the oxidation of formic acid by vanadium (IV) in aqueous solution. *Inorg. Chim. Acta,* **162(1),** 75-81.

73. **Folkesson, B., R. Larsson and J. Zander** (1989) Oxidation of methanol, formaldehyde and formic acid by vanadium (IV) ions in sulfuric acid. *J. Electroanal. Chem.,* **267(1-2)**, 149-61.

74. **Frelink, T., W. Visscher and J.A.R. Van Veen** (1995) Particle size effect of carbon -supported platinum catalysts for the electro-oxidation of methanol. *J. Electroanal. Chem.,* **382(1-2)**, 65-72.

75. **Gerand, B., G. Nowogrocki, J. Guenot and M. Figlarz** (1979) Structural study of a new hexagonal form of tungsten trioxide. *J. Solid State Chem.,* **29(3)**, 429-34.

76. **Gholamian, M. and A.Q. Contractor** (1998) Effect of the temperature of synthesis on the conductivity and electrochemical behaviour of polyaniline. *J. Electroanal. Chem.,* **252,** 291-301.

77. **Ghosh, S. and O. Inganas** (2000) Networks of electron-conducting polymer in matrices of ion conducting polymers: applications to fast electrodes. *Electrochem. Solid State Lett.,* **3**, 213-215.

78. **Golabi, S. M, and A. Nozad** (2002) Electrocatalytic oxidation of methanol on electrodes modified by platinum microparticles dispersed into poly (o-phenylenediamine) film. *J. Electroanal. Chem.,* **521**, 161–167.

79. **Gong, D., C. A. Grimes, O. K. Varghese, W. Hu, R. S. Singh, Z. Chen and E.C. Dickey** (2001) Titanium oxide nanotube arrays prepared by anodic oxidation. *J. Mater. Res.,* **16**, 3331-3334.

80. **Goodenough, J.B., A. Hamnett, B.J. Kennedy, R. Manoharan and S.A.Weeks** (1988) Methanol oxidation on unsupported and carbon supported platinum + ruthenium anodes. *J. Electroanal.Chem.,* **240(1-2)**, 133-45.

81. **Gratzel, M.** (2001) Photoelectrochemical cells. *Nature,* **414,** 338-344.

82. **Gu, Y.J. and W.T. Wong** (2006) Electro - oxidation of Methanol on Pt Particles Dispersed on RuO_2 Nanorods. *J. Electrochem. Soc.,* **153(9)**, A1714-A1718.

83. **Guay, J. and L.H. Dao** (1989) Formation of poly (4-phenylaniline) by electropolymerization of 4-aminobiphenyl or diphenylamine. *J. Electroanal. Chem.,* **274,** 135-142.

84. **Gutierrez, A. C., A.L.N. Pinheiro, E. Leiva, E.R. Gonzalez and T. Iwasita** (2003) Abnormally fast mobility of CO at electrochemical interfaces. *Electrochem. Commun.,* **5(7)**, 539-543.

85. **Hable, C.T and M.S. Wrighton** (1991) Electrocatalytic Oxidation of Methanol by Assemblies of Platinum /Tin Catalysts Particles in a conducting Polyaniline Matrix. *Langmuir,* **7,** 1305-1309.

86. **Hagfeldt, A. and M. Gratzel** (1995) Light-Induced Redox Reactions in Nanocrystalline Systems. *Chem. Rev.,* **95,** 49-68.

87. **Hamnett, A**. (1997) Mechanism and electrolysis in the direct methanol fuel cell. *Catal. Today,* **38,** 445-457.

88. **Hayden, B.E., D.V. Malevich and D. Pletcher** (2001) Platinum catalyzed nanoporous titanium dioxide electrodes in H_2SO_4 solutions. *Electrochem. Commun.,* **3(8)**, 395-399.

89. **Heegar, A.J.** (1989) Charge Transfer in Conducting Polymers. *Faraday Discuss. Chem. Soc.,* **88,** 203-211.

90. **Hepel, M., I. Kumarihamy and C.J. Zhong** (2006) Nanoporous TiO_2 - supported bimetallic catalysts for methanol oxidation in acidic media. *Electrochem. Commun.,* **8(9)**, 1439-1444.

91. **Hobbs, B.S. and A.C.C. Tseung** (1969) High-performance, platinum-activated tungsten oxide fuel cell electrodes. *Nature,* **222**, 556-56.

92. **Hogarth, M.P. and G.A. Hards** (1996) Direct methanol fuel cells. Technological advances and further requirements. *Platinum. Met. Rev.,* **40(4)**, 150-159.

93. **Hogarth, M.P. and T.R. Ralph** (2002) Catalysis for low temperature fuel cells: Part III: Challenges for the direct methanol fuel cell. *Platinum. Met. Rev.,* **46(4)**, 146-164.

94. **Hohlein, B., P. Biedermann, T. Grube and R. Menzer** (1999) Fuel cell power trains for road traffic. *J. Power Sources,* **84(2)**, 203-213.

95. **Huang, S.Y., L. Kavan, I. Exnar and M**. **Gratzel** (1995) Rocking chair lithium battery based on nanocrystalline TiO_2 (anatase). *J. Electrochem. Soc.,* **142,** L142-L144.

96. **Huang, S-Y., C-M. Chang and C-T. Yeh** (2006) Promotion of platinum-ruthenium catalyst for electro - oxidation of methanol by ceria. *J. Catal.,* **241(2),** 400-406.

97. **Huaxin,** L. (1999) The study of oxygen spillover and back spillover on Pt / TiO_2 by a potential dynamic sweep method. *J. Mol. Catal.,* **144(1)**, 189-197.

98. **Hughes, V.B. and B.D. McNichol** (1980) The stability of trifluoromethane sulfonic acid as an electrolyte in fuel cells. Comments. *J. Electrochem. Soc.,* **127(12)**, 2646-7.

99. **Hughes, V.B., B.D. McNicol, M.R. Andrew, R.B. Jones and R.T. Short** (1977) Electrolytes for methanol-air fuel cells. II. The electro-oxidation of methanol in trifluoromethane-sulfonic acid monohydrate and aqueous solutions of trifluoromethane-sulfonic acid. *J. Appl. Electrochem.,* **7(2)**, 161-74.

100. **Hyeon, T., S. Han, Y.E. Sung, K.W. Park and Y.W.Kim** (2003) High performance direct methanol fuel cell electrodes using solid-phase-synthesized carbon nanocoils. *Angew. Chem. Int. Ed*., **42**, 4352–6.

101. **Ioroi, T., Z.Siroma, N. Fujiwara, S.Yamazaki and K.Yasuda** (2005) Sub-stoichiometric titanium oxide-supported platinum electrocatalyst for polymer electrolyte fuel cells. *Electrochem. Commun*., **7(2)**, 183-188.

102. **Ismagilov, Z.R., M.A. Kerzhentsev, N.V. Shikina, A.S. Lisitsyn, L.B. Okhlopkova, Ch. N. Barnakov, M. Sakashita, T. Iijima and K. Tadokoro** (2005) Development of active catalysts for low Pt loading cathodes of PEMFC by surface tailoring of nanocarbon materials. *Catal. Today,* **102,** 58-66.

103. **Jewulski, J.R. and Z.S. Rak** (2006) Fuel cells - the opportunity for environmental protection. *Environ. Prot. Eng.*, **32(1)**, 189-194.

104. **Jia, N., R.B. Martin, Z. Qi, M.C. Lefebvre and P.G. Pickup** (2001) Modification of carbon supported catalysts to improve performance in gas diffusion electrodes. *Electrochim. Acta,* **46(18)**, 2863-2869.

105. **Jirage, K.B., J.C. Hulteen and C.R. Martin** (1997) Nanotubule based Molecular –Filtration membranes. *Science*, **278**, 655-658.

106. **Joo, S. H, S.J. Choi, I. Oh, J. Kwak, Z. Liu, O. Terasaki and R. Ryoo** (2001) Ordered nanoporous arrays of carbon supporting high dispersions of platinum nanoparticles. *Nature,* **412**, 169–172.

107. **Jun, S., S.H. Joo, R. Ryoo, M. Kruk, M. Jaroniec, Z. Liu, T. Ohsuna and O. Terasaki** (2000) Synthesis of New, Nanoporous Carbon with Hexagonally Ordered Mesostructure. *J. Am. Chem. Soc.,* **122(43)**, 10712-10713.

108. **Jurewicz, K., K. Babeł, A. Ziółkowski and H. Wachowska** (2003) Ammoxidation of active carbons for improvement of supercapacitor characteristics. *Electrochim. Acta,* **48,**1491-8.

109. **Kamat, P.** (2006) Carbon nanomaterials: building blocks in energy conversion devices. *Electrochem. Soc. Interface.,* **15(1)**, 45-47.

110. **Kasuga, T., M. Hiramatsu, A. Hoson, T. Sekino and K. Niihara** (1998) Formation of titanium oxide nanotube. *Langmuir,* **14**, 3160-3163.

111. **Kavan, L., A. Attia, F. Lenzmann, S.H. Elder and M. Gratzel** (2000) Lithium insertion into zirconia-stabilized mesoscopic TiO_2 (anatase). *J. Electrochem. Soc.,* **147,** 2897-2902.

112. **Kawamura, G., H. Okamoto, A. Ishikawa and T. Kudo** (1987) Tungsten molybdenum carbide for electrocatalytic oxidation of methanol. *J. Electrochem. Soc.,* **134,** 1653-1658.

113. **Kelaidopoulou, A., E. Abelidou and G. Kokkinidis** (1999) Electrocatalytic oxidation of methanol and formic acid on dispersed electrodes: Pt, Pt-Sn and Pt/M(upd) in poly(2-hydroxy-3-aminophenazine). *J. Appl. Electrochem.,* **29(11)**, 1255-1261.

114. **Kim, C., Y.J. Kim, Y.A. Kim, T. Yanagisawam, K.C. Park, M. Endo and M.S.Dresselhaus** (2004) High performance of cup-stacked-type carbon nanotubes as a Pt- Ru catalyst support for fuel cell applications. *J. Appl. Phys.,* **96**, 5903-5.

115. **Kim, K.J., Y.J. You, M.C. Chung, C.S. Kang, K.H. Chung, W.J. Jeong, S. W. Jeong and H.G. Ahn** (2006) Effect of nanosized gold particle addition to supported metal oxide catalyst in methanol oxidation. *J. Nanosci. Nanotech.,* **6(11)**, 3589-3593.

116. **Kim, Y.T. and T. Mitani** (2006) Surface thiolation of carbon nanotubes as supports: A promising route for the high dispersion of Pt nanoparticles for electrocatalysts. *J. Catal.,* **238(2)**, 394-401.

117. **Kinoshita, K.** (1990) Particle Size Effects for Oxygen Reduction on Highly Dispersed Platinum in Acid Electrolytes. *J. Electrochem. Soc.,* **137**, 845-48.

118. **Kost, K.M., D.E. Bartak, B. Kazee and T. Kuwana** (1988) Electrodeposition of platinum microparticles into polyaniline films with electrocatalytic applications. *Anal. Chem.,* **60(21)**, 2379-84.

119. **Kostecki, R., M. Ulmann, J. Augustynski, D.J. Strike and M. Koudelka-Hep** (1993) Enhanced Rate of Redox Conversion of Polyaniline Films Induced by the Corporation of Platinum Microparticles. *J.Phys. Chem.,* **97,** 8113-8115.

120. **Kovacic, P. and J.Oziomek** (1964) p-Polyphenyl from benzene-Lewis acid catalyst-oxidant. Reaction scope and investigation of the benzene-aluminum chloride-cupric chloride system. *J. Org. Chem.,* **29,** 100-104.

121. **Kowal, A., S.N. Port and R.J. Nichols** (1997) Nickel hydroxide electrocatalysts for alcohol oxidation reactions. An evaluation by infrared spectroscopy and electrochemical methods. *Catal. Today,* **38(4)**, 483-492.

122. **Kudo, T., A. Ishikawa, G. Kawamura and H. Okamoto** (1985) A new (W, Mo) electrocatalyts synthesized by a carbonyl process – Activity enhancement resulting from water vapour treatment in the synthesizing process. *J. Electrochem. Soc*., **132,** 1814-1819.

123. **Kudo, T., G. Kawamura and H. Okamoto** (1983) A new (W, Mo) electrocatalyts synthesized by a carbonyl process – Activity in relation to H_2, HCHO, and CH_3OH. *J. Electrochem. Soc*., **130,** 1491-1497.

124. **Kulesza, P. J., M. Matczak, A. Wolkiewicz, B. Grzybowska, M. Galkowski, M.A. Malik and A. Wieckowski** (1999) Electrocatalytic properties of conducting polymer based composite film containing dispersed platinum microparticles towards oxidation of methanol. *Electrochim. Acta,* **44(12)**, 2131-2137.

125. **Kulesza, P.J., M. Matczak, A. Wolkiewicz, B. Grzybowska, M. Galkowski, M.A. Malik and A. Wieckowski** (1999) Electrocatalytic properties of conducting polymer based composite film containing dispersed platinum microparticles towards oxidation of methanol. *Electrochim. Acta,* **44(12)**, 2131-2137.

126. **Kuo, C.W., L.M. Huang, T.C. Wen and A. Gopalan** (2006) Enhanced electrocatalytic performance for methanol oxidation of a novel Pt-dispersed poly(3,4-ethylenedioxythiophene)–poly(styrenesulfonicacid)electrode. *J. Power Sources,* **160**, 65-72.

127. **Kvarnstron, C. and A. Ivusaka** (1997) Electrochemical study on poly (paraphenylene)/poly (3-octylthiophene) bilayer electrodes. *Synth. Met.,* **84,** 593-594.

128. **Kyotani, T., I.S. Nagai, Takayuki and A. Tomita** (1997) Formation of New Type of Porous Carbon by Carbonization in Nanochannels in Zeolite. *Chem. Mater*., **9(2)**, 609-615.

129. **Laborde, H., J.M. Leger and C. Lamy** (1994) Electrocatalytic oxidation of methanol and C1 molecules on highly dispersed electrodes. Part 1. Platinum in polyaniline. *J. Appl. Electrochem.,* **24(3)**, 219-26.

130. **Laborde, H., J.M. Leger, C. Lamy, F. Garnier and A. Yassar** (1990) Electrocatalytic oxidation of hydrogen, formic acid and methanol on platinum modified copolymer (pyrrole-dithiophene) electrodes. *J. Appl. Electrochem.,* **20(3)**, 524-6.

131. **Laborde, H., J.M. Leger, C. Lamy, F. Garnier, and A. Yassar** (1990) Electrocatalytic oxidation of hydrogen, formic acid and methanol on platinum modified copolymer (pyrrole-dithiophene) electrodes. *J. Appl. Electrochem.,* **20(3)**, 524-526.

132. **Lakshmi, B. B., C.J. Patrissi and C. R. Martin** (1997) Sol-Gel Template Synthesis of Semiconductor Oxide Micro- and Nanostructures. *Chem. Mater.,* **9(11),** 2544-2550.

133. **Lamy, C., J.M. Leger and S. Srinivasan** (2001) Direct methanol fuel cells: From a twentieth century electrochemist's dream to a twenty-first century emerging technology. *Modern Aspects of Electrochemistry,* **34**, 53-118.

134. **Larsson, R. and B. Folkesson** (1993) On the catalytic oxidation of methanol with vanadium (IV) in sulfuric acid solution. *Studies Surf. Sci. Catal.,* **75**, 31-9.

135. **Larsson, R. and B. Folkesson** (2005) A catalytic oxidation of sugar by vanadium (IV). *J. Mol. Catal.,* **229(1-2),** 183-190**.**

136. **Lashway, R.W.** (2005) Fuel cells: The next evolution. *MRS Bulletin.,* **30(8)**, 581-583.

137. **Lee, C.H., C.W. Lee, D.L. Kim, D.H. Jung, C.S. Kim and D.R. Shin** (2000) Electrooxidation of methanol on Pt - Ru catalysts supported by basal plane graphite in phosphoric acid solution. *J. Power Sources,* **86(1-2)**, 478-481.

138. **Lee, J.Y. and S.M. Park** (2000) Elecrochemistry of conductive polymers. XXIV polypyrrole films grown at electrodes modified with -cyclodextrin molecular templates. *J. Electrochem. Soc.,* **147,** 4189-4195.

139. **Lee, S., C. Jeon and Y. Park** (2004) Fabrication of TiO_2 Tubules by Template Synthesis and Hydrolysis with Water Vapor. *Chem. Mater.,* **16(22)**, 4292-4295.

140. **Lefebvre, M.C, Q. Zhigang and G.P. Peter** (1999) Electronically Conducting Proton Exchange Polymers as Catalyst Supports for Proton Exchange Membrane Fuel Cells: Electrocatalysis of Oxygen Reduction, Hydrogen Oxidation, and Methanol Oxidation, *J. Electrochem. Soc.,* **146**, 2054-2058.

141. **Lei, Y., L. D. Zhang and J. C. Fan** (2001) Fabrication, characterization and Raman study of TiO_2 nanowire arrays prepared by anodic oxidative hydrolysis of $TiCl_3$. *Chem. Phys. Lett.,* **338,** 231-236

142. **Li, W. C., Liang, W. Zhou, J. Qiu, Z. Zhou and G. Sun** (2003) Preparation and characterization of multiwalled carbon nanotube-supported platinum for cathode catalysts of direct methanol fuel cells, *J. Phys. Chem. B,* **107**, 6292–6299.

143. **Li, W.Z., C.H Liang, W.J. Zhou and Q.Xin** (2003) Preparation and characterization of multiwalled carbon nanotube-supported platinum for cathode catalysts of direct methanol fuel cells. *J. Phys. Chem. B,* **107(26)**, 6292–9.

144. **Li, Y. J., R. Lenigk, X.Z. Wu, B.Gruendig, S.J.Dong, J. Shao and R. Renneberg** (1998) Investigation of oxygen and hydroge peroxide reduction on platinum particles dispersed on poly (o-phenylenediamine) film-modified glassy carbon electrodes. *Electroanalysis,* **10**, 671-676.

145. **Livage, J.** (1996) Sol-gel chemistry and electrochemical properties of vanadium oxide gels. *Solid State Ionics,* **86**, 935-942.

146. **Livraghi S, A. Votta, M. C. Paganini and E. Giamello** (2005) The nature of paramagnetic species in nitrogen doped TiO_2 active in visible light photocatalysis. *Chem. Commun.,* **4**, 498-500.

147. **Lyons, M.E.** (1994) Electrocatalysis using electroactive polymers, electroactive composites and microheterogeneous systems. *Analyst,* **119(5),** 805-26.

148. **Macak, J. M., P. J. Barczuk, H. Tsuchiya, M.Z. Nowakowska, A. Ghicov, M. Chojak, S. Bauer, S. Virtanen, P.J. Kulesza and P. Schmuki** (2005) Self-organized nanotubular TiO_2 matrix as support for dispersed Pt/Ru nanoparticles: Enhancement of the electrocatalytic oxidation of methanol. *Electrochem. Commun.,* **7(12)**, 1417-1422.

149. **Machida, K. and M. Enyo** (1990) Preparation of tungsten carbide (WCx) thin films by RF sputtering and their electrocatalytic property for anodic methanol oxidation. *J. Electrochem. Soc.,* **137(3)**, 871-6.

150. **Maiyalagan, T., B. Viswanathan and U.V. Varadaruju** (2006) Electro - oxidation of methanol on TiO_2 nanotube supported platinum electrodes. *J. Nanosci. Nanotech.,* **6,** 2067-2071.

151. **Maiyalagan,T.** and **B. Viswanathan** (2005) Template Synthesis and Characterization of Nitrogen Containing Carbon Nanotubes. *Mater. Chem. Phys.,* **93**, 291-295.

152. **Maldonado, S. and K.J. Stevenson** (2004) Direct Preparation of Carbon Nanofiber Electrodes via Pyrolysis of Iron (II) Phthalocyanine: Electrocatalytic Aspects for Oxygen Reduction. *J. Phys. Chem. B,* **108(31)**, 11375-11383.

153. **Maldonado, S., and K.J.Stevenson** (2005) Influence of Nitrogen Doping on Oxygen Reduction Electrocatalysis at Carbon Nanofiber Electrodes. *J. Phys. Chem. B,* **109,** 4707-16.

154. **Malinauskas, A.** (1999) Electrocatalysis at conducting polymers. *Synth. Met.,* **107(2)**, 75-83.

155. **Malinauskas, A.** (2001) Chemical deposition of conducting polymers. *Polymer,* **42,** 3952-3972.

156. **Mandelbaum, P. A., A. E. Regazzoni, M. A. Blesa and S. A. Bilmes** (1999) Photo-Electro-Oxidation of Alcohols on Titanium Dioxide Thin Film Electrodes. *J. Phys Chem B,* **103(26)**, 5505-5511.

157. **Markovic, N.M., A. Widelov, P.N. Ross, O.R. Monteiro and L.G. Brown** (1997) Electrooxidation of CO and CO / H_2 mixtures on a Pt - Sn catalyst prepared by an implantation method. *Catal. Lett.,* **43(3,4)**, 161-166.

158. **Martin, C. R.** (1996) Membrane-Based Synthesis of Nanomaterials. *Chem. Mater.,* **8,** 1739-1746.

159. **Martin, C. R., R .Parthasarathy and V**.**Menon** (1993) Template synthesis of electronically conductive polymers - a new route for achieving higher electronic conductivities. *Synth. Met.,* **55(2-3),** 1165 –1170.

160. **Martin, C.R.** (1994) Nanomaterials: a membrane-based synthetic approach. *Science,* **266(5193),** 1961-6.

161. **Martin, C.R., L.S. Van Dyke, Z. Cai and W. Liang** (1996) Template Synthesis of Organic Microtubules. *J. Am. Chem. Soc.,* **112,** 8976-8977.

162. **Matsumoto, T., T. Komatsu, H. Nakano, K. Arai, Y. Nagashima, E. Yoo, T. Yamazaki, M. Kijima, H. Shimizu, Y. Takasawa and J. Nakamura** (2004) Efficient usage of highly dispersed Pt on carbon nanotubes for electrode catalysts of polymer electrolyte fuel cells. *Catal. Today,* **90(3-4)**, 277-281.

163. **McNicol, B.D., D.A.J. Rand and K.R. Williams** (1999) Direct methanol –air fuel cells for road transportation. *J. Power Sources,* **83**, 15-31.

164. **Morita, M., Y. Iwanaga and Y. Matsuda** (1991) Anodic Oxidation of Methanol at a Gold-Modified Platinum Electrocatalysts prepared by RF sputtering on a glassy carbon support. *Electrochim. Acta,* **36,** 947-951.

165. **Murugan, A. V., C.W. Kwon, G. Campet, B.B. Kale, A.B. Mandale, S.R. Sainker, C.S. Gopinath, and K. Vijayamohanan** (2004) A novel approach to prepare poly(3,4-ethylenedioxythiophene) nanoribbons between V_2O_5 layers by microwave irradiation. *J. Phys. Chem. B,* **108(30)**, 10736-10742.

166. **Musiani, M.M.** (1990) Characterization of Elecroactive Polymer Layers by Electrochemical Impedance Spectroscopy. *Electrochim. Acta,* **35,** 1665-1670.

167. **Napporn, W.T., H. Laborde, J.M. Leger and C. Lamy** (1996) Electrooxidation of C1 molecules at Pt-based catalysts highly dispersed into a polymer matrix: effect of the method of preparation. *J. Electroanal. Chem.*, **404(1)**, 153-9.

168. **Neergat, M., D. Leveratto and U. Stimming** (2002) Catalysts for direct methanol fuel cells. *Fuel Cells,* **2(1)**, 25-30.

169. **Neophytides, S. G., S. Zafeiratos, G. D. Papakonstantinou, J. M. Jaksic, F. E. Paloukis and M. M. Jaksic** (2005) Extended Brewer hypo-hyper-d-interionic bonding theory. II. Strong metal-support interaction grafting of composite electrocatalysts. *Int. J. Hydrogen. Energy,* **30(4)**, 393-410.

170. **Niu, L., C. Kvarnstrom, K. Froberg and A. Ivaska** (2001) Electrochemically controlled surface morphology and crystallinity in poly (3, 4 – ethylenedioxythiophene) films. *Synth. Met.,* **122(2)**, 425-429.

171. **Obare, S. O., T.Ito and G.J. Meyer** (2005) Controlling Reduction Potentials of Semiconductor-Supported Molecular Catalysts for Environmental Remediation of Organohalide Pollutants. *Environ. Sci. Technol.,* **39(16)**, 6266-6272.

172. **Ohsaka,T., T. Watanabe, F. Kitamura, N. Oyama and K. Tokuda** (1991) Electrocatalysis of oxygen reduction at poly(o-phenylenediamine)- and poly(o- aminophenol)-coated glassy carbon electrodes. *Chem. Comm.,* **16,** 1072-1073.

173. **Okamoto, H., G. Kawamura, A. Ishikawa and T. Kudo** (1987) Activation of (W, Mo) C Methanol anodic oxidation catalyts using alkaline solution. *J. Electrochem. Soc*., **130,** 1491-1497.

174. **Park, K.W. and Y.E. Sung** (2006) Design of nanostructured electrocatalysts for direct methanol fuel cells. *J. Ind. Eng.Chem.,* **12(2)**, 165-174.

175. **Park, K.W., Y.E. Sung and M.F. Toney** (2006) Structural effect of PtRu-WO_3 alloy nanostructures on methanol electrooxidation. *Electrochem. Commun.,* **8(2)**, 359-363.

176. **Park, K-W., J.-H. Choi, K-S. Ahn and Y.-E. Sung** (2004) PtRu Alloy and PtRu-WO_3 Nanocomposite Electrodes for Methanol Electrooxidation Fabricated by a Sputtering Deposition Method. *J.Phys. Chem., B* **108**, 5989-5994.

177. **Parsons, R. and T. Vandernoot** (1988) The oxidation of small organic molecules. A survey of recent fuel cell related research. *J. Electroanal. Chem*., **257(1-2)**, 9-45.

178. **Patil, P. and P. Zegers (**1994) Fuel cell road traction: an option for a clean global society. *J. Power Sources,* **49(1-3)**, 169-84.

179. **Penner, R.M. and C.R. Martin** (1986) Controlling the Morphology of Electronically Conductive Polymers. *J. Electrochem. Soc.,* **133**, 2206-2207.

180. **Penner, R.M., L.S. Van Dyke and C.R. Martin** (1988) Electrochemical Evaluation of Charge –Transport Rates in Polypyrrole. *J. Phys. Chem.,* **92,** 5274-5282

181. **Pickup, P.G. and R.A. Osteryoung** (1984) Electrochemical Polymerization of Pyrrole and Electrochemistry of Polypyrrole Films in Ambient Temperature Molten Salts. *J. Am. Chem. Soc.,* **106,** 2294-2299.

182. **Pokhodenko, V.D. and V.A. Krylov** (1991) Effect of Electrolyte nature on the electrochemical synthesis and doping of polyanniline and Poly-3-phenylthiophene *Synth. Met.,* **41-43,** 533-536.

183. **Prabhuram, J. and R. Manoharan** (1998) Investigation of methanol oxidation on unsupported platinum electrodes in strong alkali and strong acid. *J. Power Sources,* **74(1)**, 54-61.

184. **Prabhuram, J., R. Manoharan and H.N. Vasan** (1998) Effects of incorporation of Cu and Ag in Pd on electrochemical oxidation of methanol in alkaline solution. *J. Appl. Electrochem.,* **28(9)**, 935-941.

185. **Premkumar, J. and R. Ramaraj** (1996) Permeation and electrocatalytic reduction of oxygen by poly (o-phenylenediamine) incorporated into Nafion film. *J. Appl. Electrochem.,* **26,** 763-766.

186. **Pyo, M., J.R. Reynolds, L.F. Warren, and H.O. Marcy** (1994) Longterm-term redox switching stability of polypyrrole. *Synth. Met.,* **68,** 71-77.

187. **Quan, X., S. Yang, X. Ruan and H. Zhao** (2005) Preparation of Titania Nanotubes and Their Environmental Applications as Electrode. *Environ. Sci. Technol.,* **39,** 3770-3775.

188. **Raghuveer, V. and A. Manthiram** (2004) Mesoporous Carbon with Larger Pore Diameter as an Electrocatalyst Support for Methanol Oxidation. *Electrochem. Solid State Lett.,* **7(10),** A336-A339.

189. **Raimondi F., G.G. Scherer, R. Kotz and A. Wokaun (**2005) Nanoparticles in energy technology: examples from electrochemistry and catalysis. *Angew. Chem.,* **44(15),** 2190-209.

190. **Rajesh, B. and B. Viswanathan** (2000) Polymer based oxidation catalyst for methanol fuel cell. *Indian. J.Chem.,* **39A**, 826-829.

191. **Rajesh, B., K.R. Thampi, J.M. Bonard, H.J. Mathieu, N. Xanthopoulos and B. Viswanathan** (2005) Electronically conducting hybrid material as high performance catalyst support for electrocatalytic application. *J. Power Sources,* **141,** 35-38.

192. **Rajesh, B., K.T. Ravindranathan, J.M. Bonard, N. Xanthopoulos, H.J. Mathieu and B. Viswanathan** (2003) Carbon Nanotubes Generated from Template Carbonization of Polyphenyl Acetylene as the Support for Electrooxidation of Methanol. *J. Phys. Chem. B,* **107(12)**, 2701-2708.

193. **Rajesh, B., K.T. Ravindranathan, J.M. Bonard, N. Xanthopoulos, H.J. Mathieu and B. Viswanathan** (2002) Pt-WO_3 supported on carbon nanotubes as possible anodes for direct methanol fuel cells. *Fuel,* **81(17),** 2177-2190.

194. **Rajesh, B., T.K. Ravindranathan, J.M. Bonard, H.J. Mathieu, N. Xanthopoulos and B. Viswanathan** (2005) Electronically conducting hybrid material as high performance catalyst support for electrocatalytic application. *J. Power Sources,* **141,** 35-38.

195. **Ramesh, P. and S. Sampath** (2003) Electrochemical Characterization of Binderless, Recompressed Exfoliated Graphite Electrodes: Electron-Transfer Kinetics and Diffusion Characteristics. *Anal. Chem*., **75(24),** 6949-6957.

196. **Ren, N., A-G. Dong, W-B. Cai, Y-H. Zhang, W-L. Yang, S-J. Huo, Y. Chen, S-H. Xie, Z. Gao and Y. Tang** (2004) Mesoporous microcapsules with noble metal or noble metal oxide shells and their application in electrocatalysis. *J. Mater. Chem*., **14(24)**, 3548-3552.

197. **Rodriguez, N. M., M. S. Kim and R.T. K. Baker** (1994) Carbon Nanofibers: A Unique Catalyst Support Medium. *J. Phys Chem.,* **98(50)**, 13108-11.

198. **Rodriguez, N.M.** (1993) A review of catalytically grown carbon nanofibers. *J. Mat. Res*., **8(12)**, 3233-50.

199. **Rolison, D.R. and H.S. White** (1999) Electrochemistry at Nanostructured Materials. *Langmuir,* **15(3),** 649-649.

200. **Rolison, D.R., P.L. Hagans, K.E. Swider and J.W. Long** (1999) Role of Hydrous Ruthenium Oxide in Pt-Ru Direct Methanol Fuel Cell Anode Electrocatalysts: The Importance of Mixed Electron/Proton Conductivity. *Langmuir,* **15(3)**, 774-779.

201. **Roucoux, A., J. Schulz and H. Patin** (2002) Reduced Transition Metal Colloids: A Novel Family of Reusable Catalysts. *Chem. Rev.,* **102(10)**, 3757-3778.

202. **Roy, S.C., A.W. Harding, A.E. Russell, and K.M.Thomas** (1997) Spectroelectrochemical study of the role played by carbon functionality in fuel cell electrodes. *J. Electrochem. Soc.,* **144(7)**, 2323-8.

203. **Roy, S.C., P.A. Christensen, A. Hamnett, K.M. Thomas and V. Trapp** (1996) Direct methanol fuel cell cathodes with sulfur and nitrogen-based carbon functionality. *J. Electrochem. Soc.,* **143(10)**, 3073–9.

204. **Ryoo, R., S.H. Joo and S. Jun** (1999) Synthesis of Highly Ordered Carbon Molecular Sieves via Template-Mediated Structural Transformation. *J. Phys. Chem. B,* **103(37)**, 7743-7746.

205. **Sander, M.S., M. J. Cote, W. Gu, B. M. Kile and C.P.Tripp** (2004) Template-assisted fabrication of dense, aligned arrays of titania nanotubes with well-controlled dimensions on substrates. *Adv. Mater.,* **16,** 2052-2057.

206. **Santato, C., M. Odziemkowski, M. Ulmann and J. Augustynski** (2005) (2001) Crystallographically Oriented Mesoporous WO_3 Films: Synthesis, Characterization, and Applications. *J. Am. Chem. Soc.*, **123**, 10639-49.

207. **Santhosh, P., A. Gopalan, T. Vasudevan,and K.-P Lee** (2006) Platinum particles dispersed poly(diphenylamine) modified electrode for Methanol oxidation**.** *Appl. Surf. Sci.,* **252 (22)**, 7964-7969.

208. **Schiavon, G., S. Sitran and G. Zotti** (1989) A simple two-band electrode for in situ conductivity measurements of polyconjugated conducting polymers. *Synth. Met.,* **32(2)**, 209-17.

209. **Scibioh, M.A., B. Rajesh and B. Viswanathan** (2002) Anode materials for direct methanol fuel cell. *PINSA,* **68(2),** 99-139.

210. **Serp, P., M. Corrias and P. Kalck** (2003) Carbon nanotubes and nanofibers in catalysis. *Appl. Catal. A: Gen.,* **253(2)**, 337-358.

211. **Shen, P. K., K. Y.Chen and A. C. C..Tseung** (1995) CO oxidation on Pt-Ru/WO_3 electrodes *J. Electrochem. Soc.,* **142(6)**, L85-L86.

212. **Shen, P.K. and A. C. C. Tseung** (1994) Anodic oxidation of methanol on Pt/WO_3 in acidic media. *J. Electrochem. Soc.,* **141,** 3082-90.

213. **Shen, P.K. and C. Xu** (2006) Alcohol oxidation on nanocrystalline oxide Pd/C promoted electrocatalysts. *Electrochem. Commun.,* **8(1)**, 184-188.

214. **Shim, J., C.R. Lee, H.K. Lee, J.S. Lee and E.J.Cairns** (2001) Electrochemical characteristics of Pt-WO_3/C and Pt-TiO_2/C electrocatalysts in a polymer electrolyte fuel cell. *J. Power Sources,* **102(1-2)**, 172-177.

215. **Shukla, A.K., A.S. Arico, K.M. El-Khatib, H. Kim, P.L. Antonucci and V.Antonucci** (1999) An X-ray photoelectron spectroscopic study on the effect of Ru and Sn additions to platinized carbons. *Appl. Surf. Sci.,* **137(1-4)**, 20-29.

216. **Shukla, A.K., M.K Ravikumar, A. Roy, S.R. Barman, D.D. Sarma, and A.S.Arico** (1994) Electro-oxidation of methanol in sulfuric acid electrolyte on platinized-carbon electrodes with several functionalgroup characteristics. *J. Electrochem. Soc.,* **141(6),** 1517–22.

217. **Sriramulu, S., T.D. Jarvi and E.M. Stuve** (1999) Reaction mechanism and dynamics of methanol electrooxidation on platinum(111). *J. Electroanal. Chem.,* **467(1,2)**, 132-142.

218. **Steigerwalt, E.S., G.A. Deluga and C.M.Lukehart** (2002) Pt–Ru/carbon fiber nanocomposites:Synthesis, characterization, and performance as anode catalysts of direct methanol fuel cells. A search for exceptional performance. *J. Phys. Chem. B,* **106,** 760–6.

219. **Steigerwalt, E.S., G.A. Deluga, D.E. Cliffel and C.M. Lukehart** (2001) A Pt–Ru/graphitic carbon nanofiber nanocomposite exhibiting high relative performance as a direct-methanol fuel cell anode catalyst. *J. Phys. Chem. B,* **105 (34)**, 8097–8101.

220. **Stephan, O., P. M. Ajayan, C.Colliex, Ph. Redlich, J. M. Lambert and P. Bernier** (1994) Doping graphitic and carbon nanotube structures with boron and nitrogen. *Science,* **266,** 1683-85.

221. **Stiwell, D.E. and S. MoonPark** (1988) Electrochemistry of Conductive Polymers: III. Some Physical and Electrochemical Properties Observed from Electrochemically Grown Polyaniline. *J.Electrochem. Soc.,* **135,** 2491-2496.

222. **Stoyanova, A., V. Naidenov K. Petrov L. Nikolov, T. Vitanov and E. Budevski** (1999) Effect of preparation conditions on the structure and catalytic activity of carbon-supported platinum for the electrooxidation of methanol. *J. Appl. Electrochem.,* **29(10)**, 1197-1203.

223. **Strike, D.J., N.F. De Rooij, M. Koudelka-Hep, M. Ulmann and J. Augustynski** (1992) Electrocatalytic Oxidation of Methanol on Platinum Microparticles in Polypyrrole. *J. Appl. Electrochem.,* **22,** 922-926.

224. **Su, F., J. Zeng, X. Bao, Y. Yu, J.Y. Lee and X.S. Zhao** (2005) Preparation and Characterization of Highly Ordered Graphitic Mesoporous Carbon as a Pt Catalyst Support for Direct Methanol Fuel Cells. *Chem. Mater.,* **17(15)**, 3960-3967.

225. **Subramanian, V., A.Karki, K.I,Gnanasekar, F.P. Eddy and B. Rambabu,** (2006) Nanocrystalline TiO_2 (anatase) for Li - ion batteries. *J. Power Sources,* **159(1)**, 186-192.

226. **Suffredini, H.B., V. Tricoli, N. Vatistas and L.A. Avaca** (2006) Electro - oxidation of methanol and ethanol using a Pt - RuO_2 / C composite prepared by the sol-gel technique and supported on boron - doped diamond. *J. Power Sources,* **158(1)**, 124-128.

227. **Sum, E. and M.Skyllas-Kazacos** (1985) A study of the V(II)/V(III) Redox Couple for Redox Flow Cell Applications. *J. Power Sources,* **15,** 179-190.

228. **Sum, E., M.Rychcik and M.Skyllas-Kazacos** (1985) Investigation of the V(V)/V(IV) System for Use in the Positive Half-Cell of a Redox Battery. *J. Power Sources,* **16,** 85-95.

229. **Sun, C-L., L-C. Chen, M.C. Su, L–S. Hong, O. Chyan and C-Y. Hsu** (2005) Ultrafine Platinum Nanoparticles Uniformly Dispersed on Arrayed CN_x Nanotubes with High Electrochemical Activity. *Chem. Mater.,* **17(14),** 3749-53.

230. **Sundmacher, K., T. Schultz, S. Zhou, K. Scott, M. Ginkel and E. D. Gilles** (2001) Dynamics of the direct methanol fuel cell (DMFC): experiments and Model - based analysis. *Chem. Eng. Sci.,* **56(2)**, 333-341.

231. **Swathirajan, S. and Y.M. Mikhail** (1991) Electrochemical Oxidation of Methanol at Chemically Prepared Platinum-Ruthenium Alloy Electrodes. *J. Electrochem. Soc.,* **138**, 1321-1326.

232. **Swathirajan, S. and Y.M. Mikhail** (1992) Methanol oxidation on Platinum-Tin catalysts dispersed on Poly (3-methyl) thiophene conducting polymers *J. Electrochem. Soc.,* **139**, 2105-2110.

233. **Swider, K. E. and D. R. Rolison** (2000) Reduced poisoning of platinum fuel-cell electrocatalysts supported on desulfurized carbon. *Electrochem. Solid State Lett.,* **3(1),** 4-6.

234. **Swider, K.E. and D.R. Rolison** (1996) The chemical state of sulfur in carbon-supported fuel-cell electrodes. *J. Electrochem. Soc.,* **143(3)**, 813-19.

235. **Takagahara, T. and K.Takeda** (1992) Theory of the quantum confinement effect on excitons in quantum dots of indirect-gap materials. *Phys. Rev. B,* **46**, 15578-81.

236. **Takeuchi, M., K. Sakamoto, G. Martra, S. Coluccia and M.Anpo** (2005) Mechanism of Photoinduced Superhydrophilicity on the TiO_2 Photocatalyst Surface. *J. Phys. Chem. B,* **109(32)**, 15422-15428.

237. **Tang, H., J. Chen, L. Nie , D. Liu, W. Deng, Y. Kuang and S. Yao** (2004) High dispersion and electrocatalytic properties of platinum nanoparticles on graphitic carbon nanofibers (GCNFs). *J. Colloid. Interf. Sci.,* **269(1)**, 26-31.

238. **Tang, Z. and G. Lu** (2006) High performance rare earth oxides LnOx (Ln=Sc, Y, La, Ce, Pr and Nd) modified Pt/C electrocatalysts for methanol electrooxidation. *J. Power Sources,* **162(2)**, 1067-1072.

239. **Tarasevich M.R, and V.A.Bogdanovskaya** (1987) The Surface-modified Carbon Materials for Electrocatalysis. *Russ. Chem. Rev.,* **56 (7)**, 653-69.

240. **Tarasevich M.R., L.A .Beketaeva, B.N. Efremov, N.M. Zagudaeva, L.N. Kuznetsova and K.V. Rybalka** (2004) Electrochemical Properties of Carbon Black AD-100 and AD-100 Promoted with Pyropolymer of Cobalt Tetra (p- methoxyphenyl)porphyrin. *Russ. J. Electrochem.,* 40(5), 542-51.

241. **Tauster, S. J., S. C. Fung and R. L. Garten** (1978) Strong metal-support interactions. Group 8 noble metals supported on titanium dioxide. *J.Am.Chem. Soc.,* **100(1)**, 170-5.

242. **Thess, A., R. Lee, P. Nikolaev, H. Dai, P. Petit, J. Robet, C. Xu, Y.H. Lee, S.G. Kim, A. Rinzler, D.T. Colbert, G. Scuseria, D. Tomanek, J.E. Fischer and R. Smalley** (1996) Crystalline ropes of metallic carbon nanotube. *Science,* **273**, 483-487.

243. **Thompson, S.D., L.R. Jordan and M. Forsyth** (2001) Platinum electrodeposition for polymer electrolyte membrane fuel cells. *Electrochim. Acta,* **46**, 1657-1663.

244. **Trasatti, S. and O.A. Petrii** (1991) Real surface area measurements in electrochemistry. *Pure Appl. Chem.,* **63,** 711-734.

245. **Tripkovic, A.V., K.D. Popovic, J.D. Momcilovic and D.M. Drazic** (1998) Kinetic and mechanistic study of methanol oxidation on a Pt (110) surface in alkaline media. *Electrochim. Acta,* **44(6-7)**, 1135-1145.

246. **Tsang, S.C., P. de Oliveira, J.J. Davis, M.L.H. Green and H.A.O. Hill** (1996) The structure of the carbon nanotube and its surface topography probed by transmission electron microscopy and atomic force microscopy. *Chem. Phys. Lett.,* **249,** 413-422.

247. **Uchida, M., Y. Aoyama, N. Tanabe, N. Yanagihara, N. Eda and A.Ohta** (1995) Influences of both carbon supports and heat-treatment of supported catalyst on electrochemical oxidation of methanol. *J. Electrochem. Soc.,* **142**, 2572–2576.

248. **Uchida, S., R. Chiba, M. Tomiha, N. Masaki and M. Shirai** (2002) Application of titania nanotubes to a dye-sensitized solar cell. *Electrochemistry,* **70,** 418-420.

249. **Van, M.J., G. Maggetto and P. Lataire** (2006) Which energy source for road transport in the future? A comparison of battery, hybrid and fuel cell vehicles. *Energ, Convers. Manage.,* **47(17)**, 2748-2760.

250. **Varghese, O. K., D.W.Gong, M. Paulose, K.G. Ong, E.C. Dickey and C.A.Grimes** (2003) Extreme changes in the electrical resistance of titania nanotubes with hydrogen exposure. *Adv. Mater.,* **15,** 624-627.

251. **Vielstich, W.** (2003) Interfacial Kinetics and Mass Transport, Vol. 2, **Fauze J. Anaissi** Wiley-VCH, Weinheim, pp. 466 – 511.

252. **Viswanathan, B. and M.A. Scibioh** (2006) Fuel cells Principles and Applications, The University press.

253. **Vork, E. and E. Barendrecht** (1989) Application and Characterization of Polypyrrole-Modified Electrodes with incorporated Pt Particles. *Synth. Met.,* **28,** C121-C126.

254. **Wan, W.L.M.** (1998) Porous polyaniline films with high conductivity. *Synth. Met.,* **92,** 12-16.

255. **Wang, C., M. Waje, X. Wang, J.M. Tang, R.C. Haddon and Y.S. Yan** (2004) Proton exchange membrane fuel cells with carbon nanotube based electrodes. *Nano Lett.,* **4**, 345–348.

256. **Wang, H., T. Loffler and H. Baltruschat** (2001) Formation of intermediates during methanol oxidation: a quantitative DEMS study. *J. Appl. Electrochem.,* **31(7)**, 759-765.

257. **Wang, J., J. Xi, Y. Bai, Y. Shen, J. Sun, L. Chen, W. Zhu and X. Qiu** (2007) Structural designing of Pt- CeO_2 /CNTs for methanol electro - oxidation. *J. Power Sources,* **164(2)**, 555-560.

258. **Wang, J., S. Ee, S. Lee, S.C. Ng, C.H. Chew and L.M. Gan** (1997) Reduced crystallization temperature in a microemulsion-derived zirconia precursor. *Mater. Lett.,* **30(1)**, 119-124.

259. **Wang, K., H.A. Gasteiger, N.M. Markovic, P.N. Jr. and Ross** (1996) On the reaction pathway for methanol and carbon monoxide electrooxidation on Pt-Sn alloy versus Pt-Ru alloy surfaces. *Electrochim. Acta,* **41(16)**, 2587-2593.

260. **Wang, M.** (2002) Fuel choices for fuel -cell vehicles: well-to-wheels energy and emission impacts. *J. Power Sources,* **112(1)**, 307-321.

261. **Wang, M., D.J. Guo and H. L. Li** (2005) High activity of novel Pd/TiO_2 nanotube catalysts for methanol electro-oxidation. *J. Solid State Chem.,* **178(6)**, 1996-2000.

262. **Wang, Y., J. Ren, K. Deng, L. Gui and Y. Tang** (2000) Preparation of Tractable Platinum, Rhodium, and Ruthenium Nanoclusters with Small Particle Size in Organic Media. *Chem. Mater.,* **12(6),** 1622-1627.

263. **Wasmus, S. and A. Kuver** (1999) Methanol Oxidation and Direct Methanol Fuel Cells: A Selective Review. *J. Electroanal. Chem.,* **461**, 14-31.

264. **Watanabe, M**. (2003) Design of electrocatalysts for fuel cells. *Catalysis and Electrocatalysis at Nanoparticle Surfaces,* 827-845.

265. **Watanabe, M. and S. Motto** (1975) Electroctalysis by Ad-Atoms: Part I. Enhancement of the oxidation of methanol on platinum and palladium by gold ad - atoms. *J. Electroanal. Chem.,* **60(3)**, 259-66.

266. **Watanabe, M., M. Uchida and S. Motoo** (1987) Preparation of Highly dispersed Pt-Ru alloy cluster and the activity for the electrooxidation of methanol. *J. Electroanal. Chem.,* **229**, 395-406.

267. **Wei, Z., H. Guo and Z.Tang** (1996) Methanol electro - oxidation on platinum and platinum - tin alloy catalysts dispersed on active carbon. *J. Power Sources,* **58(2)**, 239-242.

268. **Wilbourn, K. and R.W. Murray** (1988) The d.c. redox versus electronic conductivity of the ladder polymer poly(benzimidazobenzophenanthroline). *J. Phys. Chem.,* **92(12)**, 3642-8.

269. **Xia, X. H., T. Iwasita, F. Ge and W. Vielstich** (1996) Structural effects and reactivity in methanol oxidation on polycrystalline and single crystal platinum. *Electrochim. Acta,* **41(5)**, 711-18.

270. **Xiong, L. and A**. **Manthiram** (2004) Synthesis and characterization of methanol tolerant Pt/TiOx/C nanocomposites for oxygen reduction in direct methanol fuel cells. *Electrochim. Acta,* **49(24)**, 4163-4170.

271. **Xu, C. and P.K. Shen** (2004) Novel Pt/ CeO_2 /C catalysts for electrooxidation of alcohols in alkaline media. *Chem. Comm.,* **(19)**, 2238-2239.

272. **Xu, C., P.K. Shen, X. Ji, R. Zeng and Y. Liu** (2005) Enhanced activity for ethanol electrooxidation on Pt- MgO /C catalysts. *Electrochem. Commun.*, **7(12)**, 1305-1308.

273. **Yamamoto, K., D.M. Kolb, R. Kotz and G. Lehmpfuhl** (1979) Hydrogen adsorption and oxide formation on platinum single crystal electrodes. *J. Electroanal. Chem.,* **96**, 233-239.

274. **Yang, H., T. Lu, K. Xue, S. Sun, G. Lu and S. Chen** (1997) Electrocatalytic Oxidation of Methanol on Polypyrrole Film Modified with Platinum Microparticles. *J. Electrochem. Soc.,* **144,** 2302-2306.

275. **Yang, L.X., C. Bock, B. Mac Dougall and J. Park** (2004) The role of the WO_x ad-component to Pt and PtRu catalysts in the electrochemical CH_3OH oxidation *J. Appl. Electrochem.,* **34**, 427-438.

276. **Yoshiike, N. and S. Kondo** (1983) Electrochemical properties of tungsten (VI) oxide hydrate (WO_3.x (H_2O)). I. The influences of water adsorption and hydroxylation. *J. Electrochem. Soc.,* **130**, 2283-2286.

277. **Yoshiike, N. and S. Kondo** (1984) Electrochemical properties of tungsten (VI) oxide hydrate (WO_3.x (H_2O)). II. The influence of crystallization as hydration**.** *J. Electrochem. Soc.,* **131,** 809-812.

278. **Yoshitake, T., Y. Shimakawa, S. Kuroshima, H. Kimura, T. Ichihashi and Y. Kubo** (2002) Preparation of fine Platinum catalyst supported on single-wall carbon nanohorns for fuel cell application. *Physica B,* **323,**124-26.

279. **Yu, E. H. and K. Scott** (2004) Direct methanol alkaline fuel cell with catalysed metal mesh anodes. *Electrochem. Commun.,* **6(4)**, 361-365.

280. **Zeng, A., E. Liu, S.N. Tan, S. Zhang and J. Gao** (2002) Cyclic voltammetry studies of sputtered nitrogen doped diamond-like carbon film electrodes. *Electroanalysis,* **14(15-16),** 1110-1115.

281. **Zhang, D.Y., Z.F. Ma, G. Wang, K. Konstantinov, X. Yuan and H.K. Liu** (2006) Electro - oxidation of ethanol on Pt- WO_3/C electrocatalyst. *Electrochem. Solid State Lett.,* **9(9)**, A423-A426.

282. **Zhang, H., Y. Wang, E.R. Fachini and C.R. Cabrera** (1999) Electrochemically codeposited platinum/molybdenum oxide electrode for catalytic oxidation of methanol in acid solution. *Electrochem. Solid State Lett.,* **2(9)**, 437-439.

283. **Zhang, K.F., D.J. Guo, X. Liu, J. Li, H. L. Li and Z. H. Su** (2006) Vanadium oxide nanotubes as the support of Pd catalysts for methanol oxidation in alkaline solution. *J. Power Sources,* **162(2)**, 1077-1081.

284. **Zhang, X. and Y.K. Chan** (2003) Water-in-Oil Microemulsion Synthesis of Platinum-Ruthenium Nanoparticles, Their Characterization and Electrocatalytic Properties. *Chem. Mater.,* **15(2)**, 451-459.

285. **Zhao, J., X. He, J. Tian, C. Wan and C. Jiang** (2007) Reclaim/recycle of Pt/C catalysts for PEMFC. *Energ, Convers. Manage.*, **48(2)**, 450-453.

286. **Zhao, Z.W. and P.G. Pickup** (1994) Controlling the Morphology of Electrochemically Deposited Poly (3-Methyl) Thiophene Films by Electrode Rotation *Chem. Soc. Faraday Trans.,* **90,** 3097-3102.

287. **Zhou, M. and J. Heinze** (1999) Electropolymerization of Pyrrole and Electrochemical Study of Polypyrrole: 1. Evidence for Structural Diversity of Polypyrrole. *Electrochim. Acta,* **44,** 1733-1748.

288. **Zhou, S., T. Schultz, M. Peglow and K. Sundmacher** (2001) Analysis of the nonlinear dynamics of a direct methanol fuel cell. *Phys. Chem. Chem. Phy.,* **3(3)**, 347-355.

289. **Zhou, Y., L. Cao, F.Zhang, B.He and H.Li** (2003) Lithium Insertion into TiO_2 Nanotubes Prepared by the Hydrothermal Process. *J. Electrochem. Soc.,* **150,** A1246-1249.

290. **Zhou, Z., S. Wang, W. Zhou, G. Wang, L. Jiang, W. Li, S. Song, J. Liu, G. Sun and Q. Xin** (2003) Novel synthesis of highly active Pt/C cathode electrocatalyst for direct methanol fuel cell. *Chem. Comm.,* **(3)**, 394-395.

291. **Zhu, K., R. Neale Nathan, A. Miedaner and A.J. Frank** (2007) Enhanced charge-collection efficiencies and light scattering in dye-sensitized solar cells using oriented TiO_2 nanotubes arrays. *Nano lett.,* **7(1)**, 69-74.

292. **Zotti, G., S. Cattarin and N. Comisso** (1988) Cyclic potential sweep Electropolymerization of Aniline. The Role of Anions in the Polymerization Mechanism. *J. Electroanal. Chem.,* **239,** 387-396.

293. **Zoval, J.V., J. Lee, S. Gorer and R.M. Penner** (1998) Electrochemical Preparation of Platinum Nanocrystallites with Size Selectivity on Basal Plane Oriented Graphite Surfaces. *J. Phys. Chem. B,* **102(7)**, 1166-1175.

LIST OF PUBLICATIONS

REFEREED JOURNALS

1. **Maiyalagan,T.** and **B. Viswanathan** (2005) Template Synthesis and Characterization of Nitrogen Containing Carbon Nanotubes. *Mater. Chem. Phys.,* **93**, 291-295.

2. **Maiyalagan,T., B. Viswanathan** and **U.V. Varadaraju** (2005) Nitrogen containing carbon nanotubes as supports for Pt – Alternate anodes for fuel cell applications. *Electrochem. Commun.,* **7**, 905-912.

3. **Maiyalagan, T., B. Viswanathan**, **U.V. Varadaraju**, **B. K. Pradhan** and **B. Srinivas** (2005) Electro-oxidation of methanol on TiO_2 nanotube electrodes. *Proc. Fuel Cell Seminar,* Palm springs, California, USA 149.

4. **Maiyalagan, T.** and **B. Viswanathan** (2006) Template Synthesis of Carbon nanotubes by carbonization of Polyparaphenylene. *Indian .J. Chem. Sec A,* **45,** 839-844.

5. **Maiyalagan, T., B. Viswanathan** and **U.V. Varadaraju** (2006) Nitrogen Containing Carbon nanotubes as Supports for Pt – Alternate Anodes for Fuel Cell Applications- (Research Trends). *Fuel cells Bulletin* **2**, 15.

6. **Maiyalagan, T., B. Viswanathan** and **U.V. Varadaraju** (2006) Electro-oxidation of Methanol on Pt supported TiO_2 Nanotube. *J. Nanosci. Nanotech.,* **6**, 2067-2071.

7. **Maiyalagan, T., B. Viswanathan** and **U.V. Varadaraju** (2006) Fabrication and Characterization of uniform TiO_2 nanotubes. *Bull. Mater. Sci.,* **29**, 705-708.

PAPER PRESENTED IN CONFERENCES

1. **Maiyalagan, T.** and **B. Viswanathan** (2003) Carbon nanotubes as supports for Pt – a new generation anodes for DMFC Presented in National Seminar on "Fuel To Fuel Cells" on DEC 4-5, 2003 at Indian Institute of Chemical Technology, Hyderabad, India.

2. **Maiyalagan, T.** and **B. Viswanathan** (2004) Nitrogen containing carbon nanotubes as supports for Pt for fuel cell electrode applications Presented in "Advances in Catalysis" on JAN 6-7, 2004 at Loyola College, Chennai, India.

3. **Maiyalagan, T.** and **B. Viswanathan** (2004) Nitrogen containing carbon nanotubes as supports for Pt – alternate anodes for Fuel cell applications. Presented in National seminar on "Creating Infrastructure for Adoption of Fuel Cell Technology in India "on April 15, 2004 at National Thermal Power Corporation, Noida, India.

4. **Maiyalagan, T.** and **B. Viswanathan** (2004) Nitrogen containing carbon nanotubes as supports for Pt for fuel cell electrode applications. Presented in "The 13th International congress on catalysis" on JULY 11-16, 2004 at Paris, France.

5. **Maiyalagan, T.** and **B. Viswanathan** (2005) Electro oxidation of methanol on electrodeposited platinum in Poly (o-phenylenediamine) nanotubules electrodes Presented in National seminar on "National Seminar on Applied Research on Solid State Chemistry and Nanotechnology" on FEB 25, 2005 at Annamalai University, India.

6. **Maiyalagan, T., B. Viswanathan**, **U.V. Varadaraju, B.K. Pradhan,** and **B. Srinivas** (2005) Electro-oxidation of methanol on TiO_2 nanoutube electrodes in Fuel Cell Seminar on 14th NOV 2005 at Palm springs, California, USA.